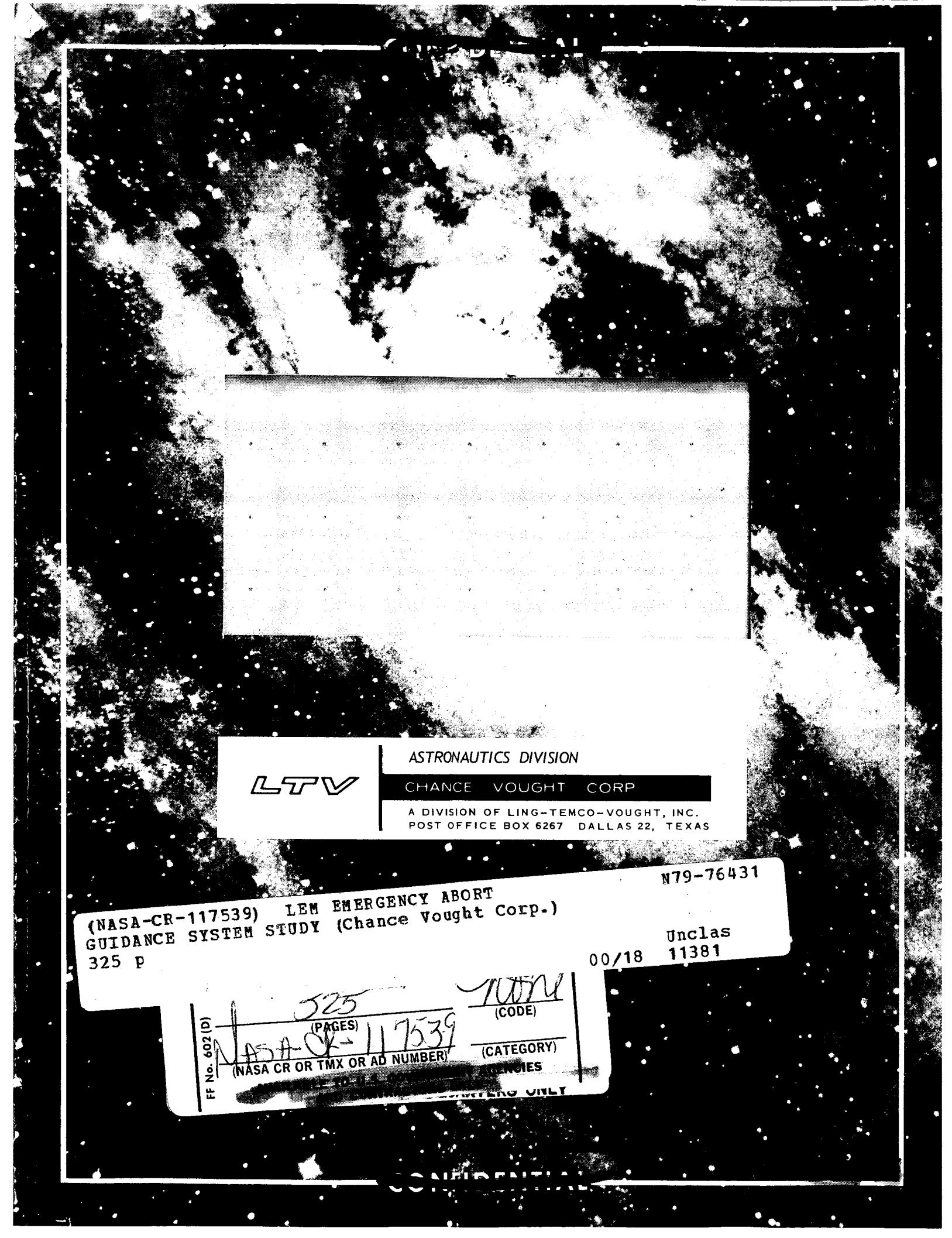

LTV

ASTRONAUTICS DIVISION

CHANCE VOUGHT CORP

A DIVISION OF LING-TEMCO-VOUGHT, INC.
POST OFFICE BOX 6267 DALLAS 22, TEXAS

~~CONFIDENTIAL~~

DOWNGRADED AT 3 YEAR INTERVALS
DECLASSIFIED AFTER 12 YEARS
DOD DIR 5200.10
4

ASTRONAUTICS DIVISION
CHANCE VOUGHT CORP.
A Division of Ling-Temco-Vought, Inc.
P. O. BOX 6267 • DALLAS 22, TEXAS

CLASSIFICATION CHANGE

To UNCLASSIFIED
By authority of GSFC E0 11652
Changed by L. Shirley Date 12/27/72
Classified Document Master Control Station, NASA
Scientific and Technical Information Facility

TITLE

LEM Emergency Abort Guidance System Study (U)

SUBMITTED UNDER

REPORT NO.	DATED
00.213	10 May 1963
PROJECT	CONTRACT NO.
	NAS 9-1051

THIS MATERIAL CONTAINS INFORMATION AFFECTING THE NATIONAL DEFENSE OF THE UNITED STATES WITHIN THE MEANING OF THE ESPIONAGE LAWS, TITLE 18, U. S. C., SECTIONS 793 AND 794. THE TRANSMISSION OR REVELATION OF WHICH IN ANY MANNER TO AN UNAUTHORIZED PERSON IS PROHIBITED BY LAW.

A. D. Schaefer
PREPARED

REVIEWED

F. S. Gaucher
APPROVED

REV.	DATE	REV. BY	PAGES AFFECTED	REMARKS

AVAIL...

~~CONFIDENTIAL~~

TITLE OF REPORT

LEM Emergency Abort Guidance System Study

ORIGINATING AGENCY AND LOCATION
Astronautics Division
Chance Vought Corp.
Post Office Box 6267
Dallas 22, Texas

CLASSIFICATION		
REPORT	ABSTRACT	TITLE
Conf.		Unclas.

AUTHORS
A. D. Schaezler

ISSUE DATE
10 May 1963

LIMITATIONS ON DISTRIBUTION (IF ANY)

ORIGINATING AGENCY'S REPORT NO.

DOD REFERENCES			OTHER IDENTIFYING REPORT NOS.
CONTRACT NO.	PROJECT NO.	TASK NO.	
NAS9-1051			

INDEXING

A. SUMMARY SENTENCE(S):

B. KEY WORDS:

WEAPON SYSTEMS NUMBERS, MODEL NUMBERS, ETC.

ABSTRACT

An analytical and simulation study has been conducted to determine LEM back-up guidance requirements in the event of failure of the primary guidance system during the powered descent. Three intercept techniques were investigated using different procedures and displays. A midcourse correction capability is necessary for close approach to the target. Attitude information and some "radar type" data are display requirements for successful intercept. A vertical velocity display during launch greatly reduces the possibility of an unsafe orbit. The required launch engine ideal velocity capability is approximately 7000 ft/sec.

Summary

An analytical and simulation study has been conducted to determine LEM back-up guidance requirements in the event of failure of the primary guidance system after initiation of the powered descent. The requirement for abort capability at any time during the powered descent results in a large range of initial conditions. The midcourse coast trajectory is different for each abort time unless a hover phase or an orbital park phase is used to standardize initial conditions for the midcourse portion. Many combinations of intercept methods and displays are possible. Three intercept techniques were investigated in this program, using different procedures and displays. A midcourse correction capability is necessary to ensure that the closest approach of the intercept trajectory to the target is even within a few miles.

Attitude displays are required for all three of the techniques investigated. The use of vertical velocity and altitude displays during launch greatly reduces the possibility of launching into a trajectory with pericynthion below the surface. These displays also permit manual launch control techniques that are easily learned and definitely preferred by pilots. Launch control under abort conditions by open loop pitch program procedures is difficult for pilots to learn, and is subject to large inaccuracies when mistakes are made. Procedures can be developed such that only attitude, time, and external vision cues are required for either launch or midcourse, but not for both. It is not probable that a successful

intercept technique can be established that requires no "radar type" information during all phases of the intercept.

The launch engine fuel requirement for the abort-intercept mission is equivalent to approximately 7000 ft/sec ideal velocity. Preliminary studies indicate that the display requirements can be mechanized for a weight of approximately 57 pounds, with a power requirement of about 259 watts.

TABLE OF CONTENTS

1.0 INTRODUCTION

The Apollo Project's manned lunar landing mission will utilize a Lunar Excursion Module (LEM) to perform the lunar landing. The LEM primary guidance system will provide basic guidance for interception of the Command-Service Modules (CSM) after launching from the lunar surface or after aborting the landing maneuver. It is necessary to have an alternate guidance scheme to enable safe return of the LEM crew to the CSM in the event of failure of the primary guidance system. The primary purpose of this study is to provide data that may be used to define back-up guidance requirements.

1.1 The objectives of this study are:

(1) To determine fundamental techniques for simplified back-up guidance for LEM abort and emergency launch due to failure of the primary guidance system.

(2) To evaluate these concepts by simulation.

1.2 The primary groundrules established for the study were:

(1) Circular Apollo orbit at 80 nautical miles altitude.

(2) Equi-period, elliptical orbit for LEM descent phase.

(3) No heading change during descent.

(4) The objective of the abort launch is to arrive at a rendezvous position. (Rendezvous and Docking Phase is not included.)

(5) Launch burnout altitude is 50,000 ft.

(6) Constant thrust launch engine.

(7) Manual control, minimum instrumentation.

(8) Rate command control system.

(9) Pericynthion of unpowered trajectories above lunar surface.

1.3 Study Procedure

This study consists of an analytical phase and a simulation phase. The analytical portion of the work includes the calculation of launch performance, pitch programs, and launch control parameter sensitivities, error analysis, the evolution of intercept techniques for launch and midcourse corrections, and a preliminary study of mechanization of guidance requirements. The simulation phase provides a means of testing the various guidance and control concepts, determining operational improvements, obtaining data on accuracy and fuel requirements, and getting pilot evaluation of several intercept techniques.

Figure 1-1 illustrates typical trajectories for a LEM landing and for aborted landings. The LEM departs from the CSM and injects into an equi-period orbit approximately 90^{o} from the landing site. Near pericynthion, the descent engine is ignited to begin the powered descent to the surface. Should the landing be aborted prior to the powered descent phase, the LEM may intercept the CSM by continuing to coast in the equi-period orbit to the point of injection (assuming an accurate injection into the equi-period orbit). Should an abort occur during the powered descent phase, the LEM must depart from the descent trajectory and launch to burnout

FIGURE 1-1
TYPICAL TRAJECTORIES

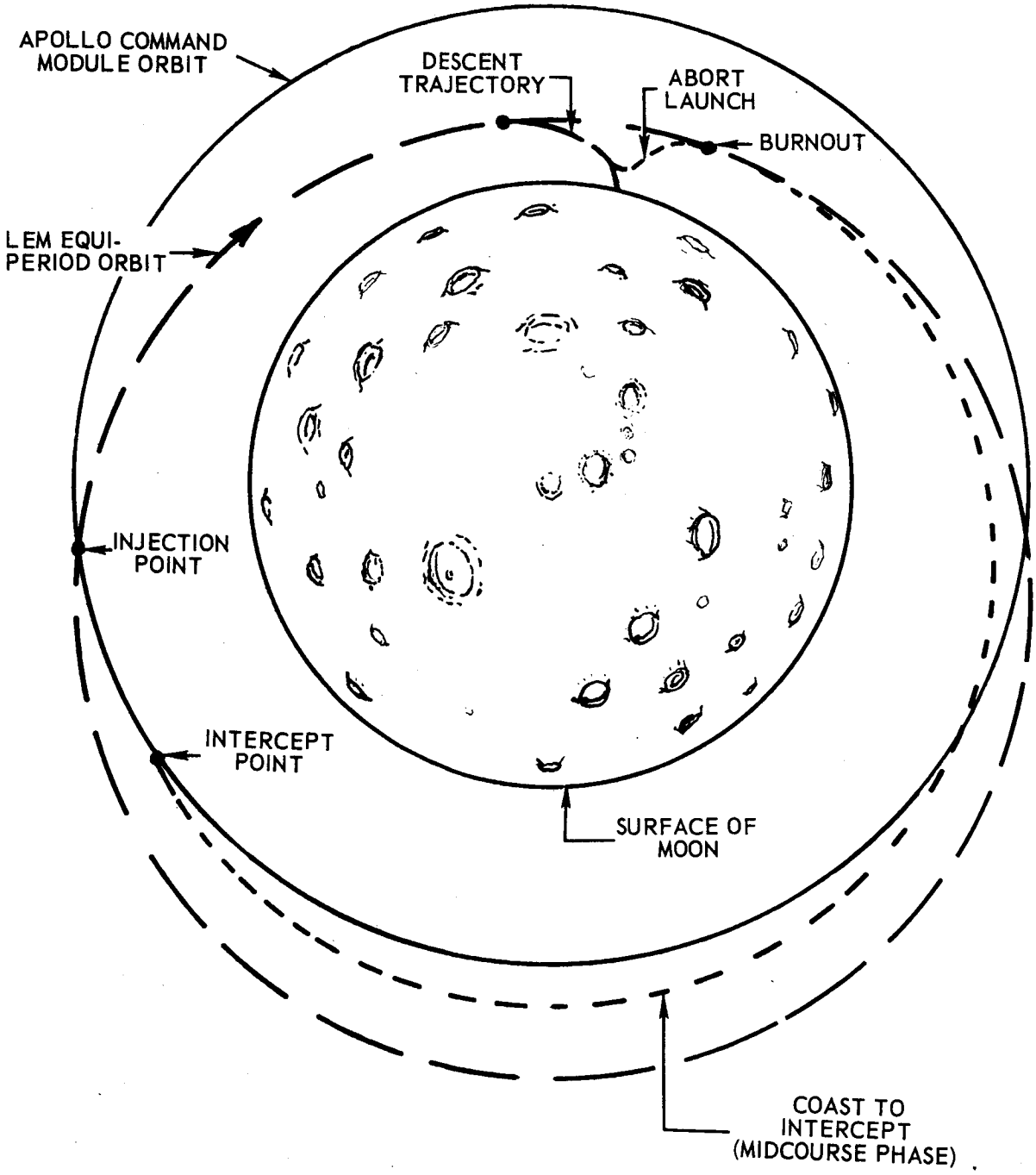

conditions from which an interception may be achieved. This study is concerned with the latter type of abort mission. Therefore, the earliest initial conditions of interest in this study are those that exist at the beginning of the powered descent. Guidance and control from initiation of abort to intercept generally involves:

(1) Descent engine use and staging.

(2) Boost with the launch engine

(3) Midcourse phase between initial boost burnout and intercept.

At the beginning of this study program, a particular abort launch technique was assumed in order to form a basis for the analytical portion of the study. This launch technique is described in section 2.1.1, and is very similar to one of the techniques investigated during the simulation. As the analytical work progressed, other intercept methods became apparent. Three basic intercept techniques were investigated with the simulator that included quite different methods for controlling the above three phases of the intercept mission.

2.0 DISCUSSION

2.1 Analytical Program

2.1.1 Abort Launch

The path of the LEM to the surface of the moon from circular orbit at an altitude of 80 nautical miles is divided into several phases, each of which is characterized by certain vehicle maneuvers. First, separation and retro maneuvers place the LEM in a coasting phase along an elliptical orbit which has a period equal to that of the original circular orbit and pericynthion at an altitude of 50,000 feet. At pericynthion, a braking phase is initiated. The braking maneuver, which serves to reduce velocity and altitude, is accomplished with constant thrust propulsion along an optimal path to a horizontal velocity of approximately 50 ft/sec at an altitude of 6,000 feet. A typical braking trajectory which is the one used for reference in this study, is presented in Table 2.1.1-I. Flare, translation, hover, and landing phases of flight follow the termination of braking.

Failure of the LEM primary guidance system during the descent coasting phase is non-critical because the vehicle orbit is a natural abort path for rendezvous with the CSM, requiring only minor midcourse and terminal adjustments. Guidance failure again becomes non-critical during the post-braking phases of flight, for then - even nominally - the flight path is controlled by the pilot who requires only his vision and simple sensor information to effect a landing. It is assumed that accurate flight path control during the braking phase is dependent upon the primary

TABLE 2.1.1-I

NOMINAL DESCENT TRAJECTORY

$(T/W)_0 = .4$ Isp = 315 Secs

Time Secs.	T/W	Thrust Angle Deg.	Range Deg.	Velocity Fps	Altitude Ft.	Flt. Path Angle Deg.
0	.400	179.13	0	5673.67	50,000	0
13	.407	178.819	.721	5500.32	50,017	.057
44.9	.424	177.969	2.4	5072.56	50,246.8	.065
77	.443	176.98	3.95	4626.47	50,207.2	- .134
93	.453	176.43	4.68	4396.24	49,927.8	- .320
109	.464	175.85	5.36	4161.04	49,403.2	- .570
125	.475	175.21	6.00	3920.7	48,587.5	- .889
141	.487	174.589	6.61	3675.07	47,442.5	- 1.285
157	.499	173.91	7.19	3423.96	45,937.7	- 1.769
173	.513	173.18	7.70	3167.18	44,052.5	- 2.352
189	.526	172.42	8.18	2904.5	41,774.5	- 3.053
205	.541	171.619	8.64	2635.76	39,101.8	- 3.898
221	.556	170.78	9.02	2360.71	36,043.9	- 4.921
237	.572	169.9	9.38	2079.17	32,622.6	- 6.198
253	.590	168.979	9.69	1791.0	28,873.1	- 7.817
269	.607	168.009	9.44	1496.23	24,845.5	- 9.972
285	.627	168.999	10.16	1195.3	20,605.8	-13.049
301	.647	165.93	10.30	889.8	16,237.7	-17.999
321	.675	164.55	10.45	512.89	10,757.2	-31.899
331	.690	163.82	10.48	346.37	8,079.8	-49.639
339	.701	163.22	10.49	260.86	6,000	-78.389

guidance for safe landing. Therefore, for crew safety considerations, it is necessary to have the capability to abort during the braking phase.

The function of the back-up guidance is that of providing the pilot with the information required to place the LEM on a trajectory which begins at any time during braking and terminates at intercept with the CSM. The type of information provided will vary with the type of abort trajectory which is followed. However, all practical return trajectories will include a powered launch phase and a coasting phase.

The powered phase, or abort launch, is marked by several events. First, the descent motion is stopped. This is particularly important during the latter portion of braking where low altitude and comparatively large negative vertical velocity can bring the LEM dangerously near the lunar surface. After the vertical motion is stopped, the descent propulsion system may, or may not be staged, depending upon the particular guidance scheme which is adopted. During the remainder of the abort launch, the pilot follows a prescribed steering program and signals engine cut-off at the proper injection point on the coasting path.

There are countless types of abort trajectories within the framework of events described above. Among the most natural are those which are used as reference trajectories in this study. These are described as follows:

(1) During the first 150 seconds of braking, there is little altitude loss and a relatively small vertical velocity

component. If the primary guidance failure occurs in this time interval, the descent engine is shut down immediately and staged. The vehicle then coasts for 10 seconds while pitching to a prescribed initial attitude angle for abort launch. If abort occurs after 150 seconds of burning (and before flare initiation at 339 seconds), the LEM is brought to a vertical position in 5 seconds and accelerated upward for 15 seconds. The descent engine is then shut down and staged, and the vehicle coasts for 5 seconds while pitching to the initial abort launch attitude. The nominal changes in significant trajectory parameters which occur between time of abort decision and abort launch are depicted in Figure 2.1.1-1.

(2) Upon arrival at the proper launch attitude, the launch engine is ignited. The vehicle is pitched at a constant rate during burning and the engine is shut down after a prescribed burning time. Values for the initial attitude angle, the pitch rate, and the burning time, and the corresponding burnout velocity are dependent upon the time of abort decision. The relation of these launch parameters to abort decision time is depicted in Figures 2.1.1-2, 2.1.1-3, and 2.1.1-4.

The launch parameters are selected so that, nominally, the abort launch terminates at an altitude of 50,000 feet with zero flight path angle. The velocity at thrust cut-off is variable and is dependent upon the

FIGURE 2.1.1-1

CHANGE IN FLIGHT CONDITIONS BETWEEN INITIATION OF ABORT AND LAUNCH ENGINE IGNITION

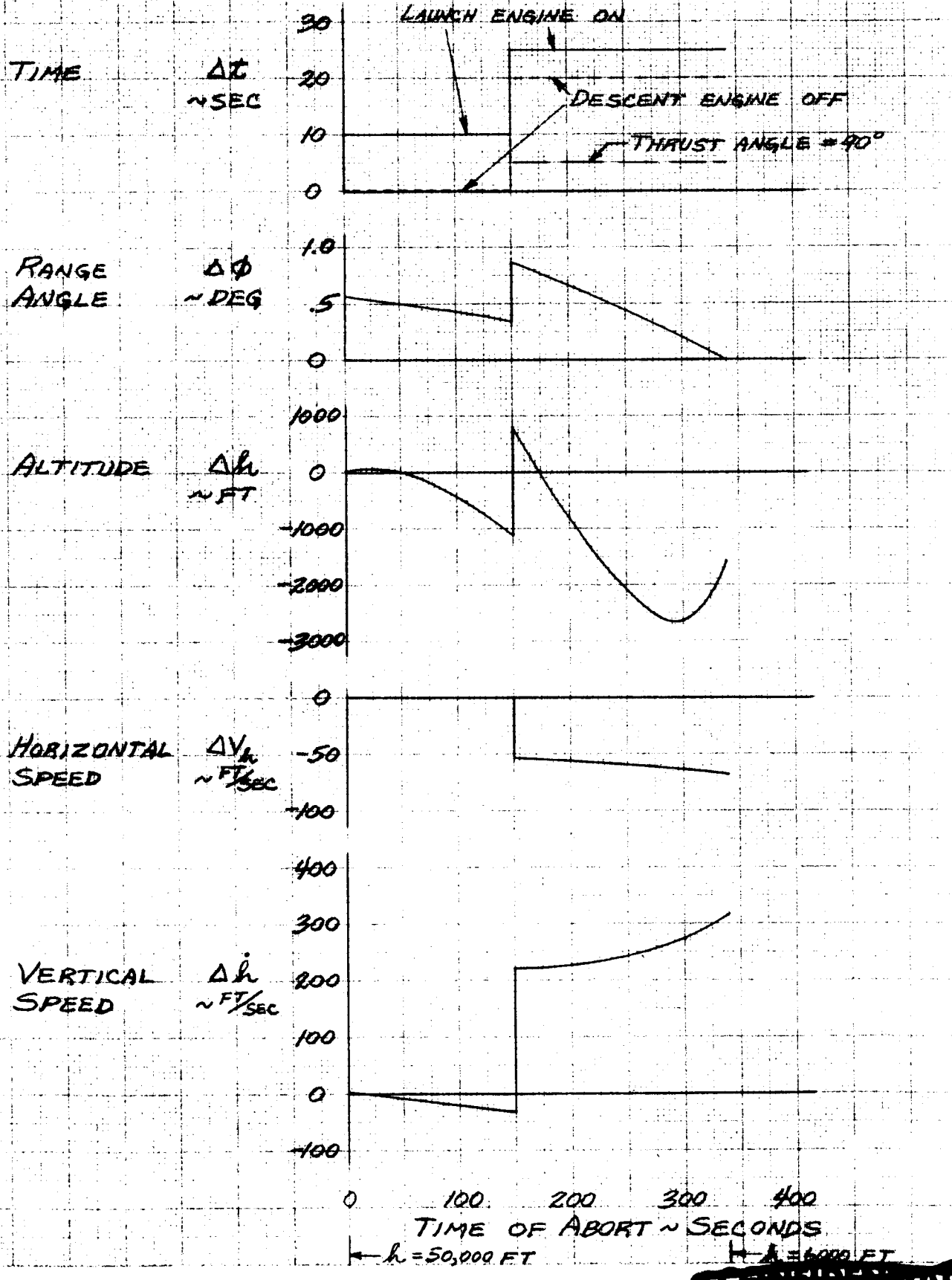

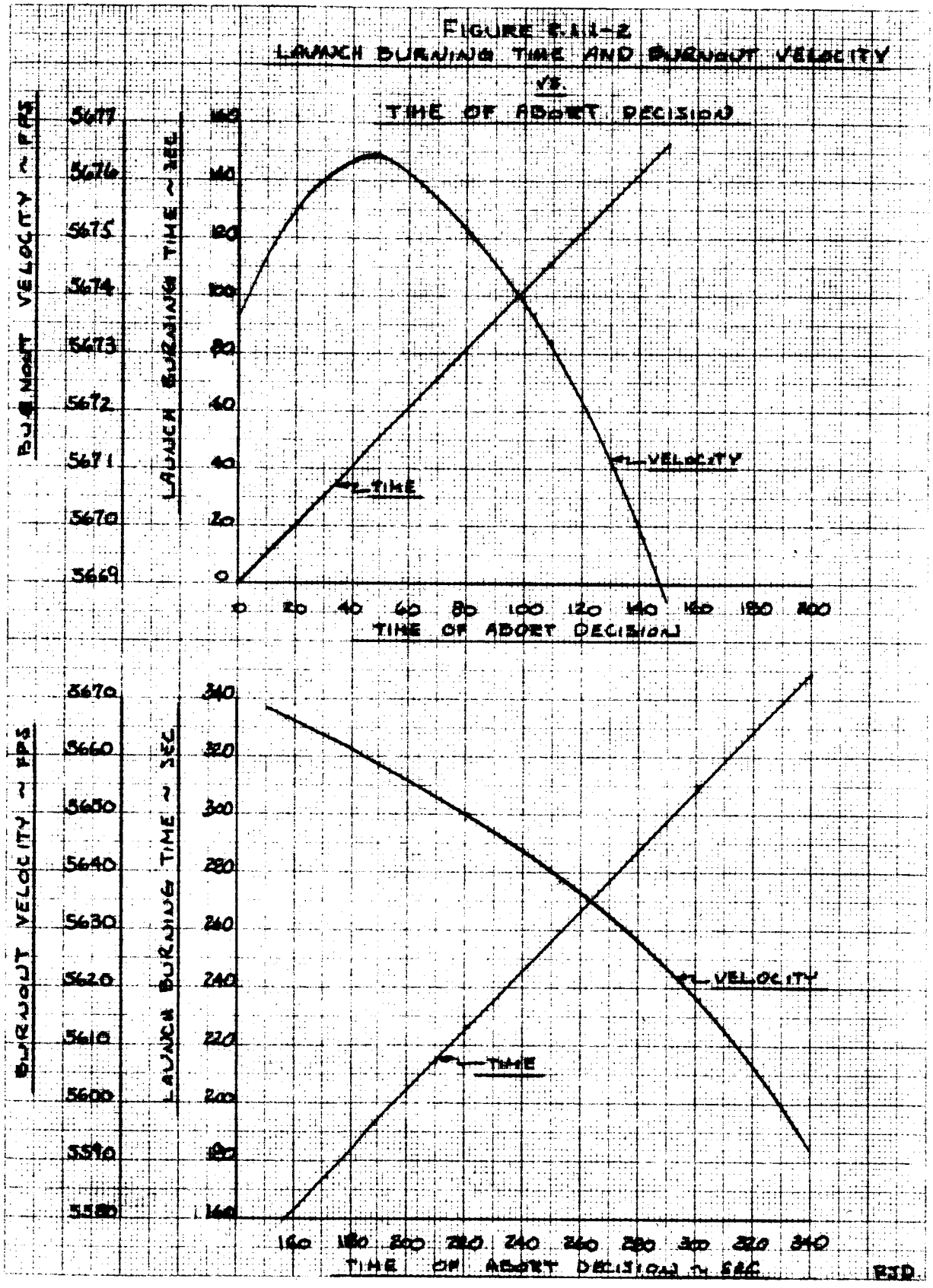

FIGURE 5.1.1-2
LAUNCH BURNING TIME AND BURNOUT VELOCITY
VS.
TIME OF ABORT DECISION

END

CONFIDENTIAL

FIGURE 2.1.1-3

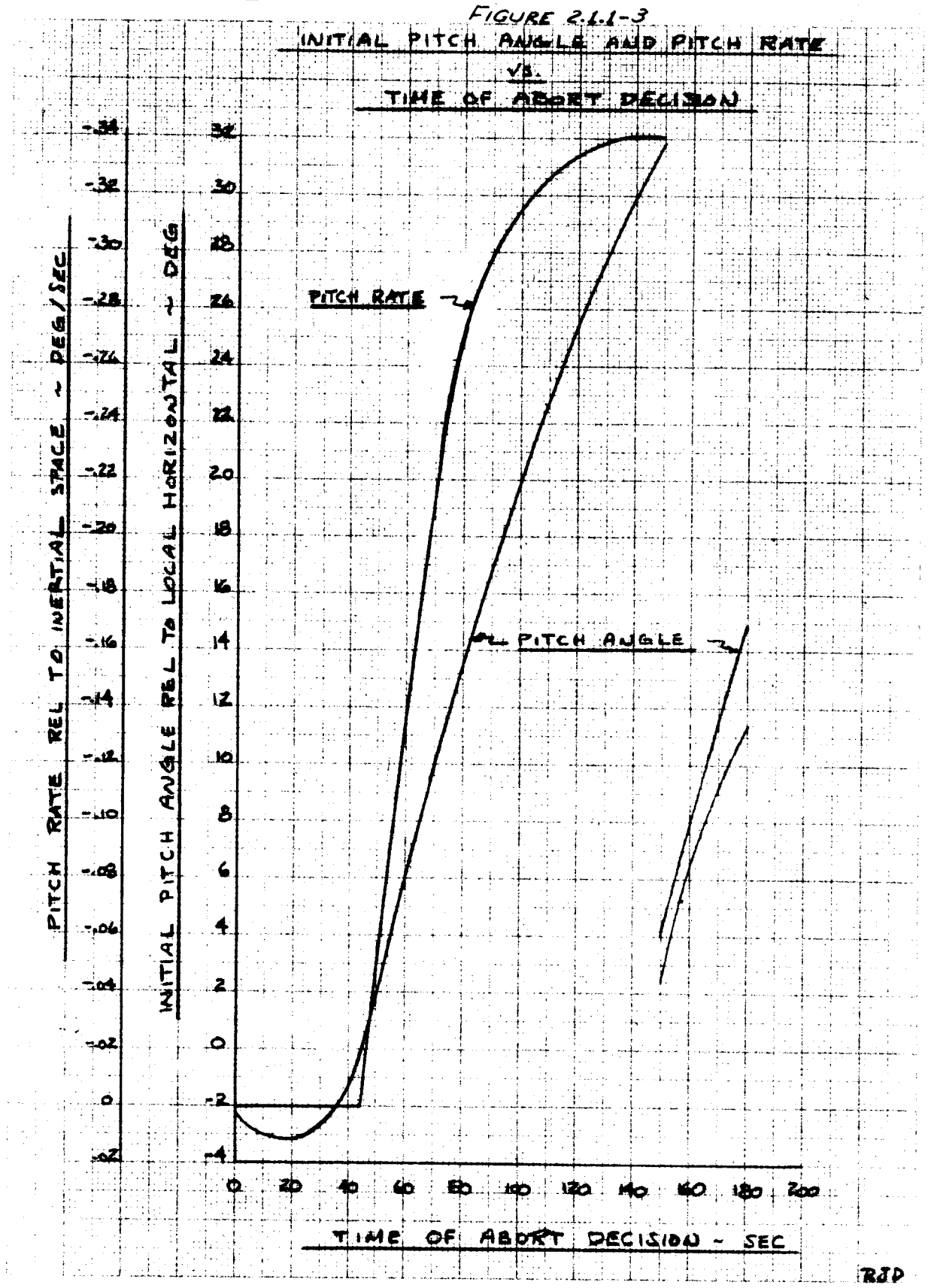

CONFIDENTIAL

CONFIDENTIAL

FIGURE 2.1.1-4

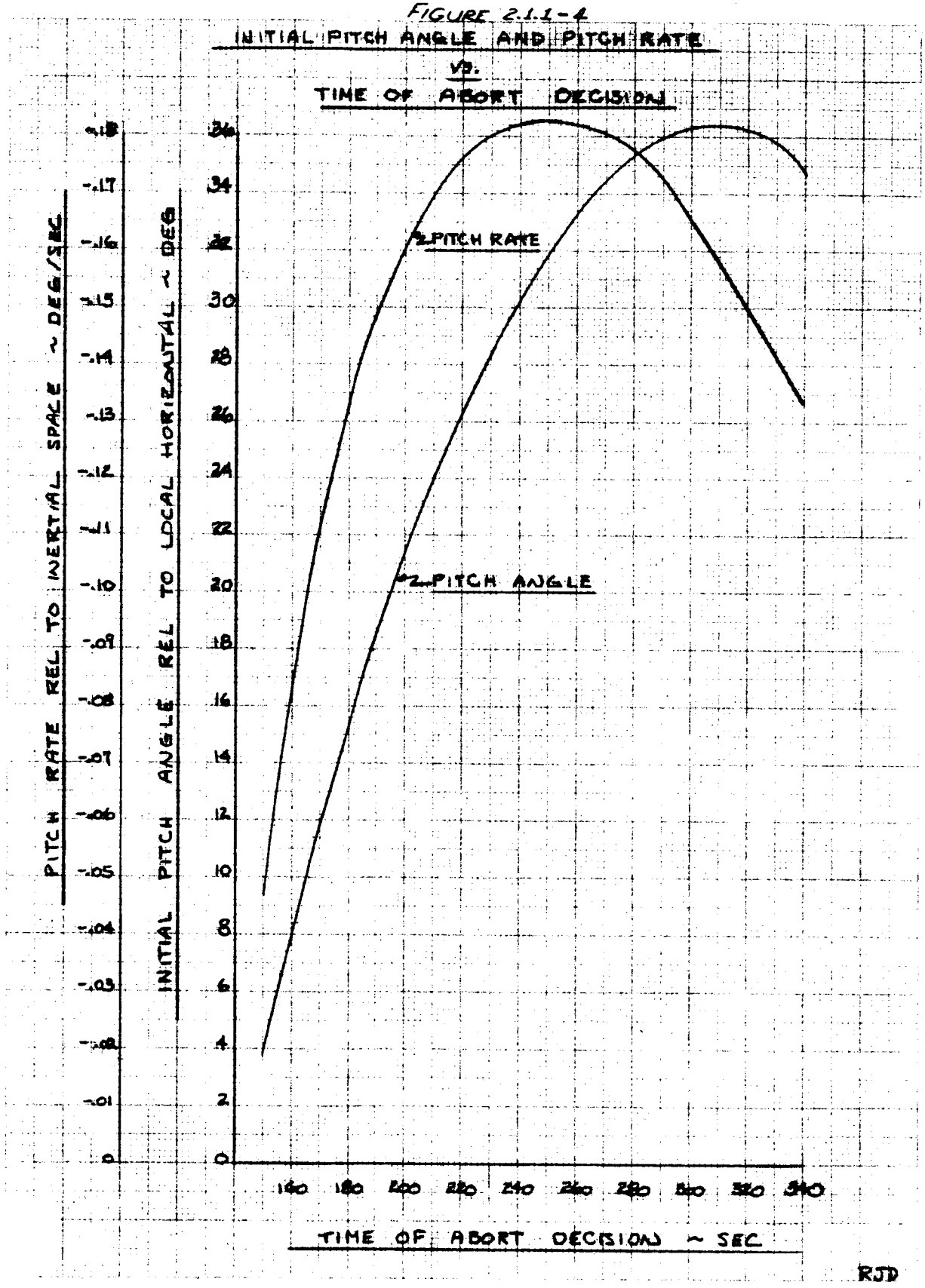

RJD

CONFIDENTIAL

lead angle, which is the angle included by the radii of the LEM and CSM. Given the lead angle at injection, the velocity can be determined so that the LEM and CSM arrive at a point in space simultaneously (i.e., intercept). For the reference trajectories described above, this point is the second intersection of the CSM circular orbit and an elliptical orbit which is the coasting path of the LEM after abort launch termination. The relation between lead angle and velocity at injection which results in intercept is illustrated in Figure 2.1.1-5.

After termination of braking, the LEM normally will be landed. Therefore, launch trajectories from ground to intercept are special cases which must be considered for back-up guidance analysis. The ground launch reference trajectory which was adopted for this study is described as follows:

The LEM is launched in a vertical position and accelerates upward for 10 seconds. The vehicle is then rapidly pitched in a plane parallel to the CSM orbit plane until it attains an attitude angle of 32.3 degrees and a pitch rate of -.132 degrees per second. The pitch rate remains constant during the remainder of powered flight which has a total duration of 351 seconds.

The nominal burnout (or injection) conditions associated with this reference trajectory are an altitude of 50,000 feet, a zero path angle, and a velocity of 5583 feet-per-second. These injection conditions describe a Hohmann transfer ellipse with an apocynthion at the CSM orbit

CONFIDENTIAL

FIGURE 2.1.1-5

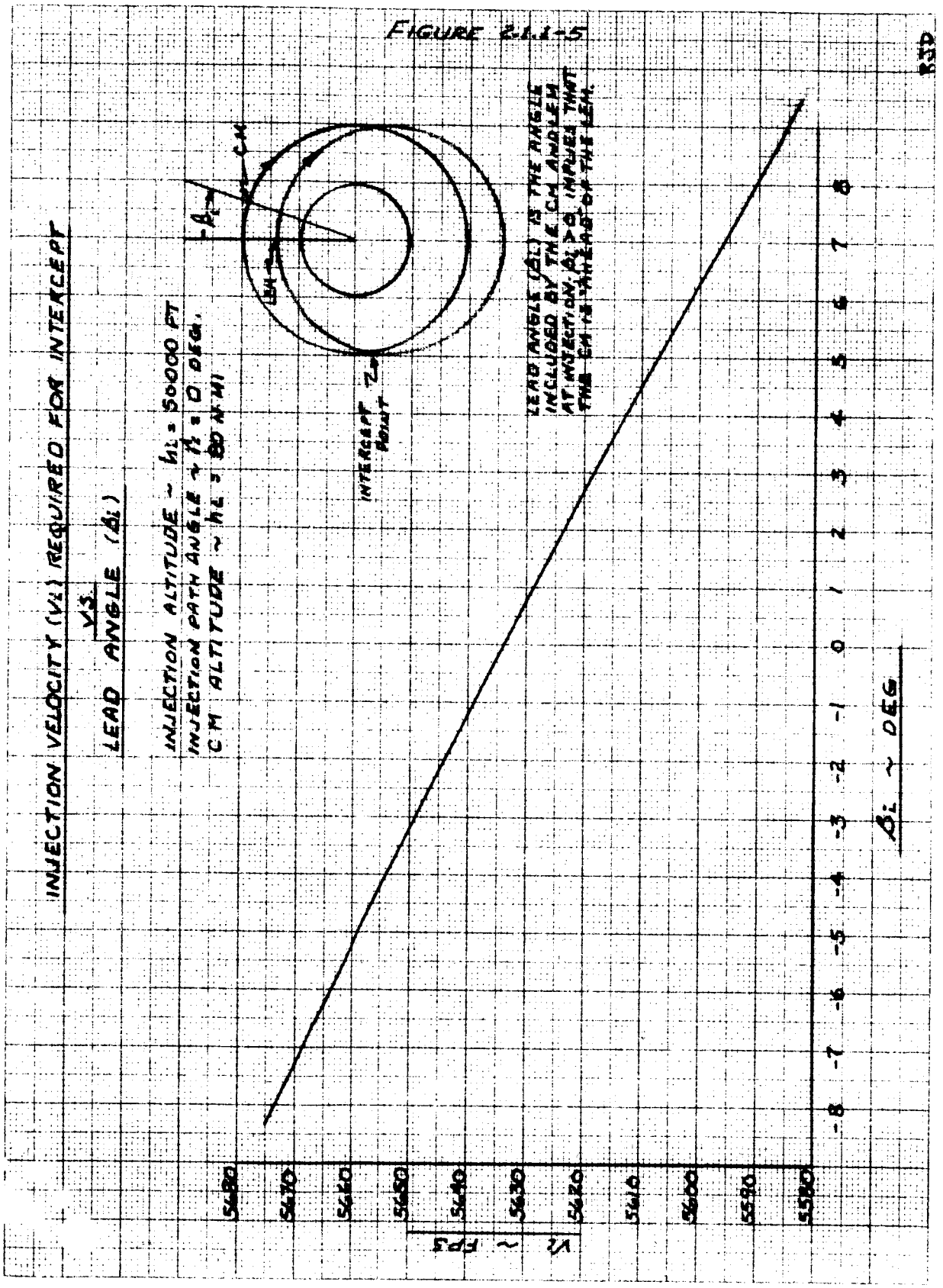

CONFIDENTIAL

altitude of 80 nautical miles. Coincident arrival of the CSM and LEM at the apocynthion point is dependent upon their relative angular position at time of launch. For this reference trajectory, the angle between the respective radii of the vehicles at launch, measured in the CSM orbit plane, is .54 degrees, with the CSM ahead.

The abort guidance scheme which is the most compatible with the reference trajectories adopted in this study is one which directly utilizes pitch attitude angle and angular rate information. If there are sensors aboard the LEM which determine and display in-flight values for these two control variables, the pilot theoretically can duplicate the computer calculated trajectories. He would note the time of abort decision; terminate descent motion according to procedures previously described; select from charts the proper initial attitude angle and attitude rate which are functions of abort decision time; null the differences between the prescribed and in-flight values of these parameters; and terminate the powered launch at a prescribed time also selected from charts.

This scheme is "open-loop" since time and body angular position determine the guidance maneuvers, rather than actual vehicle position and velocity in space. The accuracy of the injection coordinates, therefore, is dependent upon both initial condition errors and LEM system errors. Deviations from the nominal trajectory at abort launch essentially are uncontrollable by any open-loop guidance scheme, thus their effects on injection accuracy were not quantitatively analyzed in this section of the

study. Sensitivity of injection coordinates to system errors were calculated, however, in order to assess the value of the scheme and estimate tolerance bounds. The sensitivity data, in the form of partial derivatives, are presented in Figures 2.1.1-6 through 2.1.1-11.

2.1.2 Error Analysis

An analysis was made to evaluate the effects of errors in controlling the launch trajectory. Inaccuracies in launch control parameters such as pitch attitude, thrust, and burn time result in variations from nominal trajectory parameters at burnout. These errors in horizontal and vertical velocity and altitude result in failure to intercept (assuming no midcourse corrections), the distance at closest approach to the target being a function of the magnitude of the burnout errors.

The analysis is based on a launch technique that includes an immediate abort launch to burnout conditions that nominally result in a direct intercept trajectory with no hover phase or circular orbit phase. Attitude and thrust are controlled as a function of time only. This intercept technique is described in section 2.2.2.1. The nominal intercept trajectory varies with abort time because of the variation in lead angle at launch burnout. Digital computer routines used for calculating sensitivity parameters and miss distances are described in Appendix A and Appendix C.

CONFIDENTIAL

FIGURE 2.1.1-6

PARTIAL DERIVATIVES OF INJECTION COORDINATES WITH RESPECT TO INITIAL PITCH ANGLE

VS.

TIME OF ABORT DECISION

ϕ_L ~ INJECTION RANGE ANGLE
V_L ~ " VELOCITY
γ_L ~ " PATH ANGLE
h_L ~ " ALTITUDE

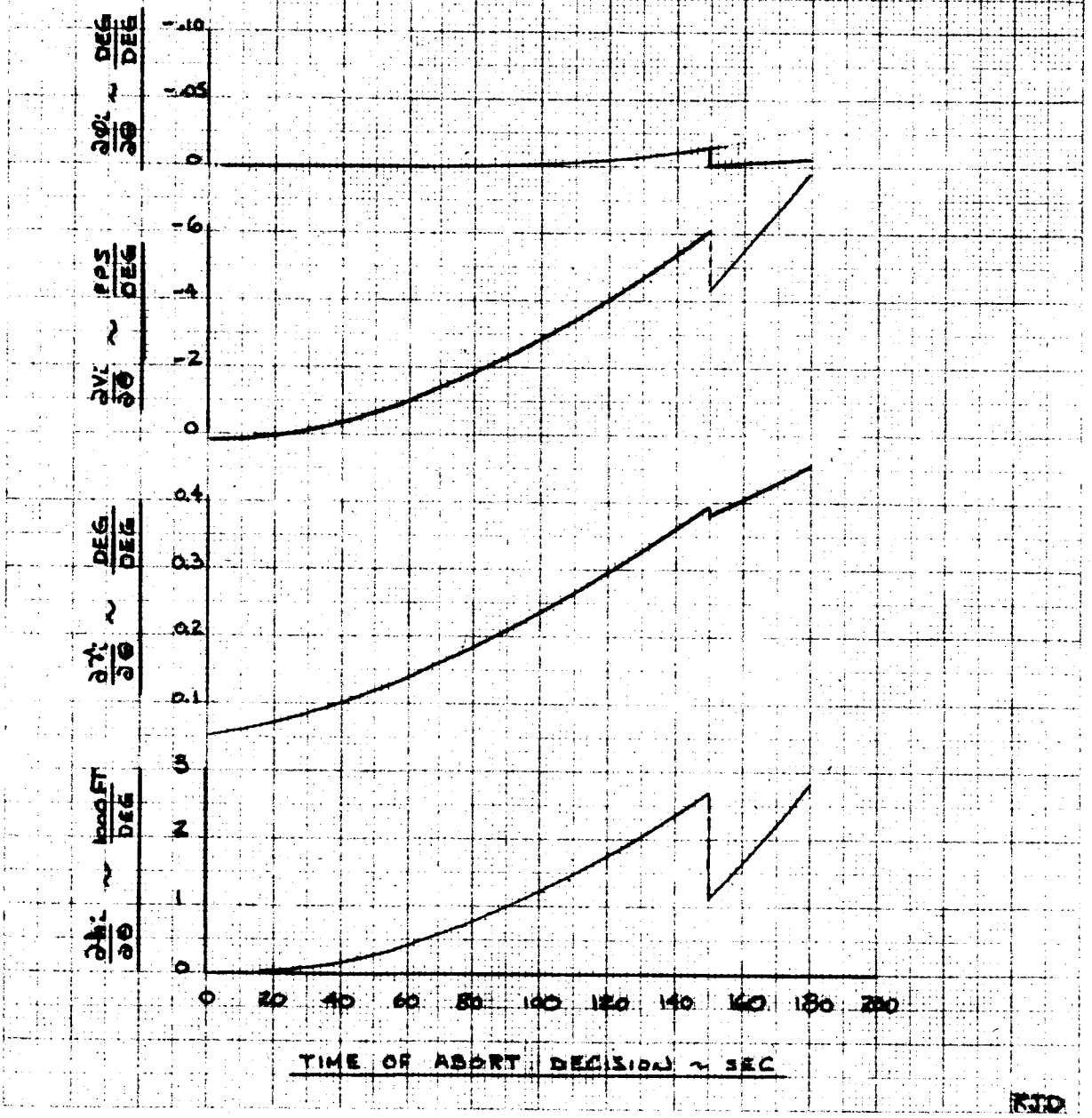

KJD

CONFIDENTIAL

CONFIDENTIAL

FIGURE 2.2.2-7
PARTIAL DERIVATIVES OF INJECTION COORDINATES WITH RESPECT TO INITIAL PITCH ANGLE
K2a
TIME OF ABORT DECISION

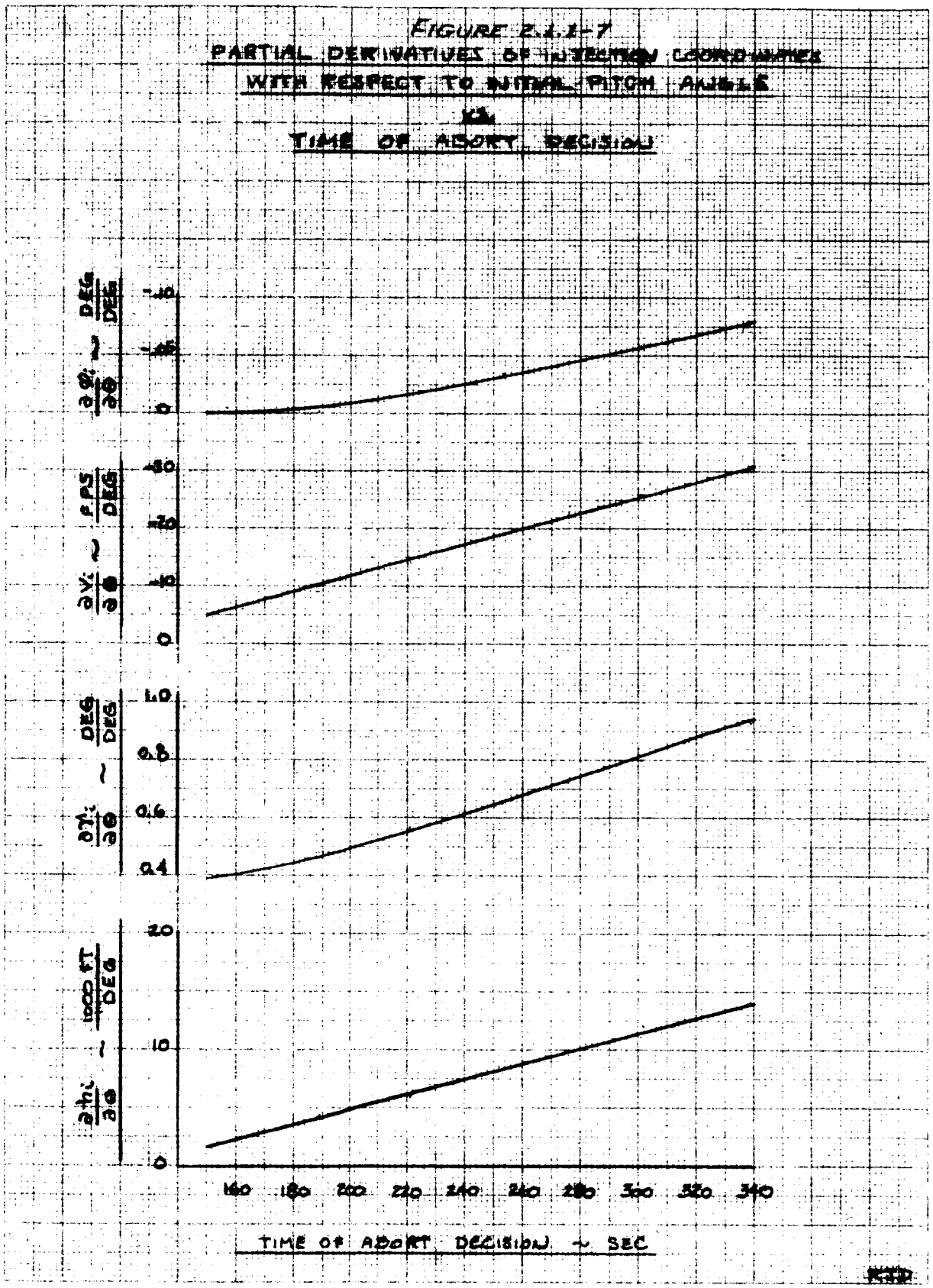

CONFIDENTIAL

CONFIDENTIAL

FIGURE 2.1.1-8
PARTIAL DERIVATIVES OF INJECTION COORDINATES WITH RESPECT TO PITCH RATE VS. TIME OF ABORT DECISION

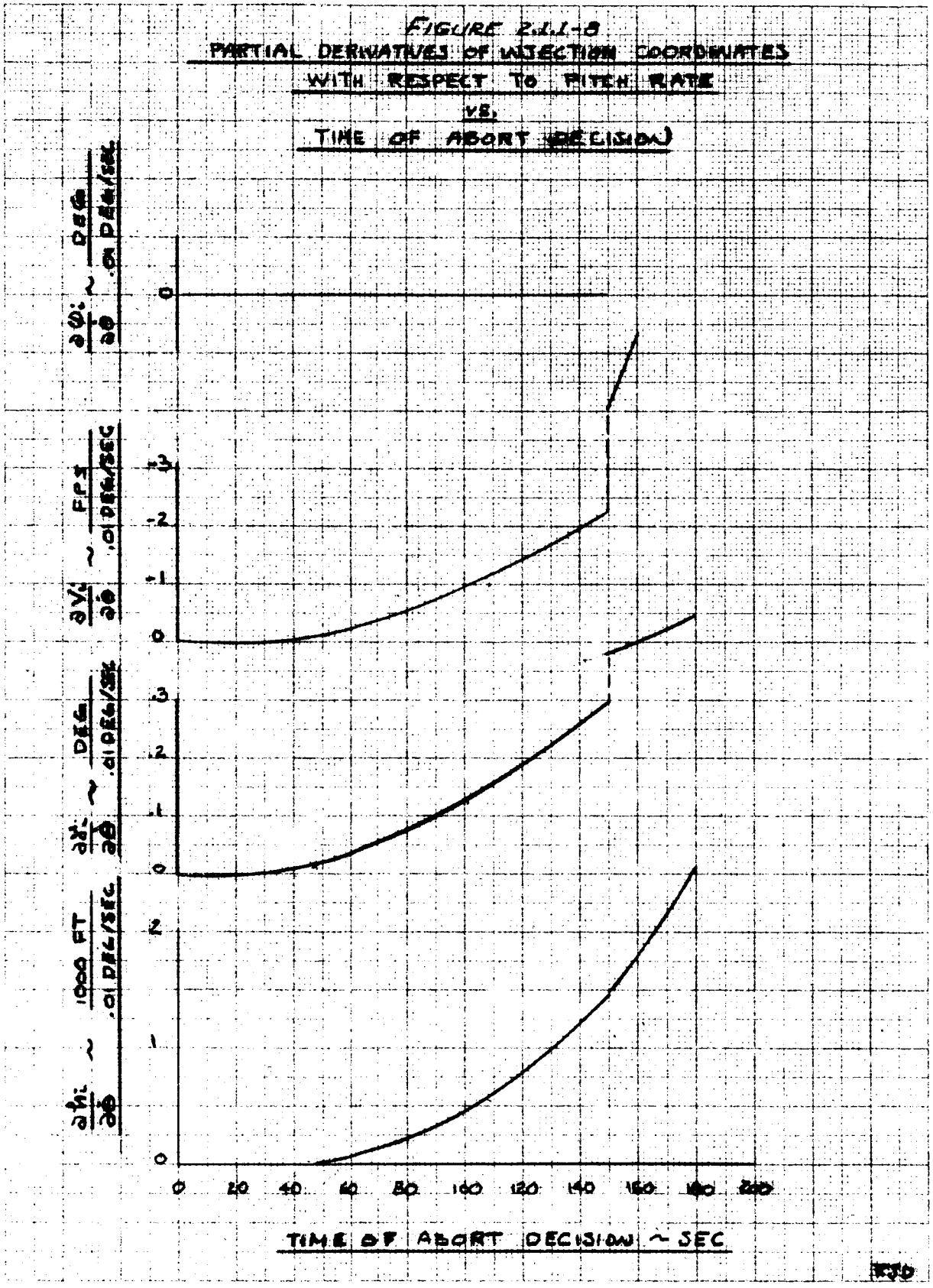

CONFIDENTIAL

FIGURE 2.11-9
PARTIAL DERIVATIVES OF INJECTION COORDINATES WITH RESPECT TO PITCH RATE VS. TIME OF ABORT DECISION

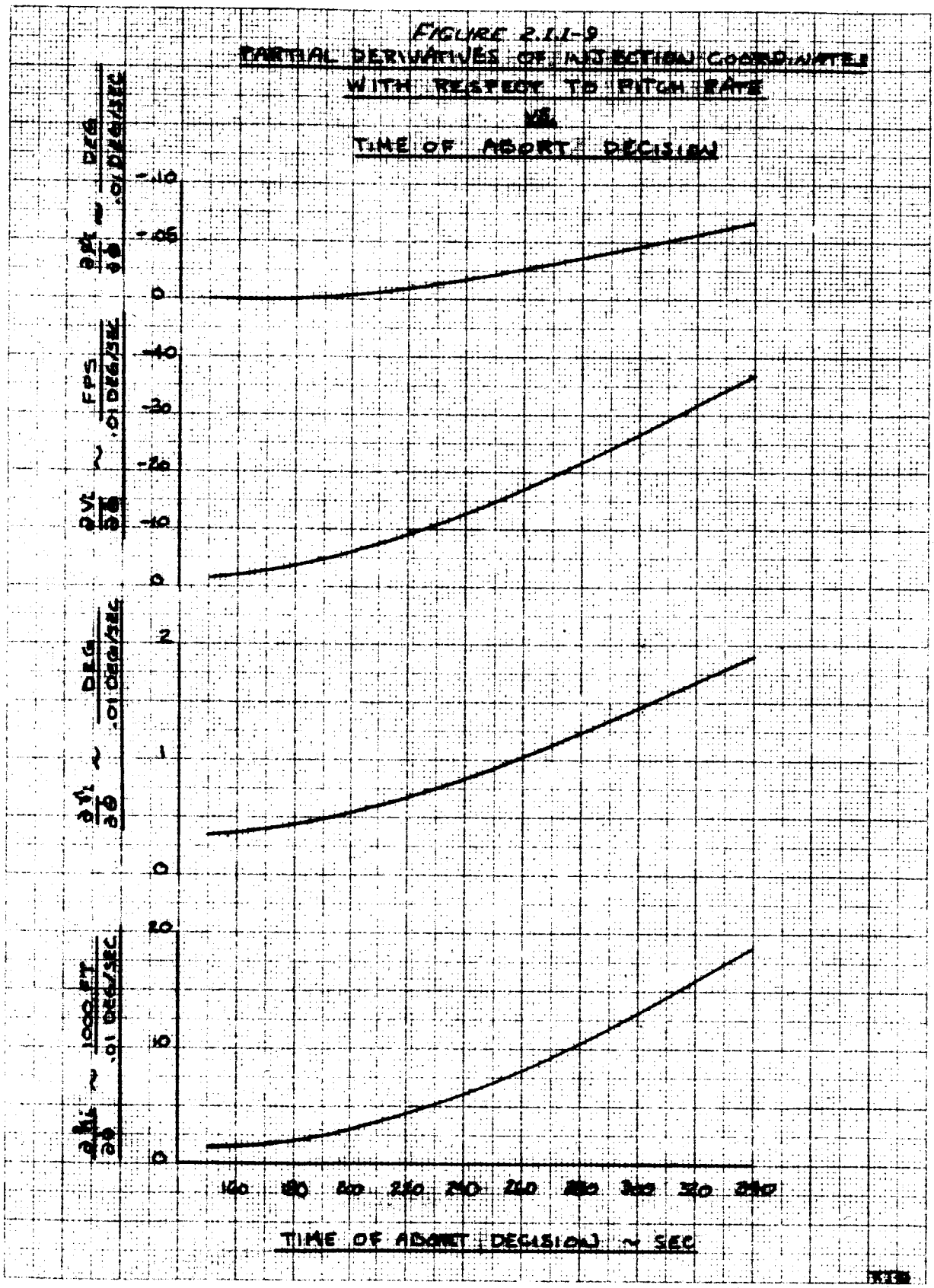

CONFIDENTIAL

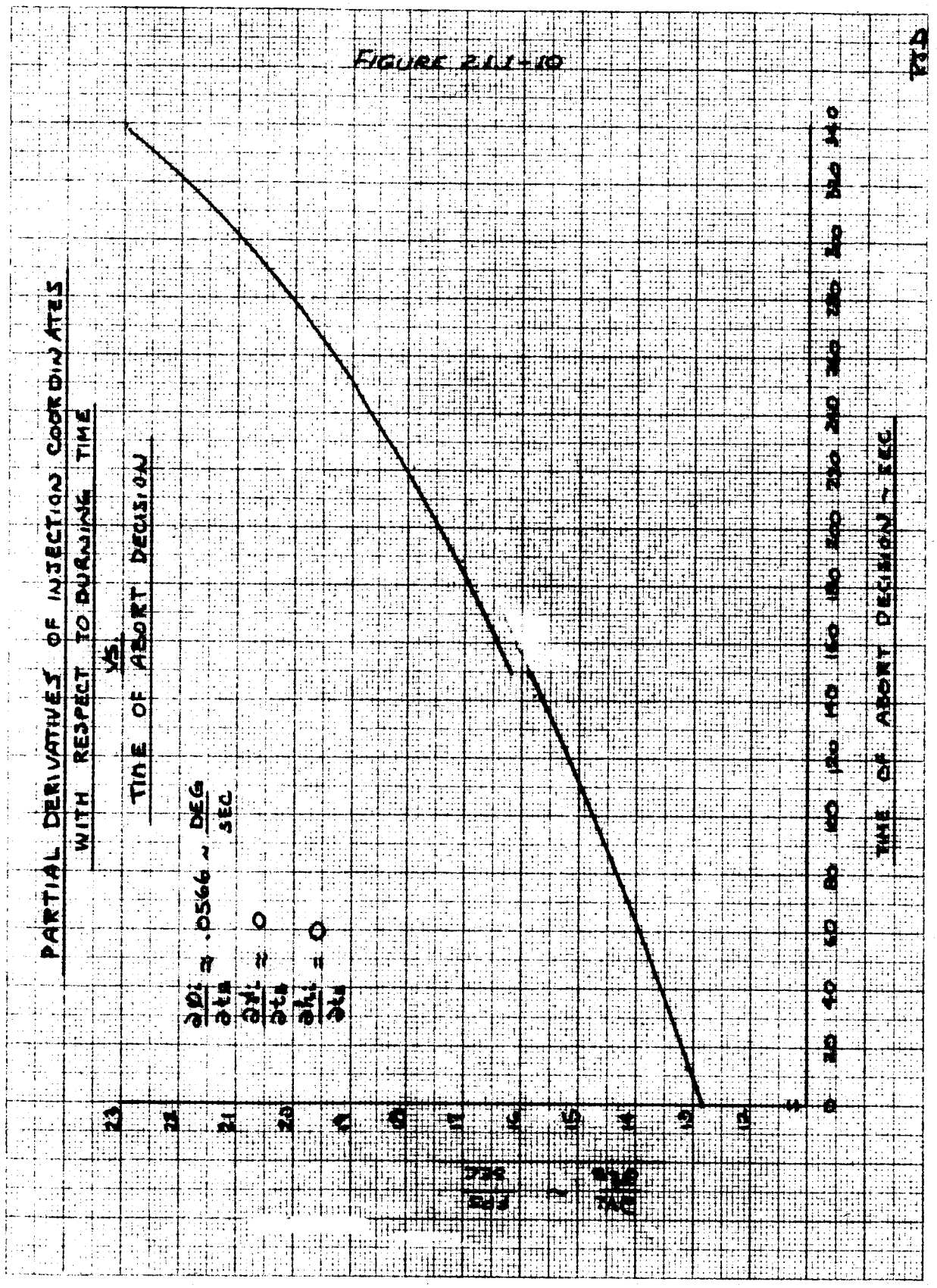

CONFIDENTIAL

FIGURE 2.1.1-11

PARTIAL DERIVATIVES OF INJECTION COORDINATES WITH RESPECT TO THRUST ERRORS VS. TIME OF ABORT DECISION

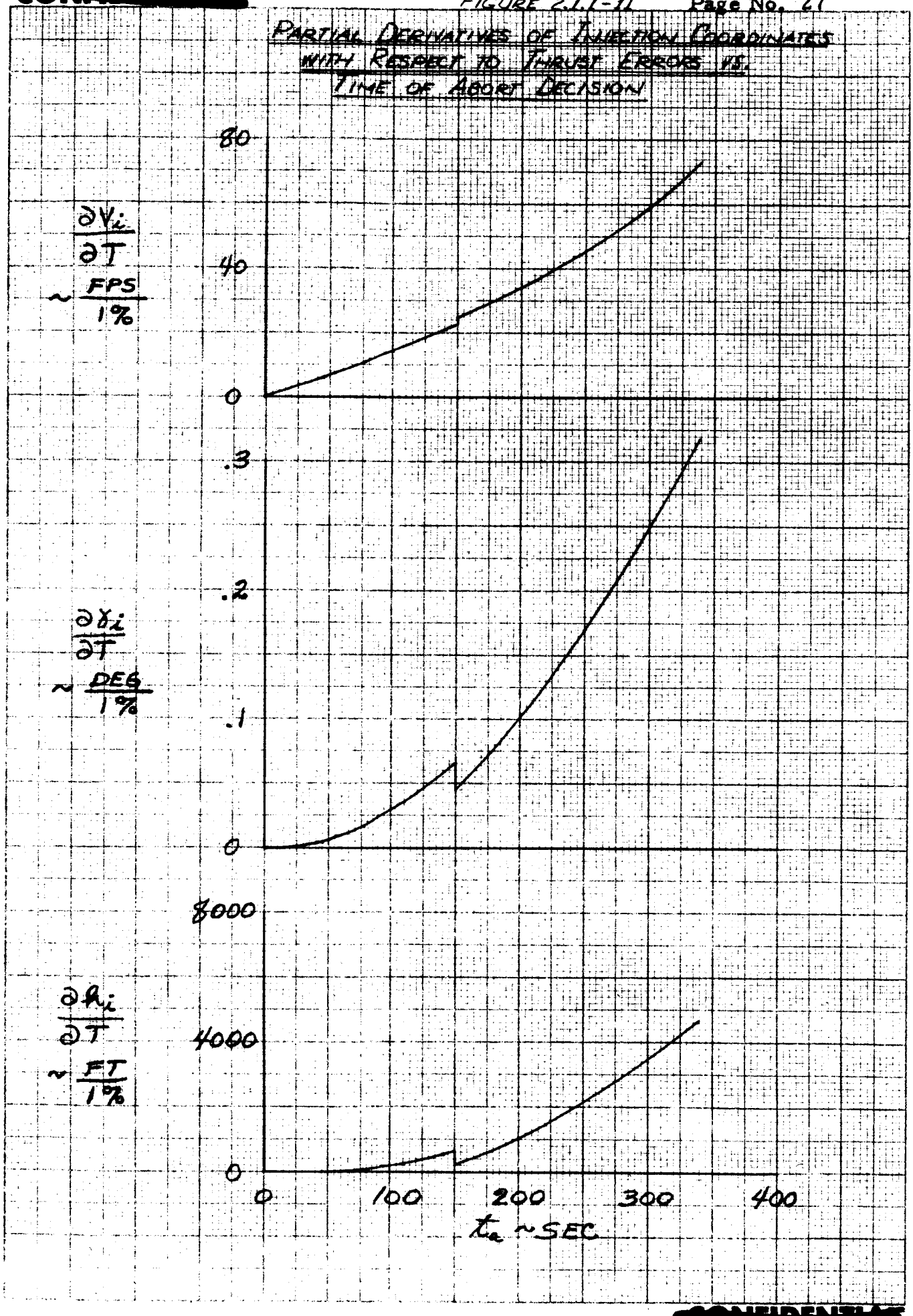

Assumed error sources used in the analysis are:

Error Source	Magnitude
Pitch attitude	1 degree
Launch engine thrust	1 per cent
Launch engine burn time	1 second

Effects of the error sources on burnout parameters are presented in Figure 2.1.2-1. Miss distances due to errors in nominal burnout conditions were calculated by varying the nominal conditions by the following increments:

$$\Delta V_i = 10 \text{ ft/sec.}$$
$$\Delta h_i = 10{,}000 \text{ ft.}$$
$$\Delta \gamma_i = .1^o$$

The resulting error sensitivities are shown in Figure 2.1.2-2. Miss distance due to an assumed error source can be calculated by summing the products of burnout errors due to the error source and the appropriate sensitivity parameters. Miss distance increments calculated in this manner are presented in Figure 2.1.2-3. It was not necessary to derive a technique for combining complex combinations of errors. For each combination of abort launch and error source, miss distance due to one of the burnout errors often predominated over the other two (the effect of horizontal velocity error usually being considerably larger than the effects of flight path angle and altitude errors). An approximate evaluation can be obtained by considering only the largest miss distance contribution.

FIGURE 2.1.2-1

LAUNCH INJECTION ERRORS

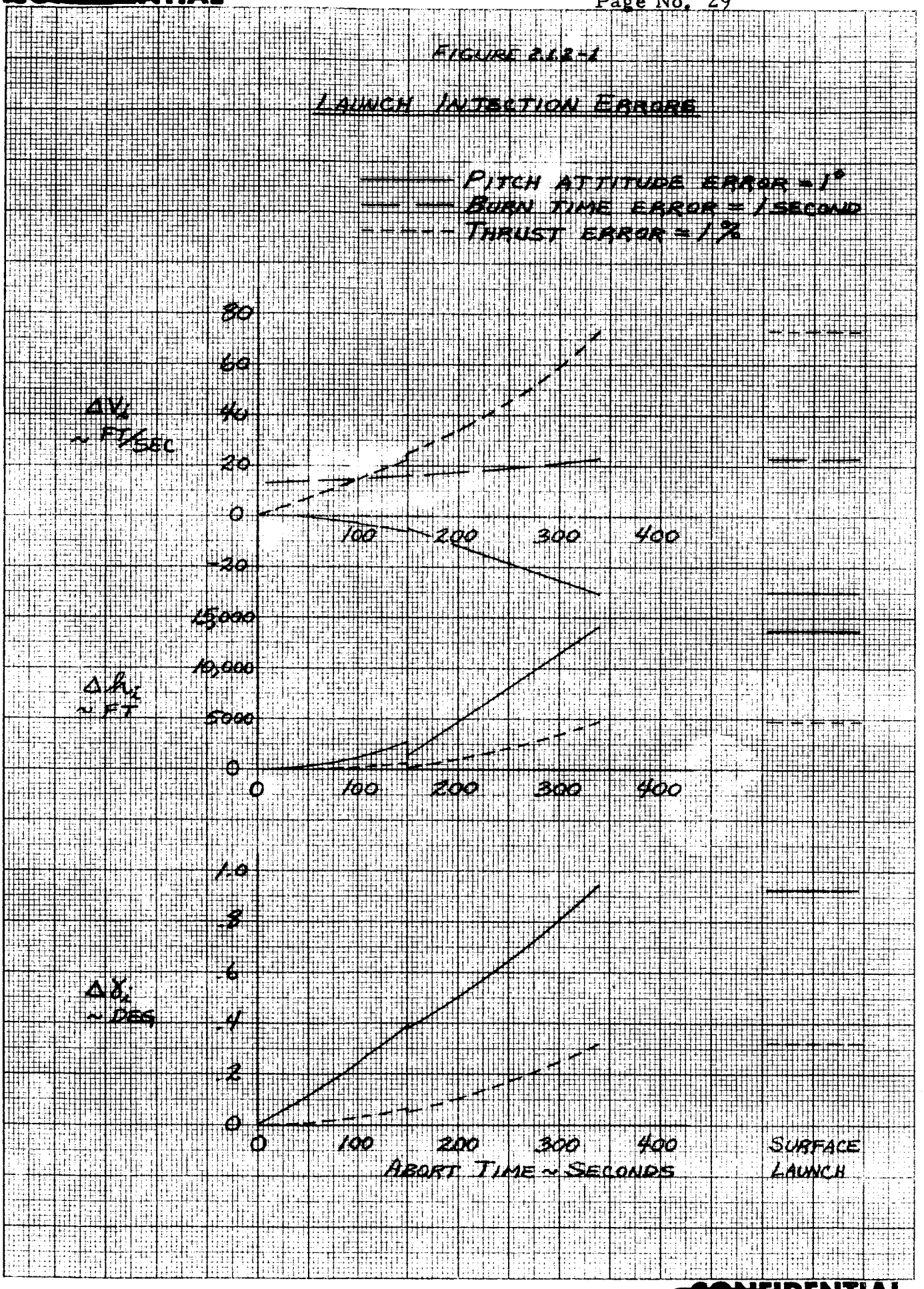

FIGURE 2.1.2-2

INJECTION ERROR SENSITIVITIES

ASSUMED INJECTION ERRORS: ——— $\Delta V_i = 10$ FPS
—— — $\Delta h_i = 10{,}000$ FT
– – – – $\Delta \delta_i = .1$ DEG

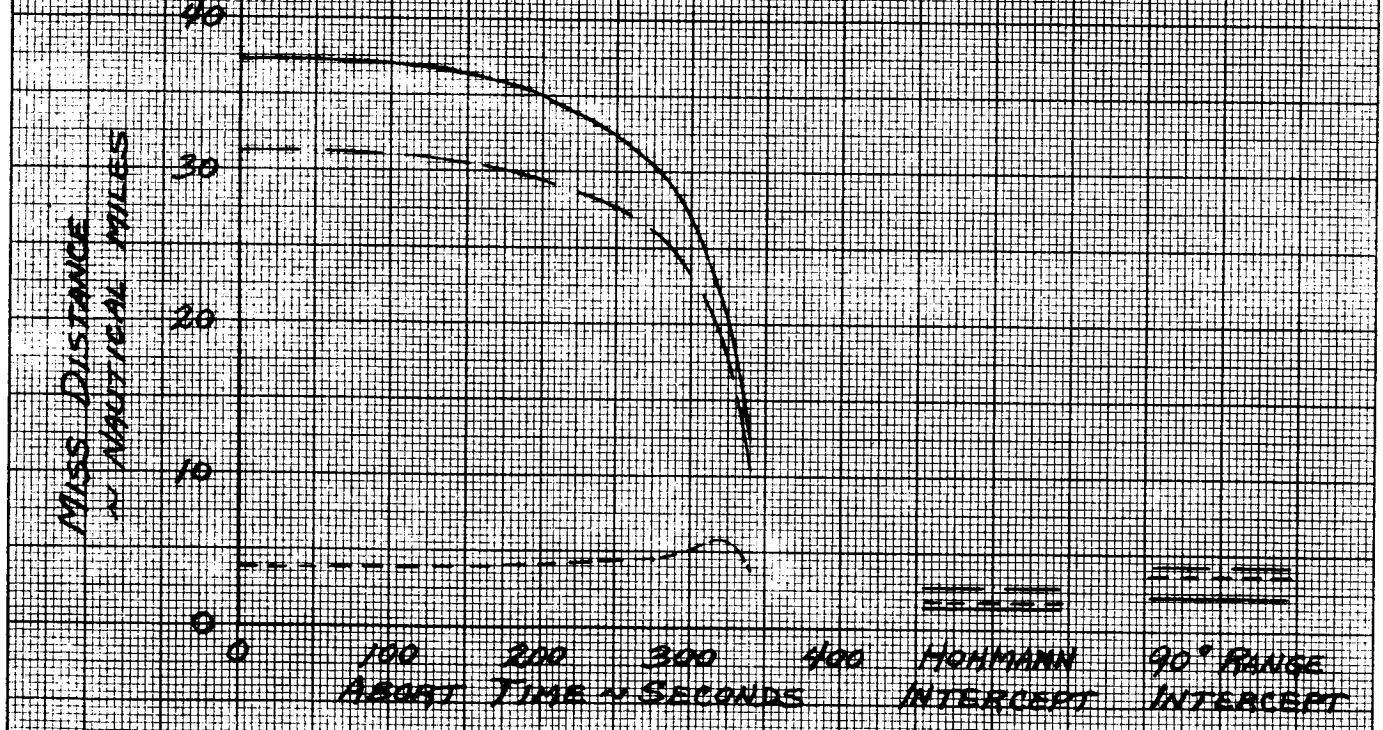

FIGURE E.1.6-3
INCREMENTAL MISS DISTANCES

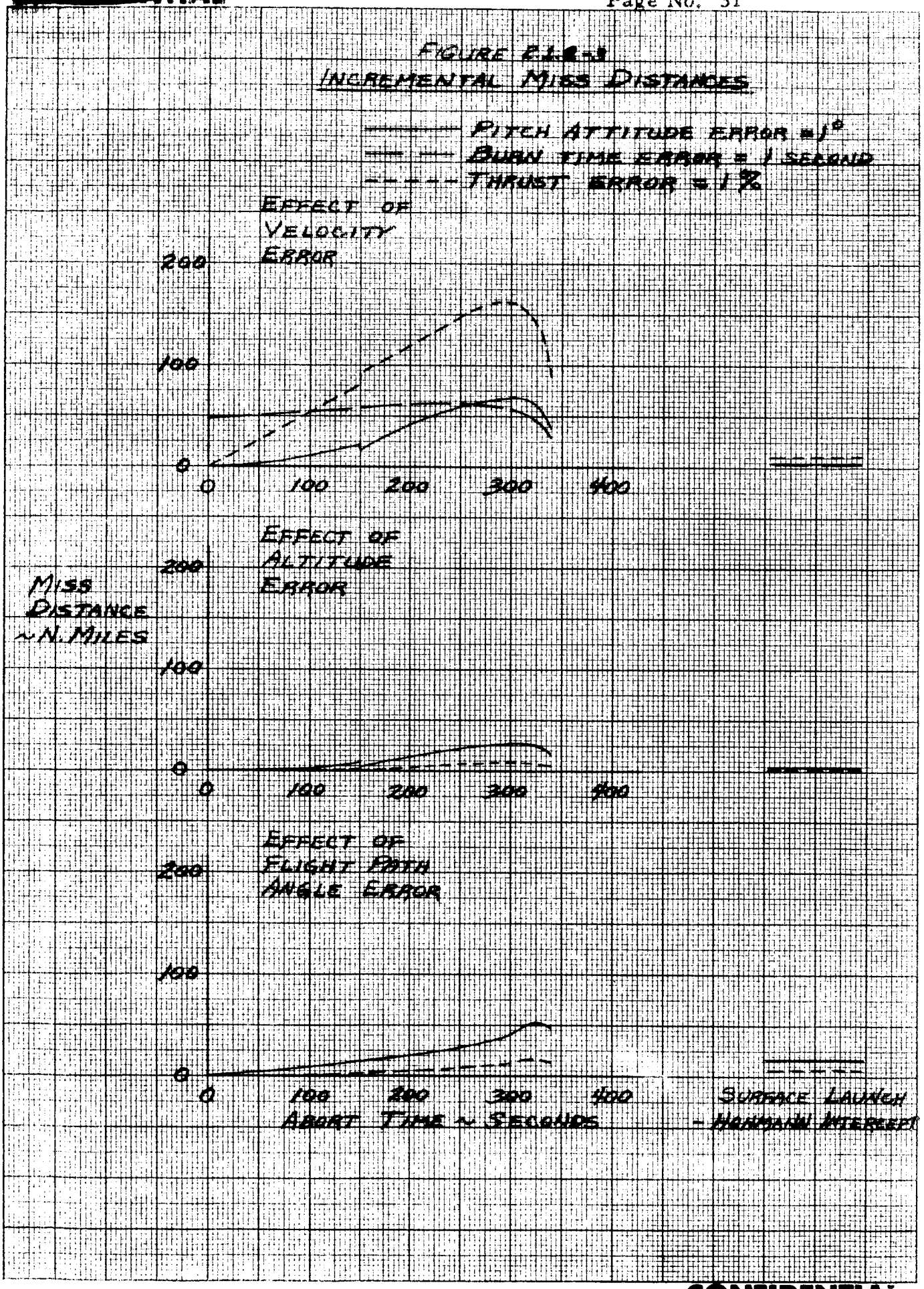

It was found that miss distances due to errors in burnout conditions are very non-linear; therefore, miss distances calculated in the above manner were inaccurate when the burnout errors used were large compared to the magnitude of burnout errors used to determine the miss distance sensitivity parameters (Figure 2.1.2-2), which is generally the case with this intercept technique. Several special computer calculations were made with representative burnout errors in order to obtain additional information concerning miss distances due to the larger burnout errors. These runs indicated a miss distance upper limit of about 70 nautical miles, or approximately the maximum altitude difference between the two orbits. In other words, for large burnout errors, the point of closest approach occurred when the LEM and the CSM were colinear with the center of the moon, and the colinear condition occurred near pericynthion of the LEM. However, since only a few special cases were investigated, it is only possible to note the trend rather than draw general conclusions concerning this upper limit. Table 2.1.2-I provides a comparison of miss distances calculated from the sensitivity parameters and miss distances computed for

TABLE 2.1.2-I

EVALUATION OF MISS DISTANCES

BASED ON SENSITIVITY PARAMETERS

Launch Trajectory	Error Source	Predominate Error Based on Sensitivity Parameters		Actual Run	
		B.O. Error	Miss Dist. N. Miles	B.O. Error	Miss Dist. N. Mi.
Abort Time of 4 minutes 36 seconds	ΔT = 1%	ΔV = 52 ft/sec	157.5	ΔV = 52 ft/sec $\Delta \gamma$ = .21° Δh = 2800 ft	71
Surface Launch	$\Delta \phi$ = 1°	$\Delta \gamma$ = .925°	16.3	ΔV = -33 ft/sec $\Delta \gamma$ = .98° Δh = 15,000 ft	39

burnout errors corresponding to specific launch error sources. The first row in the table is representative of the effect of error sources during an abort launch. A 1% thrust error is assumed for an abort 4 minutes 36 seconds after start of descent. A miss distance of 157.5 nautical miles is predicted by Figure 2.1.2-3. The miss distance based on the specific burnout errors is 71 nautical miles. The second row of the table makes a similar comparison for a surface launch, Hohmann transfer, intercept. A one degree pitch attitude error is considered. In this case, the sensitivity parameters underestimate the miss distance, predicting a miss of 16 nautical miles, compared to a 39 nautical miles miss using specific burnout errors.

Table 2.1.2-II presents results of computer calculations to determine miss distances for the case where nominal conditions at launch burnout (lead angle and LEM orbital parameters) are those required to intercept the CSM in 90^{o} lunar range angle. These data are applicable to the type of intercept technique described in section 2.2.2.2 that requires a hover phase to establish, except that the assumed burnout errors are much too large. It is seen that miss distances for this type of intercept technique are much smaller than the 70 nautical miles misses encountered by the technique that consists of a direct launch to intercept. However, the miss distances are large enough in all cases to require some form of midcourse correction unless considerable extremely accurate data are displayed to the pilot for control of burnout conditions. Figure 2.1.2-2 indicates that miss distances could be reduced to less than 5 nautical miles if

TABLE 2.1.2-II

MISS DISTANCES FOR 90°

LUNAR RANGE INTERCEPT

Error Source	Assumed Burnout Errors	Miss Distance N. Miles
ΔT = 1%	ΔV = 73 ft/sec $\Delta \gamma$ = .318° Δh = 4700 ft	16
ΔT = -1%	ΔV = -73 ft/sec $\Delta \gamma$ = -.318° Δh = -4700 ft	43
$\Delta \theta$ = 1°	ΔV = -33 ft/sec $\Delta \gamma$ = .98° Δh = 15,000 ft	34

the pilot could control his burnout velocity components to the order of accuracy of one ft/sec.

It is concluded that midcourse corrections are necessary. It is probable that more simple midcourse procedures can be utilized for launch techniques that reduce time and distance required to intercept, because of the smaller miss distances without midcourse corrections.

2.1.3 Midcourse Correction

Analyses indicate that errors at the end of the abort launch maneuver could result in substantial deviations from the nominal intercept trajectory; and further, that such deviations can lead to excessive fuel expenditure during the terminal phase of rendezvous. In order to assure an intercept and reduce fuel requirements, midcourse correction charts have been prepared. Using these charts and relative position information between the LEM and CSM, the relative velocity necessary to place the LEM on a coasting intercept path can be determined. The midcourse correction data were determined from the solution of orbital mechanics equations by means of an IBM 7090 digital computer (Appendix B).

The midcourse correction charts (Appendix B) present plots of the range rate parameter, $\frac{\dot{r}}{10^{-3}r}$ and angular rate of line of sight $\frac{\dot{\theta}}{10^{-3}}$ versus the angle of elevation (E). The charts are applicable only for a circular target orbit at an altitude of 80 nautical miles. There are six curves on each chart which correspond to intercept times from 1,000 to 6,000 sec. In order to use the charts, it is necessary to know the position

quadrant of the target with the interceptor, e.g., above and ahead. At the top of each chart there is a symbol, a circle with one quadrant darkened, which denotes the quadrant for which the particular chart is applicable. In addition, heading information is provided to indicate the variable $\frac{\dot{r}}{10^{-3}r}$ or $\frac{\dot{\theta}}{10^{-3}}$ and the range increment over which the chart is applicable. Enough range increments are used such that the errors induced due to assuming no variation over the increment is of no consequence (Appendix B).

After locating the appropriate chart, rates can be determined by entering the charts with the angle of elevation, proceeding vertically to the intercept time, and reading the corresponding value of $\frac{\dot{r}}{10^{-3}r}$ and $\frac{\dot{\theta}}{10^{-3}}$ on the ordinate. These two ratios have been plotted on separate charts. Having determine ratio values, the correct rates are given by

$$\dot{\theta} = (\text{ordinate value}) \times 10^{-3}$$

$$\dot{r} = (\text{ordinate value}) \times r \times 10^{-3}$$

If the actual rates are corrected to these values immediately after injection onto the intercept trajectory, it should not be necessary to repeat corrections more often than every 10-15 min.

The reason that relative rather than absolute velocity was selected for the midcourse correction charts was because it is thought that relative velocities could be measured with greater accuracy. Range and range rate radar sensed data could be measured with great accuracy provided a transponder on board the CSM is employed. Likewise, an optical

tracker and a flashing beacon on the CSM could provide adequate angular rate information.

A simple midcourse correction procedure is to apply thrust to maintain a constant inertial line of sight direction to the target and a negative (closing) range rate. Analysis of several special cases indicates that this procedure can be utilized efficiently after range is reduced to approximately 40 nautical miles. Figures 2.1.3-1 and 2.1.3-2 present ideal velocity requirements for constant line of sight intercept as a function of initial range for several assumed cases.

2.1.4 Out of Plane Correction

Intercept from an out-of-plane situation can become necessary due to

(1) Equi-period injection errors.

(2) Attitude errors during powered descent or launch.

(3) Thrust misalignment.

For the special case of launch from the lunar surface utilizing back-up guidance, rotation of the moon is an additional cause for an out-of-plane condition.

Analyses show that out-of-plane errors do not significantly affect midcourse correction requirements based on an in-plane assumption, if the out-of plane distance is small compared to the line of sight range. This is discussed in more detail in Appendix B. An out-of-plane correction can be made by eliminating the cross-course component of the angular

FIGURE 2.1.3-1

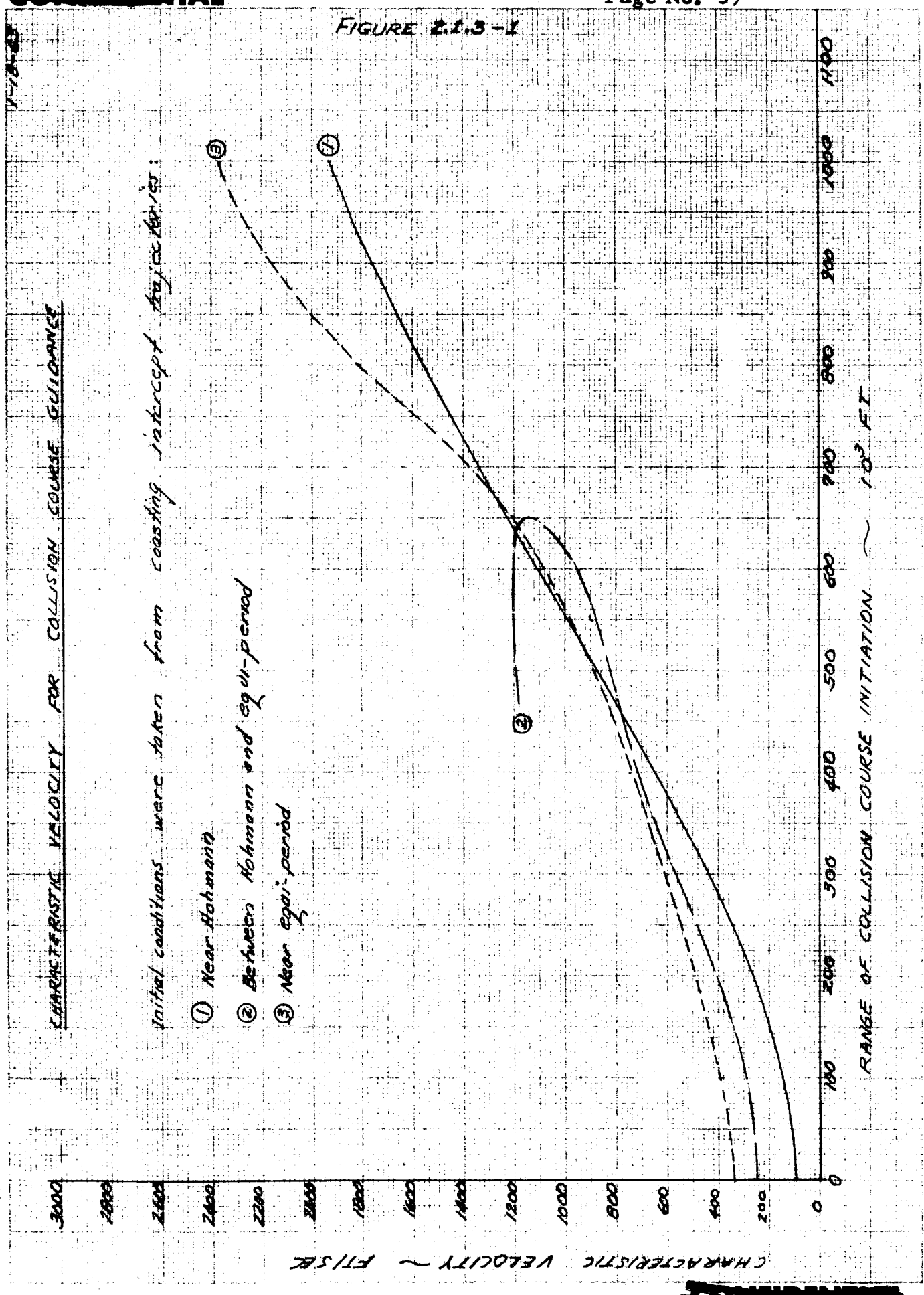
CHARACTERISTIC VELOCITY FOR COLLISION COURSE GUIDANCE
Initial conditions were taken from coasting intercept trajectories:
① Near Hohmann
② Between Hohmann and equi-period
③ Near equi-period
CHARACTERISTIC VELOCITY ~ FT/SEC
RANGE OF COLLISION COURSE INITIATION ~ 10³ FT
0
200
400
600
800
1000
1200
1400
1600
1800
2000
2200
2400
2600
2800
3000
0
100
200
300
400
500
600
700
800
900
1000
1100

Figure 2.1.8-2

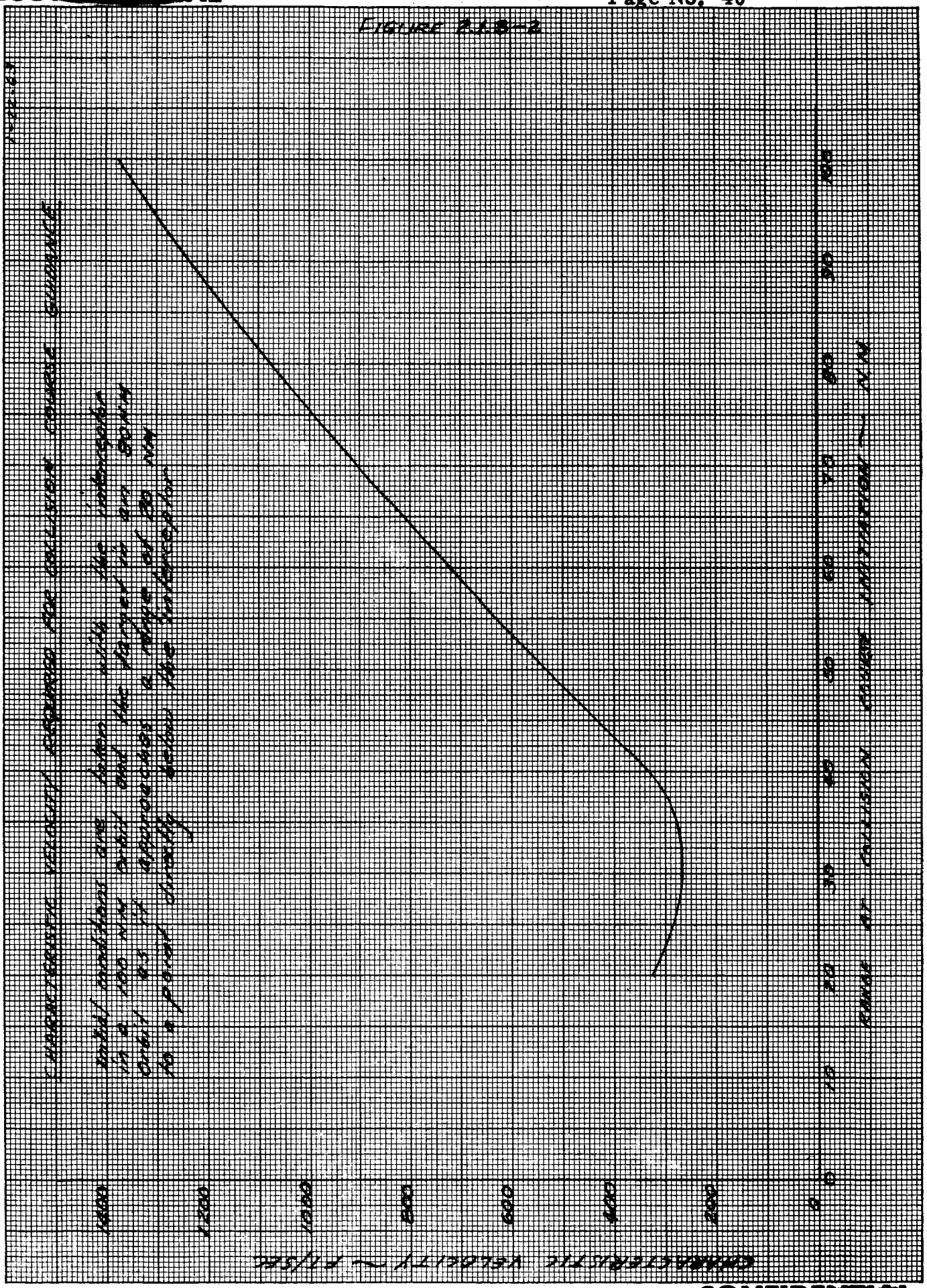

rate of the line of sight when the LEM crosses the orbital plane of the CSM.

An out-of-plane condition at short range is corrected simultaneously with the in-plane error if the terminal phase of the intercept includes maintaining zero angular rate of the line of sight.

2.1.5 Mechanization

The purpose of this study is directed more toward defining display parameters required by the pilot rather than determining methods for meeting these requirements. Optimum mechanization requires much information that was either undefined or unavailable for this study, such as:

(1) Details of LEM configuration.

(2) Details of primary guidance system.

(3) Description of components remaining (if any) after failure of the primary guidance system.

However, a preliminary study of mechanization of requirements was conducted to ensure the evolvement of realistic and reasonable requirements.

Table 2.1.5-I is a summary of the display parameters required for the abort launch techniques investigated during the simulation and described in section 2.2.2. The remainder of this section is a discussion of possible mechanization methods for these combinations of requirements.

Attitude Reference

All of the abort techniques considered require complete attitude display for at least limited periods during the mission. An attitude reference system which would provide complete attitude display during the

TABLE 2.1.5-I

DISPLAY PARAMETER REQUIREMENTS
(Time display required for all cases)

Abort Launch Technique	Requirements for Launch	Additional Requirements for Midcourse Correction
A	Attitude	Range to target
	Pitch (either inertial or local reference)	Range Rate
	Yaw	Direction of target (azimuth & elevation)
	Roll	Inertial angular rate of LOS resolved into two body axis components
B	Attitude	None
	Pitch (local reference)	
	Yaw	
	Roll	
	Vertical Velocity	
C	Attitude	Inertial angular rate of line of sight
	Pitch (local reference)	
	Yaw	Either range or local angle of elevation of target
	Roll	
	Vertical Velocity	
	Altitude	
	Body Axis Velocity Increments	

entire abort mission would have to be the equivalent of a stable platform. However, a stable platform would seem to be too complex for use in a back-up guidance system. A "strapped-down" system which would provide all attitude display would in a sense substitute electronic complexity for the mechanical complexity of a platform.

Such a strapped-down system would consist of three body mounted integrating gyros operating in a caged mode with the output converted to a pulse rate. The digital output would then be processed in a simple (incremental) digital computer. The computer would convert the integrated body rates into inertial angular displacements. The primary design problems of such a system would be associated with the computer, specifically, the major difficulty would be designing the computer to operate in real time.

In all three abort techniques, it would be possible to perform the mission with a more limited attitude reference system. One such system would use three body mounted wide angle integrating gyros, one body mounted free gyro, and a horizon scanner. There would obviously be a certain amount of redundancy inherent in this system.

The system would have three modes of operation. Mode one operation would be based entirely on the three integrating gyros and would be used in the early stages of the abort. The pitch gyro would be operated in a caged mode with digital output, and the output pulses, representing unit displacements, would be fed into a counter. The yaw and roll gyros would

maintain yaw and roll zero reference and correction factors for the pitch output as long as all maneuvers are within the operating limits of the gyros.

Near the end of the powered ascent, the system goes into mode two operation. Mode two operation would be the same as mode one with the exception that pitch reference is taken from the horizon scanners and, therefore, pitch would be referenced to the local vertical.

Mode three operation would be used during extended maneuvers about all three axes, as when making out of plane corrections. The free gyro would be uncaged while the vehicle was at zero yaw and roll and would thus retain the yaw and roll reference during the maneuver. Reference for pitch could be taken from the horizon scanners.

Radar

In the midcourse and terminal phases of abort techniques A and C, information on the relative position and velocities of the command module and LEM must be supplied by radar. Radar systems will soon be available which will give range, range rate, azimuth, elevation, azimuth rate, and elevation rate to a target (equipped with a suitable transponder) from 0 to 500 n-mi away.

The reflected signal is processed to give range rate data from the doppler shift. Range information is obtained by a method which essentially measures the travel time of the signal. However, the method used (interrupted continuous wave) requires only moderate bandwidths within the receiver, thus reducing noise problems.

Inertial angular rates of the lines of sight could be obtained from rate gyros mounted on the radar antenna.

The same radar system could be used to provide altitude and altitude rate for abort technique C.

Velocity Increment

Abort technique C requires body axis velocity increment measurement and display. This could be mechanized quite easily by using a body mounted integrating accelerometer.

The estimated power and weight requirements for the system components are summarized in Tables 2.1.5-II and 2.1.5-III. The radar data are based on reference (4).

2.2 Simulator Program

2.2.1 General Setup

The hardware components used for the simulation consisted of the following items:

(1) ASI-210 Digital Computer.

(2) PACE Analog Equipment (100 amplifiers with accessories).

(3) Digital to Analog and Analog to Digital Conversion Equipment.

(4) Moving Base Cockpit Simulator inside Spherical Screen.

(5) Target and Starfield Projector.

TABLE 2.1.5-II

BACK-UP GUIDANCE SYSTEM POWER BREAKDOWN

Horizon Scanner	4 Watts
Integrating Gyro Unit	100 Watts*
Free Gyro	15 Watts
Radar	110 Watts**
Integrating Accelerometer	30 Watts
Total	259 Watts

* Maximum power required (including 75 watts for heating used intermittently).

** Includes 6 watts for Display Unit and 24 watts for Antenna Drive

TABLE 2.1.5-III

BACK-UP GUIDANCE SYSTEM WEIGHT BREAKDOWN

Horizon Scanner	3 lbs.
Integrating Gyro Unit	15 lbs.
Free Gyro	4.5 lbs.
Radar	29.3 lbs.
Integrating Accelerometer	5 lbs.
Total	56.8 lbs.

(6) Lunar Scene Projector.

(7) Recording Equipment.

(8) Master Control Console.

Appendix D gives a detailed description of the simulator facility.

The digital computer was coded for the automatic descent to the manual abort command or to the 6000 ft. altitude level whichever occured first. Manual control was then available to the pilot for the remainder of the flight. All of the space mechanics calculations, control system computations, etc. were performed in the digital computer on a real time basis. The analog equipment was used chiefly to drive instruments, the moving base cockpit, the plotters, and the projectors. There was also a provision to operate the digital computer on a 4:1 speeded up time basis wherein it did the space mechanics calculations although all pilot control was eliminated. The purpose was to speed up those runs which contained long transfer orbit waiting periods.

The target projector was set up so that a spot of light, representing the target, was produced by the outer gimbal, and a patch of smaller light spots was projected by the inner gimbal to give the illusion of a starfield (target positioned inside starfield). The purpose of this arrangement was to give the target a fixed reference in order for the pilot to determine relative motion between the LEM and the target.

Appendix E contains the basic equations used for the simulation.

2.2.2 Procedure

The Manned Aero-space Flight Simulator was programmed so that the problem started at the initiation of powered descent when the pilot turned on the "operate" switch. The LEM was automatically controlled along the nominal descent trajectory until a switch was closed at the control station that terminated automatic control and turned on an "abort" light on the pilot's display. The pilot then manually controlled the LEM for the remainder of the run, utilizing the descent and landing engines as required by the particular launch technique and making midcourse corrections with the descent or launch engines or with the reaction control thrusters until an intercept was achieved. The pilot performed all of the required tasks on a few of the runs; however, it was found that the second crew member could be very helpful. Midcourse corrections were usually determined by an engineer and transmitted to the pilot over the intercom. A few runs were made in which the pilot maneuvered to within a few hundred feet of the CSM and reduced the closing rate to less than 10 ft/sec. However, the scope of this program does not include investigation of the rendezvous and docking phase; therefore, the runs were usually terminated when the range became less than 5000 ft., with no attempt to control closing rate as a function of range. It was assumed that this requirement would be included in the rendezvous and docking phase. Pertinent trajectory data and fuel used were recorded at launch burnout and run termination. Fuel in the descent engine was assumed to be equivalent to an ideal

velocity of 6600 ft/sec. Calculated fuel required by the launch engine includes all required for translational control by both the launch engine and the reaction control thrusters, but does not include rotational requirements of the reaction control system. The LEM control system was not simulated in sufficient detail to warrant calculation of rotational impulse requirements. (See Appendix E.)

Eight astronauts and several other pilots participated in the program as simulator-LEM pilots. An LTV pilot (W. J. North, Jr.) assigned to the simulator group, participated as pilot in more of the tests than any of the other pilots. Some of the maneuvers required for this program require considerable study and training to perfect, even for experienced pilots. Therefore, due to the greater simulator experience, on other similar porgrams as well as this, the results of Mr. North's runs are emphasized as more representative of a pilot thoroughly trained for this mission.

2.2.2.1 Intercept Technique A

Parameters displayed to the pilot for this technique are:

Launch	Midcourse
Time	Time
Attitude	Attitude
	Range
	Range Rate
	Direction (bearing and elevation angles of target)
	Body Axis Components of Angular Rate of Line of Sight

The procedure for this intercept technique is illustrated in Figure 2.2.2-1. During the abort launch, the pilot terminates descent engine thrust, controls attitude, and ignites and shuts down the launch engine according to a precalculated schedule. The schedule is presented in Table 2.2.2-I, and is based on the analytical calculations discussed in section 2.1.1. The descent engine is used for 20 seconds for aborts initiated later than 2-1/2 minutes after start of descent in order to prevent excessive loss of alittude for low altitude aborts. The data of section 2.1.1 are based on constant pitch rate trajectories. The data of Table 2.2.2-I are calculated to approximate the same trajectories with step changes in relative pitch attitude. The pitch program procedure is to start the launch at the attitude specified in the table, then decrease the pitch attitude 10^{o} (nose down) every 90 seconds.

After launch burnout, midcourse corrections are made as required to intercept. The midcourse correction procedure is to determine the quadrant, range, and angle of elevation of the target, use midcourse correction charts to determine range rate and line of sight angular rate to intercept, then apply thrust to establish the required rates. Use of the midcourse correction charts is explained in Appendix B. Final closure may be controlled by occasionally applying thrust to maintain near zero angular rate of line of sight.

2.2.2.2 Intercept Technique B

Display parameters are:

FIGURE 2.2.2-1

INTERCEPT TECHNIQUE A – DIRECT LAUNCH TO INTERCEPT

A. INITIATE ABORT (STAGE DESCENT ENGINE WITHIN 20 SEC.)

B. ABORT LAUNCH:

1. REFER TO ABORT LAUNCH TABLE.
2. PITCH TO REQUIRED INITIAL ATTITUDE.
3. IGNITE LAUNCH ENGINE.
4. LOWER NOSE 10° EVERY 90 SEC.
5. BURNOUT AT SPECIFIED TIME.

C. COAST MIDCOURSE CORRECTION PROCEDURE:

1. OBSERVE RANGE AND DIRECTION OF TARGET.
2. USE MIDCOURSE CORRECTION CHARTS TO DETERMINE RANGE RATE AND ANGULAR RATE REQUIRED.
3. APPLY THRUST UNTIL REQUIRED RATES ARE OBSERVED.

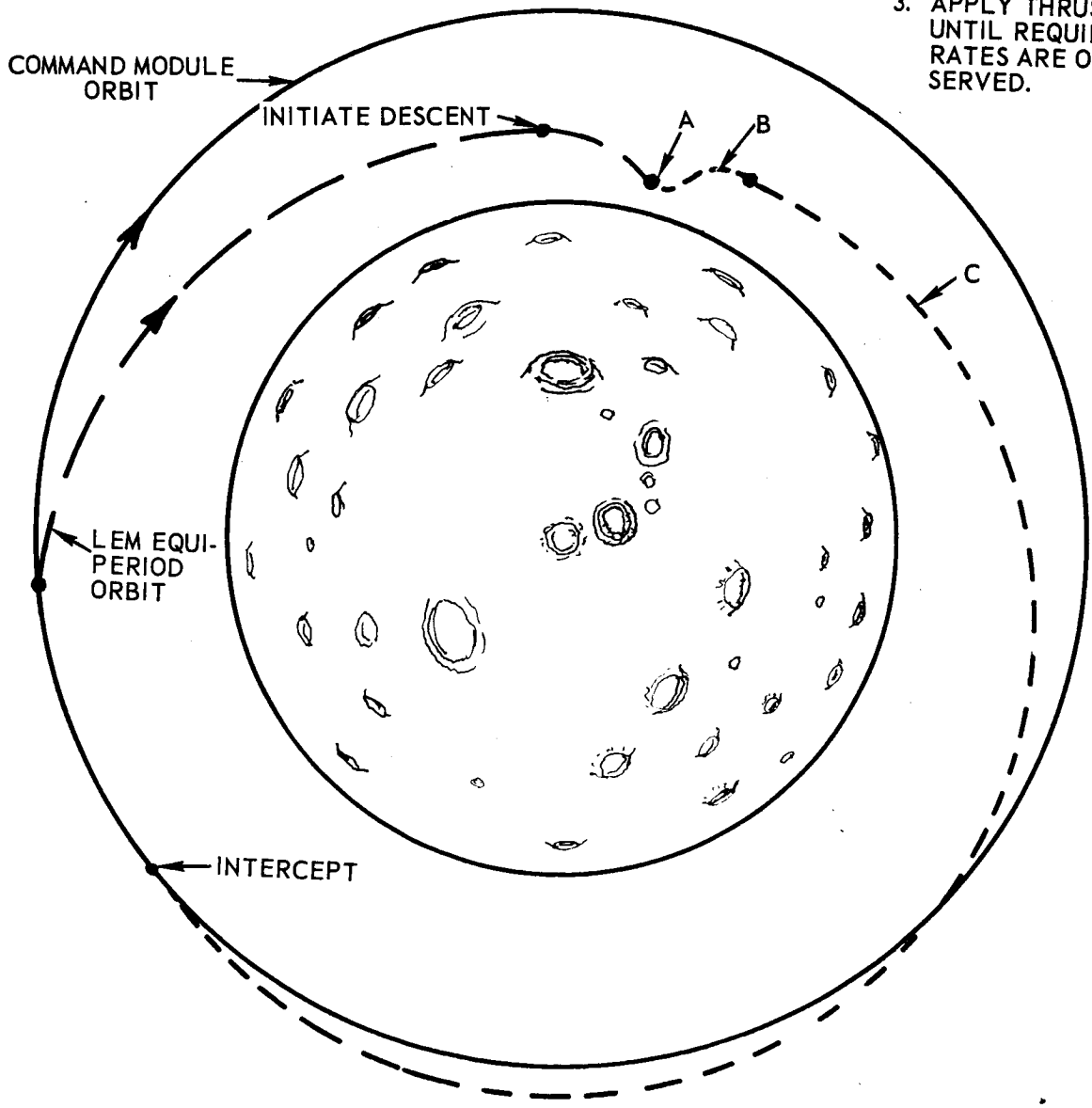

TABLE 2.2.2-I

ABORT LAUNCH TECHNIQUE A
DIRECT LAUNCH TO INTERCEPT
(Time Measured from Start of Powered Descent)

Abort Time Min:Sec	Descent Eng. B.O. Time Min:Sec	Initial Pitch Attitude Degrees	Launch Ign. Time Min:Sec	B.O. Time Min:Sec	Intercept Time Hr:Min
0:00	Stage Immed.				1:33
0:20		- 90	0:40	1:00	1:35
0:40		- 89	1:00	1:41	1:35
1:00		- 87	1:20	2:21	1:36
1:20		- 85	1:40	3:02	1:36
1:40		- 82	2:00	3:42	1:37
2:00		- 79	2:20	4:22	1:37
2:20		- 76	2:40	5:02	1:37
2:40	3:04	- 81	3:15	5:58	1:38
3:00	3:24	- 78	3:35	6:39	1:37
3:20	3:44	- 75	3:55	7:19	1:37
3:40	4:04	- 72	4:15	8:00	1:37
4:00	4:24	- 69	4:35	8:41	1:36
4:20	4:44	- 67	4:55	9:21	1:35
4:40	5:04	- 65	5:15	10:02	1:34
5:00	5:24	- 63	5:35	10:43	1:32
5:20	5:44	- 62	5:55	11:23	1:28
5:40	6:04	- 61	6:15	12:04	1:21

Launch	Midcourse
Time	Time
Attitude	
Vertical Velocity	

This type of intercept is illustrated in Figure 2.2.2-2 and utilizes a launch technique that includes retrograde and hover phases for the purpose of establishing a nominal midcourse trajectory that is simple to control and is the same for all abort times. All the descent engine fuel is used. Table 2.2.2-II describes the launch method. If the abort occurs earlier than three minutes after start of descent, the pilot maneuvers the vehicle to maintain zero vertical velocity for the entire launch. For later aborts, the procedure is similar except for an immediate vertical thrust phase to stop the vertical descent and a pitch program to regain altitude. A nominal variation of burnout altitude from 40,000 to 80,000 feet is expected due to variation of initial abort conditions. Control to zero vertical velocity during the final seconds of launch ensures small flight path angle errors at burnout.

The error in circular speed may be determined from Figure 2.2.2-4 by timing the change in vertical velocity after launch burnout. A horizontal velocity increment of approximately 200 ft/sec is required to inject into the intercept trajectory. High accuracy is not required for this injection increment because of the smaller error sensitivities for this type of intercept. (See section 2.1.2.) Therefore, the injection may be made by relighting the launch engine for an estimated time required to achieve the

FIGURE 2.2.2-2
INTERCEPT TECHNIQUE B
90° LUNAR RANGE ANGLE INTERCEPTION

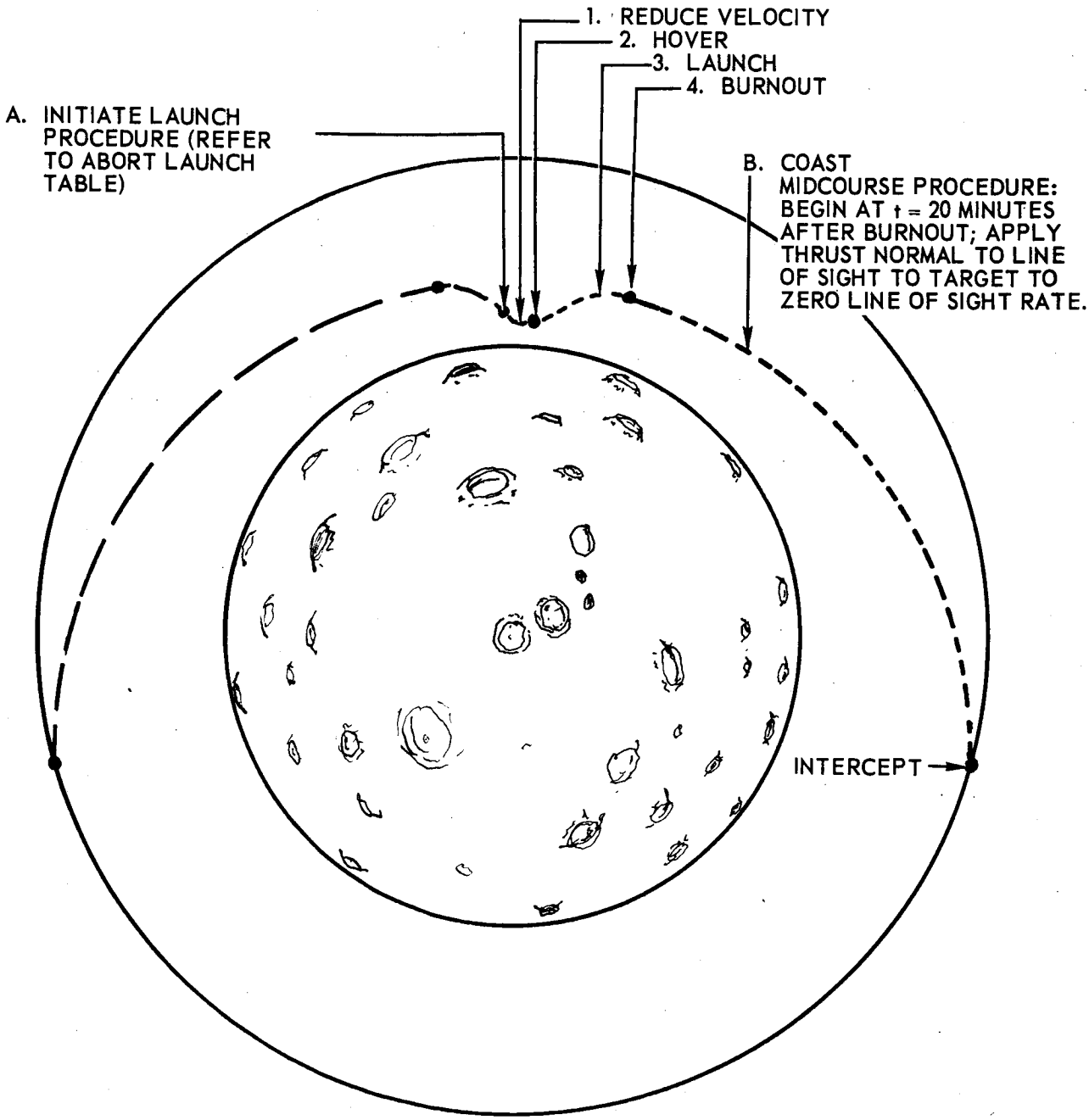

TABLE 2.2.2-II

ABORT LAUNCH TECHNIQUE B

(Time in min:sec from start of powered descent)

Abort Time	100% Vertical Thrust $\theta = 0$	Retrograde, 100% Thrust, $\dot{h} = 0$, $\theta \approx +80^{\circ}$	Hover, Low Thrust $\theta = 0$	100% Vertical Thrust $\theta = 0$	Posigrade, $\theta_o \approx -70^{\circ}$
Before t = 3:00	0	5:41	7:03	0	$\dot{h} = 0$ 100% descent eng. to t = 7:18. Stage. Ignite launch eng. Terminate launch circular at approx. t = 12:35
After t = 3:00	20 sec.	5:58	6:54	6:57 (Stage)	Ignite launch eng. at $\theta = -63^{\circ}$ $\theta = -63^{\circ}$ to t = 8:27 $\theta = -73^{\circ}$ to t = 9:57 $\theta = -83^{\circ}$ to t = 11:32 $\dot{h} = 0$ to circular at approx. t = 12:34

required ΔV. Compensation for the burnout velocity error may also be made at this time with an adjustment in estimated thrust time required to inject. Injection nominally requires relighting the launch engine for approximately 9 seconds.

The midcourse procedure is to wait 20 minutes after injection, then maintain constant line of sight direction until intercept. Constant line of sight angle may be maintained by occasionally applying thrust to eliminate motion of the target across the background of stars. Intercept nominally requires about 30 minutes after injection. The 20 minute waiting period appears to be near optimum from the standpoint of starting line of sight control close to the target and controlling effects of errors at injection. That is, if line of sight control is started earlier, it is less efficient due to the larger initial range. If it is initiated later than 20 minutes, an insufficient closing rate may exist due to the divergent effect of errors at injection.

2.2.2.3 Intercept Technique C

Parameters displayed to the pilot are:

Launch	Midcourse
Time	Time
Attitude	Attitude
Vertical Velocity	Vertical Velocity
Altitude	Altitude
Body Axis Velocity Increment	Body Axis Velocity Increment

Launch

Midcourse

Angular Rate of Line of Sight

Either Angle of Elevation or
Range of Target

This procedure resulted from the desire to find a method that consists of an immediate launch to orbital conditions, with no retrograde thrusting or hovering, and a simple midcourse procedure that is standard for all abort times. This is possible by transferring to a circular orbit ahead of and above the CSM, and waiting for the CSM to "catch up" to a selected relative position for initiation of the intercept trajectory. Intercept technique C is illustrated in Figure 2.2.2-3.

The purpose of the launch is to achieve circular orbit at approximately 50,000 feet. The launch engine is not used until the descent engine is out of fuel. The pilot sets up approximately 300 ft/sec vertical velocity for late aborts (slightly less for earlier aborts), levels out at 50,000 feet, maintains zero vertical velocity until approximate circular speed is achieved, then terminates thrust. He can detect circular speed (to within about 100 ft/sec) by observing the pitch attitude required to maintain zero vertical velocity, and terminating thrust when it appears that no vertical component of thrust is required to maintain zero vertical velocity. Figure 2.2.2-4 may be used to determine the incremental error in horizontal velocity. This is corrected by thrusting until the required increment is observed.

FIGURE 2.2.2-3

INTERCEPT TECHNIQUE C

LAUNCH TO CIRCULAR ORBIT – DOUBLE TRANSFER INTERCEPT

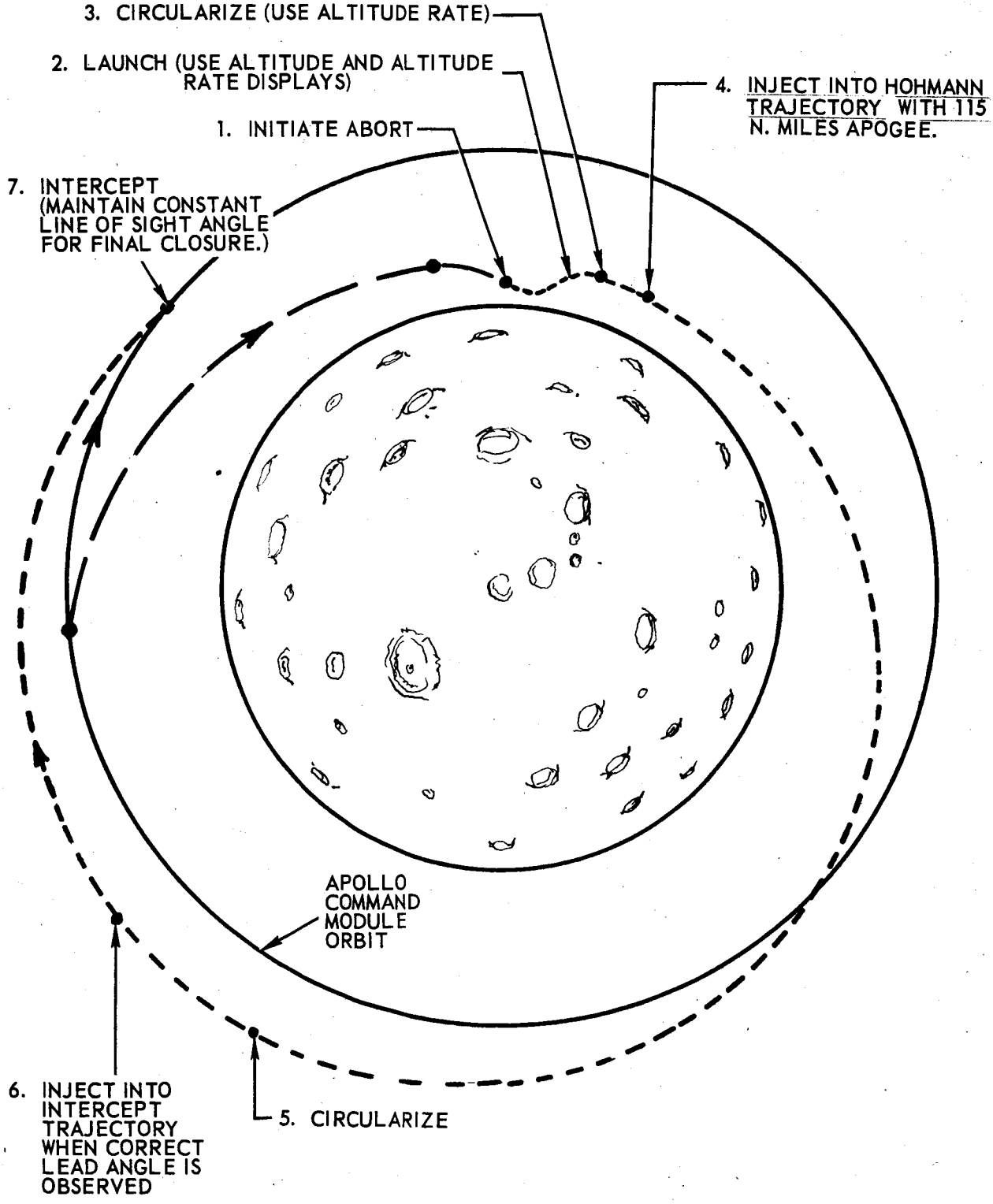

In order to allow sufficient time for performing the required maneuvers for all abort times, the Hohmann transfer to the higher orbit is not initiated until the CSM is behind and at an angle of elevation less than 73^{o} (or range $\geq$ 454,000 ft). When this condition is satisfied, a velocity increment of 144 ft/sec is applied to obtain an apogee of 115 nautical miles. Figure 2.2.2-6 is used to determine vertical velocity corrections as apogee is approached. At apogee, a velocity increment of 141 ft/sec is applied to circularize. Figure 2.2.2-5 is used to refine the circularization if required. The CSM approaches from behind and below. When the angle of elevation becomes -28^{o}, a retrograde velocity increment of 88 ft/sec is applied to establish the intercept trajectory. Nominal intercept occurs approximately 30 minutes later.

Final intercept correction procedure may be started about 20 minutes after initiating the intercept trajectory by maintaining constant line of sight direction. Control of the target's motion against a background of stars is not directly usable at this time because the background is generally obscured by the moon. It appears that inertial line of sight angular rate must be displayed to the pilot, or possibly an optical device could be designed that would superimpose an image of stars above the LEM on a sighting instrument aligned with the target, thus providing an artificial celestial "background." Design problems for such an optical device have not been studied in this program.

2.2.3 Results

Results of simulator abort-intercept runs using Techniques A, B, and C are summarized in Figures 2.2.3-1 through 2.2.3-7, Launch

FIGURE 2.2.2-4

ORBIT CIRCULARIZATION CHART

ORBIT ALTITUDE = 50,000 FT.

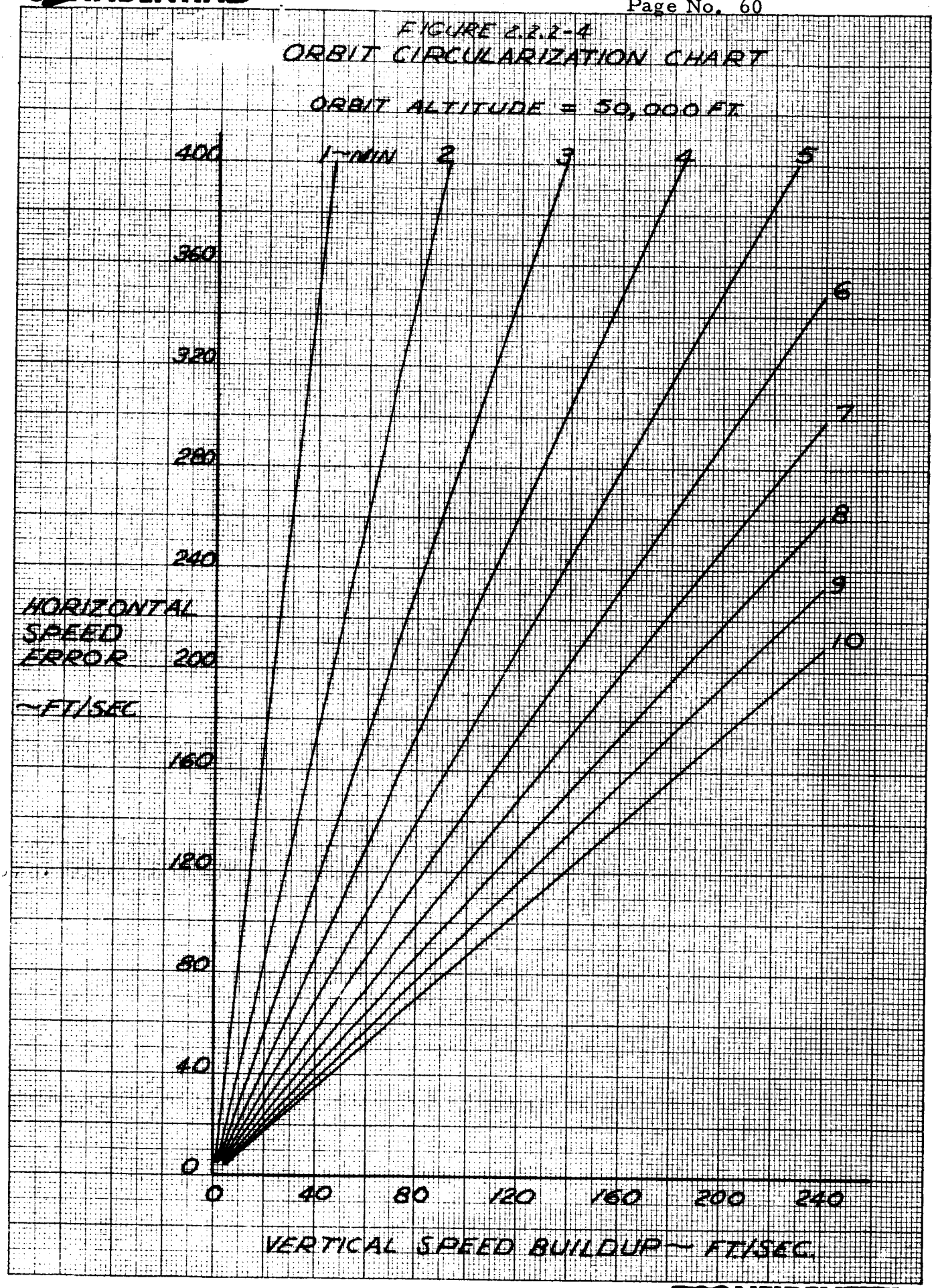

FIGURE 2.2.2 -5

ORBIT CIRCULARIZATION CHART

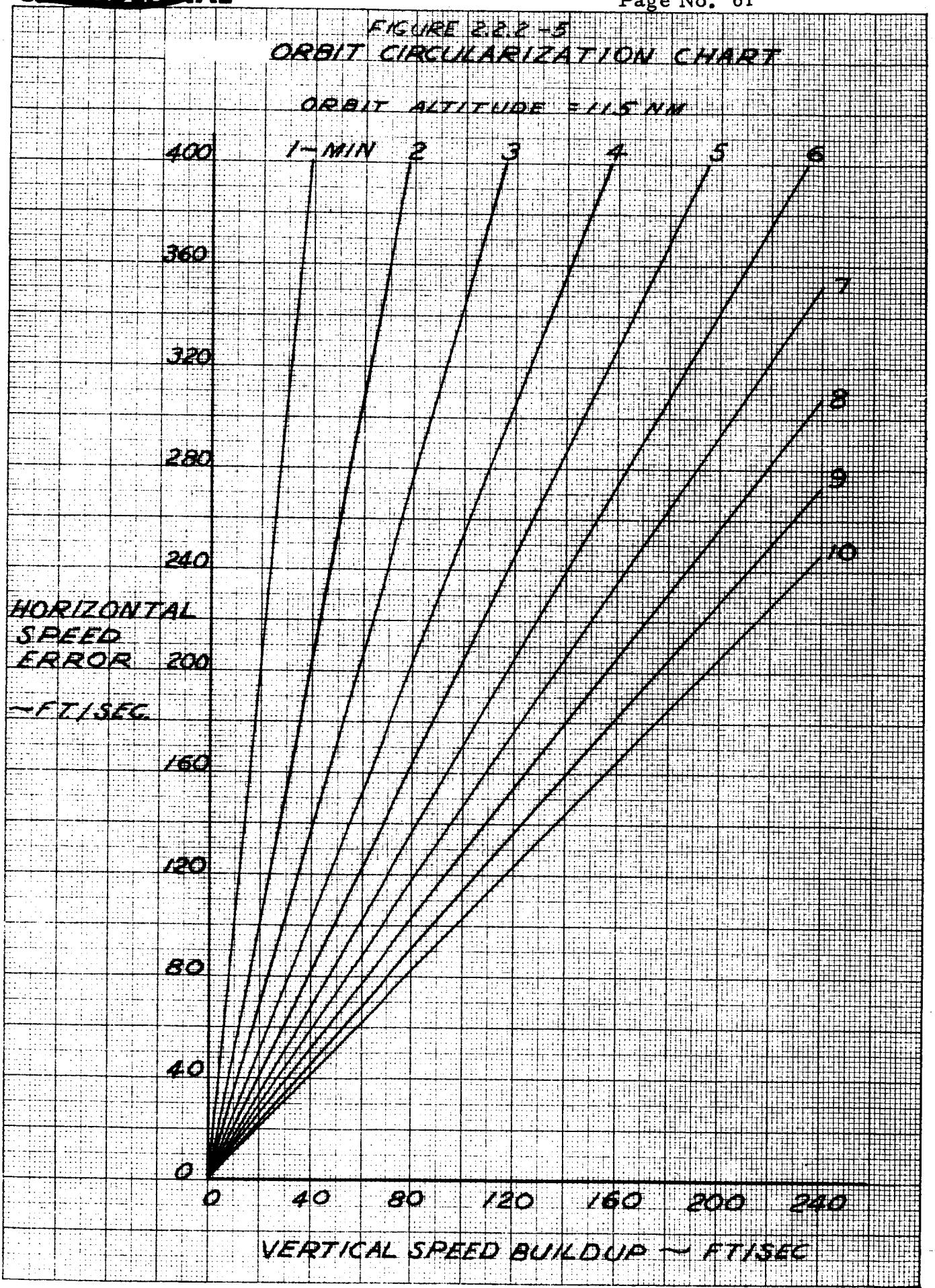

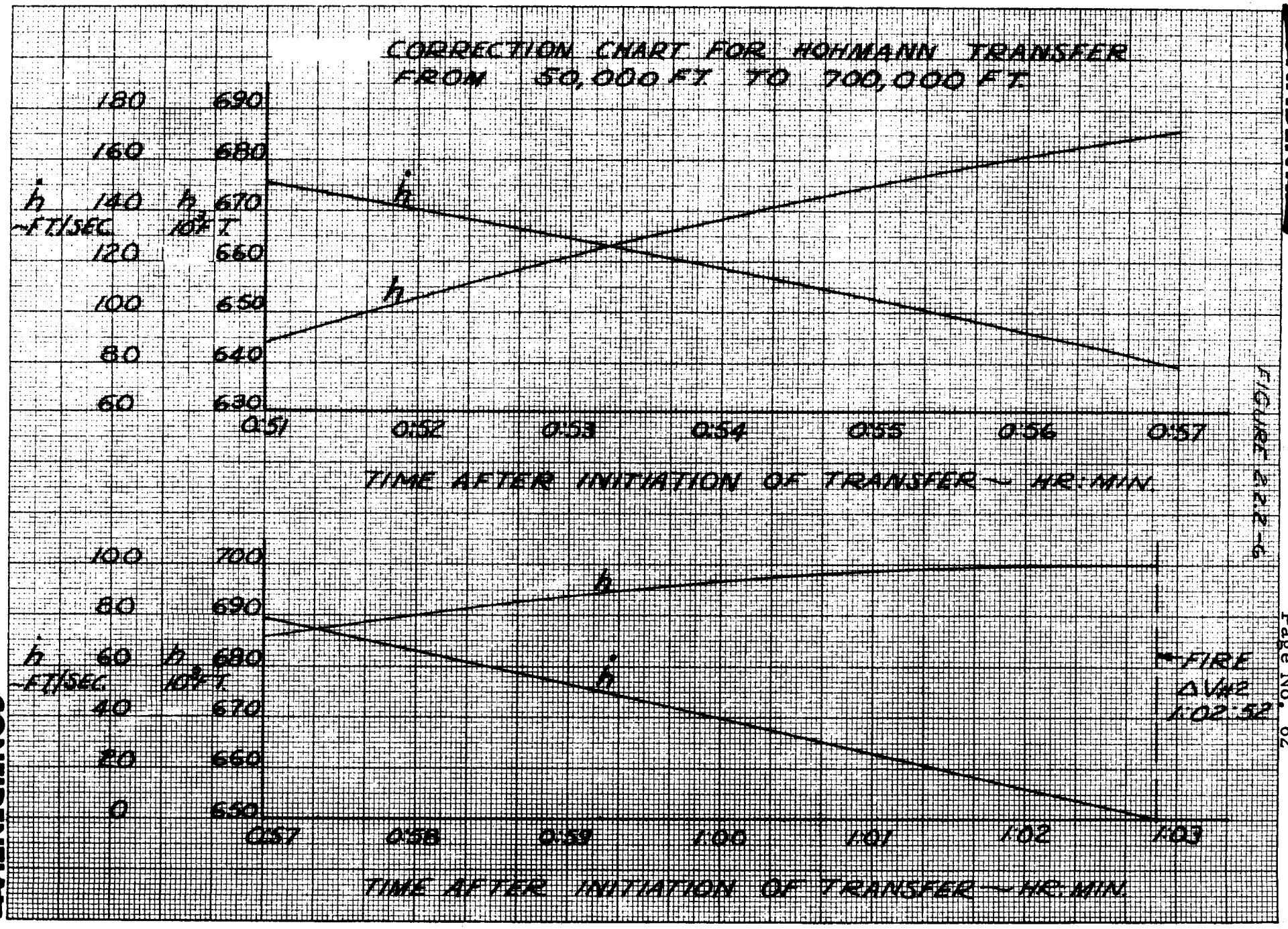

FIGURE 2.2.2-6

Report No. 00.213
Page No. 62

engine fuel requirements were calculated by adding the closing rate at termination of the run to the ideal velocity actually used. Therefore, the fuel requirement includes that required to reduce closing rate as range approaches zero, even though that phase was generally not attempted. This fuel requirement does not include docking and body axis rotational requirements.

Fuel required is greatest for Technique B and least for Technique C, although for very late aborts, requirements for all three techniques are about the same. Techniques A and B are difficult for pilots to fly until a certain experience level is reached; therefore, fairing of the curves was weighted toward the data of Mr. North's runs to be more representative of a high level of pilot training. Improvement in fuel requirements could possibly be realized with further training. The midcourse requirements for some of the Technique A data appear especially excessive compared to the theoretical minimum. A contributing factor is thought to be a low experience level in utilization of the midcourse correction charts.

Fuel required for Technique A would be approximately the same as for Technique C if the launch instructions (Table 2.2.2-I) were modified to allow full use of the descent engine fuel, but accurate control would become more difficult due to the additional phases of the procedure. The reason for the larger fuel requirements for Technique B is the necessity to fire retrograde and hover in order to set up a favorable lead angle at burnout. It is interesting to note that, if the equi-period orbit were established 270° from the landing site (rather than 90°), a very

FIGURE 2.2.3-1

IDEAL VELOCITY SUMMARY

TECHNIQUE A

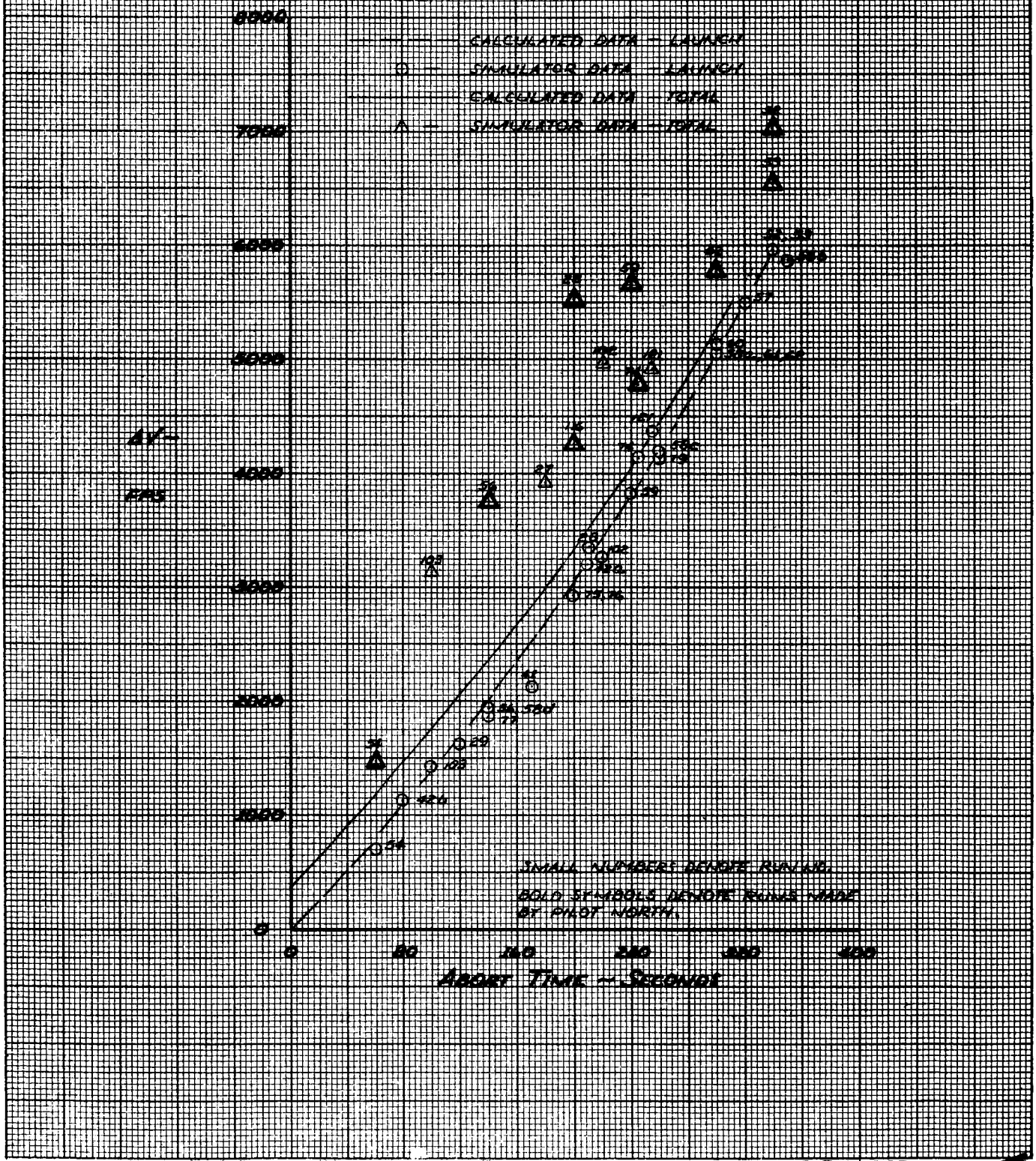

FIGURE 2.d.3-2

IDEAL VELOCITY SUMMARY

TECHNIQUE C

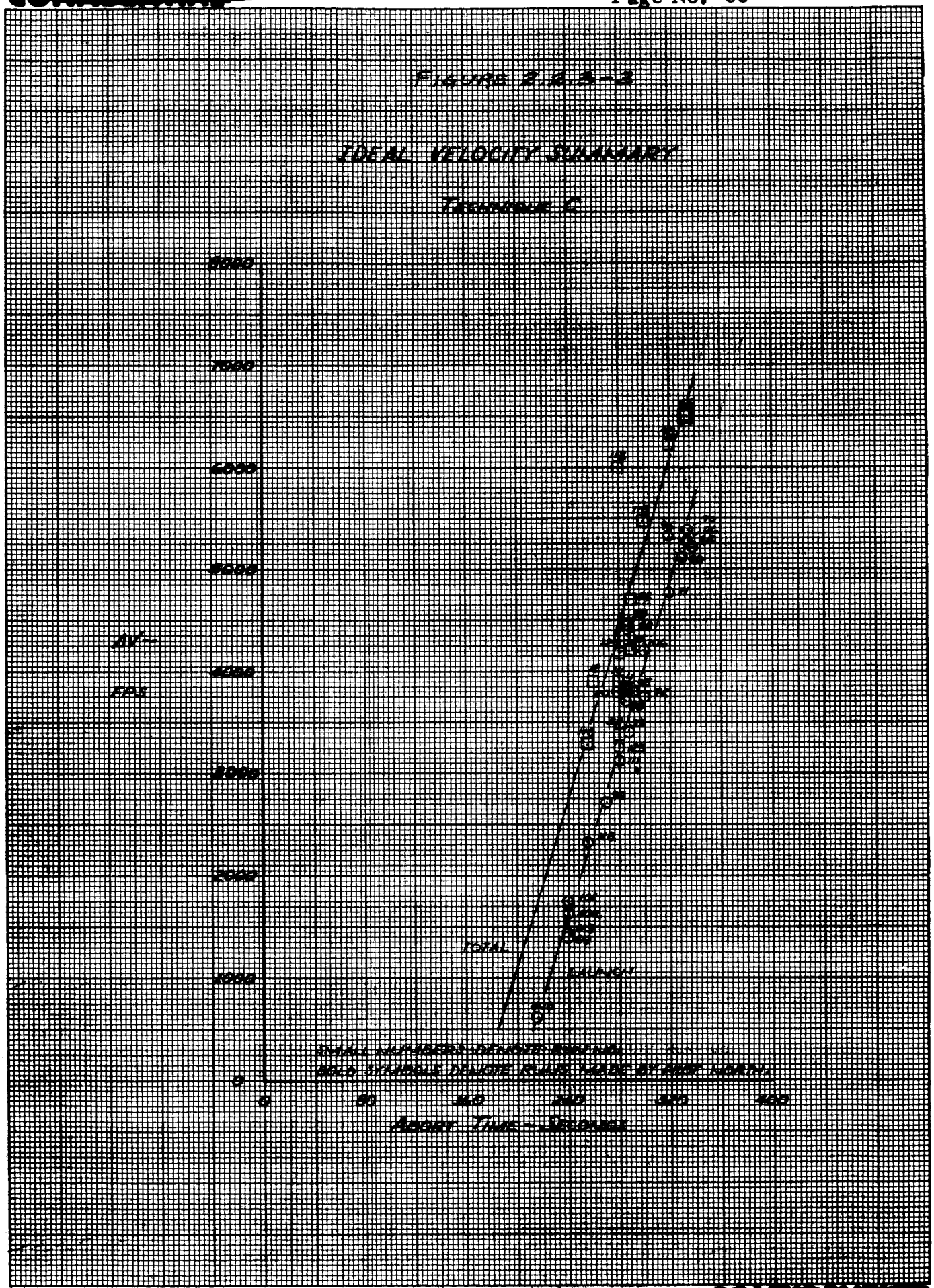

FIGURE 2.2.3-4

COMPARISON OF TOTAL IDEAL VELOCITY REQUIREMENTS

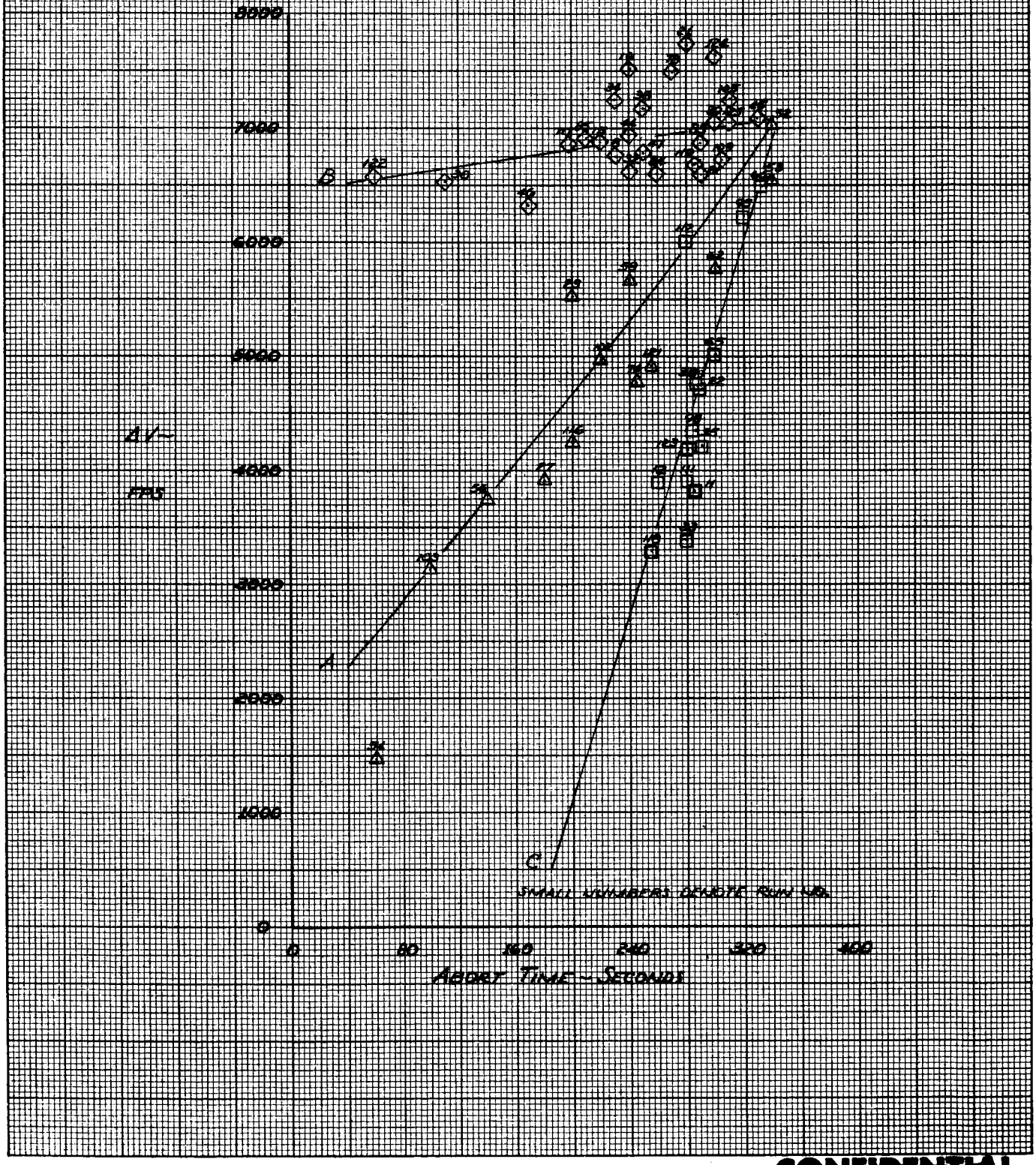

attractive abort intercept technique could be arranged. It would consist of a direct launch to a low circular orbit, a short orbital park period, then an injection and midcourse phase similar to that of Technique B. Fuel required would be about the same as for Technique C.

Figure 2.2.3-5 was used to determine if launch engine burnout resulted in a safe orbit. The possibility of shutdown of the launch engine in a trajectory with pericythion below the lunar surface appears to be greater for Technique A than for B or C. Figure 2.2.3-6 shows that a high percentage of burnout conditions for Technique A are unsafe. The primary reason is the large vertical velocity errors. The use of a vertical velocity display with Techniques B and C eliminates that source of error. The first launch engine shutdown can result in a pericynthion below the surface for Techniques B and C if it occurs at approximately 15 ft/sec below circular speed (or less). This often occurred during the simulation runs; however, no specific effort had been made to avoid this. Underspeed at first shutdown could have been prevented with Technique C by providing the pilot with a schedule of earliest launch engine shutdown time as a function of abort time. In the case of Technique B, the launch schedule (Table 2.2.2-II) could be revised to eliminate the orbital park phase and to burnout at a specified time approximately 200 ft/sec above circular speed, providing a safety margin above minimum safe speed. Actual speed above circular could be determined after burnout (from Figure 2.2.2-4) and adjusted.

The closing rates at near intercept terminal conditions are shown in Figure 2.2.3-7. Each run was generally terminated when the

FIGURE 2.2.3-5

VERTICAL VELOCITY REQUIRED FOR PERICYNTHION AT LUNAR SURFACE

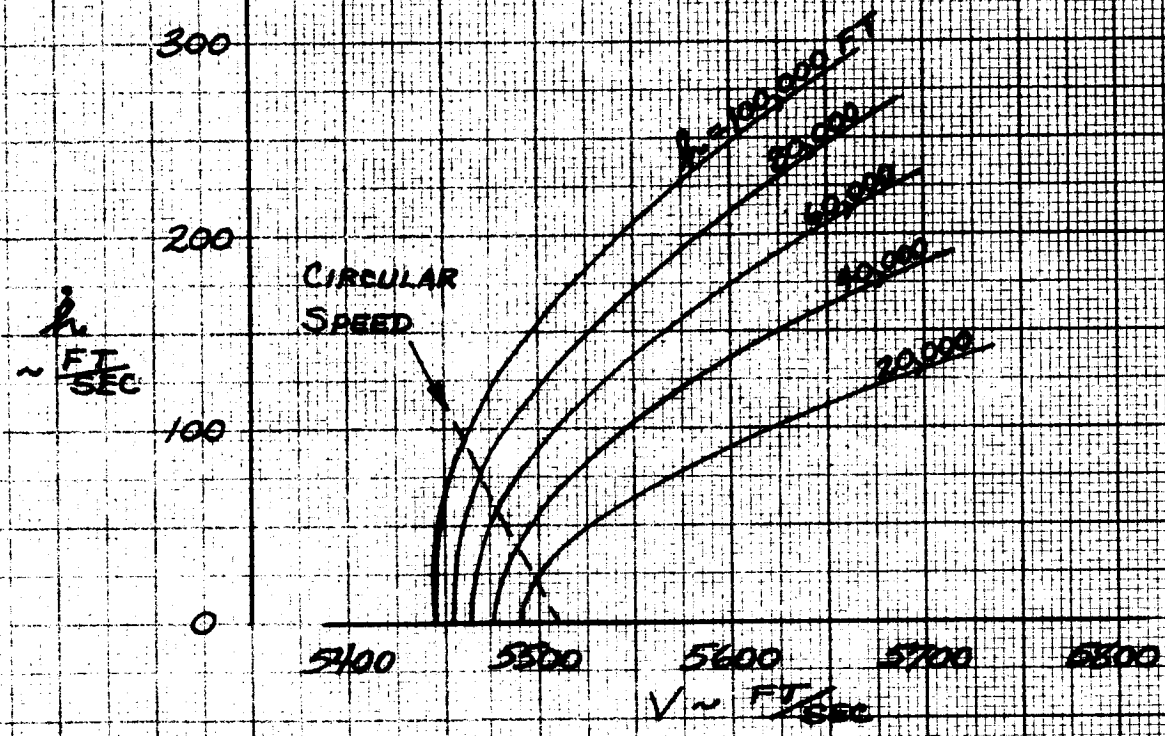

FIGURE 2.2.3-6
LAUNCH BURNOUT SUMMARY

TECHNIQUE A

PILOT: NORTH

FLAGGED SYMBOLS DENOTE PERICYNTHION BELOW SURFACE.

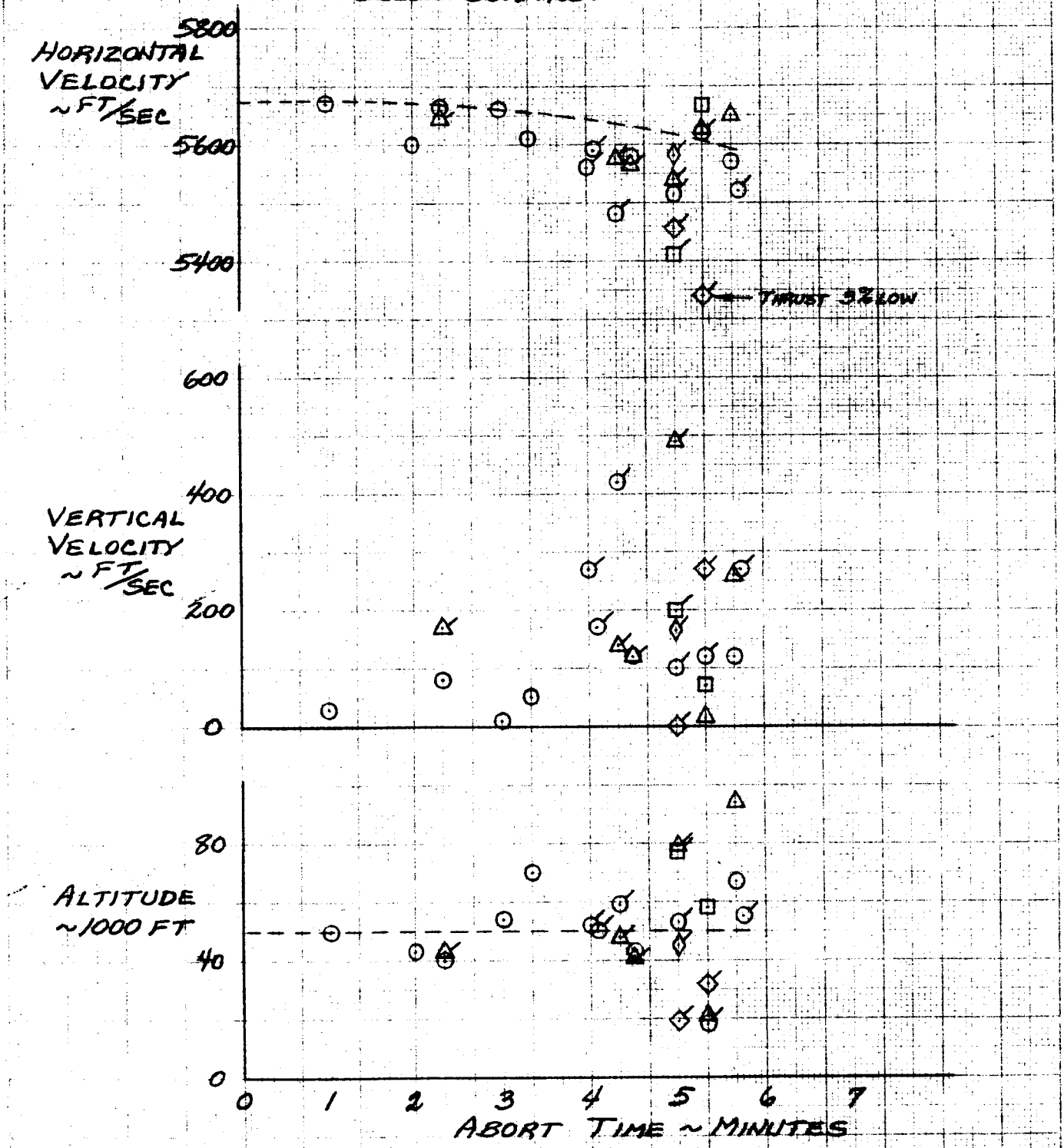

CONFIDENTIAL

FIGURE 2.2.3-7

SUMMARY OF FINAL CLOSING RATE

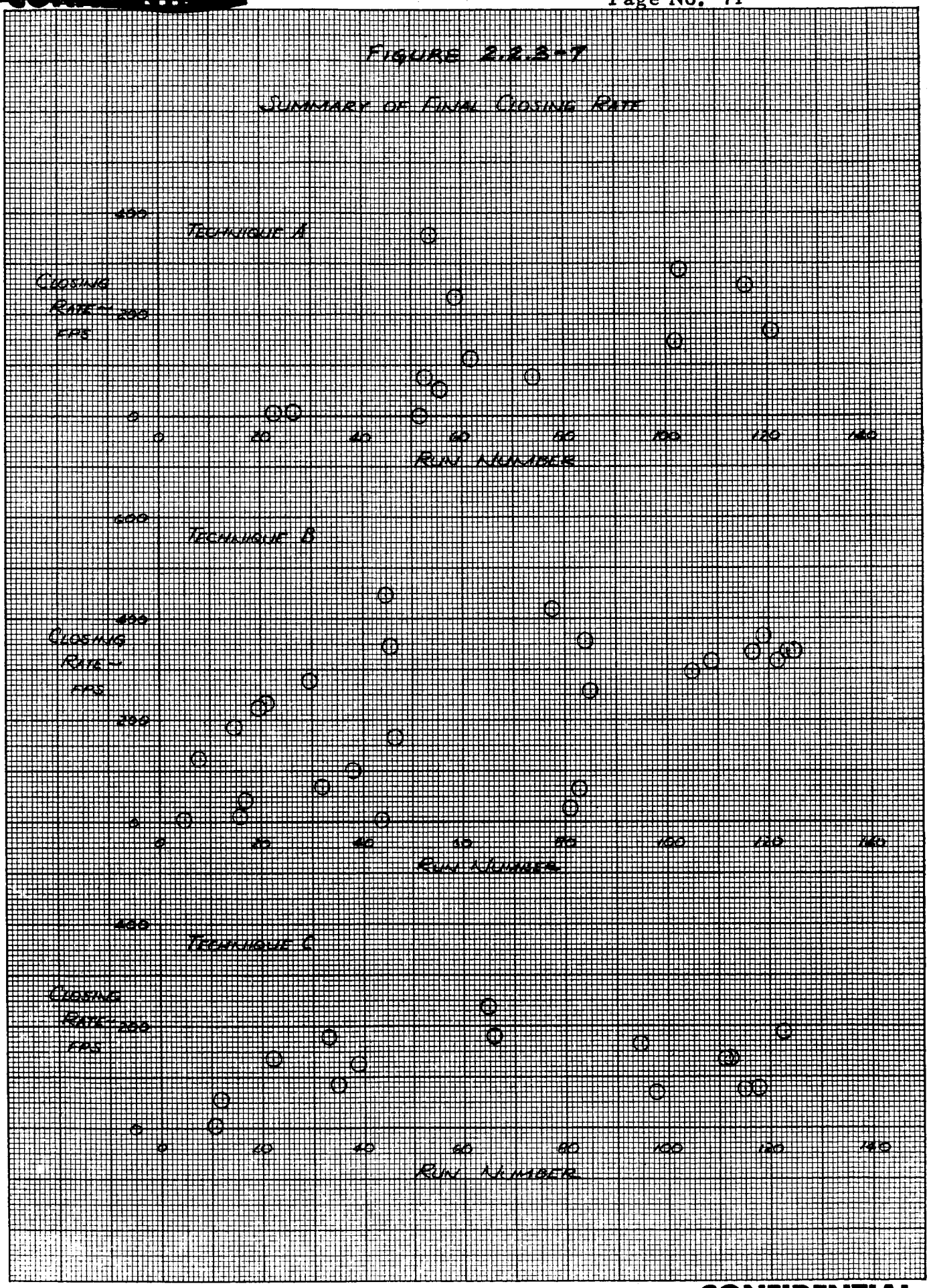

CONFIDENTIAL

range became less than 5000 feet. Reduction of the closing rate as range approached zero was usually not attempted. The closing rate is nearly constant over the final few miles of range. Therefore, the data of Figure 2.2.3-7 may be useful in the selection of realistic initial conditions for future rendezvous and docking studies.

Accurate control of the launch was definitely easier for Technique C than for A and B. Manual control of an abort launch by following a precalculated procedure (such as Tables 2.2.2-I and 2.2.2-II) is difficult for pilots to learn and is subject to large errors when mistakes are made. Control of altitude and vertical velocity (rather than a pitch program schedule) is similar to airplane maneuver requirements and is learned quickly and performed accurately by experienced pilots. Technique C was unanimously favored by the pilots participating in the simulation program. Technique B was less difficult to perform than A.

Off-nominal conditions were investigated by two methods.

(1) Abort launches were performed with a three percent reduction in launch engine thrust.

(2) The powered descent was initiated from off-nominal orbital conditions corresponding to an assumed 10 ft/sec increase in velocity at injection into the equi-period orbit. (At start of powered descent, altitude was approximately 20,000 feet too high and vertical velocity was about +20 ft/sec).

It was found that the three techniques investigated are capable of successful intercepts from these off-nominal conditions. No adverse

effects were noted for Techniques B and C. Reduced thrust caused low burnout speed for Technique A; however, this was compensated by the first midcourse correction.

Two intercept runs were performed in which the launch was initiated from the surface of the moon, 5^{o} out of the plane of the orbit of the CSM. The initial lead angle was optimum for a Hohmann intercept. The pitch program and results of the runs are presented in Table 2.2.3-I.

The procedure for run 93 was

(1) Use only attitude and time displays for launch (as in Technique A).

(2) Use midcourse correction charts to determine corrections required after burnout.

(3) Perform a plane change maneuver when crossing the plane of the target. (Attitude, target direction components, and line of sight angular rate components were the display data required.)

On Run 94, the procedure was more like Technique B.

(1) Vertical velocity was used during launch to circularize.

(2) A four minute park period was used to set the approximate lead angle desired.

(3) A velocity increment of 200 ft/sec was applied to inject into an intercept trajectory.

(4) After 20 minutes from injection, constant line of sight was maintained using the target and starfield background. No separate

TABLE 2.2.3-I

SURFACE LAUNCHES

Pitch Program	t~Sec	0	10	20	20-110	110-200	200-290	290-351
	θ~Deg	0	0	-63	-63	-73	-83	-93

Results

	Burnout			Intercept		
Run No.	V~Fps	h~Ft	$\dot{h}$~Fps	t~Min	*Fuel ΔV~Fps	Closing Rate~Fps
93	5570	53,000	32	74.2	6810	60
94		50,000	0	36.6	7360	503

* Includes Closing Rate

plane change maneuver is required because intercept occurs near the line of nodes.

Both runs were successful. Run 94 (Technique B) required more fuel. Some improvement in fuel required could possibly be realized with further practice.

An interesting quick intercept abort technique was briefly investigated during the simulator program. It consisted of launching into a circular orbit, thrusting toward the target to a closing rate of about 400 ft/sec, then maintaining constant line of sight direction to intercept. The technique was easy to control. Fuel requirements appeared to be reasonable. Unfortunately, the trajectory resulting from this procedure will always intersect the lunar surface if the rendezvous should fail to occur on the first attempt. However, it may be desirable to risk this type of procedure for certain emergencies requiring quick intercept.

3.0 CONCLUSIONS

(1) Launching directly to intercept burnout conditions results in a different intercept trajectory for each abort time. A hover phase or an orbital park phase is necessary if it is desired to standardize the intercept trajectory.

(2) A midcourse correction capability or highly accurate velocity and altitude displays are necessary to ensure that the intercept trajectory passes within a few miles of the target.

(3) Many different intercept techniques are possible. Any of the three methods investigated could be developed into successful abort techniques.

(4) Complete attitude information is required. Either a vertical velocity display during launch or tracking of the CSM during the midcourse coast phase is required for successful intercepts. It is not probable that a successful technique can be devised that utilizes no "radar type" information during all phases of the intercept mission.

(5) Fuel required for very late aborts is equivalent to an ideal velocity of approximately 7000 ft/sec for any of the three techniques investigated. The reduction in fuel requirements for earlier aborts is a function of the intercept technique.

(6) The use of a vertical velocity display near launch burnout greatly reduces the possibility of launching into a trajectory with pericynthion below the surface.

(7) Constant line of sight direction to the target can be maintained using the celestial background behind the target if it is not obscured by the moon's surface.

(8) The use of vertical velocity and altitude displays during launch enables a launch method to be used (Technique C) that is similar to airplane control techniques and is easily learned by experience pilots. All the pilots participating in the simulation program preferred this type of technique over the other two that were investigated.

(9) Manual control of an abort launch by following a pre-calculated procedure (Technique A) requires more time for pilots to learn and is subject to large errors when mistakes are made. However, with adequate training, this type of procedure can be successful.

(10) Preliminary studies indicate that the primary components for the display requirements for Technique C can be mechanized for a weight of approximately 57 pounds. The power requirement is estimated to be 259 watts.

REFERENCES

1. Moulton, F. R., "An Introduction to Celestial Mechanics," The McMillan Company, New York, 1915

2. Harrison, E., "Minimum Energy Space Rendezvous," Ph. D. Thesis, Michigan State University, 1962

3. Eggleston, John M., and Beck, Harold, D., "A Study of Positions and Velocities of a Space Station and a Ferry Vehicle and Return," NASA Technical Report R-87, 1961

4. LFE Electronics, "Radar System for Lunar Landing and Rendezvous," Volume II, 20 August 1962

APPENDIX A

LAUNCH CALCULATIONS

List of Symbols

ϕ - Central angle included by CSM radius and reference radius (radius through pericynthion of descent transfer orbit).

ϕ - Central angle included by LEM radius and reference radius.

β - Lead angle (the difference, $\phi - \phi$).

R - CSM radius in circular orbit.

r - LEM radius.

v - LEM velocity.

γ - LEM path angle.

i - Subscript denoting value at LEM injection into return transfer orbit.

$\Delta\eta(r)$ - Central angle traversed by LEM from injection to point on orbit with radius .

$\Delta t(r)$ - Time elapsed from LEM injection to point on orbit with radius .

ω_c - CSM angular orbital velocity.

T - Period of LEM return orbit.

a - Semi-major axis of LEM return orbit.

e - Eccentricity.

EN - Energy of LEM return orbit.

p - Semilatur rectum of LEM return orbit.

H - Angular momentum of LEM return orbit.

α - Angle included by LEM thrust vector and velocity vector.

List of Symbols (Cont'd)

h - LEM altitude.

$\left(\frac{T}{W_i}\right)$ - Initial thrust-to-weight of LEM.

I_s - Specific impulse of LEM rocket engine.

θ - Angle included by LEM longitudinal axis and horizontal at position of abort launch.

LAUNCH CALCULATIONS

The calculations required to describe the family of reference abort launch trajectories for the LEM, which intercept with the CSM, involve two analyses: (1) the determination of injection condition values and (2) the calculation of abort launch trajectories which meet the injection conditions. The equations and approach used in performing the calculations for these two analyses are described in the following paragraphs.

Development of Injection Requirements

Let ϕ_i and ϕ_i denote the angles included by the radius vector through the pericynthion of the equi-period descent transfer orbit and the respective radii of the CSM and LEM at the time of abort launch termination. Their difference, $\phi_i - \phi_i$, is the lead angle denoted by β_i. The symbols R (a constant) and $r(t)$ denote the respective radii of the CSM and the LEM. The relative position of the two vehicles at any time after abort launch termination, or transfer orbit injection, is completely determined by β_i, the LEM injection velocity (v_i), injection altitude (h_i), and injection path angle (γ_i).

The injection altitude is fixed at 50,000 feet and the flight path angle is zero. This choice is made primarily to assure that the transfer orbit does not intersect with the surface of the moon. There remains to be determined the relation between β_i and v_i which leads to intercept.

We may write the general expression for the central angle (change in true anamoly) traversed from injection by the LEM and the time elapsed from injection in terms of the LEM radius.

1. $\Delta\eta = \Delta\eta(r)$

2. $\Delta t = \Delta t(r)$

The first condition for intercept is that the LEM and CSM radii are equal. The second condition is that their respective central angles, measured from a common reference, are equal. Then the intercept equation is,

3. $\phi = [\Delta t(R)] = \phi(R)$

and, expressed in terms of injection conditions,

$$[\phi_i + \omega_c \Delta t(R)] - [\phi_i + \Delta\eta(R)] = 0$$

or

4. $\beta_i = -[\omega \Delta t(R) - \Delta\eta(R)]$

where, (recalling that the injection path angle is zero)

ω = constant angular velocity of CSM

R = constant radius magnitude of CSM

5. $$\Delta t(R) = T - \frac{T}{2\pi}\left\{\cos^{-1}\left(\frac{a-R}{ae}\right) - e\sin\left[\cos^{-1}\left(\frac{a-R}{ae}\right)\right]\right\}$$

6. $$T = 2\pi a\sqrt{\frac{a}{\mu}} \qquad (\mu = 1.7298717 \times 10^{16}\ FT^3/SEC^2)$$

7. $$a = \frac{-\mu}{2EN}$$

8. $$EN = \frac{v_i^2}{2} - \frac{\mu}{(r_m + h_i)} \qquad (r_m = 5{,}702{,}400\ FT)$$

9. $$\Delta\eta(R) = 2\pi - \cos^{-1}\left(\frac{p-R}{eR}\right)$$

10. $$p = \frac{H^2}{\mu}$$

11. $$H = (r_m + h_i)\, v_i$$

12. $$e = \sqrt{1 - \frac{p}{a}}$$

These equations are written for the case of intercept occuring at the second intersection of the orbits of the two vehicles. Evaluating the equations 4 - 12, with values for V_i over a range from Hohmann velocity to equi-period velocity, yields the desired relation between lead angle and injection velocity required for intercept. This relation is shown in the body of the report by Figure 2.1.1-5.

Abort Launch Trajectories

Assumptions made for simulation of the abort launch trajectories are: (1) point mass LEM, (2) planar flight, (3) constant thrust and fuel consumption, and (4) a spherical, non-rotating moon. The equations of motion may be written,

1. $\dot{v} = a(t) \cos\alpha - g \sin\gamma$
2. $\dot{\gamma} = a(t) \frac{\sin\alpha}{v} - \left(\frac{g}{v} - \frac{v}{r}\right) \cos\gamma$
3. $\dot{h} = v \sin\gamma$
4. $\dot{\phi} = \frac{v}{r} \cos\gamma$

where

5. $a(t) = g_c \left(\frac{T}{W_i}\right) \frac{I_s}{I_s - \left(\frac{T}{W_i}\right)t}$ $\qquad (g_c = 32.174 \text{ FT/SEC}^2)$
6. $g = \frac{\mu}{r^2}$
7. $\alpha = \theta - (\phi - \gamma)$

For all reference abort launch trajectories,

$\left(\frac{T}{W_i}\right) = 0.4 \qquad I_s = 315$

$\theta = \theta_i + \dot{\theta} t \qquad (\theta_i, \dot{\theta} = \text{constants})$

At selected points in the nominal braking phase, the values for significant trajectory parameters were noted and transformed into initial conditions for abort launch, considering the maneuvers assumed to take place

between abort decision and abort launch. The initial conditions being fixed in this manner, only the values for θ_i, θ, and burning time, t_b, are free for selection in order to meet injection variables requirements. Systematic selection of the launch parameters and subsequent trajectory calculation by numerical integration on the IBM 7090 was used to iteratively converge upon the values which satisfied the injection conditions,

$$8. \begin{cases} h_i = 50{,}000 \\ \gamma_i = 0 \\ v_i = v_i(\beta_i) \end{cases}$$

The values for the launch parameters which were determined in this manner are given in Figures 2.1.1-2, 2.1.1-3, and 2.1.1-4.

A valuable by-product of this iterative approach for determining the launch parameters which result in intercept are system error sensitivity data also presented in the body of the report.

APPENDIX B

MIDCOURSE CORRECTIONS

This appendix describes the method of data determination and presentation for midcourse corrections to be used for LEM to CSM rendezvous. Orbital mechanics equations were solved by means of a digital computer to determine the velocity required to place the LEM on a coasting intercept trajectory with respect to the CSM. This problem and the method of solution is described in the following paragraphs.

Problem Statement

The space intercept problem is one of determining the velocity required to place a vehicle on a coasting trajectory between two points in space such that it traverses the path in a specified time. One terminal of the trajectory is determined by the position of the interceptor at initiation of the intercept maneuver and the other terminal by the predicted target position at the end of the specified intercept time. Thus, for the intercept problem, the following parameters are specified:

R_1, R_2 = Radii of terminal points (P_1, P_2)

$\Delta\phi$ = Difference between the true anomalies of P_1 and P_2 on the transfer ellipse.

T = Intercept time.

With these quantities specified, it is desired to determine the initial velocity, V_1, on the intercept trajectory.

Assumptions

The following assumptions were made in order to facilitate the solution of the orbital equations:

(1) The moon is spherical.

(2) Lunar gravity is the only outside disturbing force.

(3) The LEM and CSM are in coplanar orbits. The problem of out-of-plane effect is discussed in a special section on out-of-plane considerations.

Method of Solution

Under the assumption that the ephemeris of the CSM orbit will be known precisely, the aforementioned parameters (R_1, R_2, $\Delta\phi$) can be determined from position measurements relative to the CSM and the transfer time, T. The intercept trajectory between P_1 and P_2 can be determined by employing the method of Gauss (References 1, 2). This method makes use of equations developed from a comparison of the areas of the elliptical sector and the triangle between R_1 and R_2. The basic equation that must be solved is

$$\pm a_1 = \left[b_1 + \sin^2\left(\frac{\Delta E}{4}\right)\right]^{1/2} + \frac{(\Delta E - \sin \Delta E)}{\sin^3\left(\frac{\Delta E}{2}\right)} \left[b_1 + \sin^2(\Delta E/4)\right]^{3/2} \qquad \text{(B.1)}$$

where

$$a_1 = \frac{(\mu)^{1/2}}{\left[2 (R_1 R_2)^{1/2} \cos\left(\frac{\Delta\phi}{2}\right)\right]^{3/2}}$$

$$b_1 = \frac{R_1 + R_2}{4 (R_1 R_2)^{1/2} \cos\left(\frac{\Delta\phi}{2}\right)} - 1/2$$

where μ is the gravity constant of the moon.

The sign for a_1 is taken as

\+ for $\Delta\phi < 180°$

\- for $\Delta\phi > 180°$

The case for $\Delta\phi = 180°$ requires a separate equation which is

$$\mu^{1/2} T \left[2/(R_1 + R_2)\right]^{3/2} = \frac{\Delta E - \text{Sin}\ \Delta E}{\text{Sin}^3 \frac{\Delta E}{2}} \qquad (B.2)$$

Equations (B.1) and (B.2) must be solved by trial and error to obtain ΔE, the change in eccentric anomaly corresponding to $\Delta\phi$. With ΔE known, the transfer ellipse elements, of which the coasting trajectory is a segment, can be determined by solving the equations:

semilatus rectum -

$$p = \frac{2 R_1 R_2 \ \text{Sin}^2 \left(\frac{\Delta\phi}{2}\right)}{R_1 + R_2 - 2(R_1 R_2)^{1/2} \ \text{Cos}\left(\frac{\Delta\phi}{2}\right) \ \text{Cos}\left(\frac{\Delta E}{2}\right)} \qquad (B.3)$$

semimajor axis -

$$a = \frac{R_1 + R_2 - 2(R_1 R_2)^{1/2} \ \text{Cos}\left(\frac{\Delta\phi}{2}\right) \ \text{Cos}\left(\frac{\Delta E}{2}\right)}{2 \ \text{Sin}^2 \left(\frac{\Delta E}{2}\right)} \qquad (B.4)$$

eccentricity -

$$e = \left(\frac{a - p}{a}\right)^{1/2} \qquad (B.5)$$

After these ellipse elements are determined, the initial and final value of the true anomaly, ϕ, can be determined from the orbital mechanics equation

$$\phi_n = \text{Cos}^{-1} \left(\frac{p - R_n}{e R_n}\right); \quad n = 1, 2. \qquad (B.6)$$

The velocities and flight path angles can be obtained by first determining the vertical and horizontal components of velocity at P_1 and P_2 from the equations

$$(V_x)_n = (R\dot{\phi})_n = \frac{(\mu p)^{1/2}}{R_n} \quad ; \quad n = 1, 2 \tag{B.7}$$

$$(V_y)_n = \dot{R}_n = \left(\frac{\mu}{p}\right)^{1/2} e \sin \phi_n; \; n = 1,2 \tag{B.8}$$

and then, the total velocity is given by

$$V_n = \sqrt{(V_x)_n^2 + (V_y)_n^2} \; ; \quad n = 1, 2 \tag{B.9}$$

The flight path angle is given by

$$\gamma_n = \tan^{-1}\left(\frac{V_y}{V_x}\right); \; n = 1, 2 \tag{B.10}$$

A routine was developed for the solution of the above equations on an IBM 7090 digital computer.

Results

Velocity intercept data was obtained in several forms and for a wide range of initial conditions.

With respect to the axis system shown on Figure B.1, data was obtained for initial conditions corresponding to target positions in the first three quadrants (θ = 0° to 270°), and for separation distances up to 2 x 10^6 ft. Data was not obtained for the fourth quadrant (θ = 270° - 360°) because an examination of relative position during the traversal of trajectories that could be used shows that the target vehicle would never be in the fourth quadrant except at very close ranges.

The initial velocity required for intercept was obtained from the computer runs in three forms: (1) total velocity and flight path angle, (2) radial and tangential components of velocity, and (3) relative velocity in terms of range rate and angular rate of the line of sight between the LEM and CSM.

The relative velocity data was selected for further study and application because it is believed that it could be measured with greater accuracy than would be possible for the other forms listed.

Midcourse correction charts were prepared using the relative position and velocity data and are included at the end of this appendix. From these charts, the range rate, $\dot{r}$, and line-of-sight inertial angular rate, $\dot{\theta}$, necessary to achieve an intercept can be determined. The variables $\frac{\dot{r}}{10^{-3}r}$ and $\frac{\dot{\theta}}{10^{-3}}$ are plotted versus elevation angle, E. These ratios are plotted for each 1000 seconds of intercept time up to 6000 seconds. In order to use the charts, it is necessary to know the position quadrant of the target (I ~ θ = 0°-90°; II - 90°-180°; etc.). At the top of each chart there is a symbol, a circle with one quadrant shaded, which denotes the quadrant for which the particular chart is applicable. In addition, heading information indicates the variable sought and the range increment over which the chart is applicable. It was originally hoped that only one chart would be needed for the entire range of interest, but the variation in parameters proved to be too great. Consequently, plots were made for each 200,000 feet increment of range between 400,000 and 2×10^6 ft. It was found that one chart was sufficient for a range up to 400,000 feet. Each curve is exact for the midpoint of each range increment. Thus, maximum error would exist at an increment boundary. However, the error introduced is not large. The approximate error can be determined by taking one-half the difference of values read from curves for two adjacent increments. For example, from the 600,000 - 800,000 feet and 800,000 - 1,000,000 feet increments in the second quadrant, the $\dot{\theta}$ error is found to be approximately 0.012×10^{-3} rad/sec and the $\dot{r}$ error approximately 4 ft/sec at the

increment boundaries for E = 10° and a rendezvous time of 3000 sec. Errors decrease as range decreases.

Out-of-Plane Considerations

Two items are of primary interest concerning non-coplanar maneuvers. One is the procedure to be used to maneuver into the target plane and the other is the effect upon values obtained from the previously described midcourse correction charts.

For moderate out-of-plane distances, the midcourse correction chart values would not be significantly affected. This may be seen by first writing the equations for the in-plane velocities in term of velocities out-of-plane (Figure B.2).

The relationship is given by

$$\begin{matrix} \text{In-plane} \\ \begin{bmatrix} \dot{r}_{ip} \\ V_{Eip} \\ V_{Bip} \end{bmatrix} \end{matrix} = \begin{bmatrix} \text{Cos B} & 0 & \text{-Sin B} \\ 0 & 1 & 0 \\ \text{Sin B} & 0 & \text{Cos B} \end{bmatrix} \begin{matrix} \text{Out-of-plane} \\ \begin{bmatrix} \dot{r}_{op} \\ V_{Eop} \\ V_{Bop} \end{bmatrix} \end{matrix} \quad \text{(B.11)}$$

or

$$V_{ip} = D\, V_{op}$$

Now the desired in-plane velocities can be stated as

$$\dot{r}_{ip} = C_1 \qquad r_{ip} = C_1\, r_{op}\, \text{Cos B}$$

$$V_{Eip} = C_2 \qquad r_{ip} = C_2\, r_{op}\, \text{Cos B}$$

$$V_{Bip} = V_3$$

where C_1 and C_2 are the values read from the midcourse correction charts for $\frac{\dot{r}}{10^{-3}r}$ and $\frac{\dot{\Theta}}{10^{-3}}$.

The out-of-plane velocities required to achieve these desired in-plane values can be determined by substitution into equation B.11 and

solving for the sought parameters as

$$\begin{bmatrix} \dot{r}_{op} \\ V_{Eop} \\ V_{Bop} \end{bmatrix} = D^{-1} Vi = \begin{bmatrix} \text{Cos } B & 0 & \text{Sin } B \\ 0 & 1 & 0 \\ -\text{Sin } B & 0 & \text{Cos } B \end{bmatrix} \begin{bmatrix} C_1 r_{op} \text{ Cos } B \\ C_2 r_{op} \text{ Cos } B \\ V_3 \end{bmatrix} \quad \text{(B.12)}$$

As B approaches zero, this equation becomes

$$\begin{bmatrix} \dot{r}_o \\ V_{Eop} \\ V_{Bop} \end{bmatrix} = \begin{bmatrix} 1 & 0 & 0 \\ 0 & 1 & 0 \\ 0 & 0 & 1 \end{bmatrix} \begin{bmatrix} C_1 & r_{ip} \\ C_2 & r_{ip} \\ & V_3 \end{bmatrix} \quad \text{(B.13)}$$

The effect of a small out-of-plane distance can best be determined by showing an example. Let the out-of-plane distance be 10 NM and the range 50 NM, then B = 11.5°. Also assume values of

$$\dot{r}_{cp} = C_1 r_{op} = 400 \text{ ft/sec}$$

$$V_{Eop} = C_2 r_{op} = 400 \text{ ft/sec}$$

$$V_{Bop} = V_3 = 20 \text{ ft/sec}$$

where the first two are values that would be obtained from the midcourse correction charts and the value for V_3 corresponds to a representative value for the considered out-of-plane distance. These velocities are the values that would be used if out-of-plane effects were neglected.

From a substitution into equation (B.12), the correct velocities are determined as

$$\dot{r}_{op} = 388 \text{ ft/sec}$$

$$V_{Eop} = 392 \text{ ft/sec}$$

Thus errors would be 12 and 8 ft/sec, respectively. This is not enough error to seriously affect the intercept trajectory for early corrections.

Actually, out-of-plane error effects can be minimized by a procedure which allows the interceptor and target to become coplanar after a time period equal to one-fourth of the target orbit period or less.

Motion perpendicular to the target plane is described quite accurately by the equation $y = y_o \text{ Cos } \omega t + \frac{\dot{y}_o}{\omega} \text{ Sin } \omega t$.[3] (B.14)

Thus, if $\dot{y}_o$ can be brought to zero or given a negative value (corresponding to motion toward the target plane), y will go to zero in a time of

$$t = \frac{\pi}{2\omega}$$

or less. Such can be achieved by thrusting to make the angular rate, $\dot{B}$, zero or negative. Then, when the interceptor and target become coplanar, $\dot{B}$ is once again brought to zero in order that subsequent motion remain coplanar.

LIST OF SYMBOLS

a	-	Semimajor axis of transfer ellipse.
a_1	-	Dimensionless group.
B	-	Angle formed between the orbital plane of the interceptor and the line-of-sight between the interceptor and target.
b_1	-	Dimensionless group.
E	-	Angle of elevation. Angle between the line-of-sight from interceptor to target and local horizontal. Angle is measured from 0-90 degrees.
ΔE	-	Difference between the eccentric anomalies of P_1 and P_2 on the transfer ellipse.
e	-	Eccentricity of transfer ellipse.
P	-	Space terminal.
p	-	Semilatus rectum of transfer ellipse.
R	-	Radius of orbiting vehicle measured from the center of the moon.
$\dot{r}$	-	Range rate.
T	-	Total transfer time.
V	-	Velocity along the flight path.
γ	-	Flight path angle measured between velocity vector and local horizontal.
μ	-	Moon gravity constant = $1.7298717 \times 10^{14} \frac{ft^3}{sec^2}$
ϕ	-	True anomaly of transfer ellipse.
$\Delta\phi$	-	Difference between the true anomalies of P_1 and P_2 on the transfer ellipse.

LIST OF SYMBOLS (Cont'd)

θ - Angle between line-of-sight from the interceptor to target and local horizontal. Angle is measured from 0-360 degrees.

$\dot{\theta}$ - Line-of-sight inertial angular rate.

ω - Angular velocity of circular orbit.

Subscripts

1, 2 - Denote starting point and destination on a transfer trajectory respectively.

ip, op - Denote in-plane and out-of-plane, respectively.

FIGURE B.1

ORBITAL INTERCEPT ILLUSTRATION

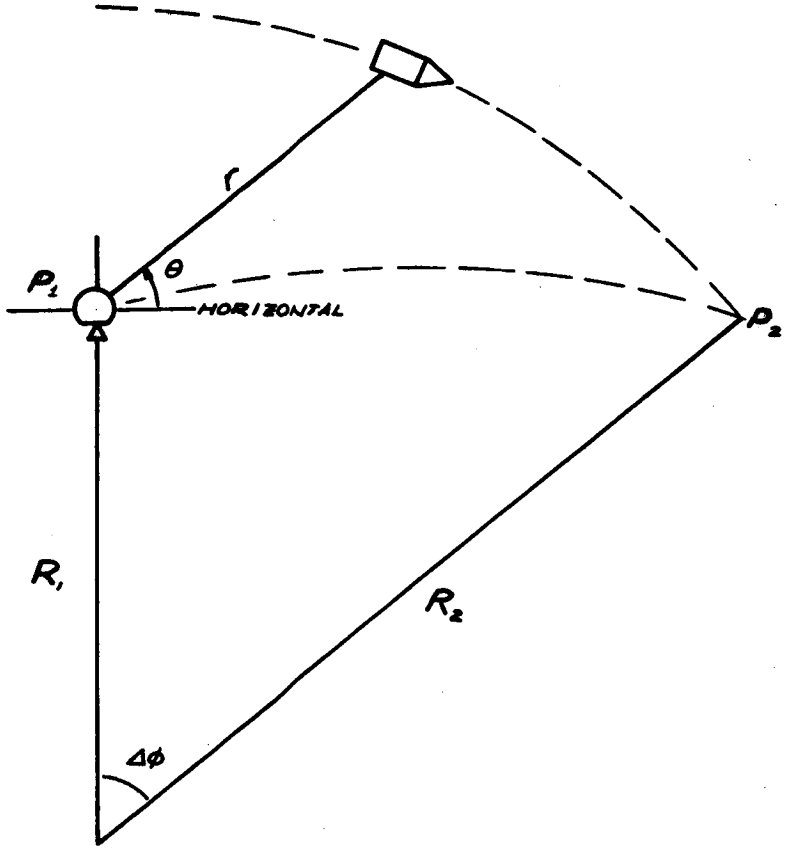

FIGURE B.2

IN PLANE AND OUT-OF-PLANE VELOCITIES

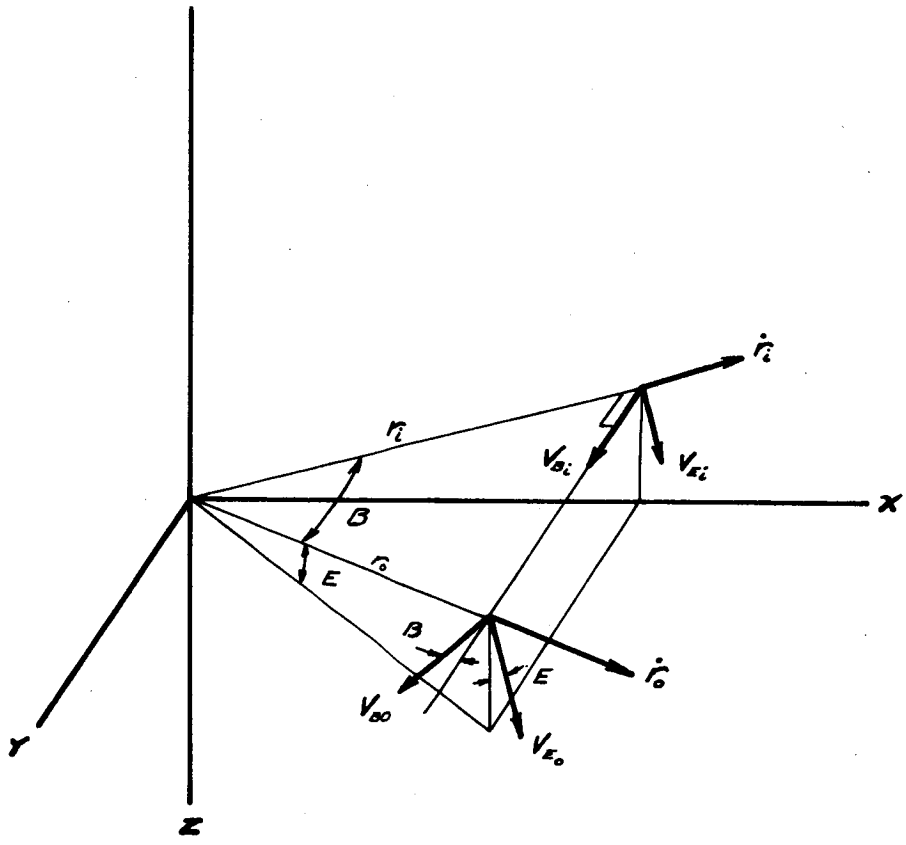

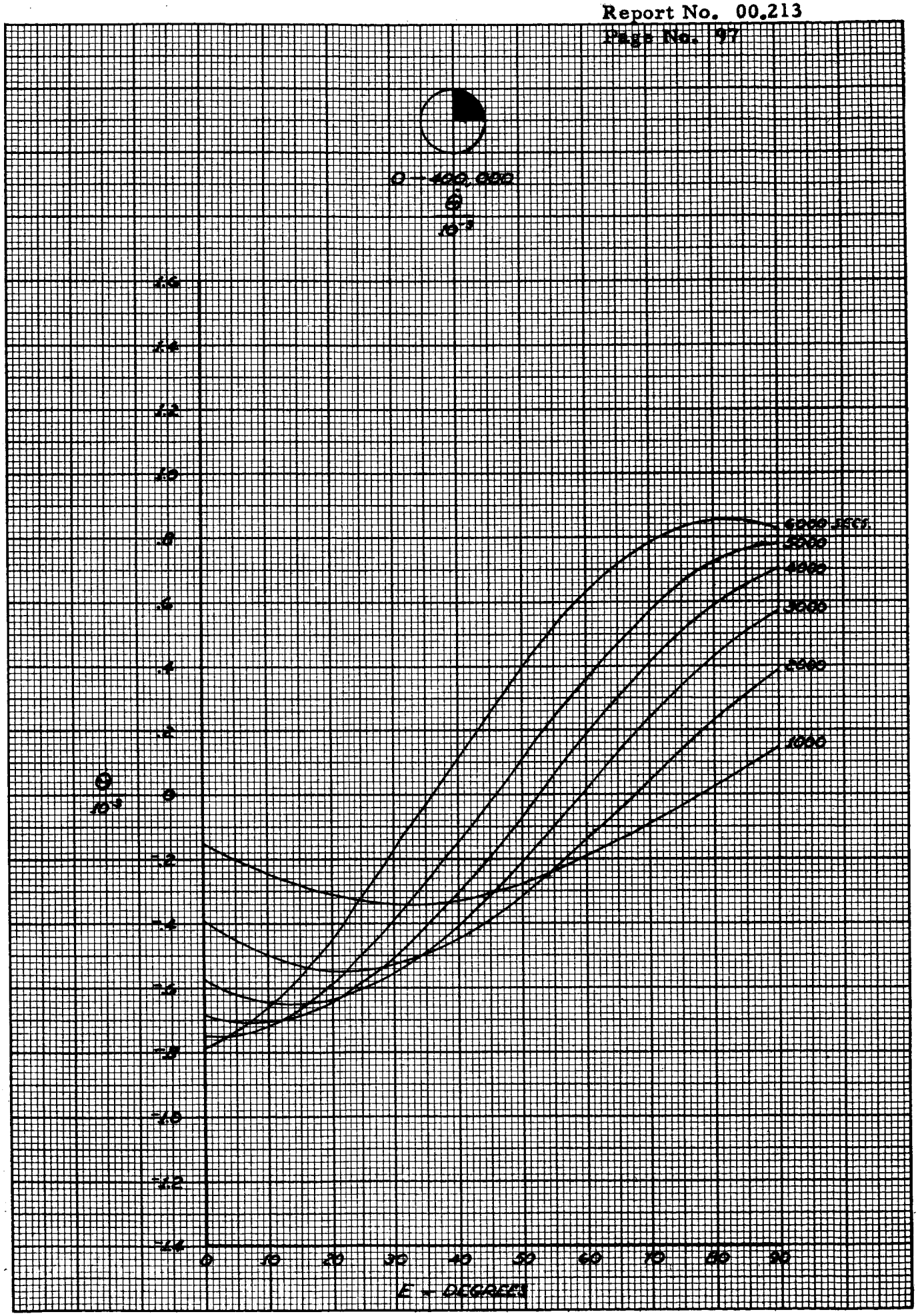
Θ - 400,000
Θ
10⁻³
.16
.14
.12
.10
.8
.6
.4
.2
0
-.2
-.4
-.6
-.8
-.10
-.12
-.14
Θ
10⁻³
6000 RPM
5000
4000
3000
2000
1000
0
10
20
30
40
50
60
70
80
90
E - DEGREES

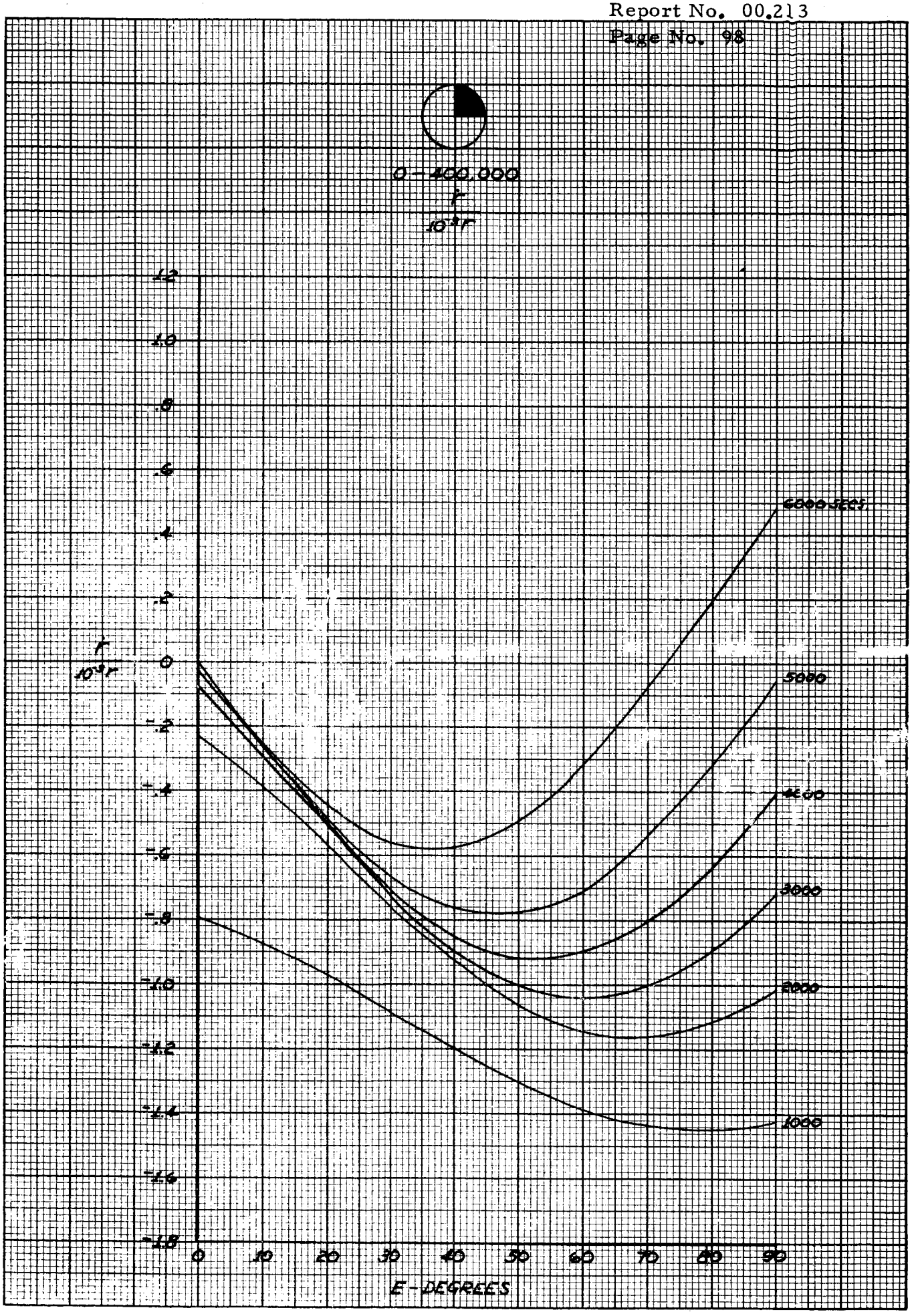
0 - 400,000
r
10^{-3}r
1.2
1.0
.8
.6
.4
.2
0
-.2
-.4
-.6
-.8
-1.0
-1.2
-1.4
-1.6
-1.8
r
10^{-3}r
6000 SECS.
5000
4000
3000
2000
1000
0
10
20
30
40
50
60
70
80
90
E - DEGREES

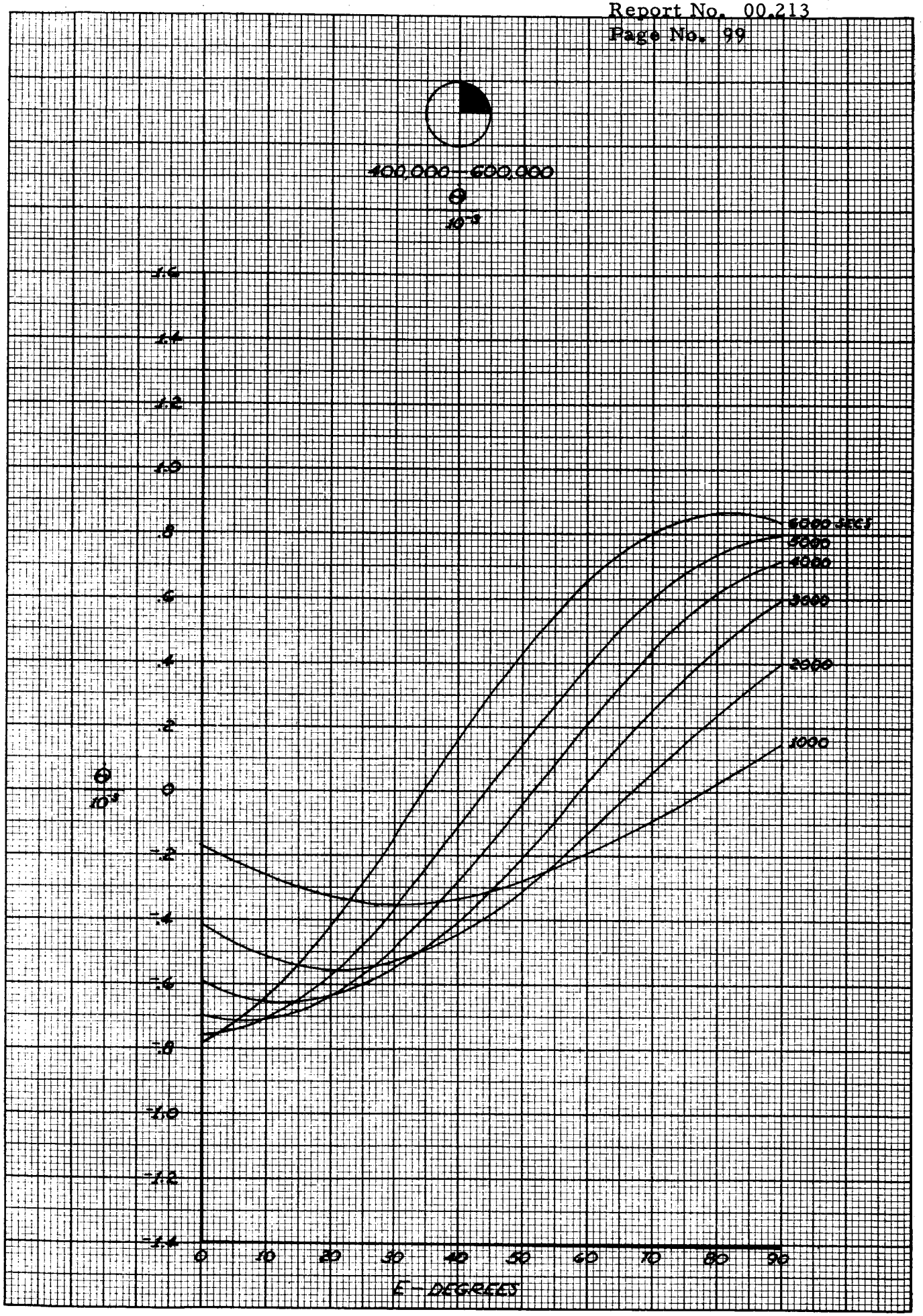
400,000 – 600,000
Φ
10⁻³
1.6
1.4
1.2
1.0
.8
.6
.4
.2
0
-.2
-.4
-.6
-.8
-1.0
-1.2
-1.4
Φ
10⁻³
6000 Kc/s
5000
4000
3000
2000
1000
0
10
20
30
40
50
60
70
80
90
E – DEGREES

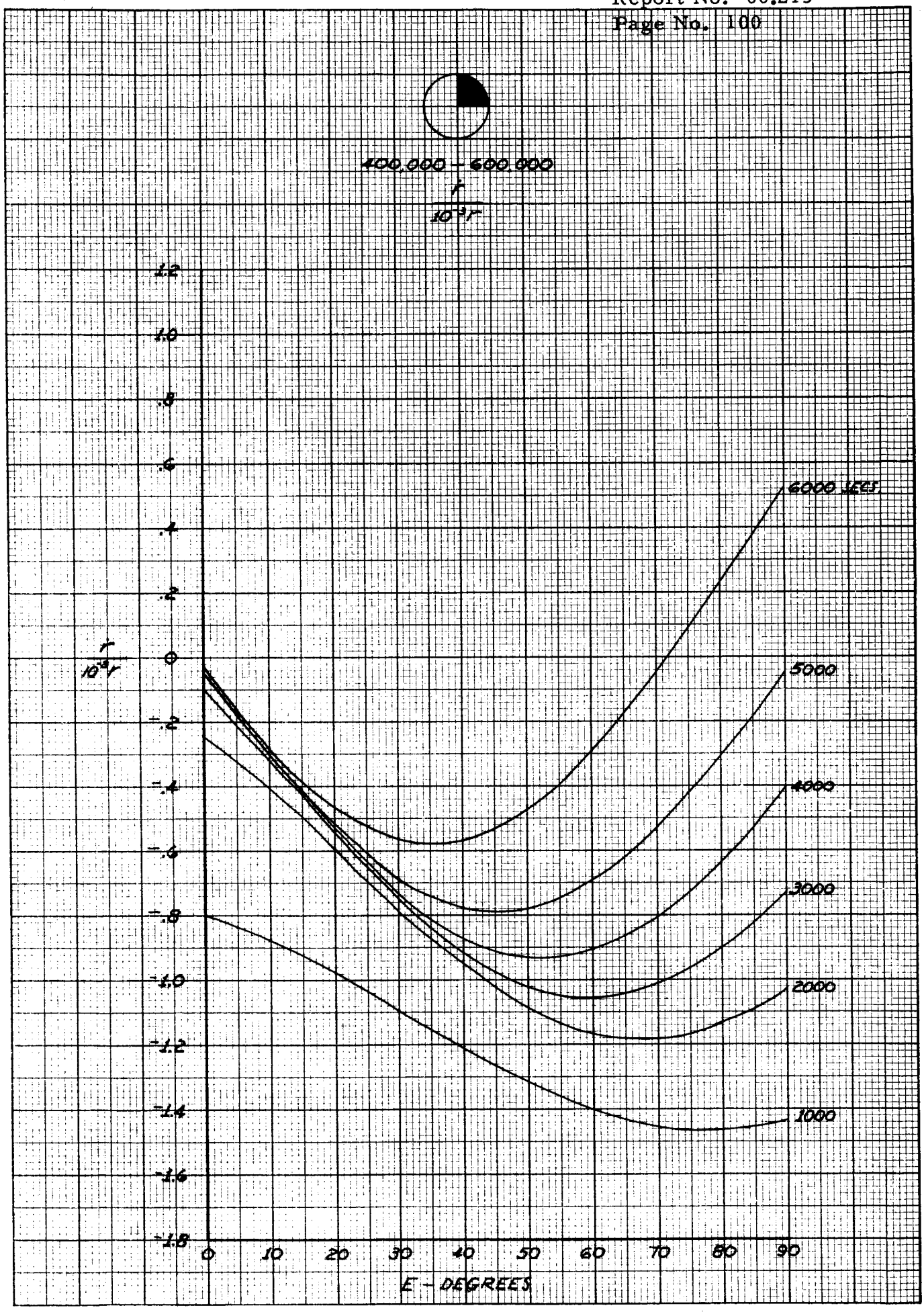
400,000 – 600,000
r
10⁻³r
1.2
1.0
.8
.6
.4
.2
0
-.2
-.4
-.6
-.8
-1.0
-1.2
-1.4
-1.6
-1.8
r
10⁻³r
6000 FEET
5000
4000
3000
2000
1000
0
10
20
30
40
50
60
70
80
90
E - DEGREES

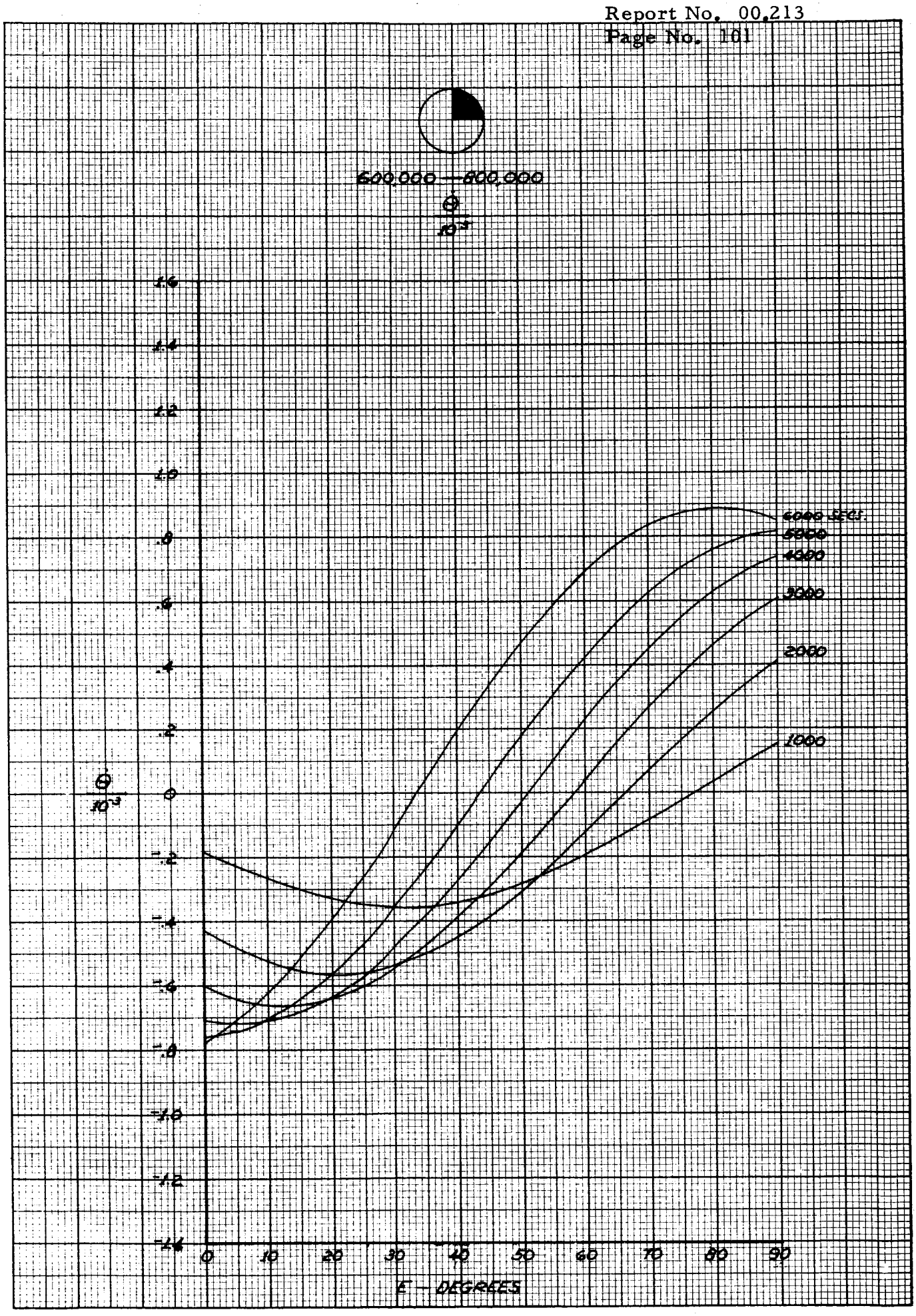
600,000 — 800,000
Φ / 10⁻³
1.6
1.4
1.2
1.0
.8
.6
.4
.2
0
-.2
-.4
-.6
-.8
-1.0
-1.2
-1.4
6000 SEC.
5000
4000
3000
2000
1000
0
10
20
30
40
50
60
70
80
90
ε — DEGREES

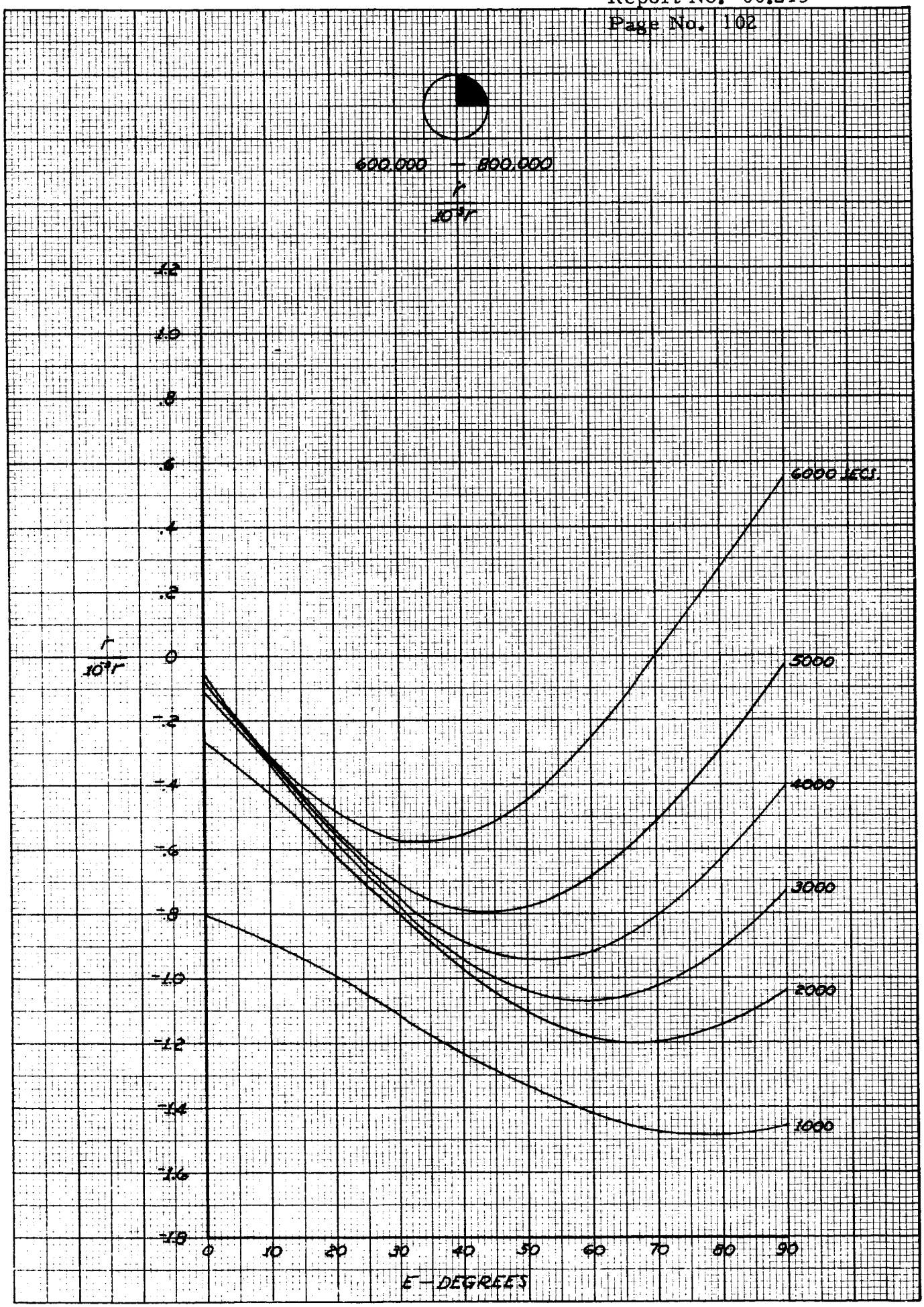
600,000 — 800,000
r
10^{3}r
4.2
4.0
.8
.6
.4
.2
0
-.2
-.4
-.6
-.8
-1.0
-1.2
-1.4
-1.6
-1.8
r
10^{3}r
6000 LEGS.
5000
4000
3000
2000
1000
0
10
20
30
40
50
60
70
80
90
ε — DEGREES

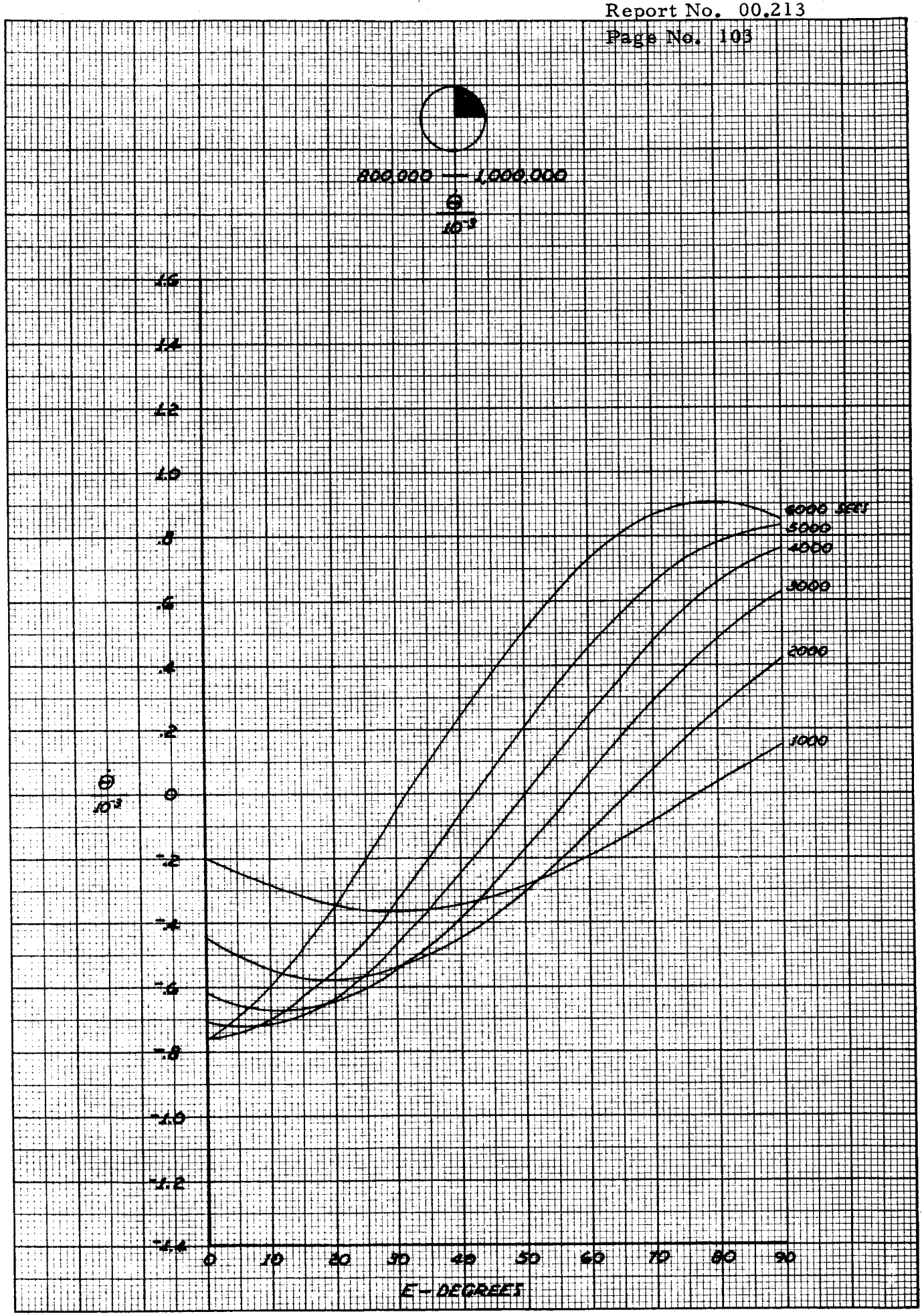
800,000 — 1,000,000
Φ / 10⁻³
1.6
1.4
1.2
1.0
.8
.6
.4
.2
0
-.2
-.4
-.6
-.8
-1.0
-1.2
-1.4
Φ / 10⁻³
6000 RPM
5000
4000
3000
2000
1000
0
10
20
30
40
50
60
70
80
90
E - DEGREES

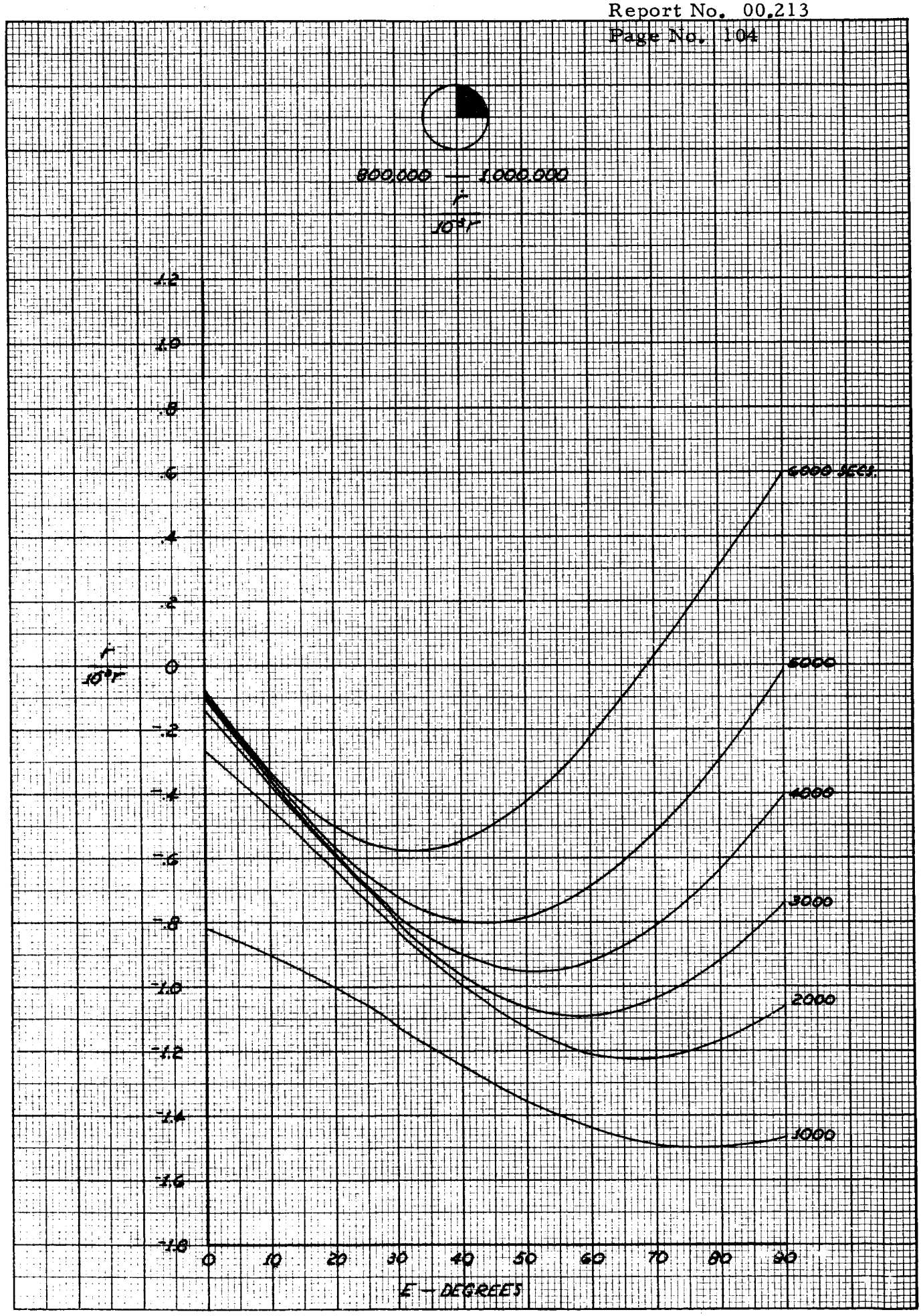
800,000 — 1,000,000
$\frac{\dot{r}}{10^3 r}$
$\frac{\dot{r}}{10^3 r}$
-1.2
-1.0
-.8
-.6
-.4
-.2
0
-.2
-.4
-.6
-.8
-1.0
-1.2
-1.4
-1.6
-1.8
6000 SEC.
5000
4000
3000
2000
1000
0
10
20
30
40
50
60
70
80
90
ε — DEGREES

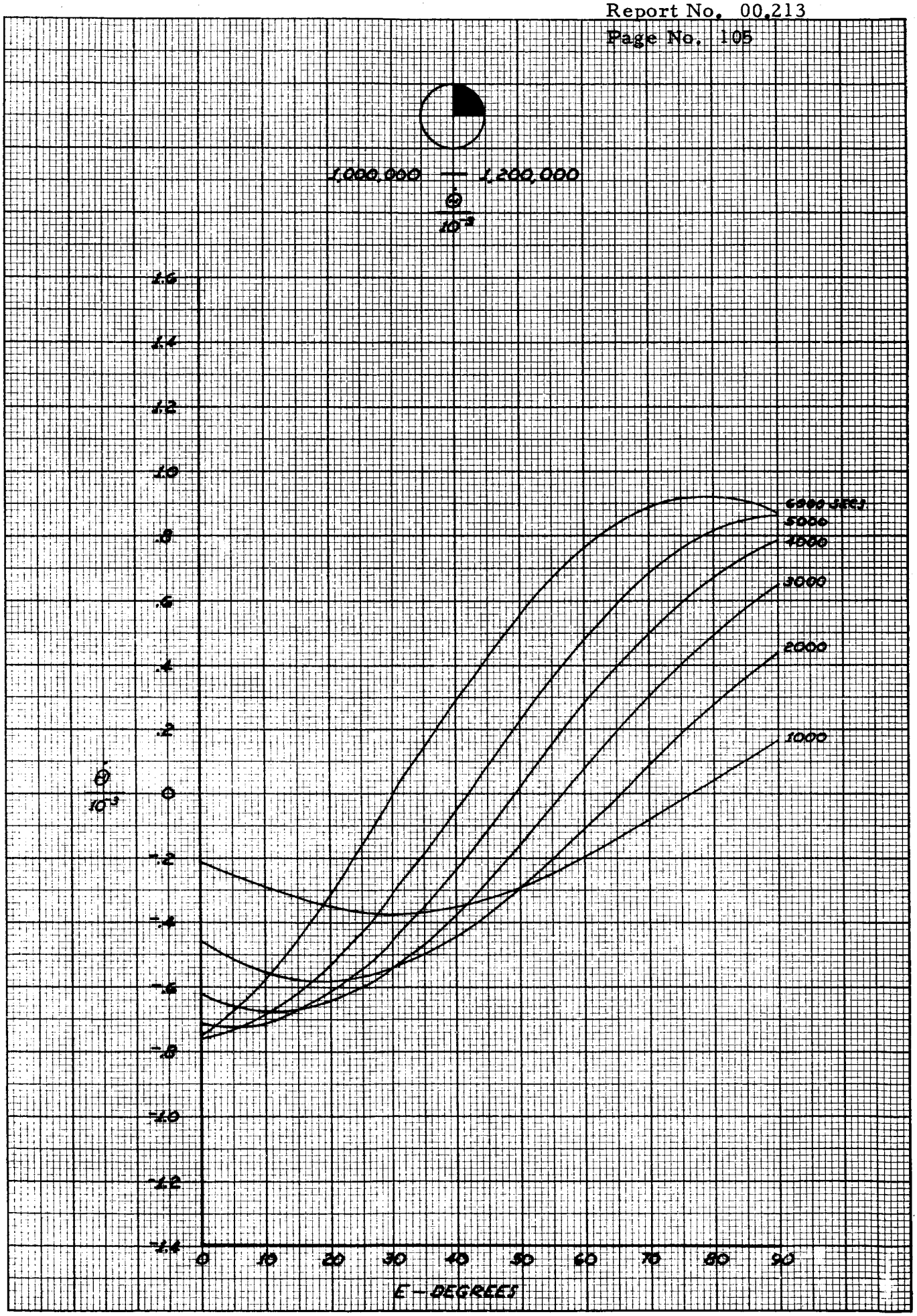
1,000,000 — 1,200,000
Φ / 10⁻³
1.6
1.4
1.2
1.0
.8
.6
.4
.2
0
-.2
-.4
-.6
-.8
-1.0
-1.2
-1.4
6000 (EST.)
5000
4000
3000
2000
1000
0
10
20
30
40
50
60
70
80
90
E - DEGREES

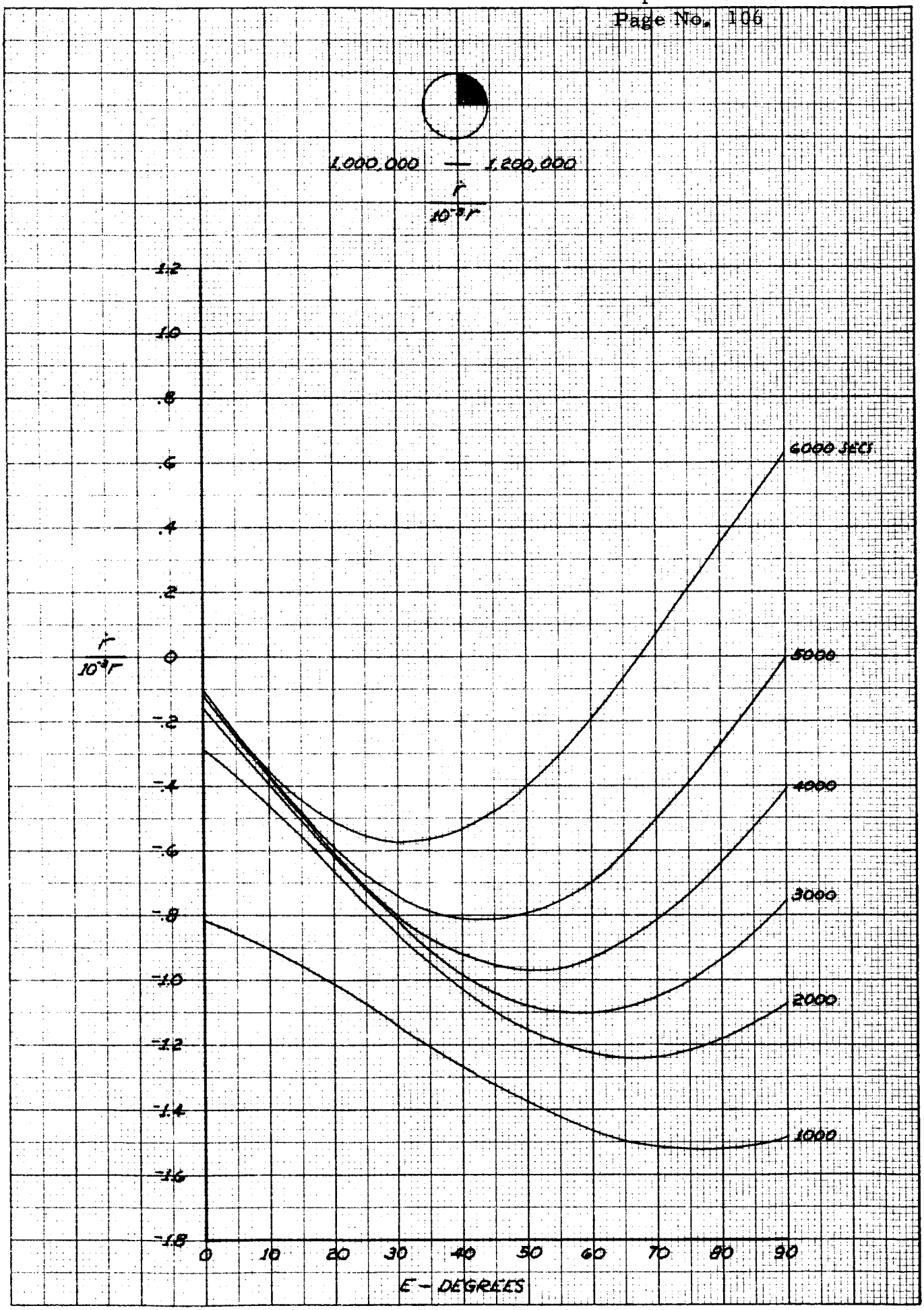
1,000,000 — 1,200,000
$\frac{\dot{r}}{10^{-3}r}$
1.2
1.0
.8
.6
.4
.2
0
-.2
-.4
-.6
-.8
-1.0
-1.2
-1.4
-1.6
-1.8
6000 SECS
5000
4000
3000
2000
1000
0
10
20
30
40
50
60
70
80
90
E - DEGREES

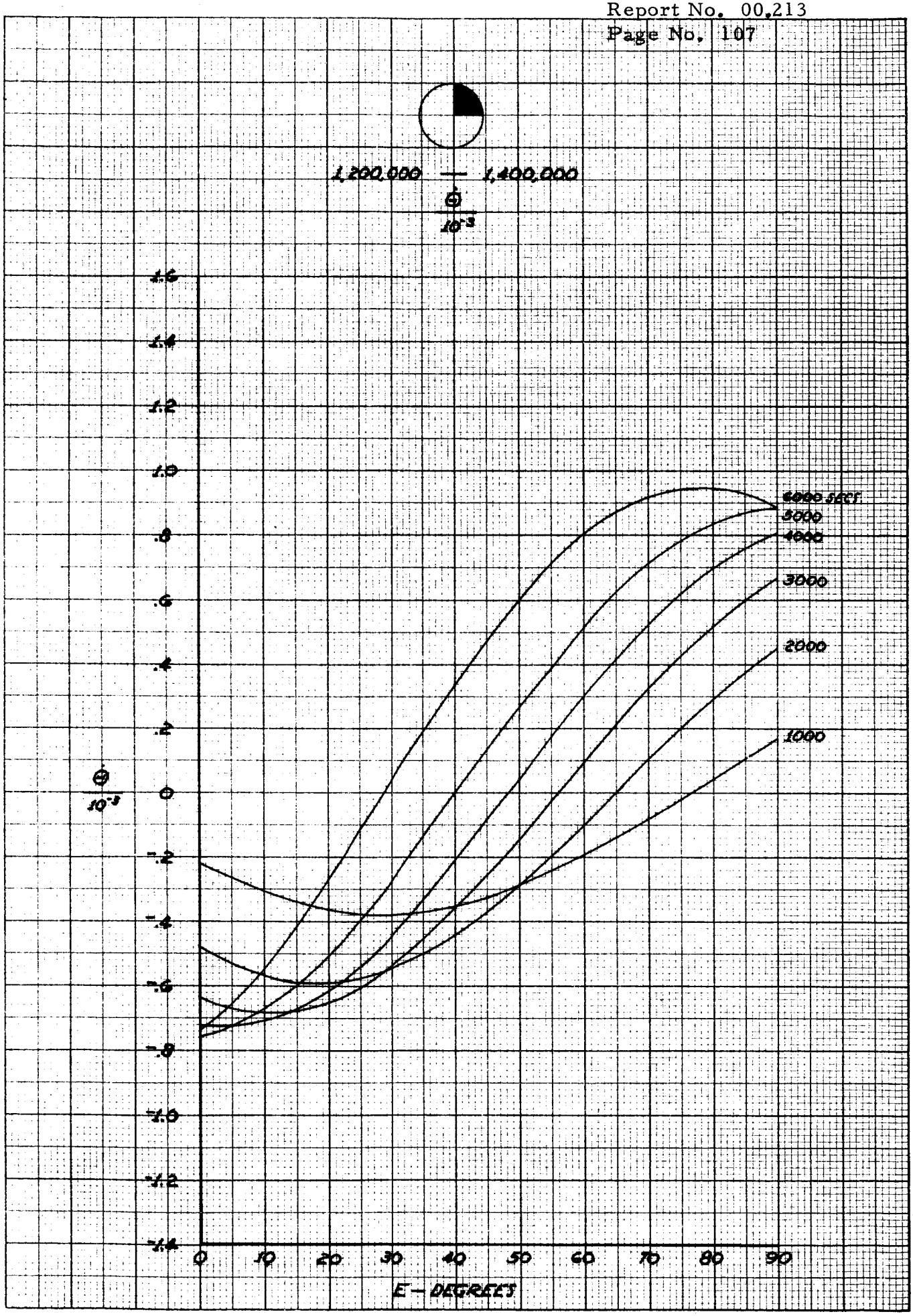
1,200,000 — 1,400,000
Φ / 10⁻³
1.6
1.4
1.2
1.0
.8
.6
.4
.2
0
-.2
-.4
-.6
-.8
-1.0
-1.2
-1.4
6000 SECT.
5000
4000
3000
2000
1000
0
10
20
30
40
50
60
70
80
90
E - DEGREES

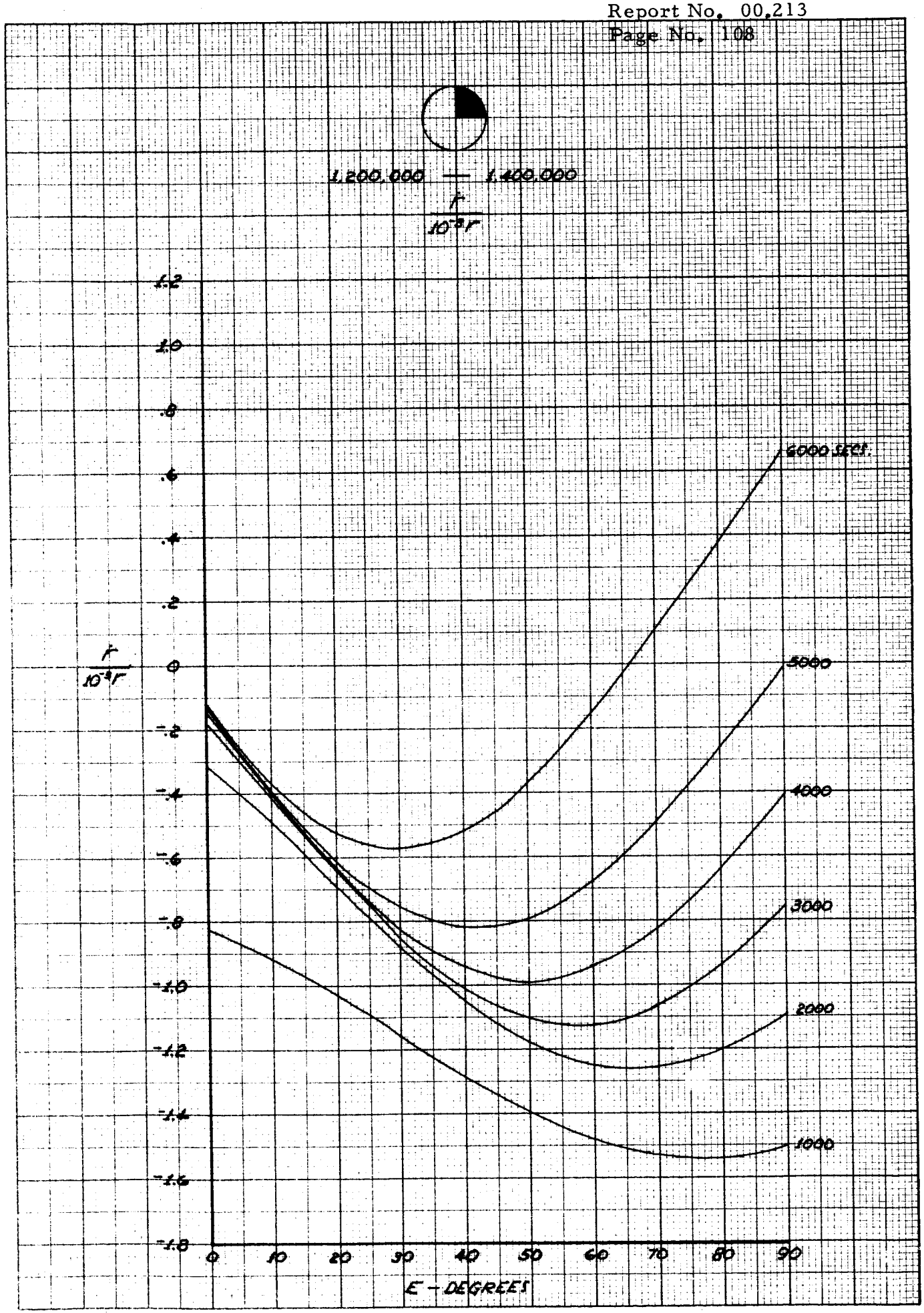
1,200,000 — 1,400,000
F
10⁻³F
1.2
1.0
.8
.6
.4
.2
0
-.2
-.4
-.6
-.8
-1.0
-1.2
-1.4
-1.6
-1.8
F
10⁻³F
6000 FEET
5000
4000
3000
2000
1000
0
10
20
30
40
50
60
70
80
90
E - DEGREES

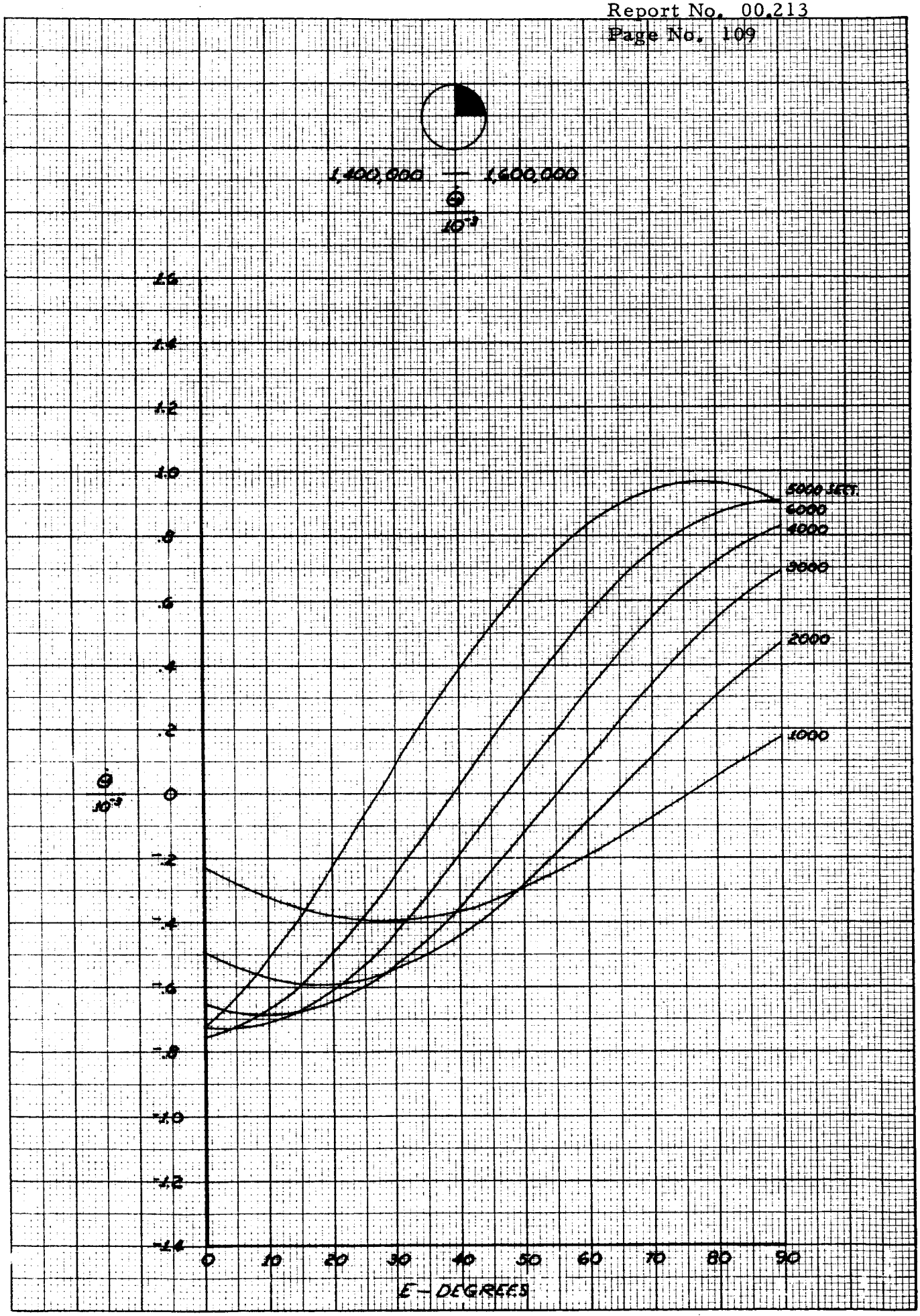
1,400,000 — 1,600,000
Φ
10⁻⁹
1.6
1.4
1.2
1.0
.8
.6
.4
.2
0
-.2
-.4
-.6
-.8
-1.0
-1.2
-1.4
Φ
10⁻⁹
0
10
20
30
40
50
60
70
80
90
E - DEGREES
5000 ALT.
6000
4000
3000
2000
1000

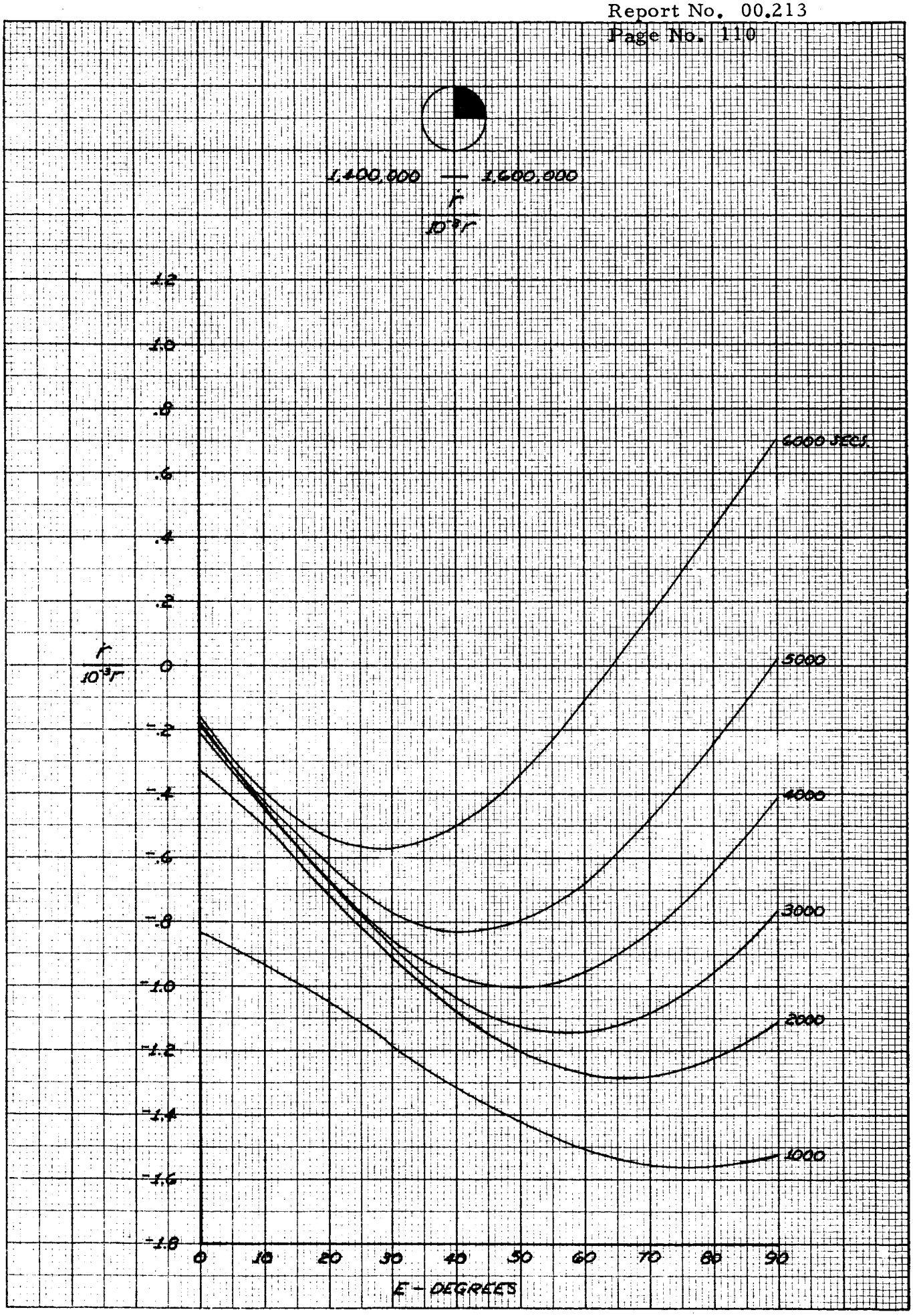
1,400,000 — 1,600,000
$\dot{r}$
$10^{-3}r$
1.2
1.0
.8
.6
.4
.2
0
-.2
-.4
-.6
-.8
-1.0
-1.2
-1.4
-1.6
-1.8
6000 SECS.
5000
4000
3000
2000
1000
0
10
20
30
40
50
60
70
80
90
E - DEGREES

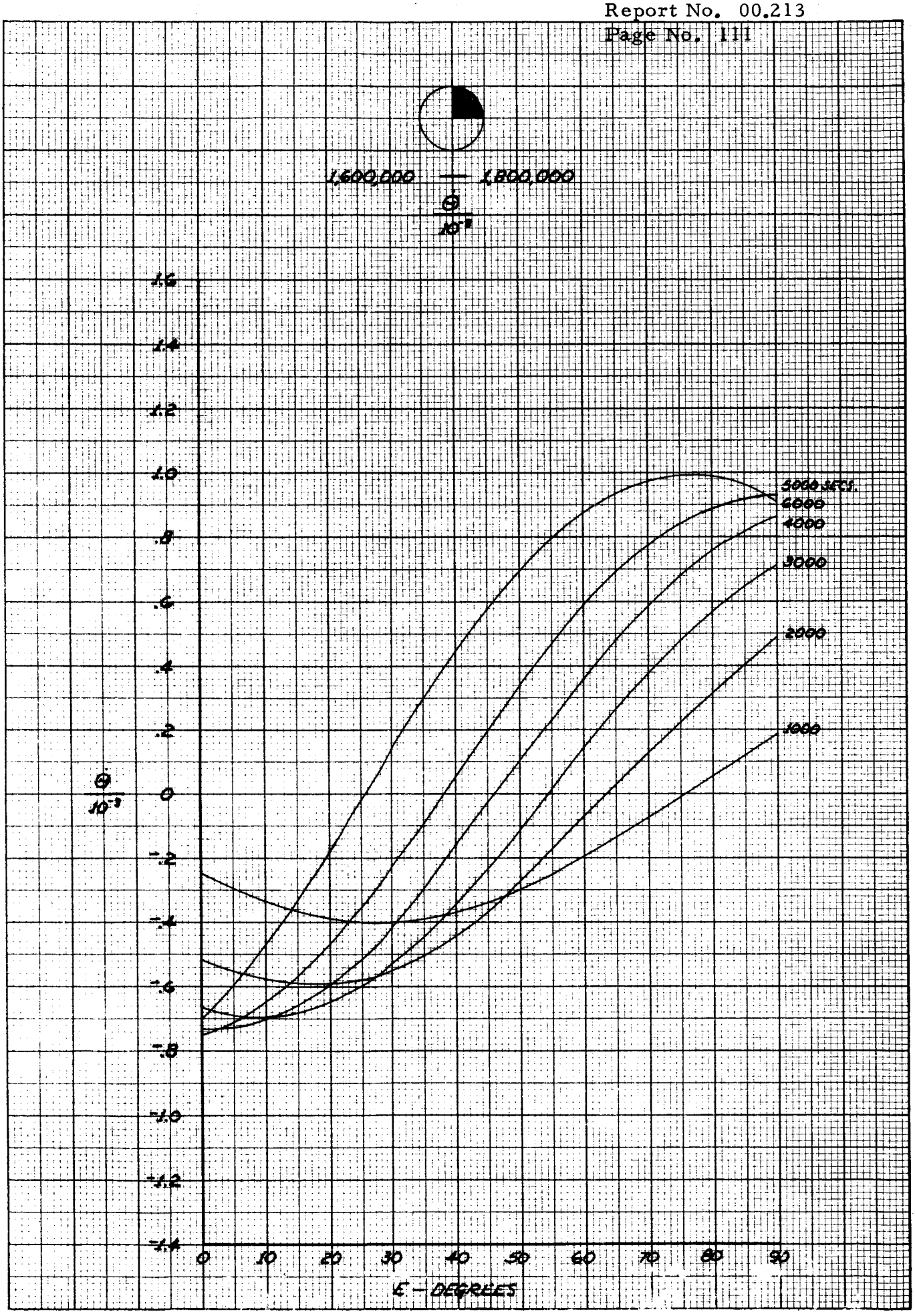
1,600,000 — 1,800,000
Θ/10⁻³
1.6
1.4
1.2
1.0
.8
.6
.4
.2
0
-.2
-.4
-.6
-.8
-1.0
-1.2
-1.4
5000 SECS.
4000
3000
2000
1000
0
10
20
30
40
50
60
70
80
90
ε - DEGREES

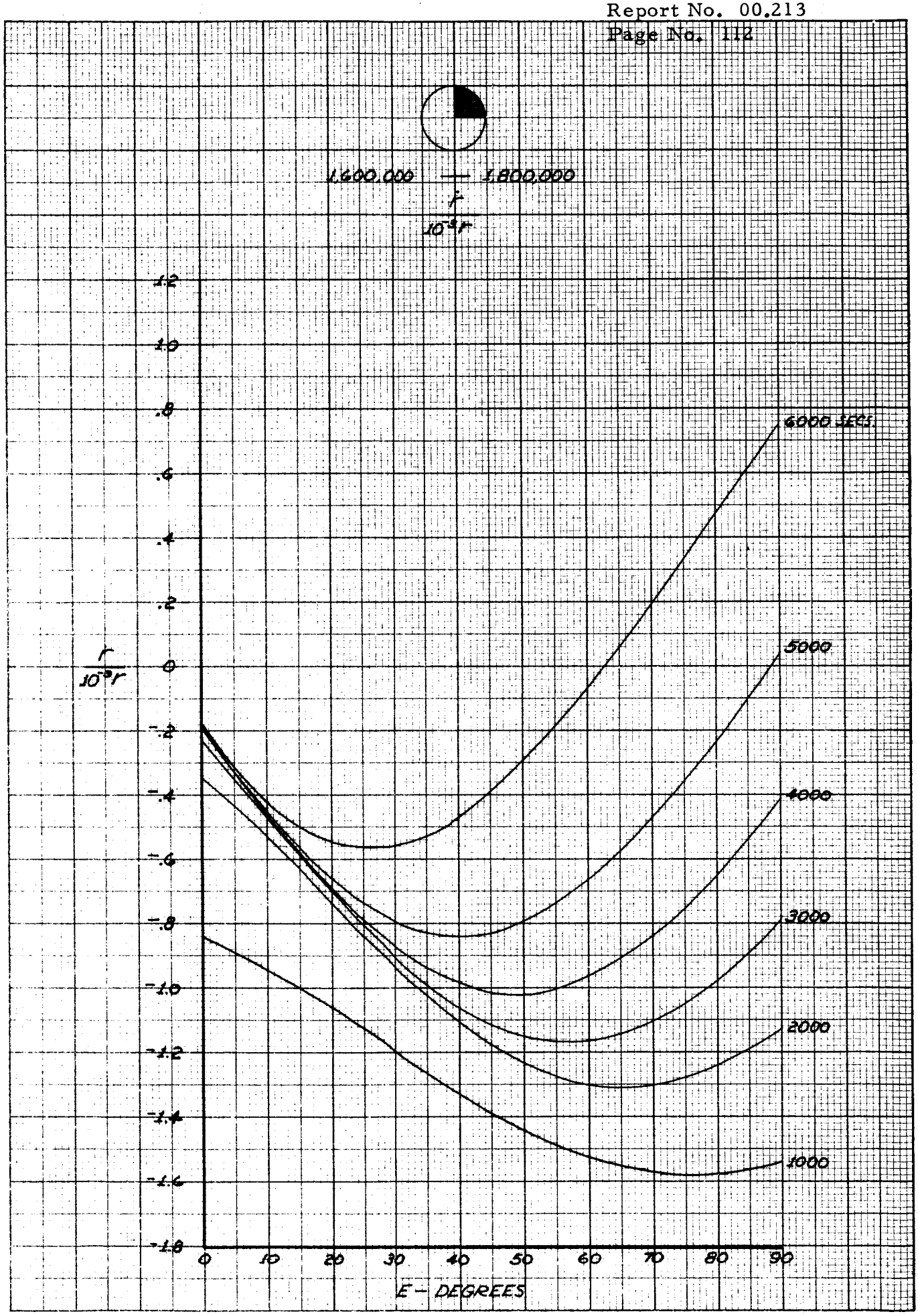
1,600,000 — 1,800,000
f
10^{-9}f
1.2
1.0
.8
.6
.4
.2
0
-.2
-.4
-.6
-.8
-1.0
-1.2
-1.4
-1.6
-1.8
$\frac{r}{10^{-9}r}$
6000 SECS.
5000
4000
3000
2000
1000
0
10
20
30
40
50
60
70
80
90
E - DEGREES

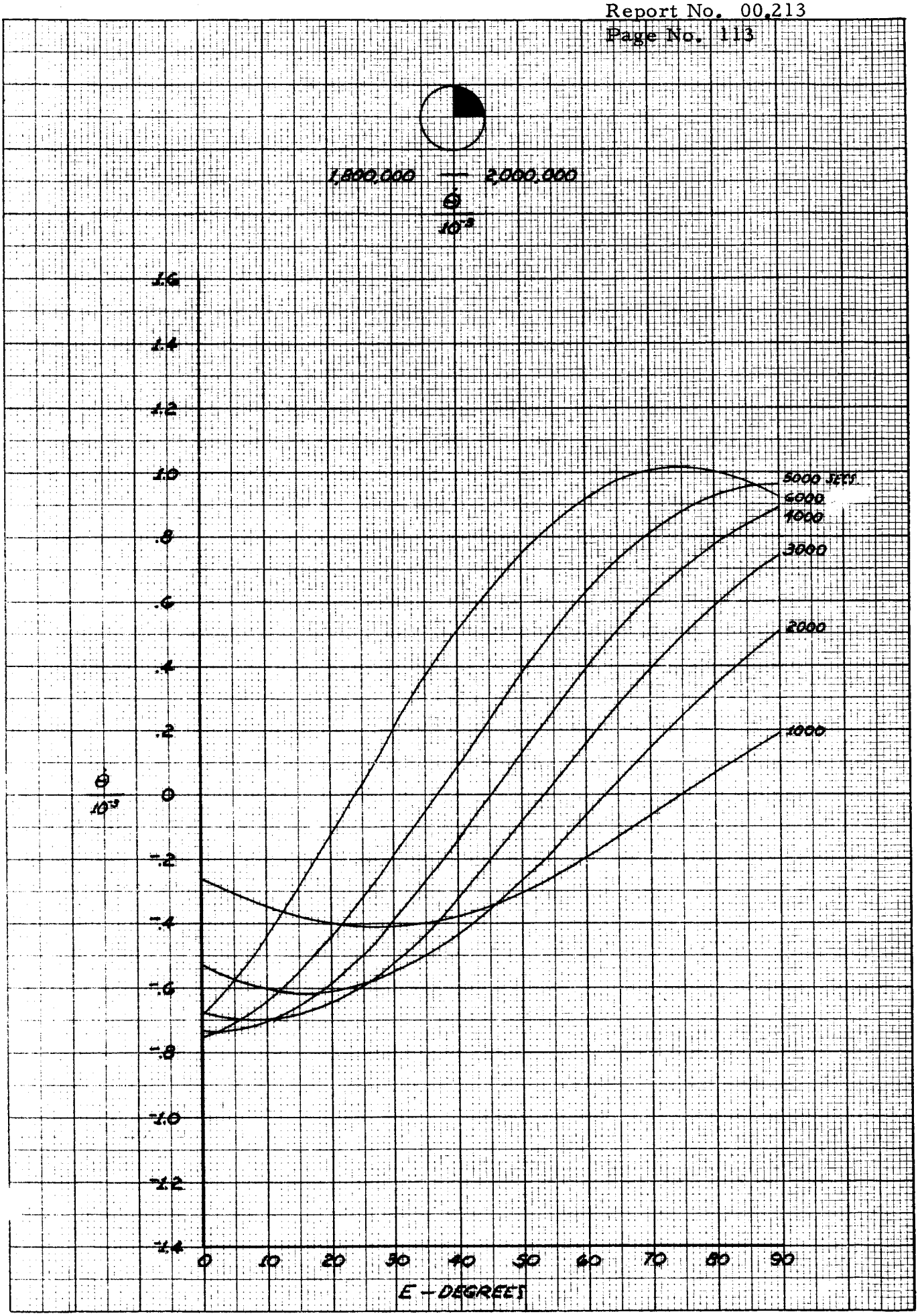
1,800,000 — 2,000,000
Φ
10⁻³
1.6
1.4
1.2
1.0
.8
.6
.4
.2
0
-.2
-.4
-.6
-.8
-1.0
-1.2
-1.4
Φ
10⁻³
5000 FEET
4000
3000
2000
1000
0
10
20
30
40
50
60
70
80
90
E - DEGREES

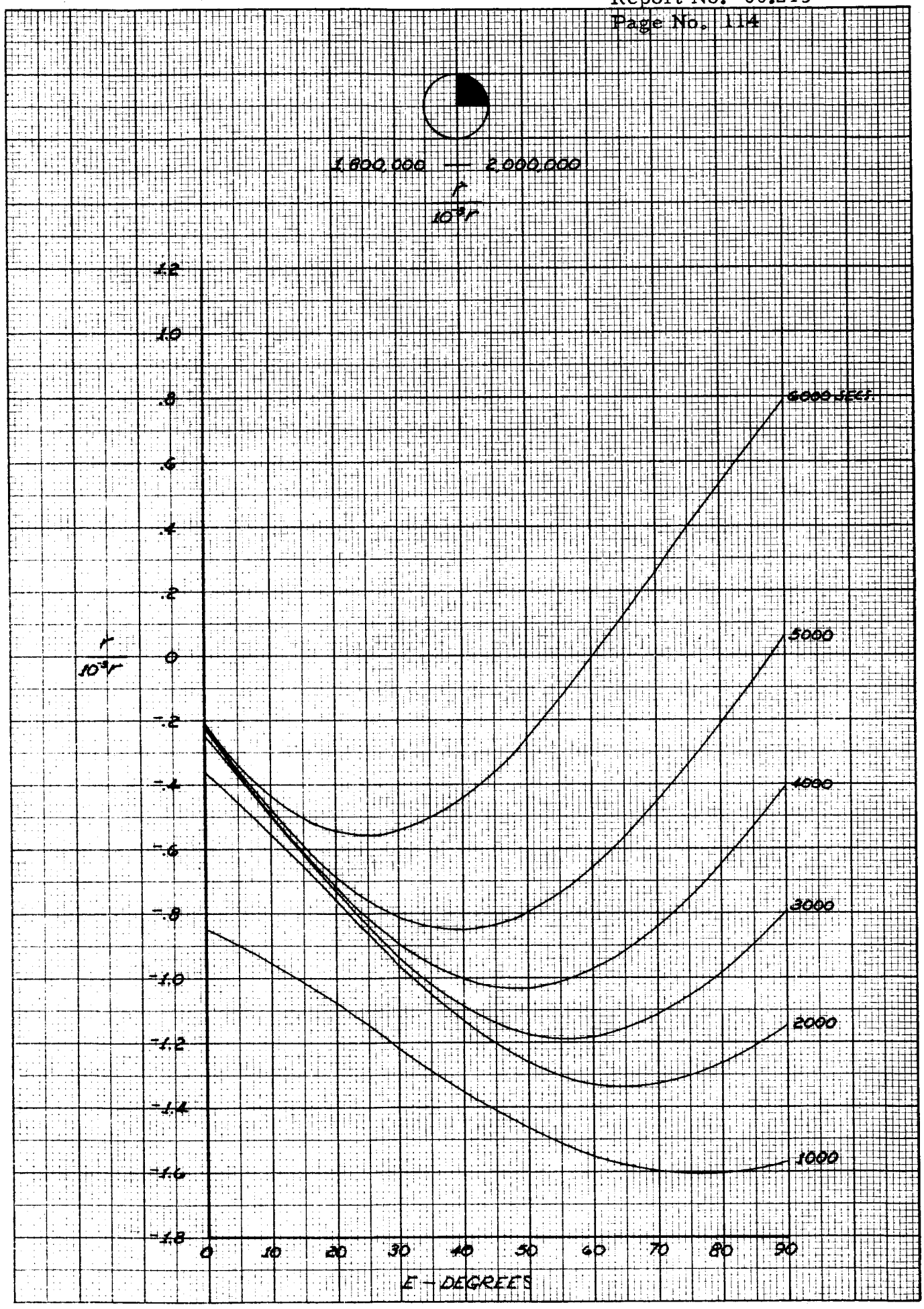
1,600,000 — 2,000,000
r
$10^{-3}r$
1.2
1.0
.8
.6
.4
.2
0
-.2
-.4
-.6
-.8
-1.0
-1.2
-1.4
-1.6
-1.8
6000 FEET
5000
4000
3000
2000
1000
0
10
20
30
40
50
60
70
80
90
E - DEGREES

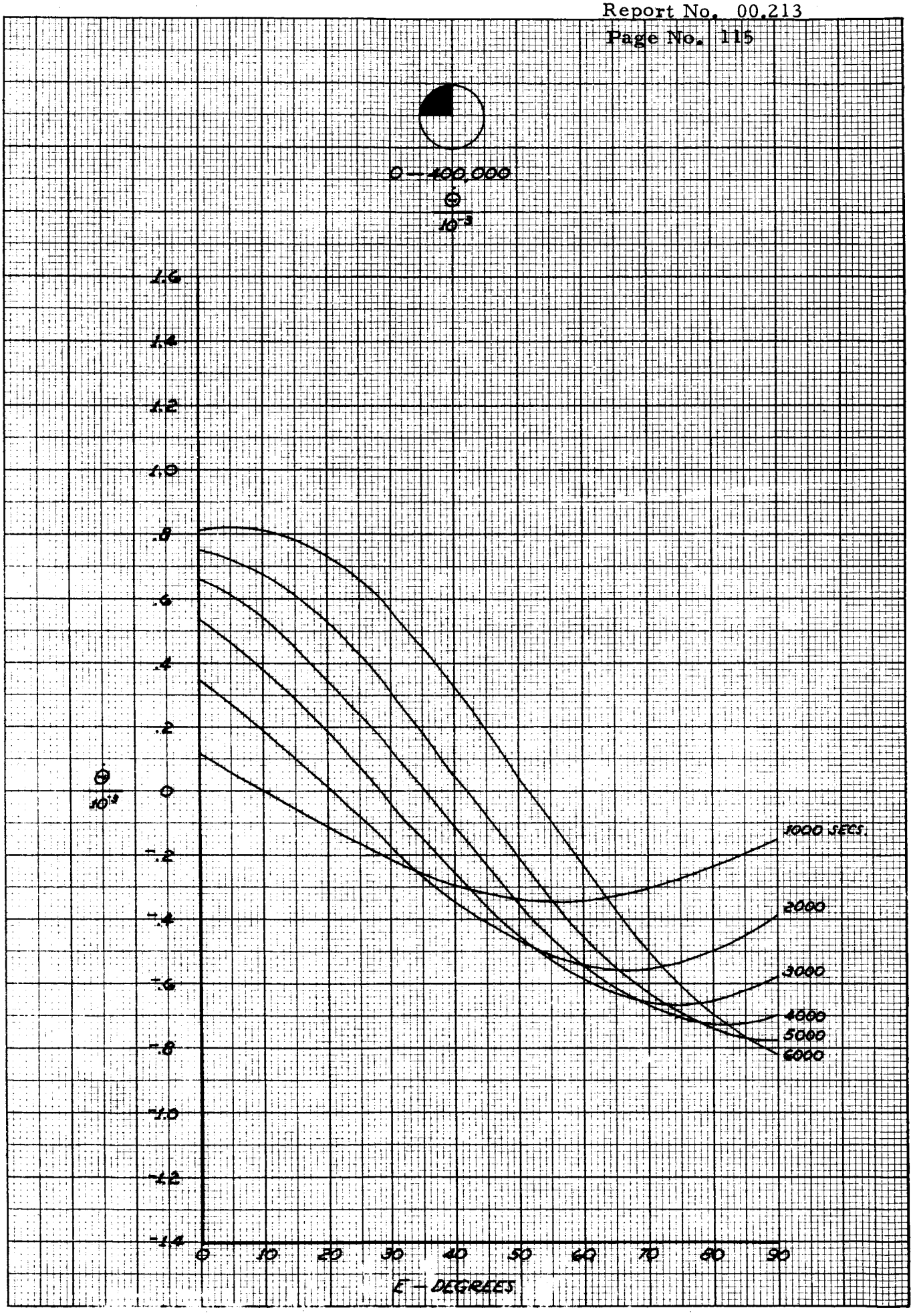
0 — 100,000
Θ
10⁻³
1.6
1.4
1.2
1.0
.8
.6
.4
.2
0
-.2
-.4
-.6
-.8
-1.0
-1.2
-1.4
Θ
10⁻³
1000 SECS.
2000
3000
4000
5000
6000
0
10
20
30
40
50
60
70
80
90
E — DEGREES

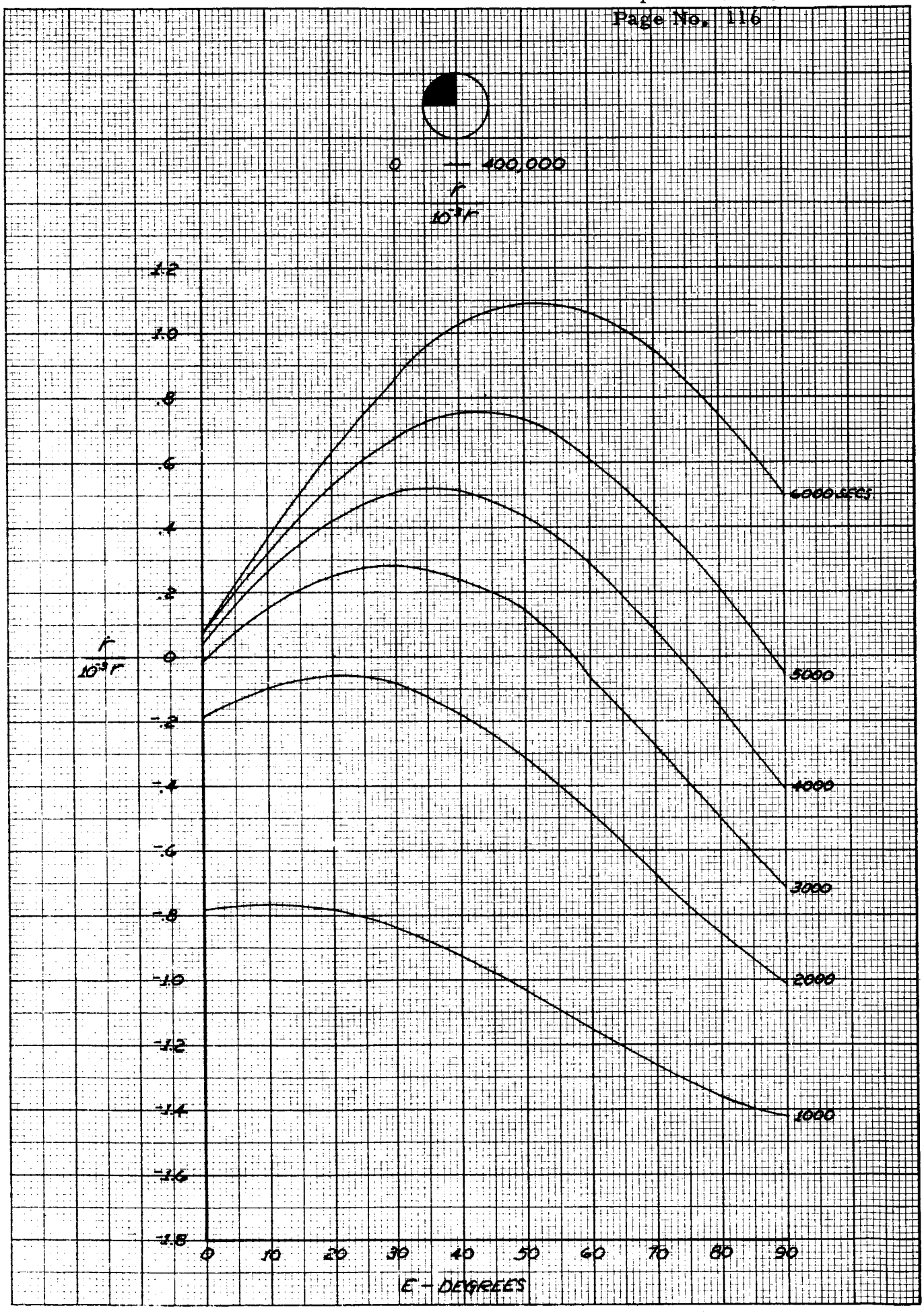
Q — 400,000
f
10^{-3} f
1.2
1.0
.8
.6
.4
.2
0
-.2
-.4
-.6
-.8
-1.0
-1.2
-1.4
-1.6
-1.8
6000 LEGS
5000
4000
3000
2000
1000
0
10
20
30
40
50
60
70
80
90
E - DEGREES

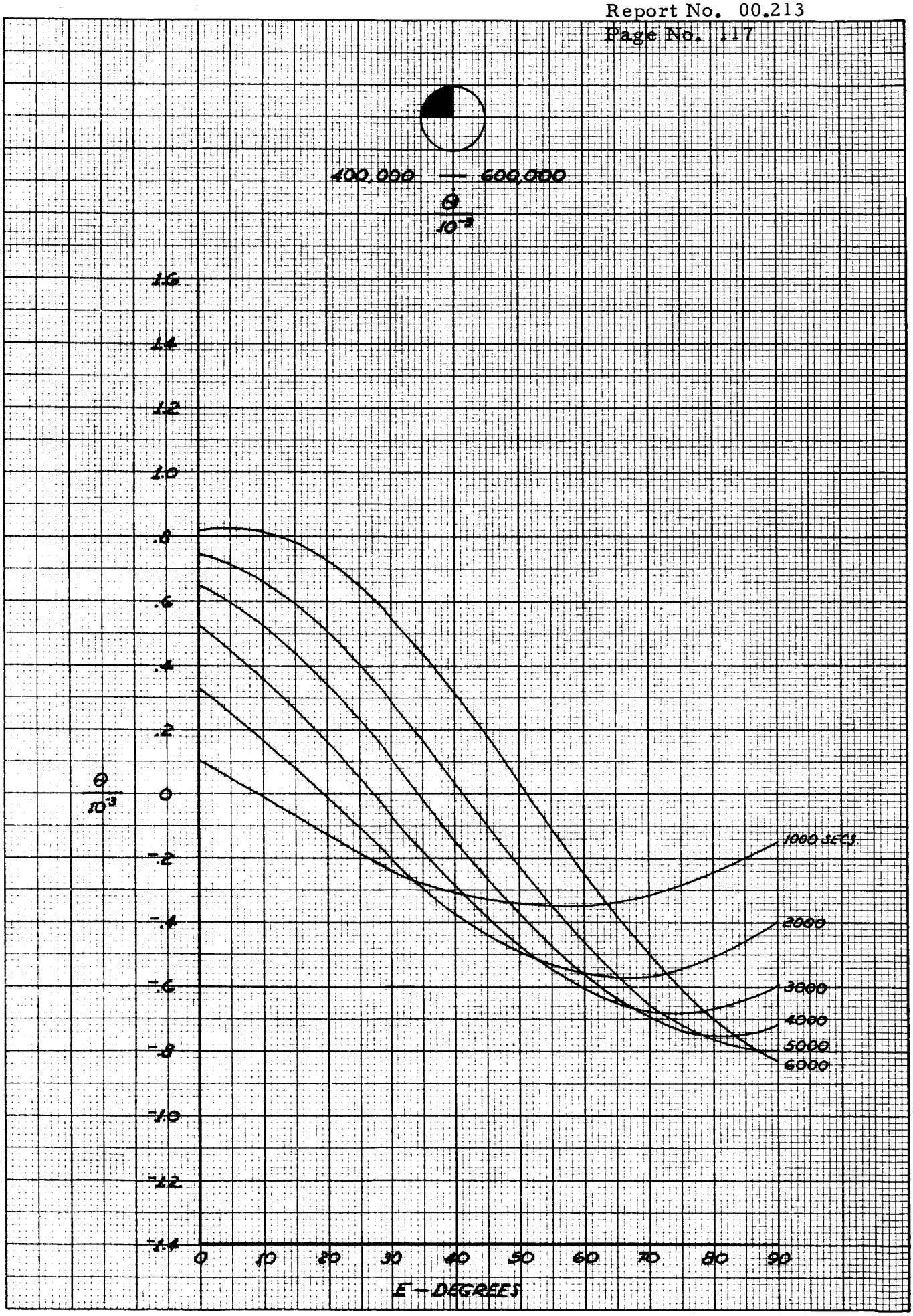
400,000 — 600,000
Θ / 10⁻³
1.6
1.4
1.2
1.0
.8
.6
.4
.2
0
-.2
-.4
-.6
-.8
-1.0
-1.2
-1.4
Θ / 10⁻³
0
10
20
30
40
50
60
70
80
90
E — DEGREES
1000 SECS.
2000
3000
4000
5000
6000

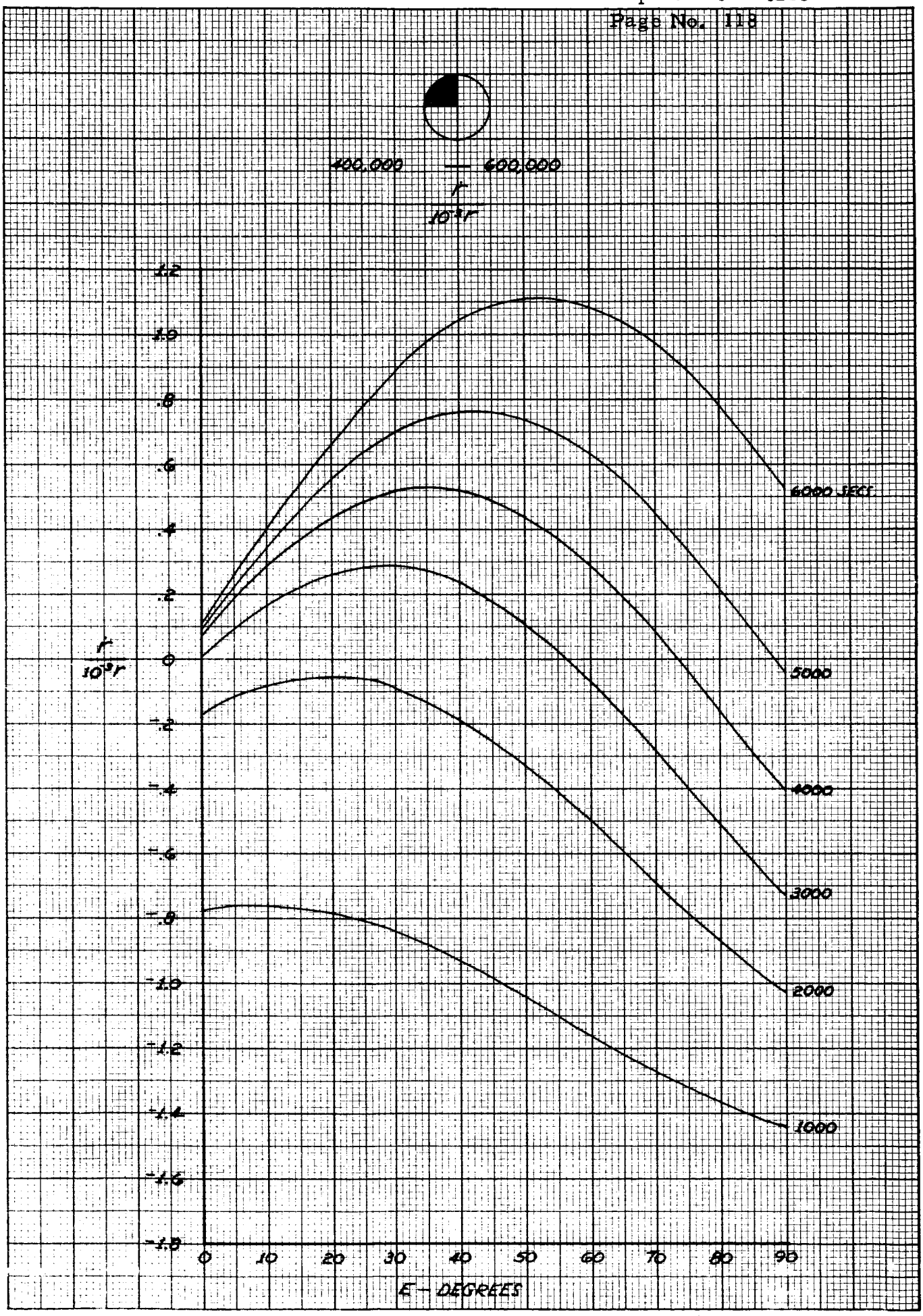
400,000 — 600,000
$\frac{r}{10^3 r}$
1.2
1.0
.8
.6
.4
.2
0
-.2
-.4
-.6
-.8
-1.0
-1.2
-1.4
-1.6
-1.8
6000 JECT
5000
4000
3000
2000
1000
0
10
20
30
40
50
60
70
80
90
E - DEGREES

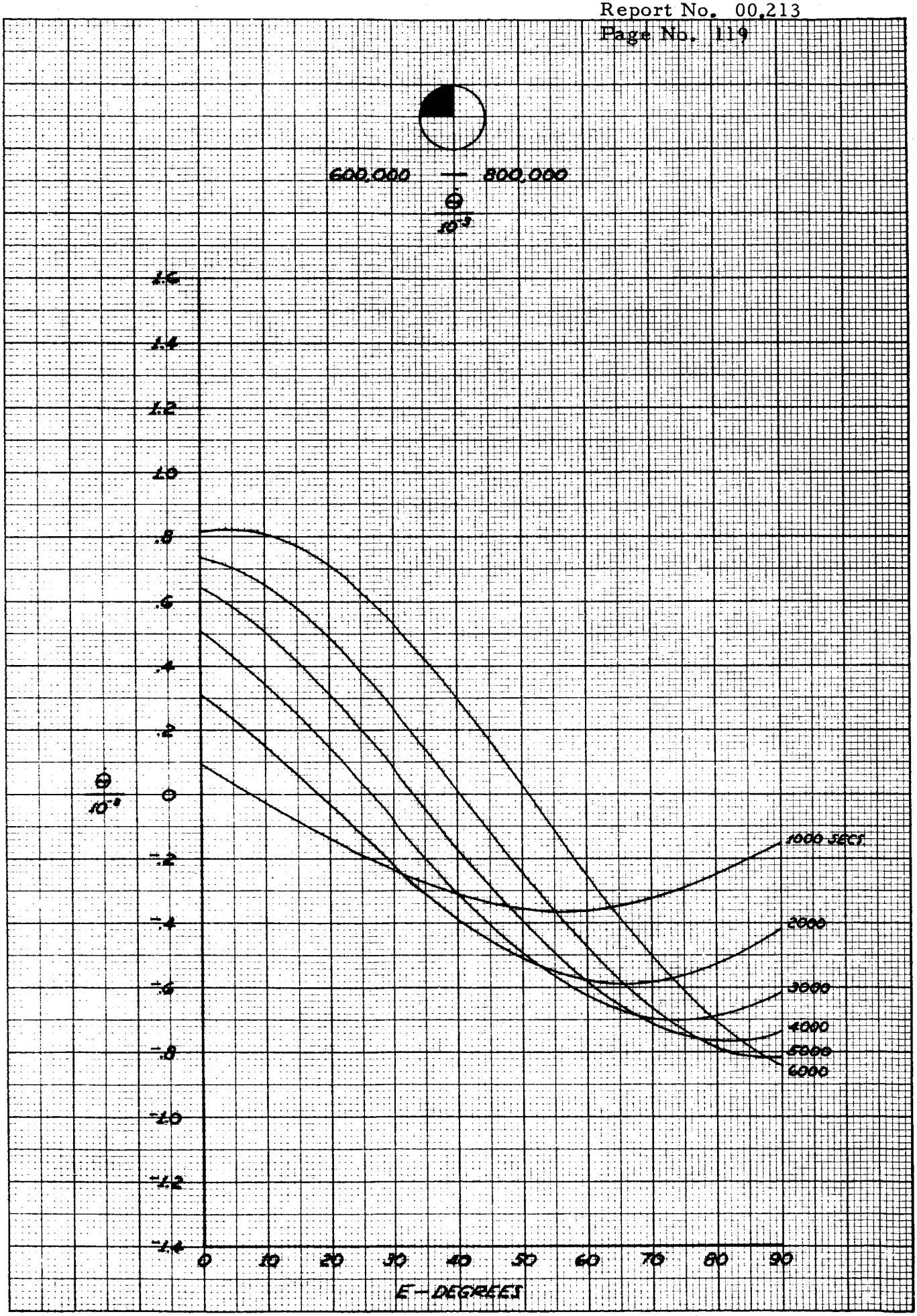
600,000 — 800,000
$\frac{\dot{\Theta}}{10^{-9}}$
1.6
1.4
1.2
1.0
.8
.6
.4
.2
0
-.2
-.4
-.6
-.8
-1.0
-1.2
-1.4
$\frac{\dot{\Theta}}{10^{-9}}$
1000 SECS
2000
3000
4000
5000
6000
0
10
20
30
40
50
60
70
80
90
E — DEGREES

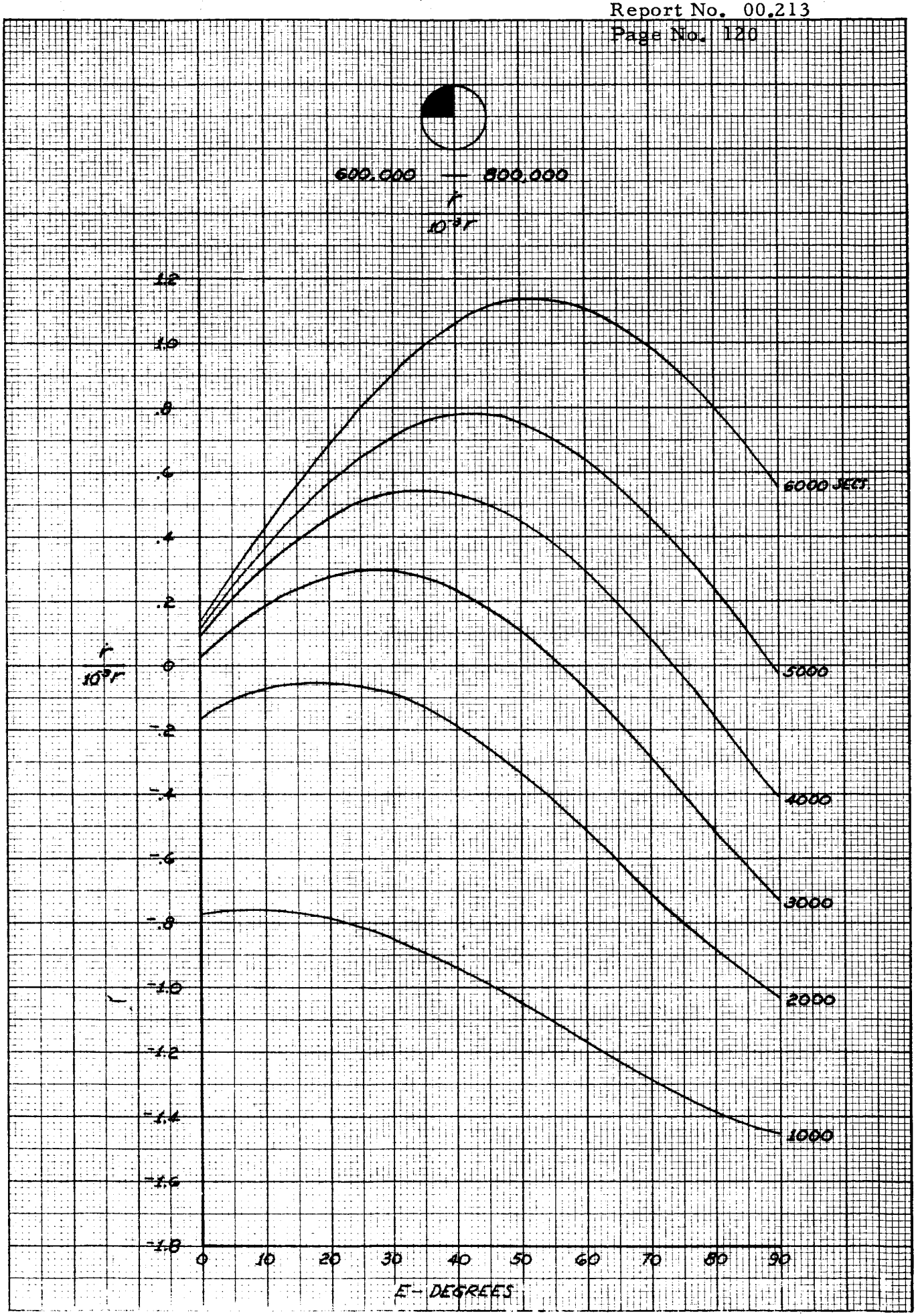
600,000 — 800,000
$\frac{\dot{r}}{10^3 r}$
1.2
1.0
.8
.6
.4
.2
0
-.2
-.4
-.6
-.8
-1.0
-1.2
-1.4
-1.6
-1.8
6000 FEET
5000
4000
3000
2000
1000
0
10
20
30
40
50
60
70
80
90
E - DEGREES

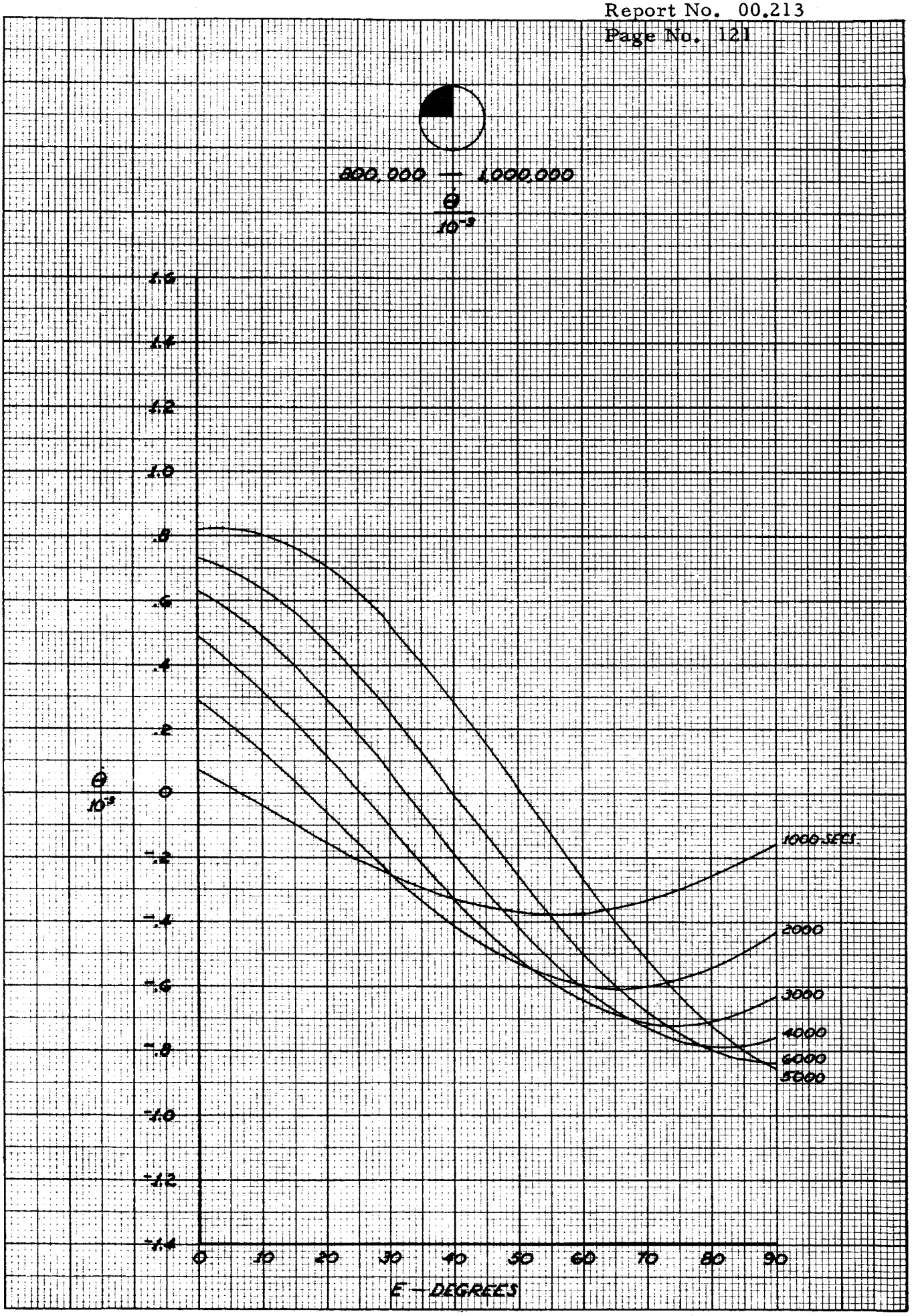
800,000 — 1,000,000
θ̇ / 10⁻⁹
1.6
1.4
1.2
1.0
.8
.6
.4
.2
0
-.2
-.4
-.6
-.8
-1.0
-1.2
-1.4
θ̇ / 10⁻⁹
1000 SECS.
2000
3000
4000
6000
5000
0
10
20
30
40
50
60
70
80
90
E — DEGREES

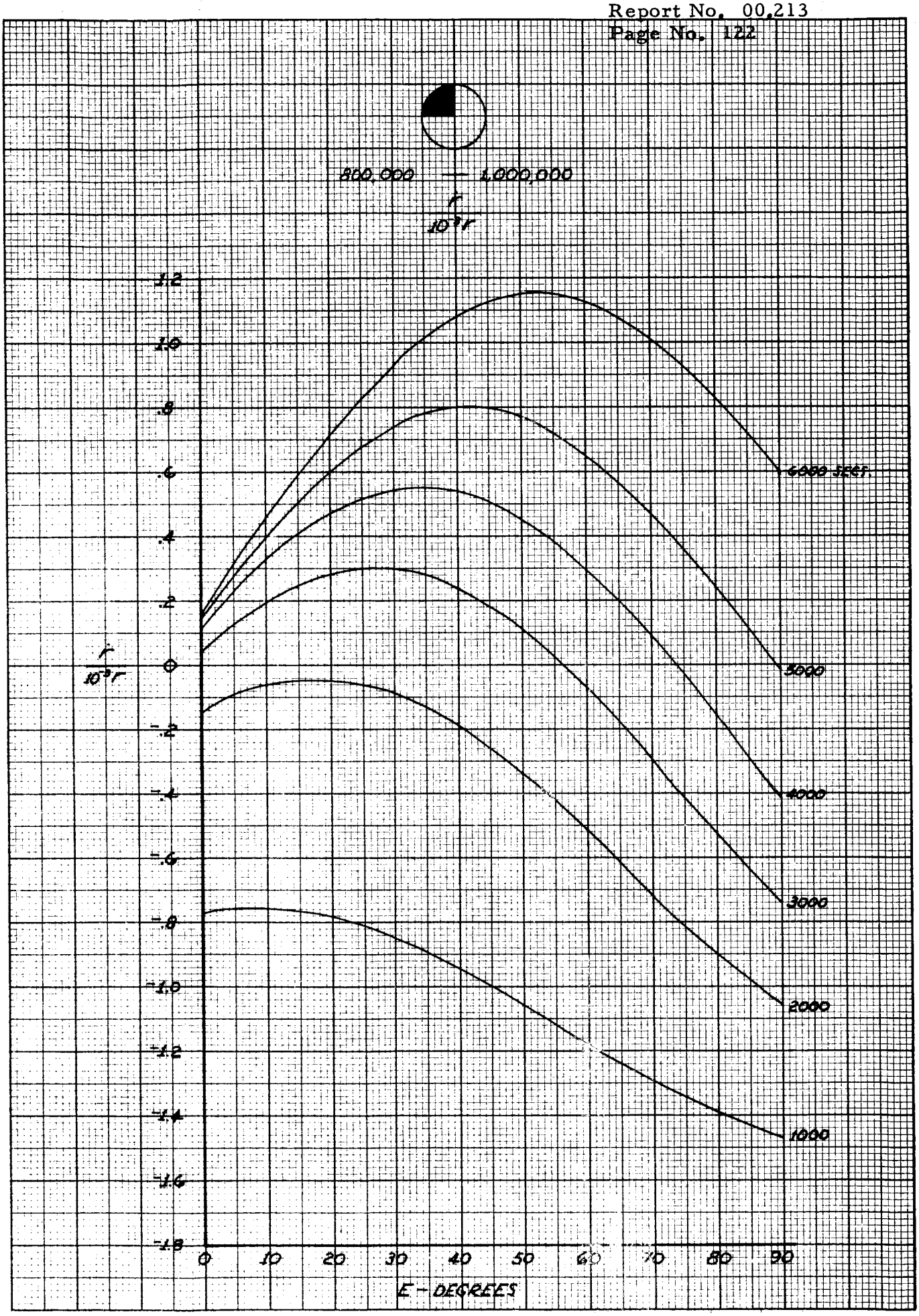
800,000 — 1,000,000
r / 10^9 r
1.2
1.0
.8
.6
.4
.2
0
-.2
-.4
-.6
-.8
-1.0
-1.2
-1.4
-1.6
-1.8
r / 10^9 r
6000 SEC.
5000
4000
3000
2000
1000
0
10
20
30
40
50
60
70
80
90
E - DEGREES

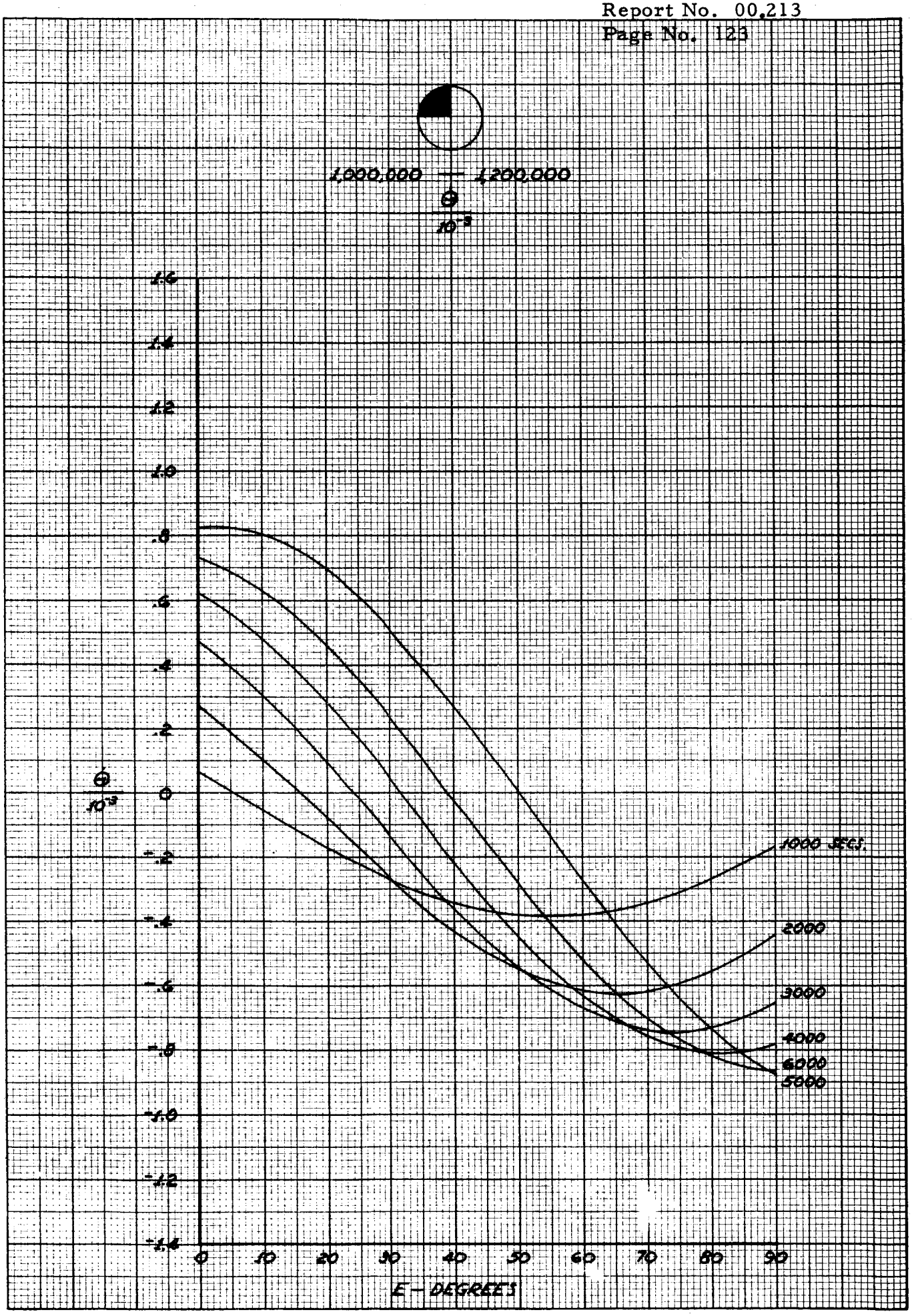
1,000,000 — 1,200,000
Θ / 10⁻³
1.6
1.4
1.2
1.0
.8
.6
.4
.2
0
-.2
-.4
-.6
-.8
-1.0
-1.2
-1.4
0
10
20
30
40
50
60
70
80
90
E – DEGREES
1000 JEC.
2000
3000
4000
6000
5000

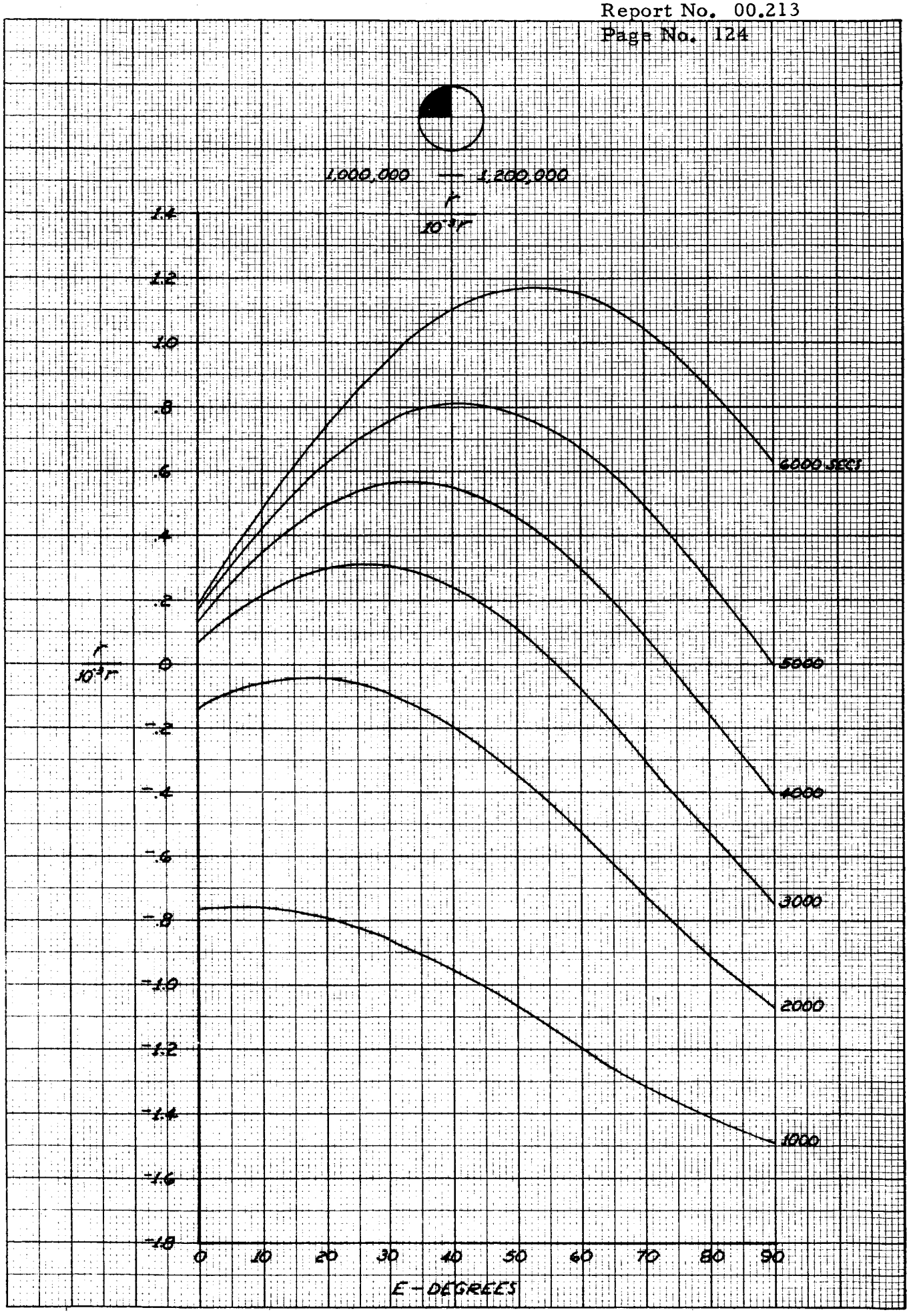
1,000,000 — 1,200,000
r
10⁻³r
1.4
1.2
1.0
.8
.6
.4
.2
0
-.2
-.4
-.6
-.8
-1.0
-1.2
-1.4
-1.6
-1.8
6000 SEC.
5000
4000
3000
2000
1000
0
10
20
30
40
50
60
70
80
90
E - DEGREES

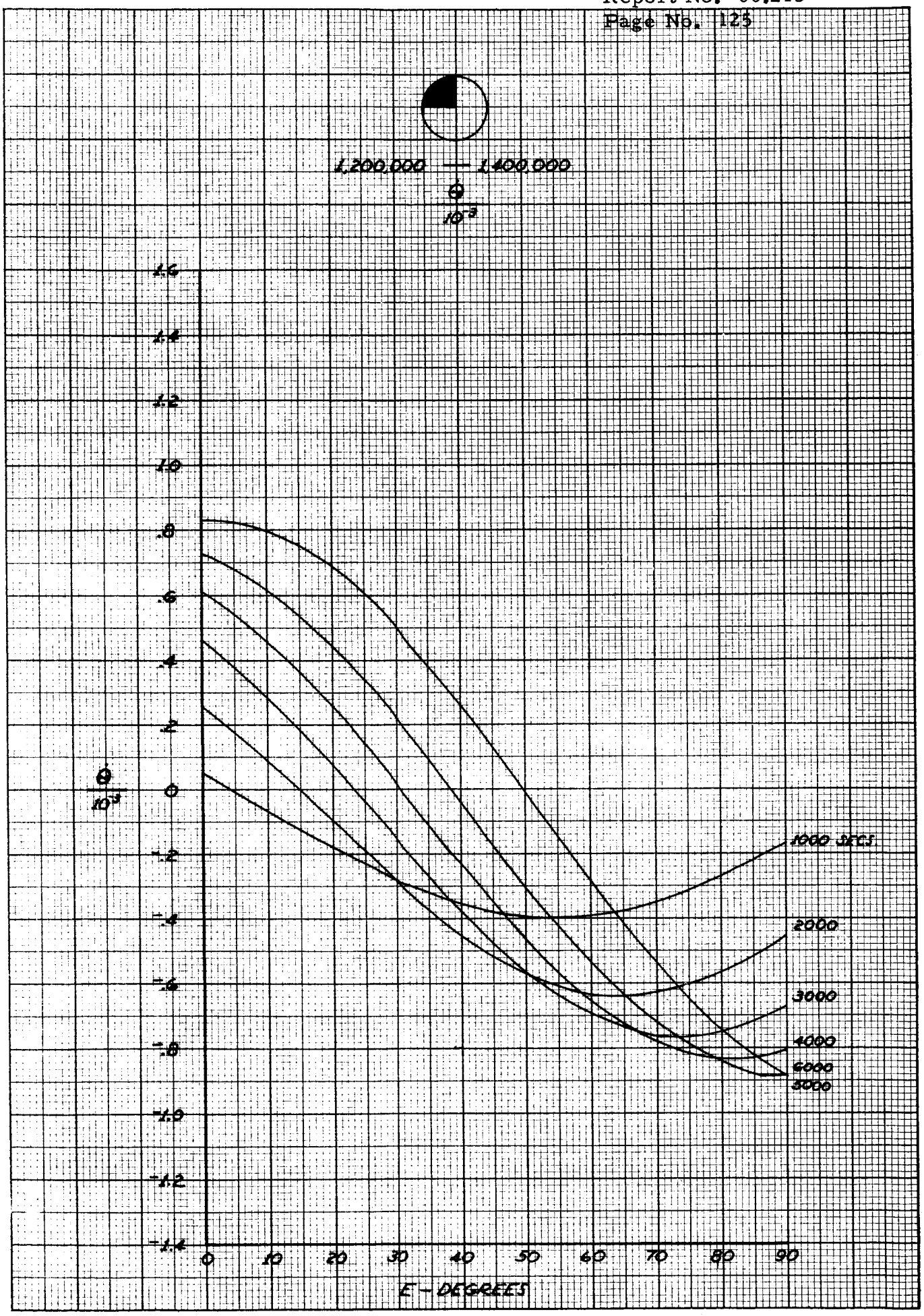
1,200,000 — 1,400,000
Φ
10⁻³
1.6
1.4
1.2
1.0
.8
.6
.4
.2
0
-.2
-.4
-.6
-.8
-1.0
-1.2
-1.4
Φ
10⁻³
0
10
20
30
40
50
60
70
80
90
ε - DEGREES
1000 SECS
2000
3000
4000
6000
5000

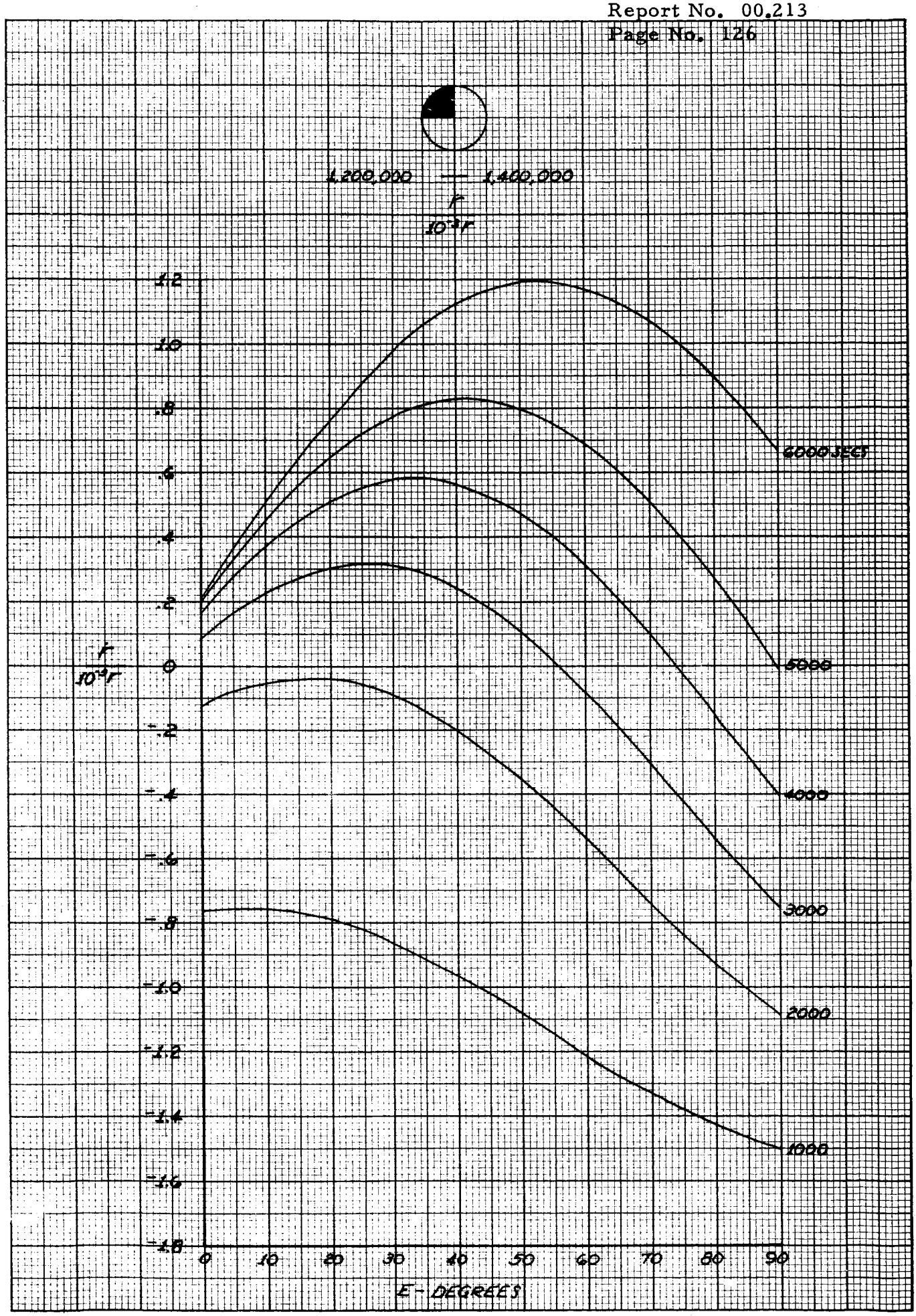
1,200,000 — 1,400,000
F
10^{-9}F
1.2
1.0
.8
.6
.4
.2
0
-.2
-.4
-.6
-.8
-1.0
-1.2
-1.4
-1.6
-1.8
F
10^{-9}F
6000 SECS
5000
4000
3000
2000
1000
0
10
20
30
40
50
60
70
80
90
E - DEGREES

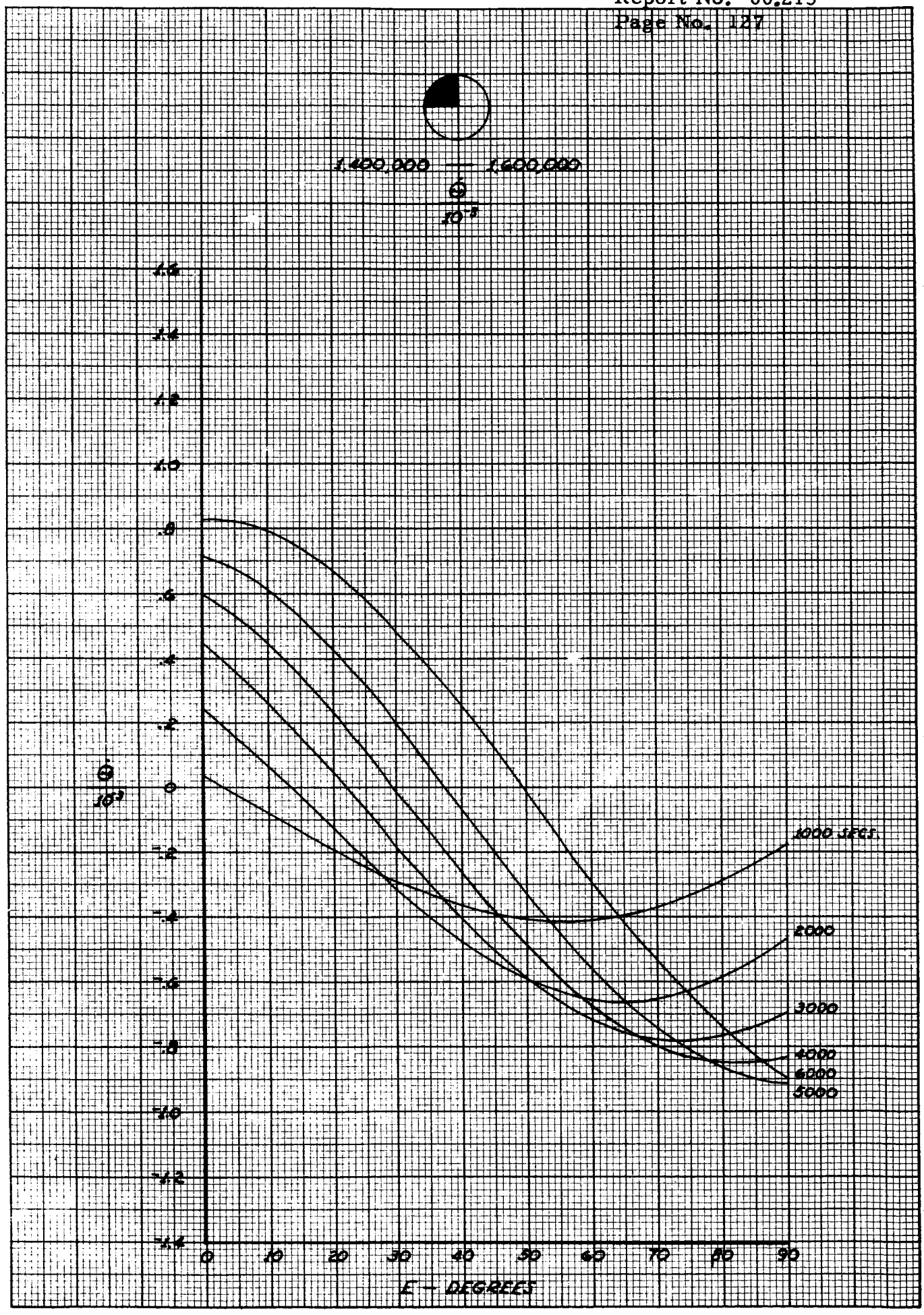
1,400,000 — 1,600,000
$\frac{\dot{\Theta}}{10^{-3}}$
1.6
1.4
1.2
1.0
.8
.6
.4
.2
0
-.2
-.4
-.6
-.8
-1.0
-1.2
-1.4
$\frac{\dot{\Theta}}{10^{-3}}$
1000 secs.
2000
3000
4000
5000
6000
0
10
20
30
40
50
60
70
80
90
ε - DEGREES

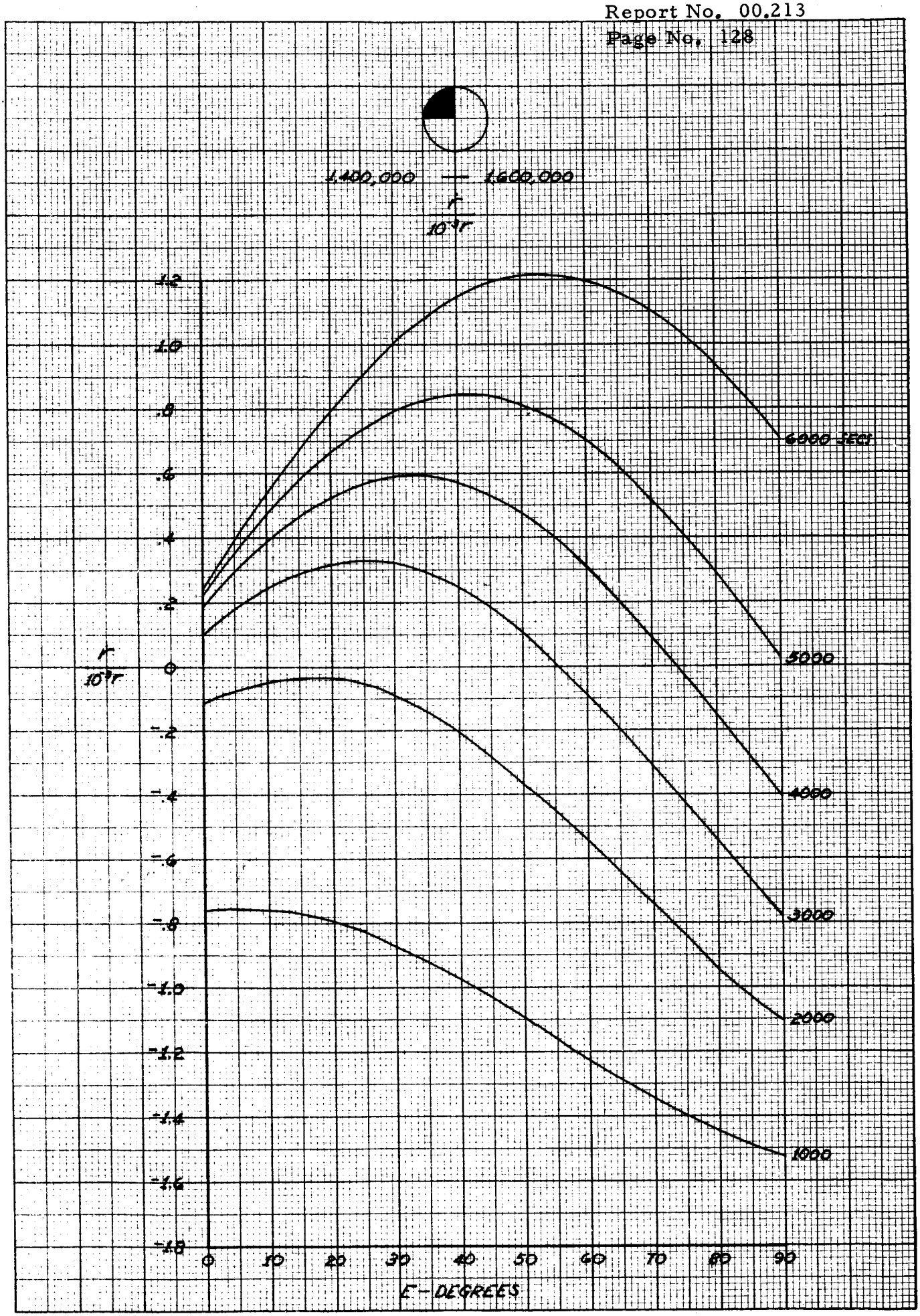
1,400,000 — 1,600,000
r
$10^{-3}r$
1.2
1.0
.8
.6
.4
.2
0
-.2
-.4
-.6
-.8
-1.0
-1.2
-1.4
-1.6
-1.8
6000 JECI
5000
4000
3000
2000
1000
0
10
20
30
40
50
60
70
80
90
ε - DEGREES

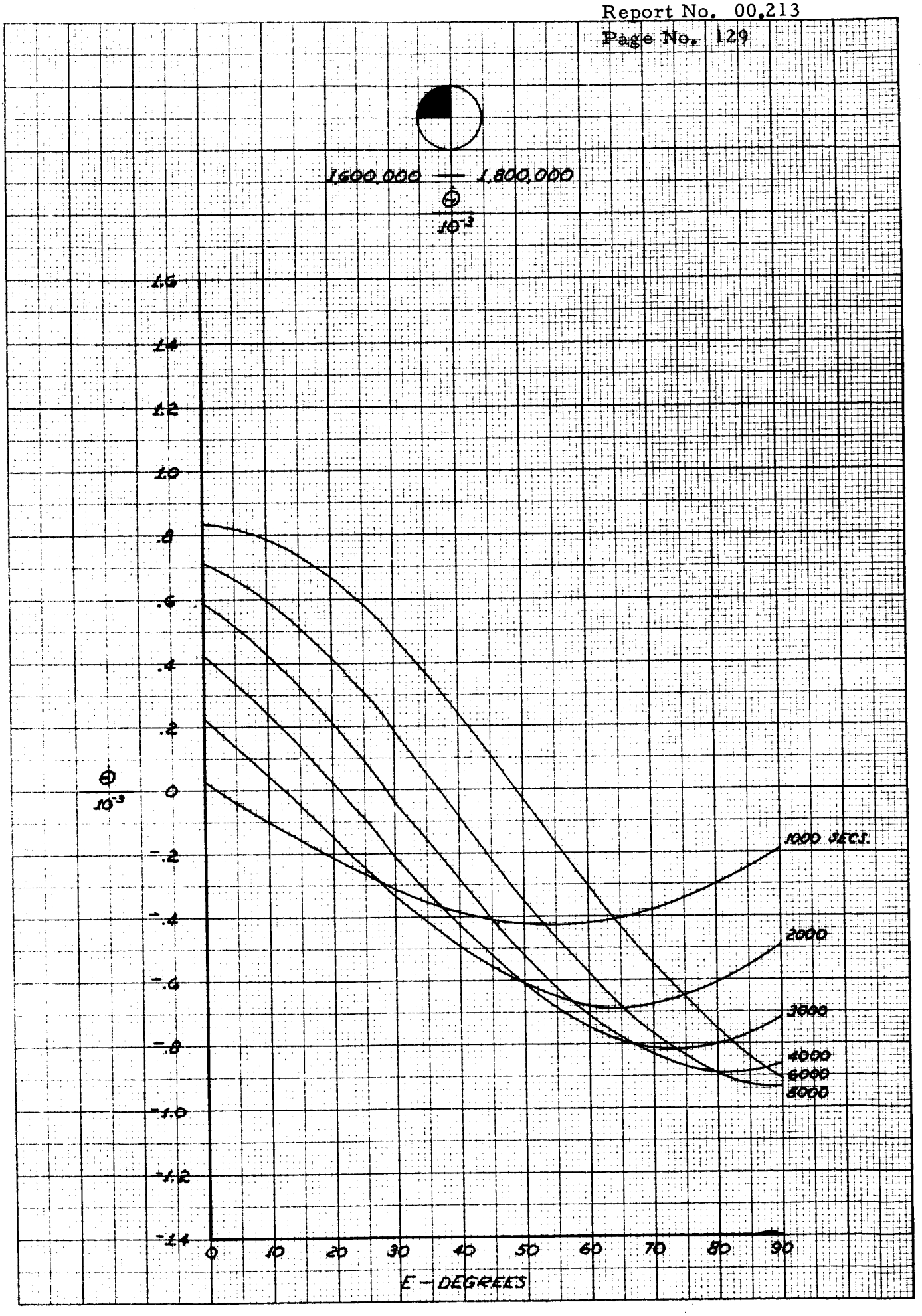
1,600,000 — 1,800,000
Θ / 10⁻³
1.6
1.4
1.2
1.0
.8
.6
.4
.2
0
-.2
-.4
-.6
-.8
-1.0
-1.2
-1.4
0
10
20
30
40
50
60
70
80
90
E - DEGREES
1000 SECS.
2000
3000
4000
6000
8000

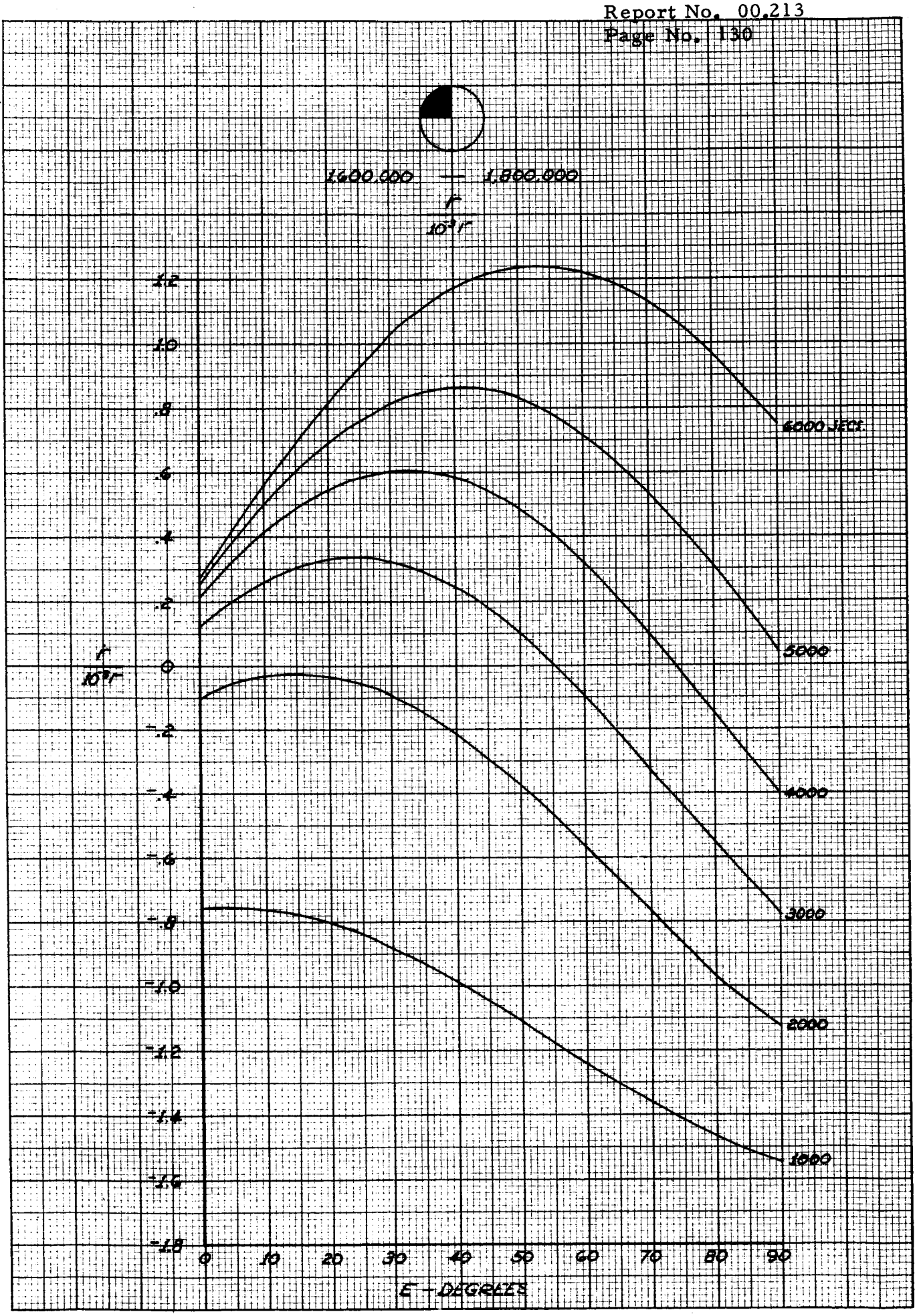
1,400,000 — 1,800,000
f
$10^3 f^r$
1.2
1.0
.8
.6
.4
.2
0
-.2
-.4
-.6
-.8
-1.0
-1.2
-1.4
-1.6
-1.8
6000 JECS.
5000
4000
3000
2000
1000
0
10
20
30
40
50
60
70
80
90
E - DEGREES

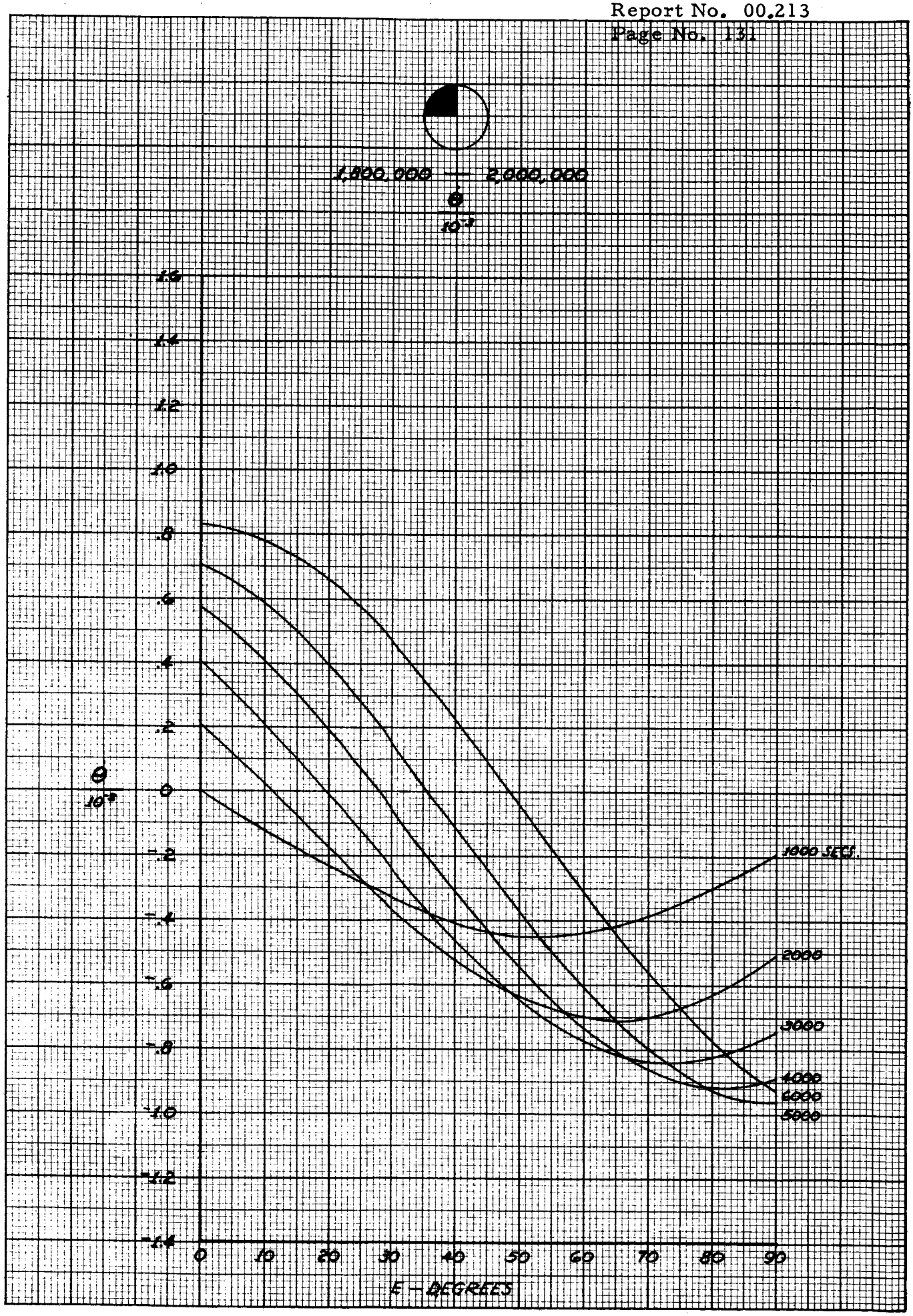
1,800,000 — 2,000,000
θ
10⁻³
1.6
1.4
1.2
1.0
.8
.6
.4
.2
0
-.2
-.4
-.6
-.8
-1.0
-1.2
-1.4
θ
10⁻³
1000 SECS.
2000
3000
4000
6000
5000
0
10
20
30
40
50
60
70
80
90
E — DEGREES

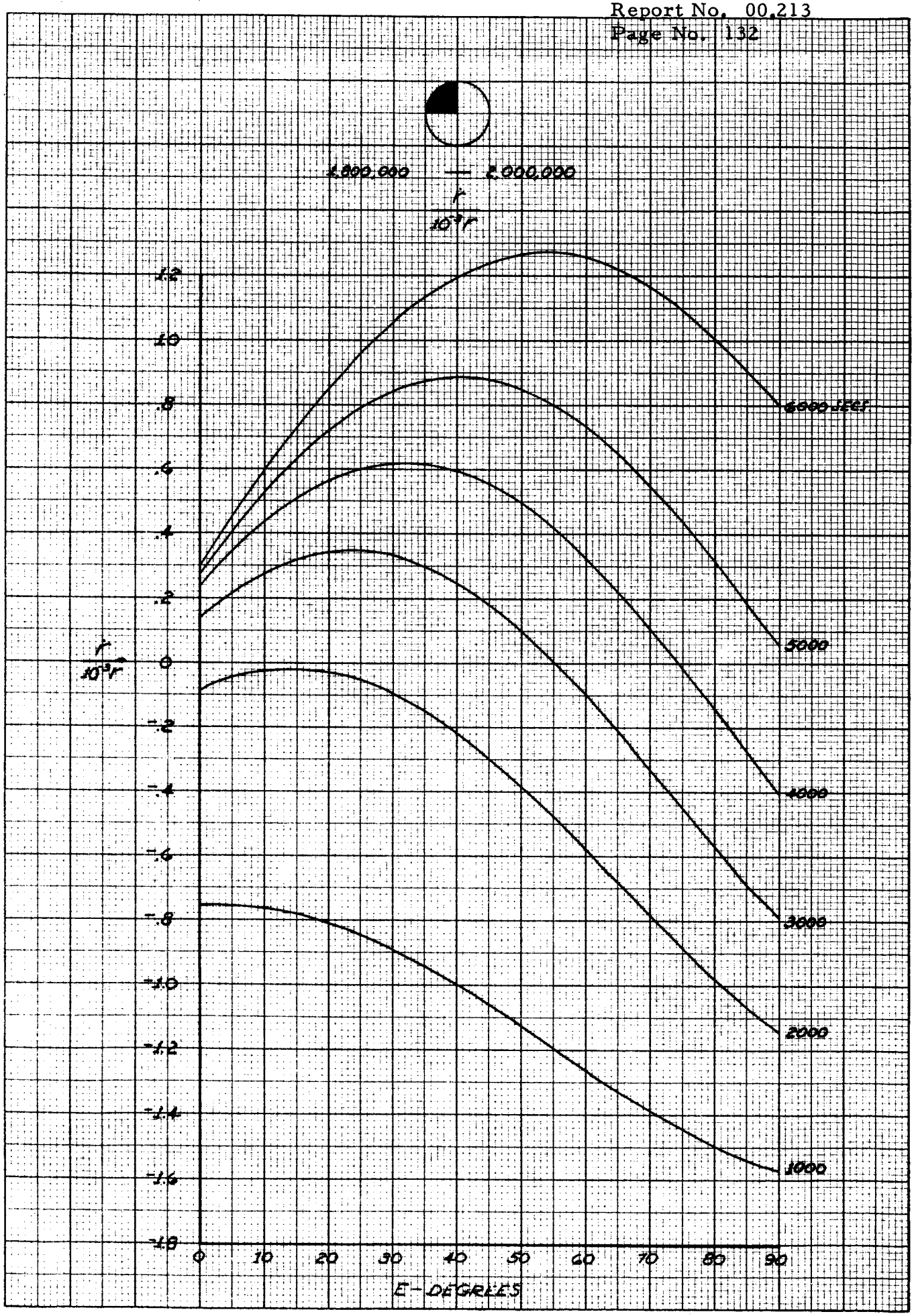
1,800,000 — 2,000,000
f
$10^{-3}f$
1.2
1.0
.8
.6
.4
.2
0
-.2
-.4
-.6
-.8
-1.0
-1.2
-1.4
-1.6
-1.8
6000 FEET
5000
4000
3000
2000
1000
0
10
20
30
40
50
60
70
80
90
E - DEGREES

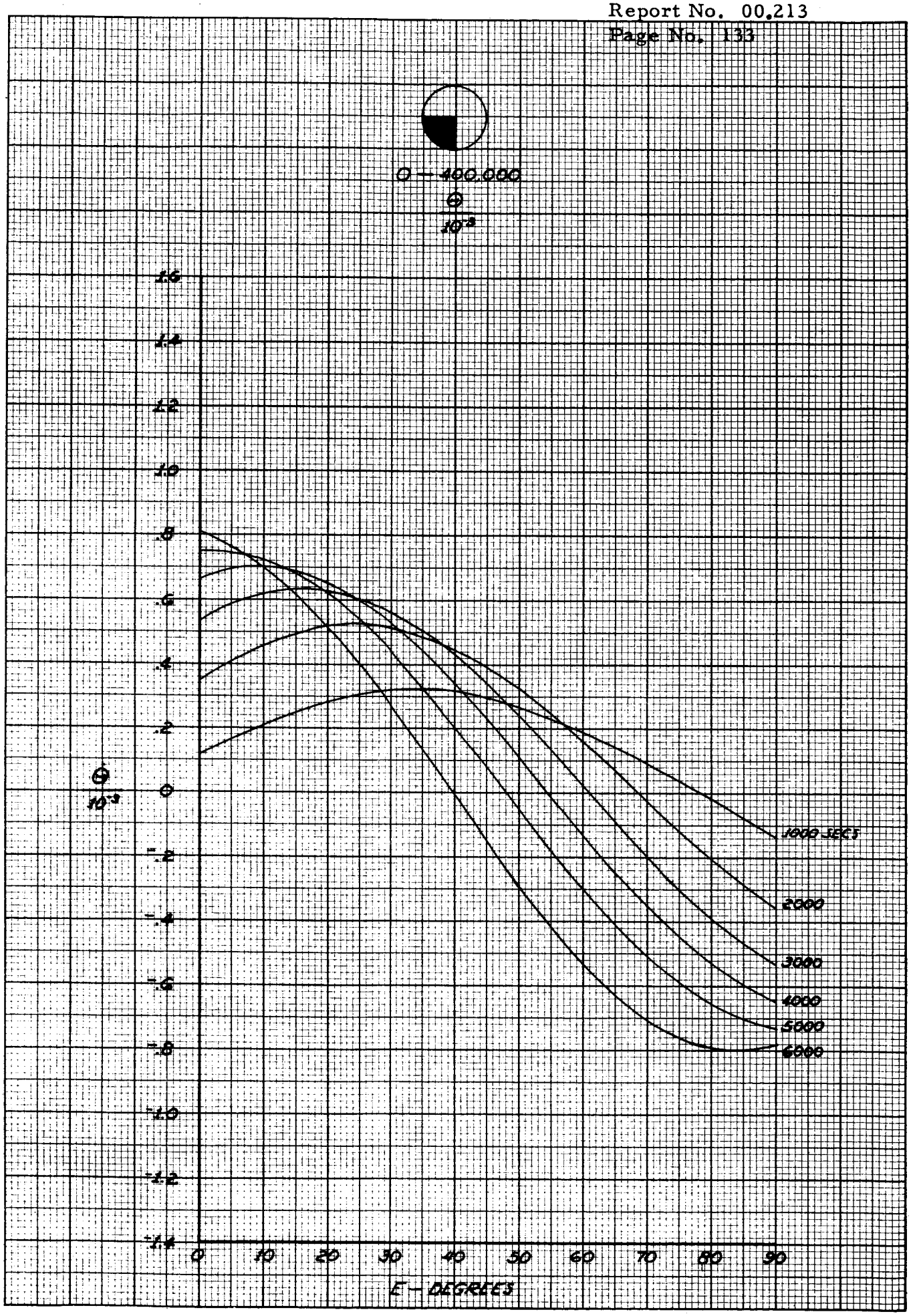
O — 400,000
Φ
10⁻³
1.6
1.4
1.2
1.0
.8
.6
.4
.2
0
-.2
-.4
-.6
-.8
-1.0
-1.2
-1.4
Φ
10⁻³
1000 SECS
2000
3000
4000
5000
6000
0
10
20
30
40
50
60
70
80
90
ζ — DEGREES

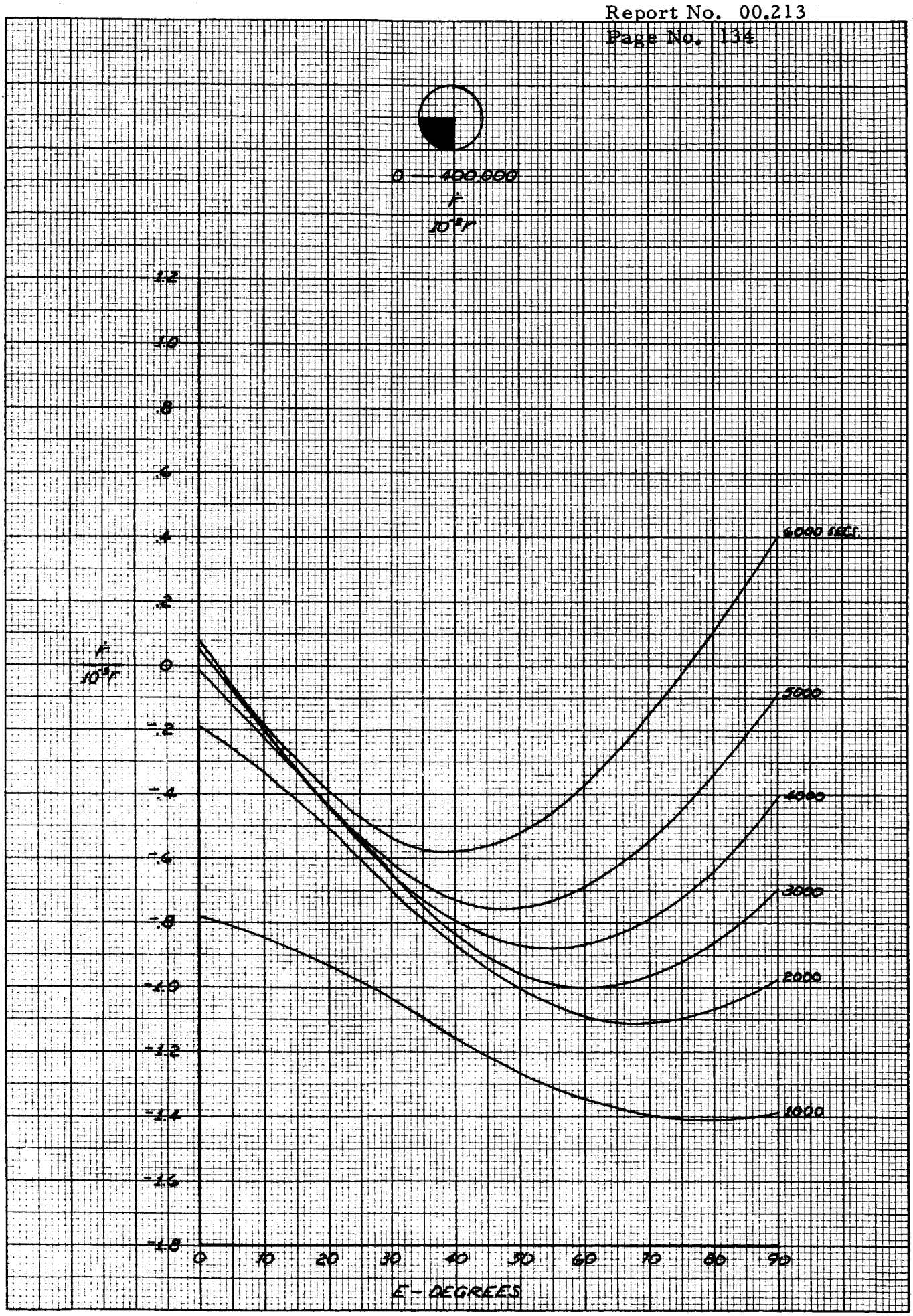
0 — 400.000
f
10^{-9}r
1.2
1.0
.8
.6
.4
.2
0
-.2
-.4
-.6
-.8
-1.0
-1.2
-1.4
-1.6
-1.8
f
10^{-9}r
6000 KC.
5000
4000
3000
2000
1000
0
10
20
30
40
50
60
70
80
90
E - DEGREES

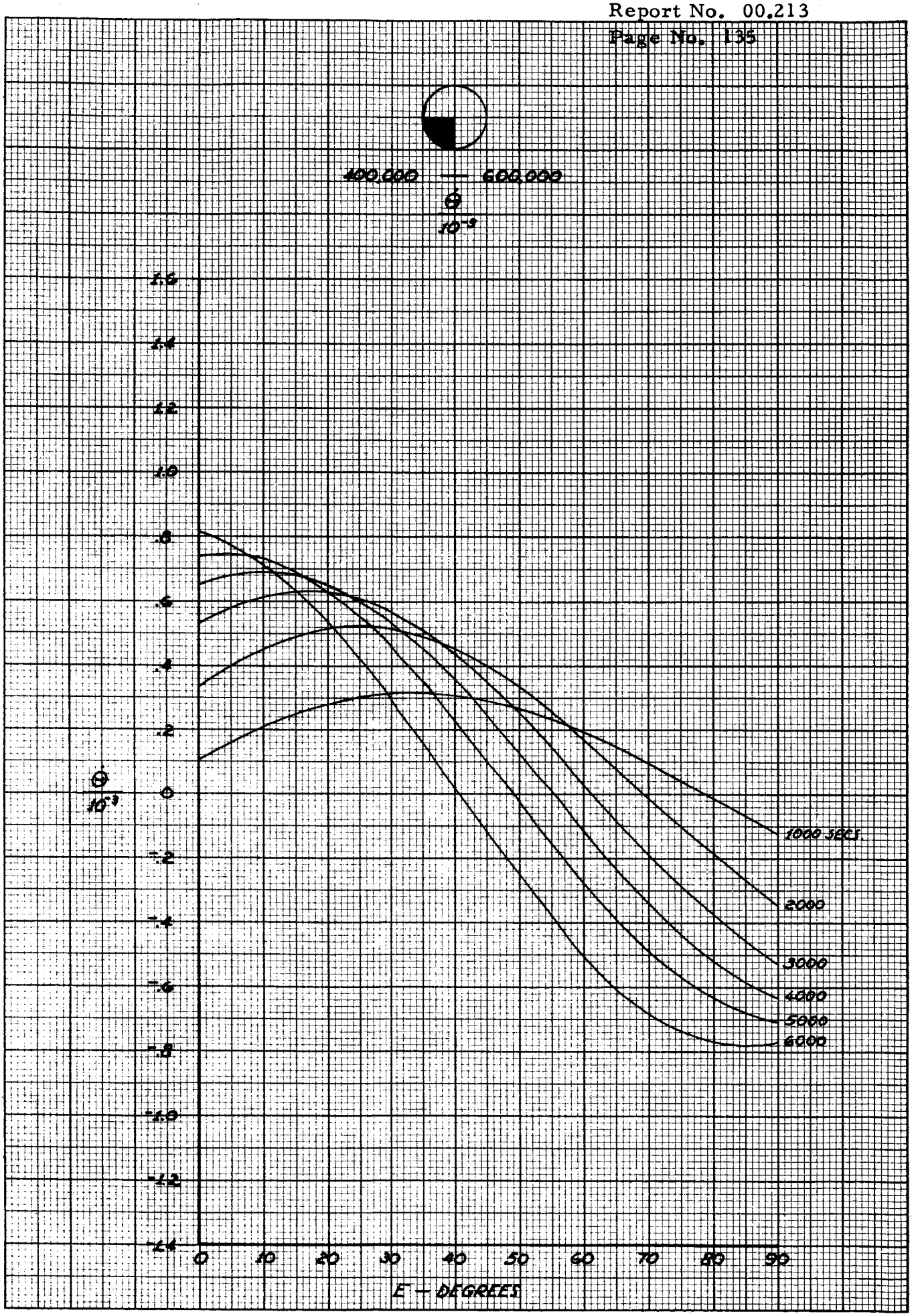
400,000 — 600,000
$\dot{\Theta}$
10^{-3}
1.6
1.4
1.2
1.0
.8
.6
.4
.2
0
-.2
-.4
-.6
-.8
-1.0
-1.2
-1.4
$\dot{\Theta}$
10^{-3}
1000 SECS.
2000
3000
4000
5000
6000
0
10
20
30
40
50
60
70
80
90
E — DEGREES

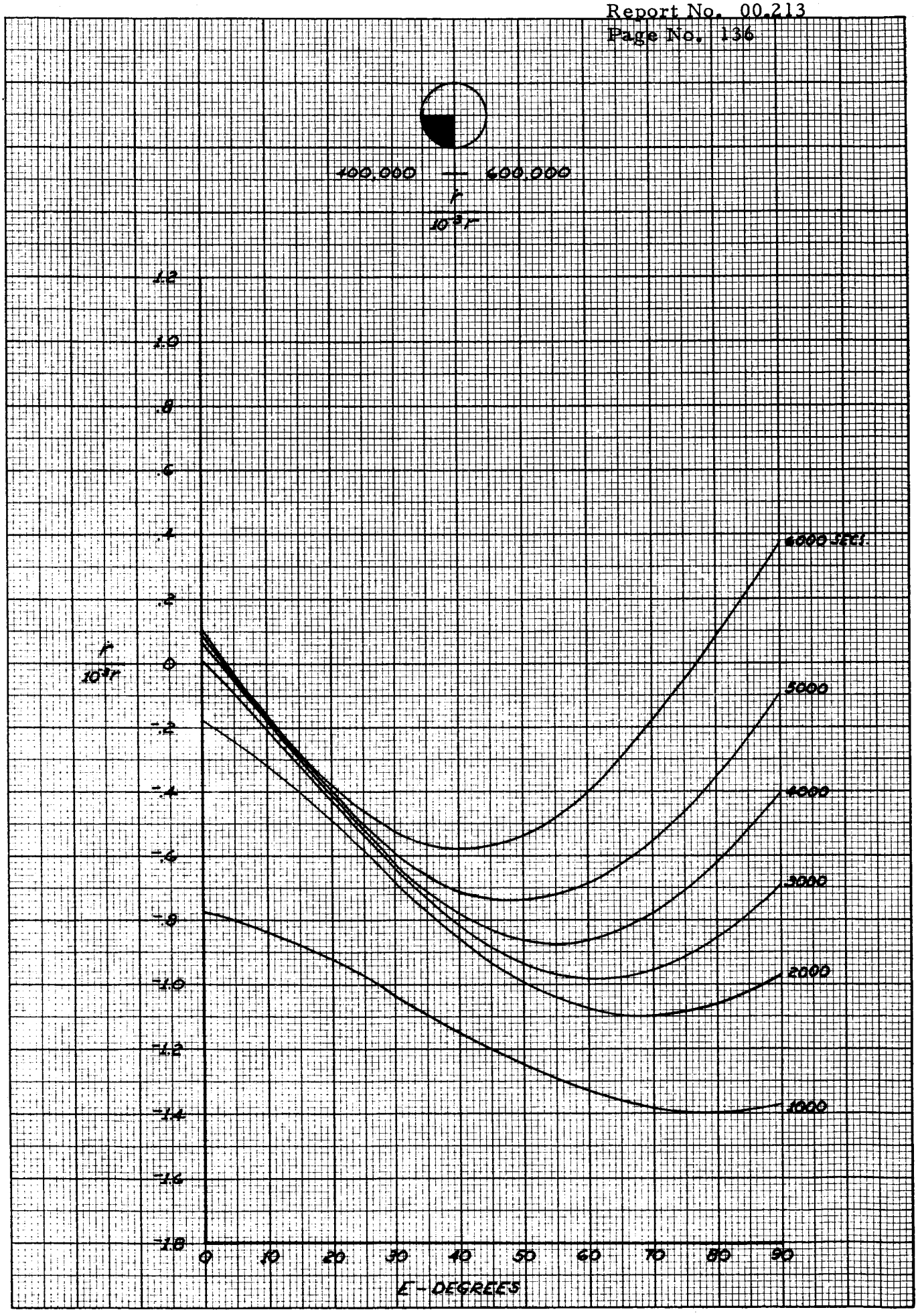
400,000 — 600,000
$\frac{\dot{r}}{10^{-3}r}$
1.2
1.0
.8
.6
.4
.2
0
-.2
-.4
-.6
-.8
-1.0
-1.2
-1.4
-1.6
-1.8
6000 SEC.
5000
4000
3000
2000
1000
0
10
20
30
40
50
60
70
80
90
E - DEGREES

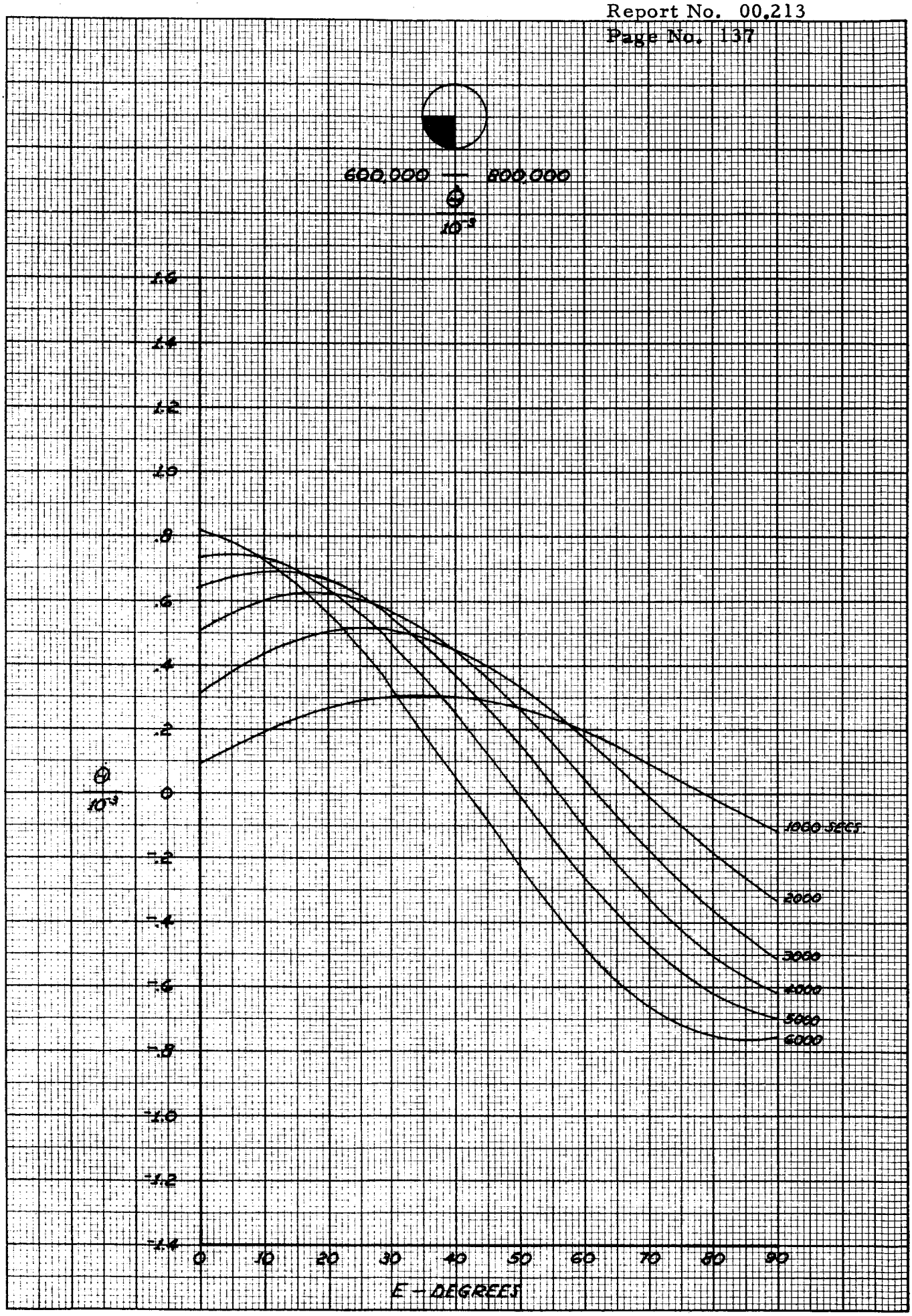
600,000 — 800,000
$\frac{\dot{\Theta}}{10^{-3}}$
1.6
1.4
1.2
1.0
.8
.6
.4
.2
0
-.2
-.4
-.6
-.8
-1.0
-1.2
-1.4
1000 SECS.
2000
3000
4000
5000
6000
0
10
20
30
40
50
60
70
80
90
E — DEGREES

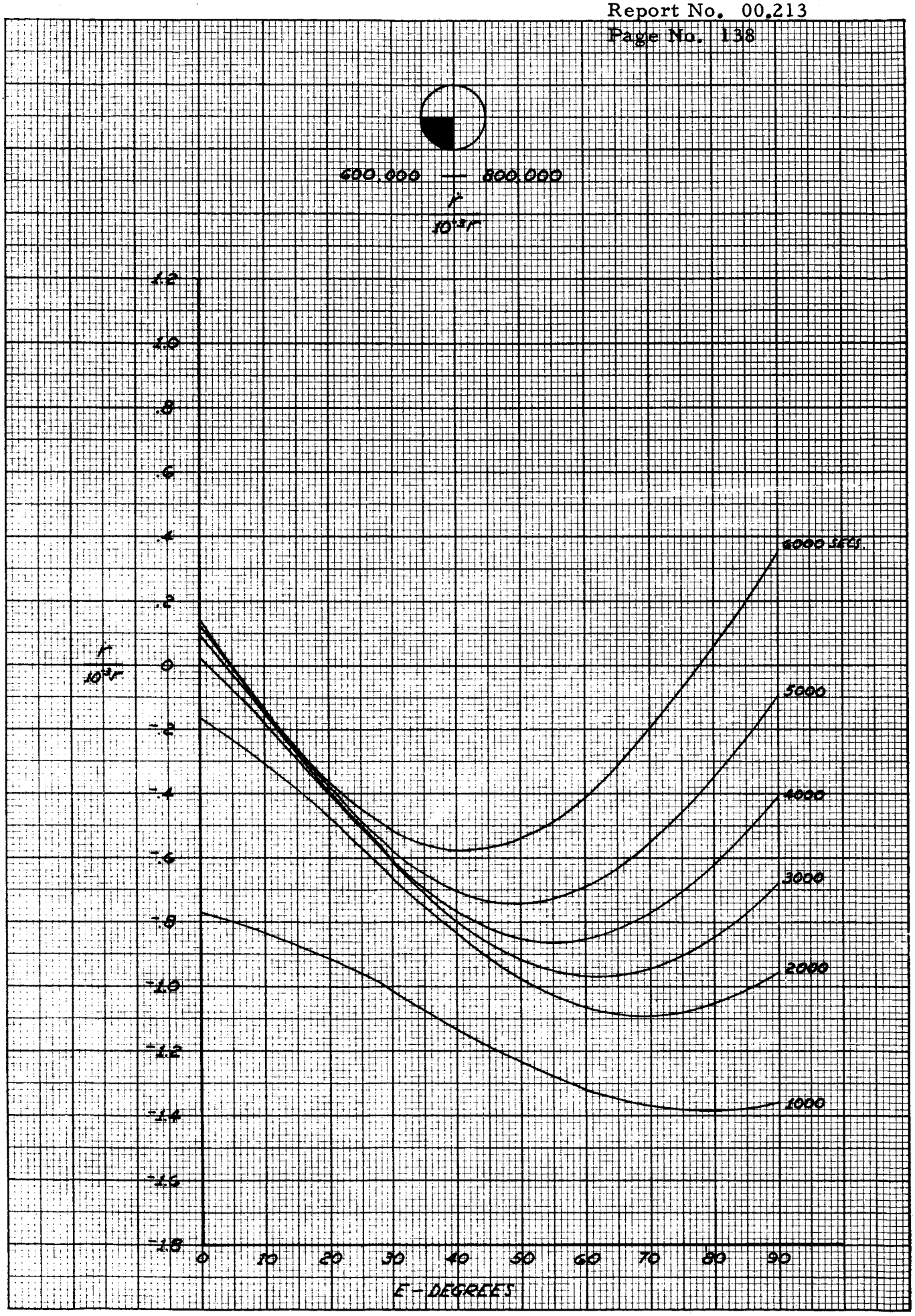
600,000 — 800,000
f²
10⁻³f
1.2
1.0
.8
.6
.4
.2
0
-.2
-.4
-.6
-.8
-1.0
-1.2
-1.4
-1.6
-1.8
f
10⁻³f
6000 SECS.
5000
4000
3000
2000
1000
0
10
20
30
40
50
60
70
80
90
E - DEGREES

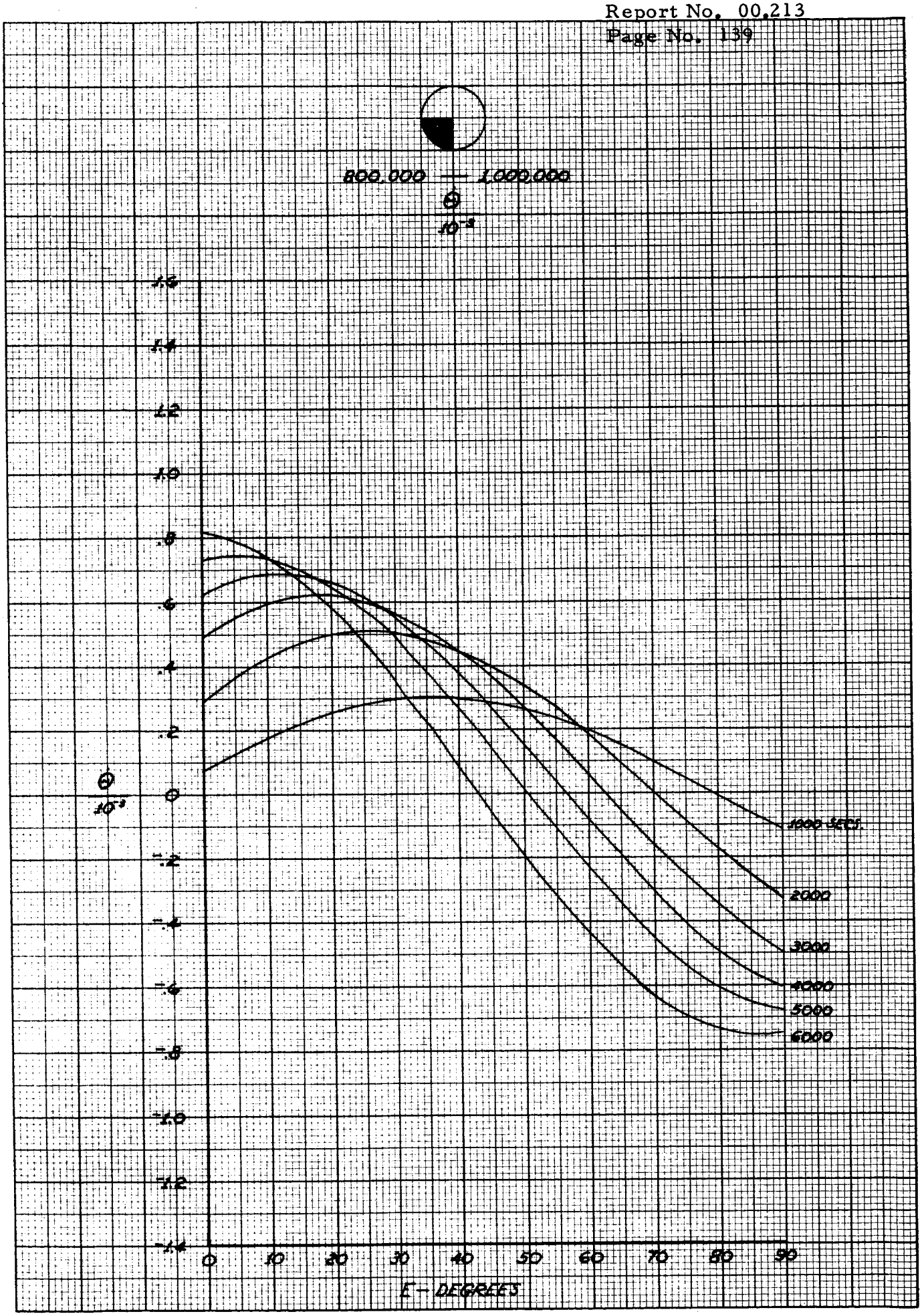
800,000 — 1,000,000
Θ
10⁻³
1.6
1.4
1.2
1.0
.8
.6
.4
.2
0
-.2
-.4
-.6
-.8
-1.0
-1.2
-1.4
1500 SECS.
2000
3000
4000
5000
6000
0
10
20
30
40
50
60
70
80
90
E - DEGREES

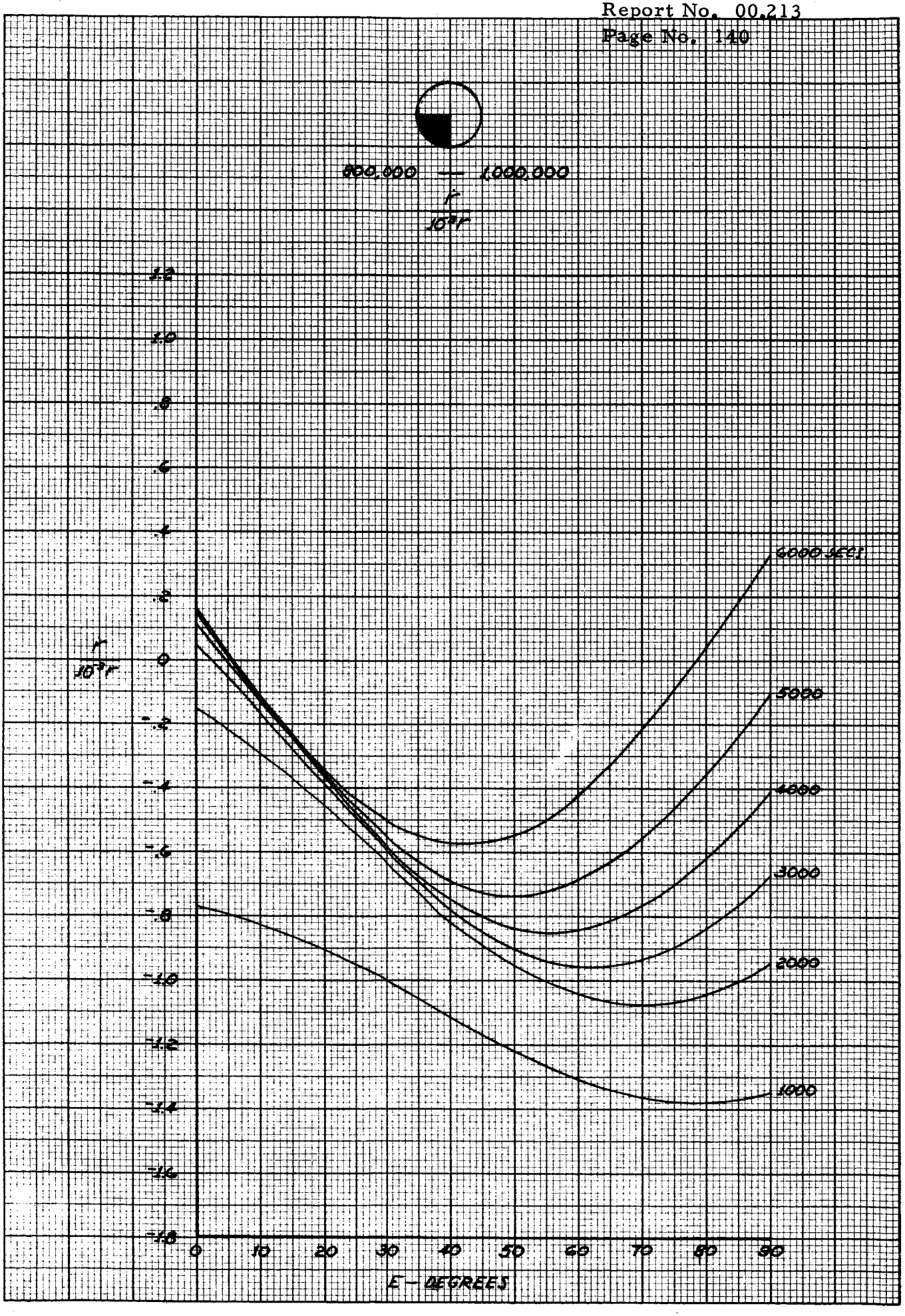
800,000 — 1000,000
f
10^{-3}f
1.2
1.0
.8
.6
.4
.2
0
-.2
-.4
-.6
-.8
-1.0
-1.2
-1.4
-1.6
-1.8
$\frac{f'}{10^{-3}f}$
6000 sec.
5000
4000
3000
2000
1000
0
10
20
30
40
50
60
70
80
90
E - DEGREES

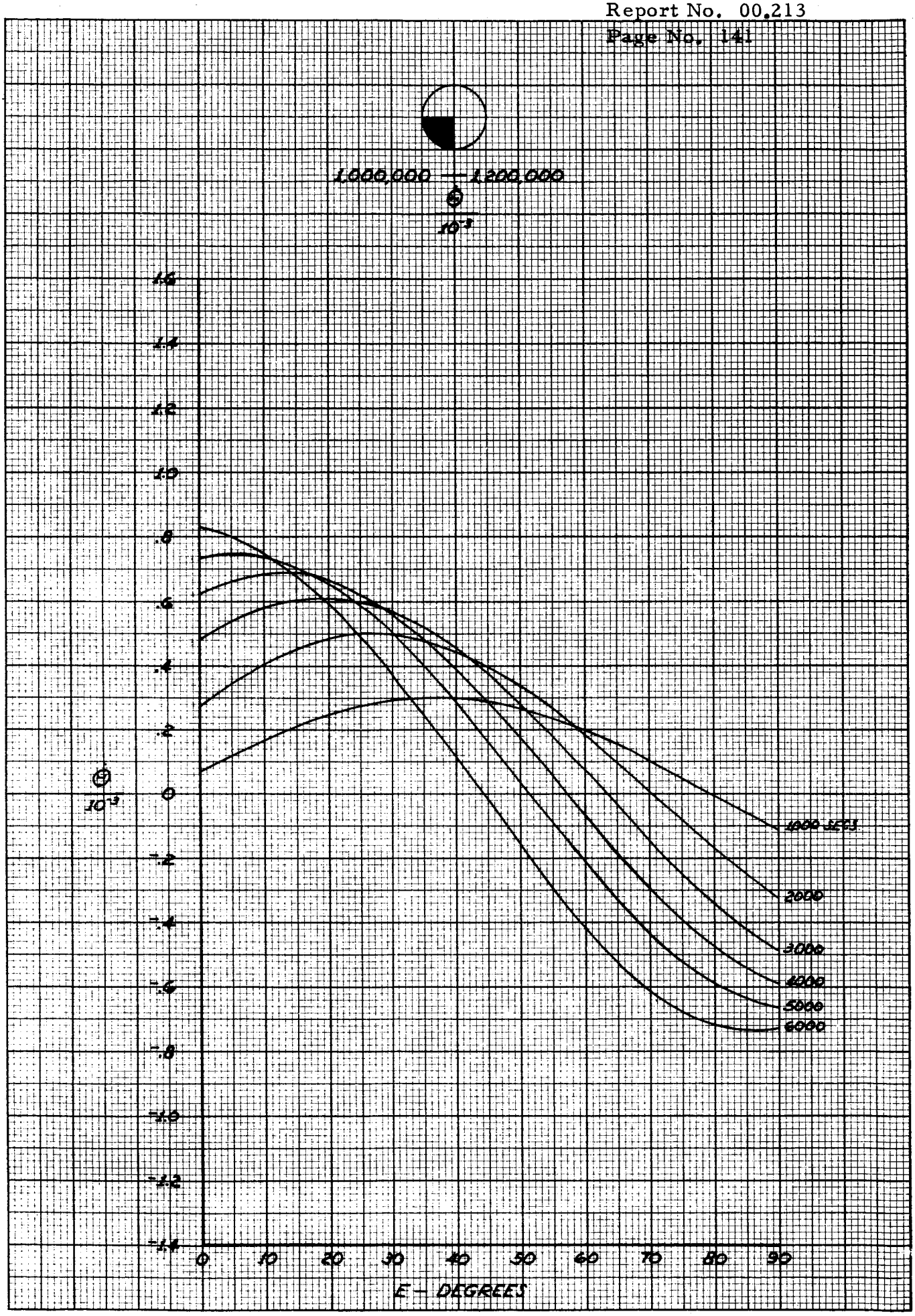
1,000,000 — 1,200,000
Φ
10^{-3}
1.6
1.4
1.2
1.0
.8
.6
.4
.2
0
-.2
-.4
-.6
-.8
-1.0
-1.2
-1.4
Φ
10^{-3}
1000 SECS
2000
3000
4000
5000
6000
0
10
20
30
40
50
60
70
80
90
E – DEGREES

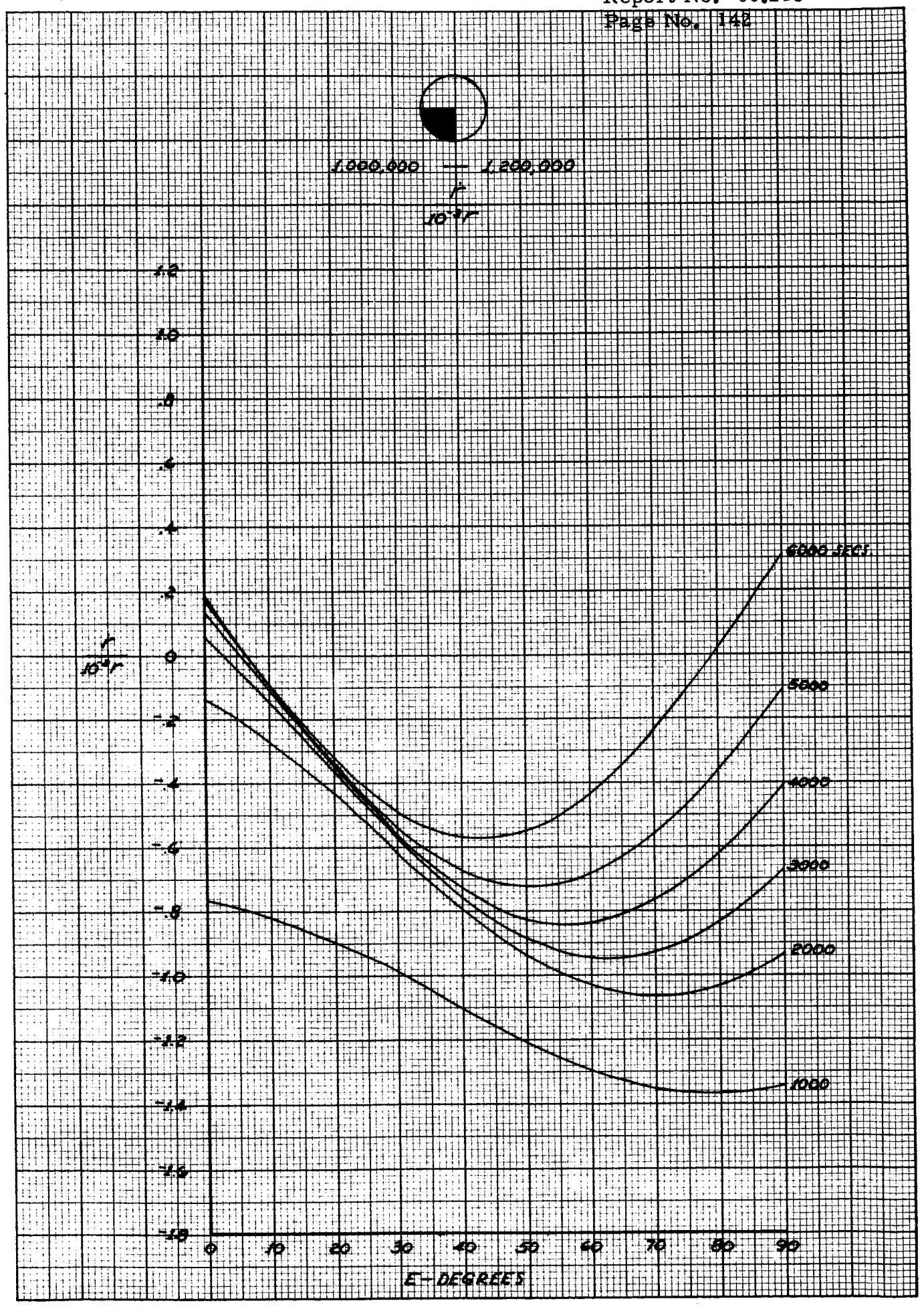
1,000,000 — 1,200,000
f
10⁻¹²f
1.2
1.0
.8
.6
.4
.2
0
-.2
-.4
-.6
-.8
-1.0
-1.2
-1.4
-1.6
-1.8
6000 SECS
5000
4000
3000
2000
1000
0
10
20
30
40
50
60
70
80
90
E-DEGREES

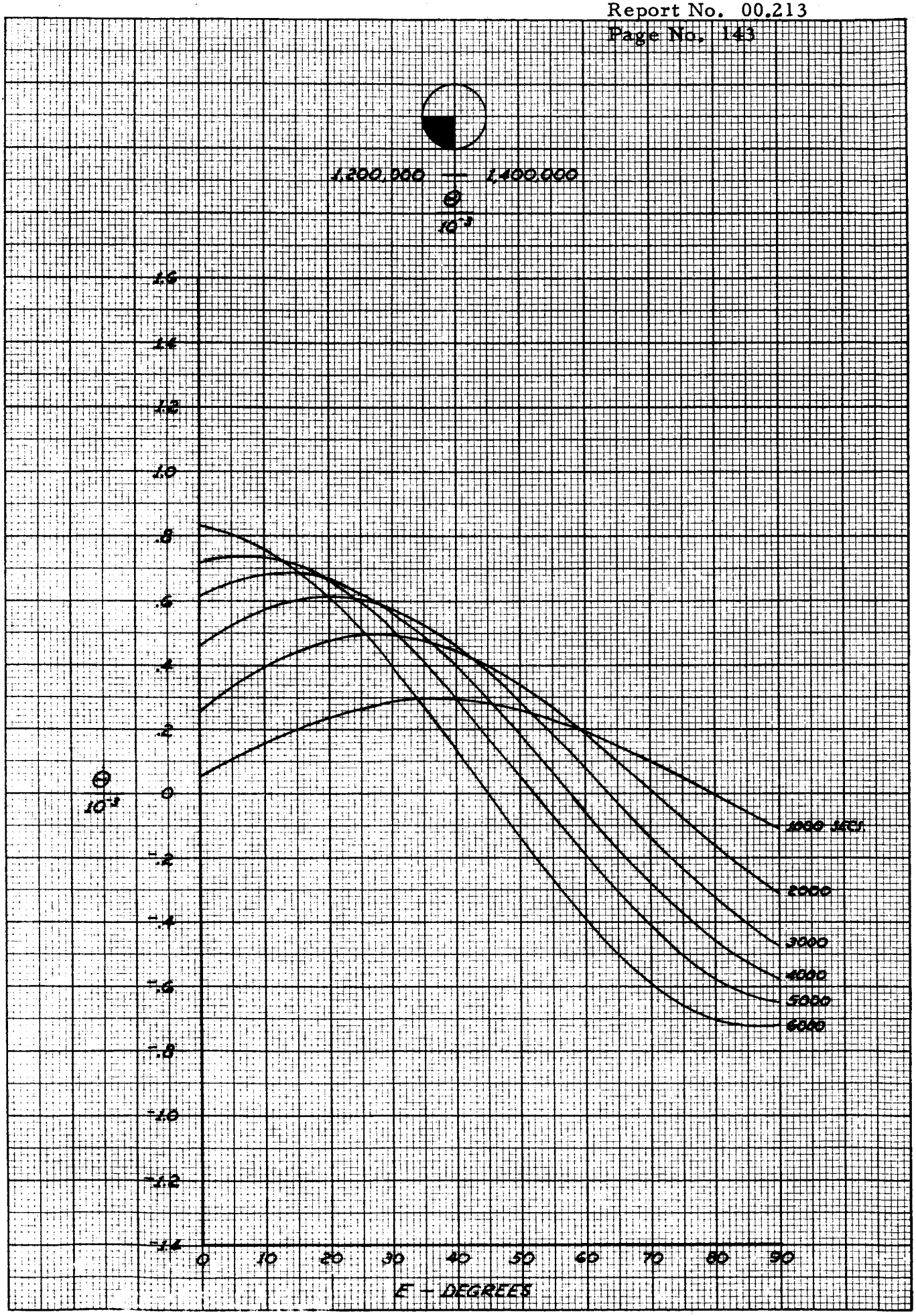
1,200,000 — 1,400,000
Θ
10⁻³
1.6
1.4
1.2
1.0
.8
.6
.4
.2
0
-.2
-.4
-.6
-.8
-1.0
-1.2
-1.4
Θ
10⁻³
1000 MEV
2000
3000
4000
5000
6000
0
10
20
30
40
50
60
70
80
90
F - DEGREES

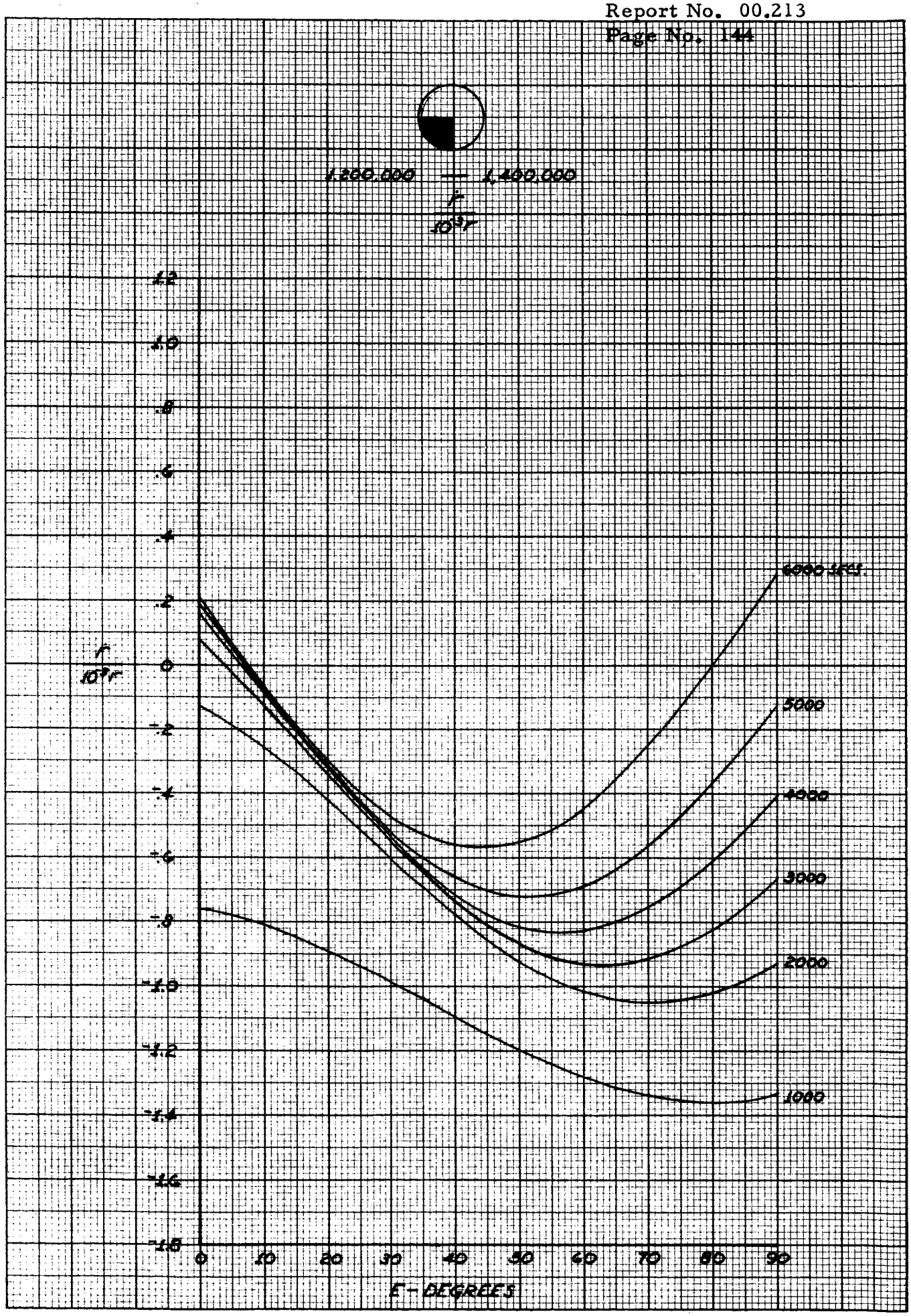
1,200,000 — 1,400,000
f
10^3 r
1.2
1.0
.8
.6
.4
.2
0
-.2
-.4
-.6
-.8
-1.0
-1.2
-1.4
-1.6
-1.8
f
10^3 r
6000 RPM
5000
4000
3000
2000
1000
0
10
20
30
40
50
60
70
80
90
E - DEGREES

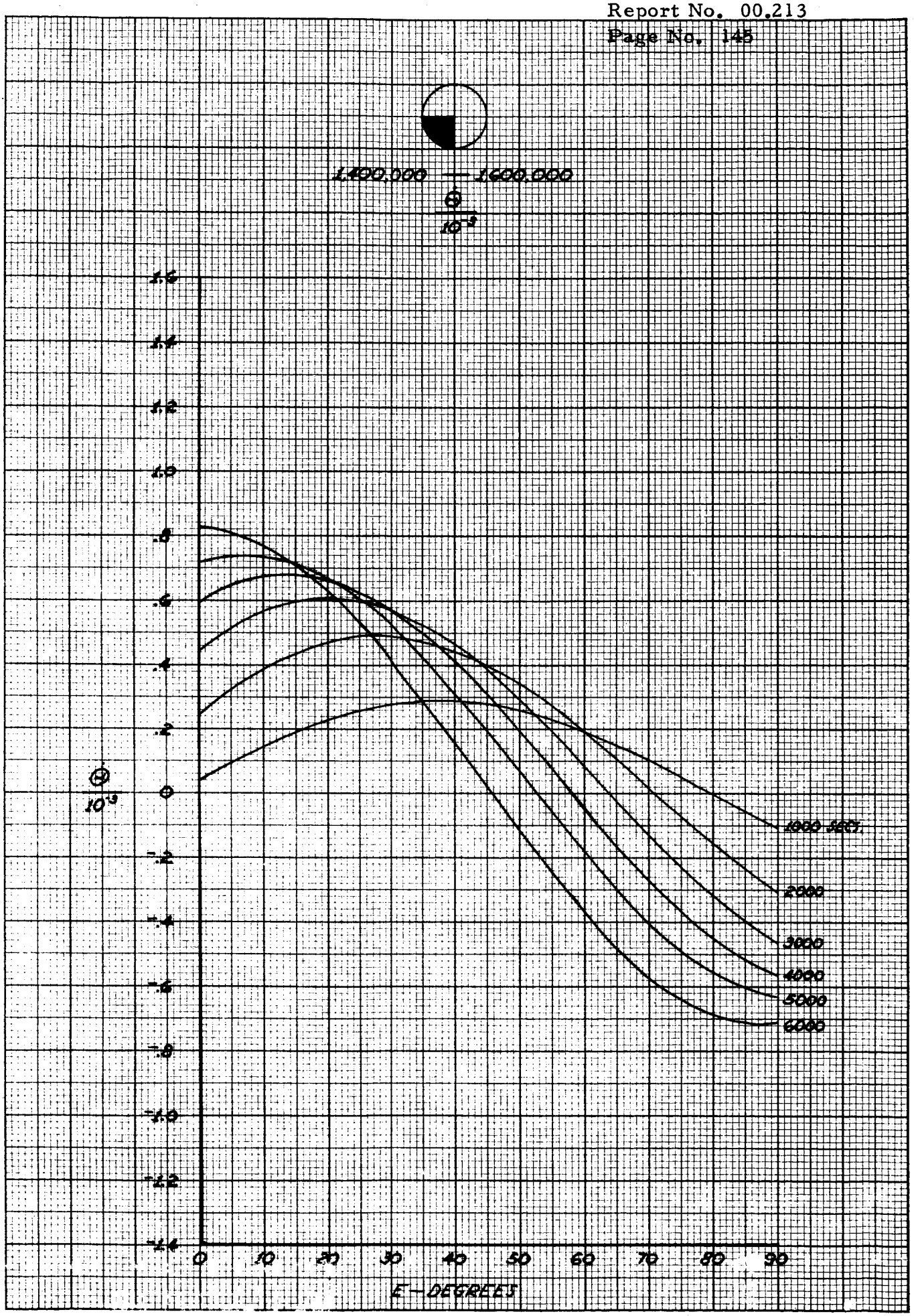
1,400,000 — 1600,000
Φ/10⁻⁹
1.6
1.4
1.2
1.0
.8
.6
.4
.2
0
-.2
-.4
-.6
-.8
-1.0
-1.2
-1.4
Φ/10⁻⁹
1000 RPM
2000
3000
4000
5000
6000
0
10
20
30
40
50
60
70
80
90
E - DEGREES

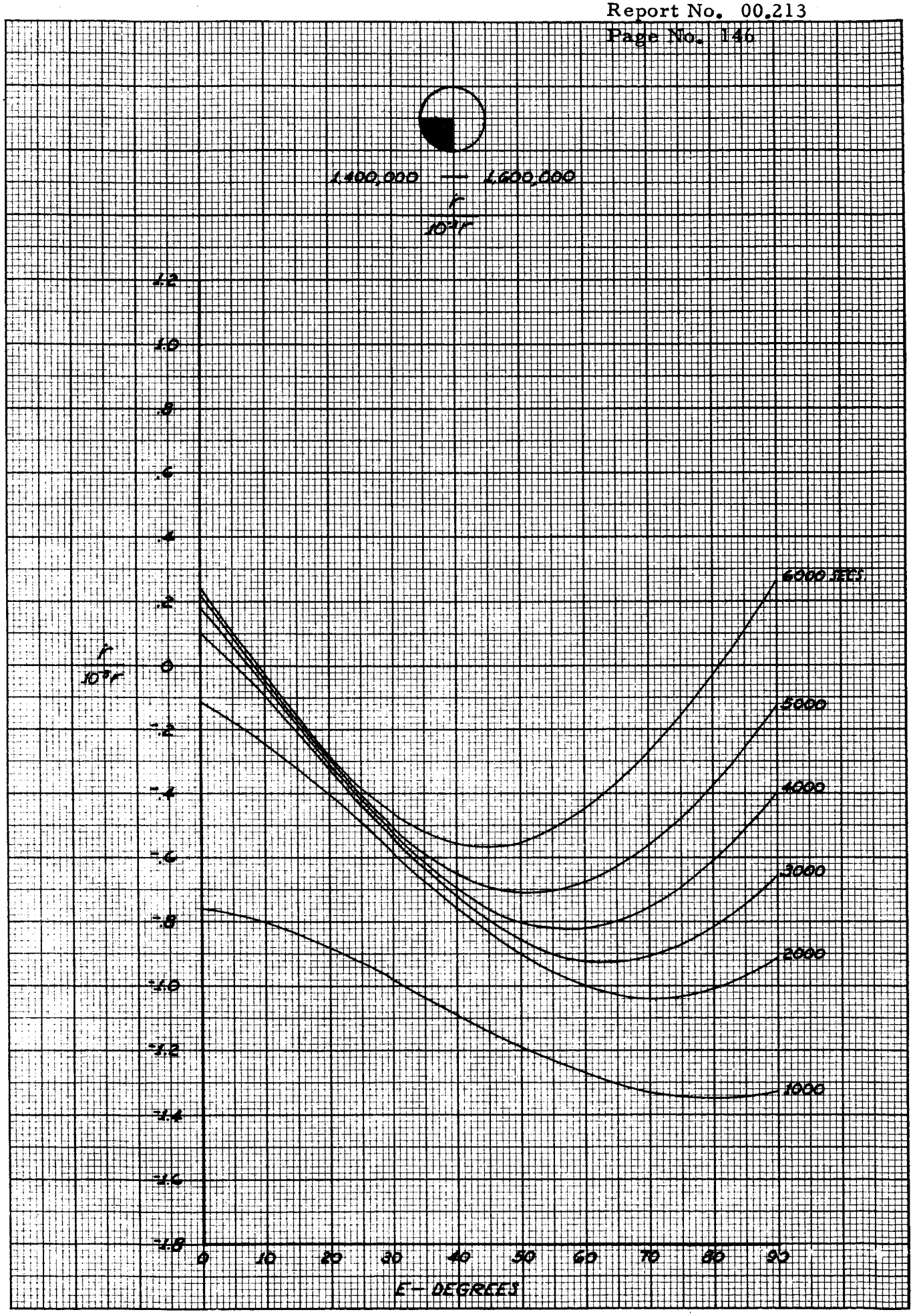
1400,000 — 1,600,000
f
10^{-9}f
1.2
1.0
.8
.6
.4
.2
0
-.2
-.4
-.6
-.8
-1.0
-1.2
-1.4
-1.6
-1.8
f
10^{-9}f
6000 SECS
5000
4000
3000
2000
1000
0
10
20
30
40
50
60
70
80
90
E — DEGREES

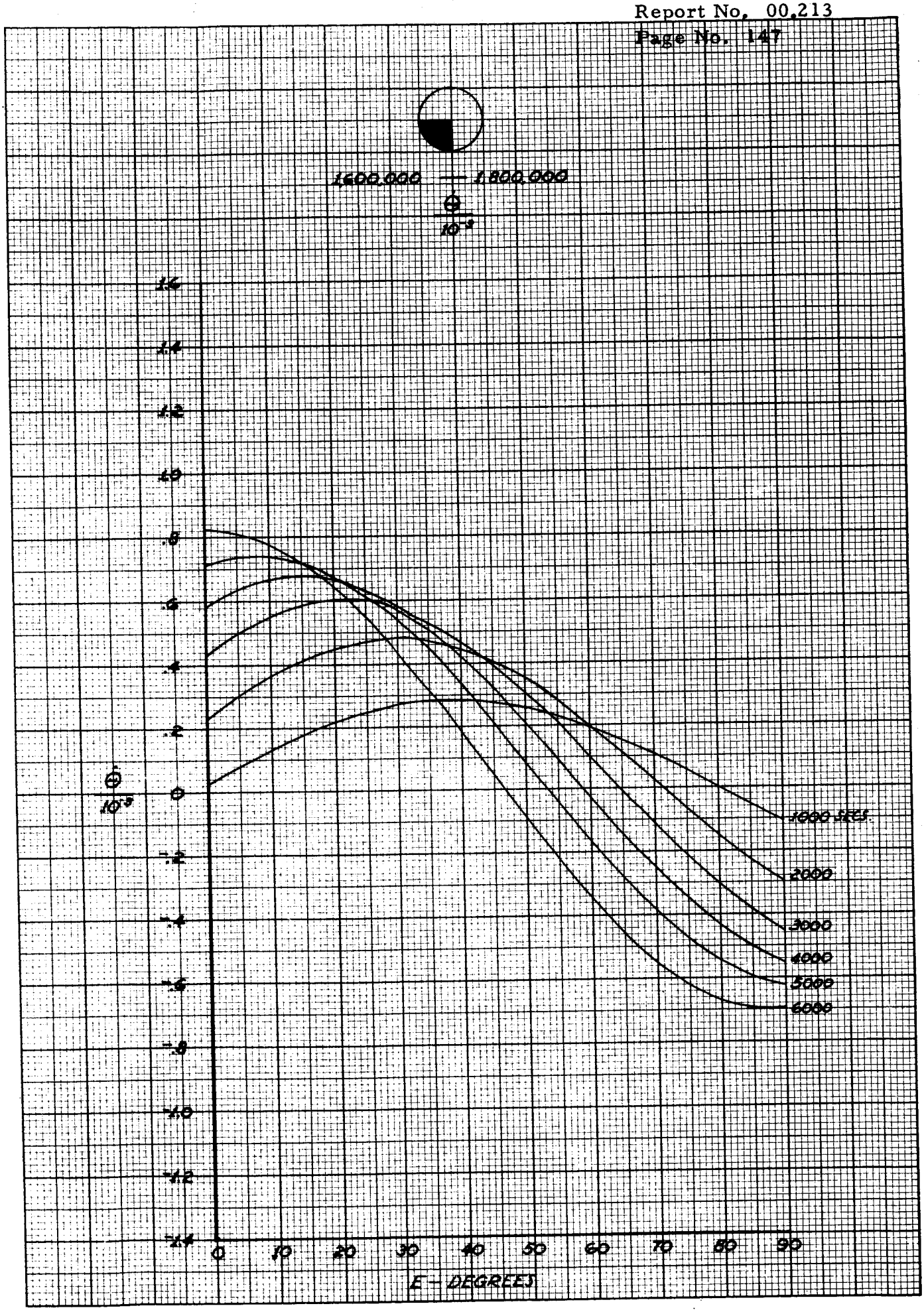
1,600,000 — 1,800,000
$\frac{\dot{\Theta}}{10^{-3}}$
1.6
1.4
1.2
1.0
.8
.6
.4
.2
0
-.2
-.4
-.6
-.8
-1.0
-1.2
-1.4
1000 SECS.
2000
3000
4000
5000
6000
0
10
20
30
40
50
60
70
80
90
E - DEGREES

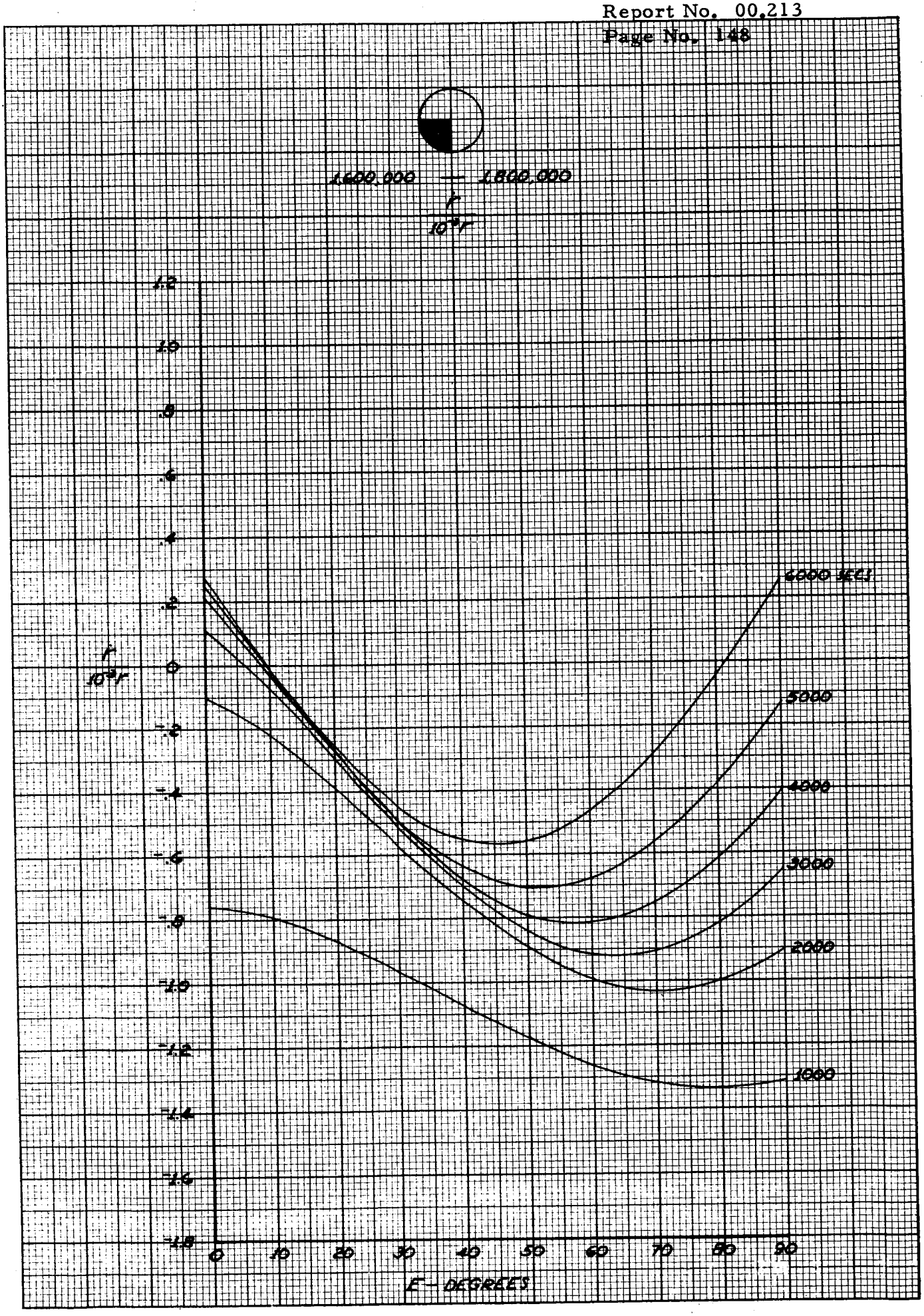
1,600,000 — 1,800,000
f
10⁻³f
1.2
1.0
.8
.6
.4
.2
0
-.2
-.4
-.6
-.8
-1.0
-1.2
-1.4
-1.6
-1.8
f
10⁻³f
6000 SECS
5000
4000
3000
2000
1000
0
10
20
30
40
50
60
70
80
90
E - DEGREES

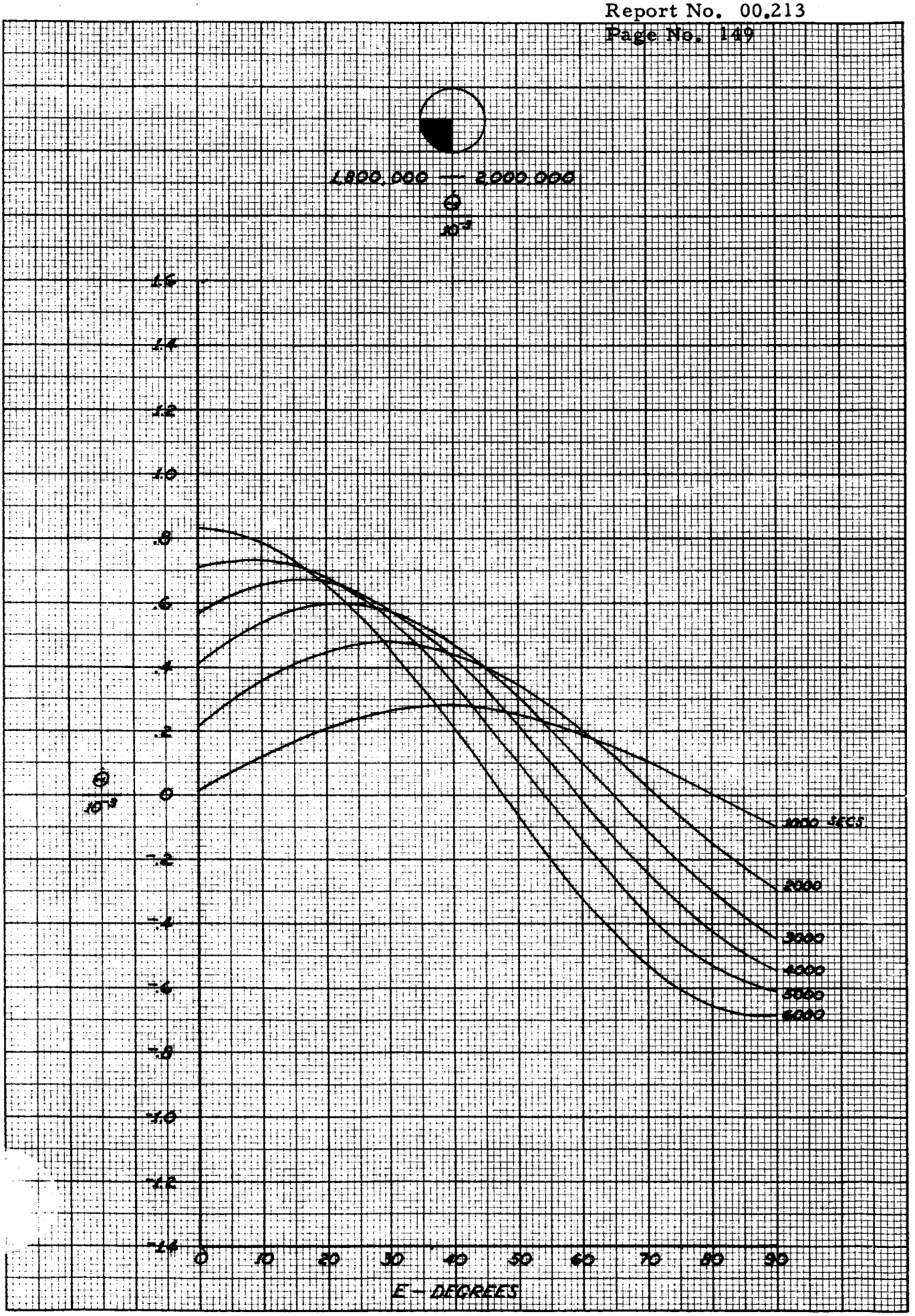
1,800,000 — 2,000,000
Φ
10⁻⁹
1.6
1.4
1.2
1.0
.8
.6
.4
.2
0
-.2
-.4
-.6
-.8
-1.0
-1.2
-1.4
0
10
20
30
40
50
60
70
80
90
E – DEGREES
1000 secs
2000
3000
4000
5000
6000

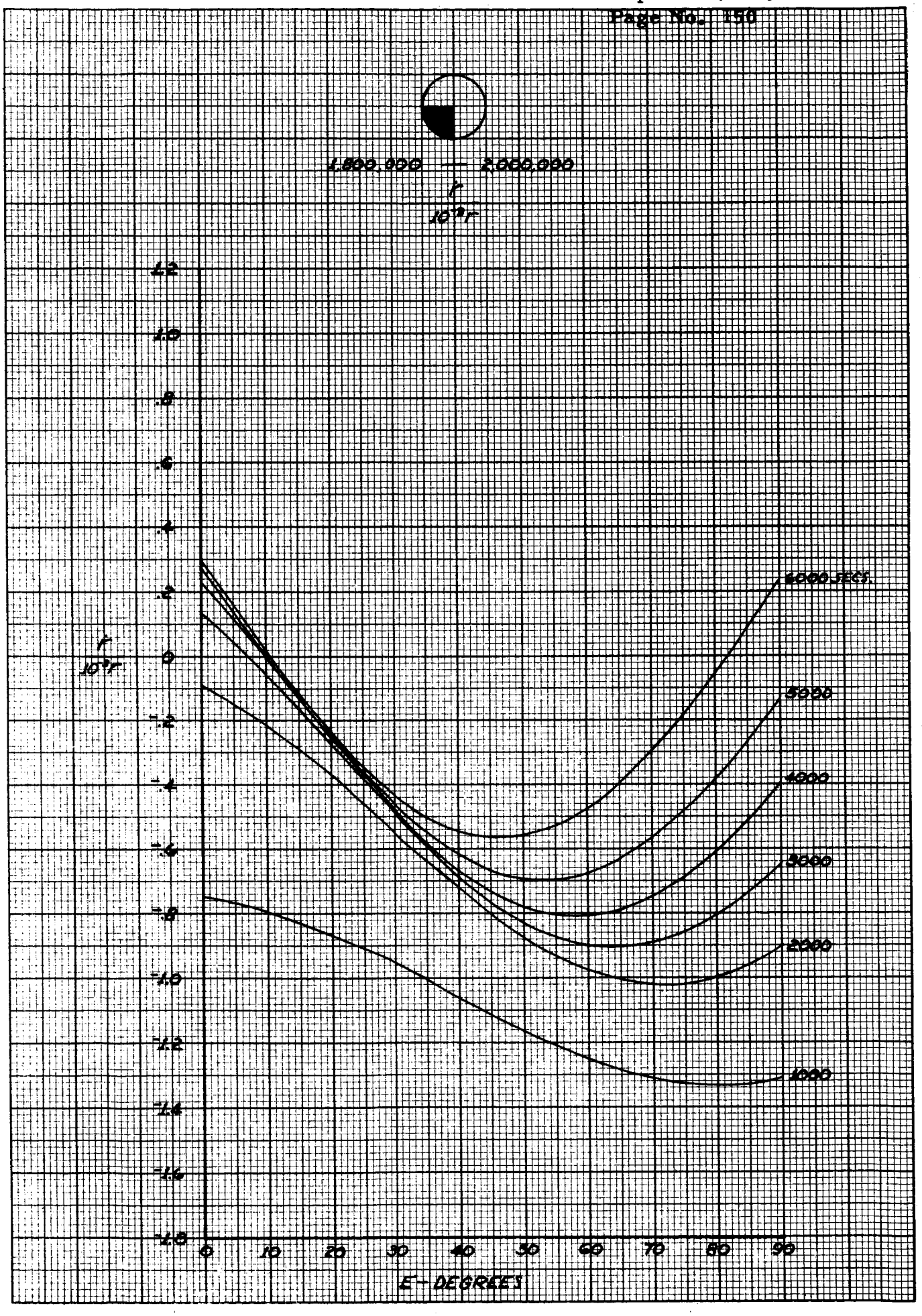
1,800,000 — 2,000,000
f
10^{12}r
.12
1.0
.8
.6
.4
.2
0
-.2
-.4
-.6
-.8
-1.0
-1.2
-1.4
-1.6
-1.8
f
10^{12}r
6000 JECS.
5000
4000
3000
2000
1000
0
10
20
30
40
50
60
70
80
90
E - DEGREES

APPENDIX C

MIDCOURSE INTERCEPT TRAJECTORY DATA CALCULATIONS

INTRODUCTION

This appendix to the LEM Back-up Guidance Report presents an explanation of the computer program used to calculate midcourse intercept trajectory data. Included in this appendix are discussions of the desired data, equations used, and method of utilization. This program is useful not only in determining nominal intercept trajectories, but also to investigate the effects on intercept accuracy of injection errors. The routine is restricted to coasting trajectories with both vehicles in the same plane.

The program was written in machine language for the Autonetics Recomp III Computer and retained for future use in similar studies.

LIST OF SYMBOLS

r_i - Radius vector of interceptor orbit.

v_i - Velocity of interceptor.

γ - Interceptor flight path angle.

r_t - Radius of target circular orbit.

v_t - Velocity of target.

$\Delta\phi_o$ - Difference in angular position of two vehicles.

$\Delta\phi_i$ - Increment in true anomaly of interceptor.

ϕ_{i_T} - Angular portion of intercept trajectory investigated.

μ - Gravitational constant.

τ_c - Orbital period of target vehicle.

a - Length of semimajor axis of intercept trajectory.

p - Semilatus rectum.

e - Eccentricity of trajectory.

r_p - Radius at pericynthion.

r_a - Radius at apocynthion.

ϕ_o - Initial true anomaly of interceptor with respect to pericynthion.

ϕ_i - True anomaly of interceptor with respect to pericynthion.

E - Eccentric anomaly of intercept.

t - Time from pericynthion.

ϕ_{t_o} - Initial angular position of target.

ϕ_t - Angular position of target.

r - Line of sight range to target.

β - Line of sight elevation to target (ref. to local vertical).

LIST OF SYMBOLS (Cont'd)

α - Line-of-sight elevation to target (ref. to local horizontal).

$\dot{r}$ - Line-of-sight range rate.

$\dot{\theta}$ - Line-of-sight inertial angular rate.

Desired Output

The program was written to calculate intercept trajectory data for a transfer from any arbitrary lunar orbit (LEM) to a vehicle (Apollo Command Module) that is moving in a lunar circular orbit. The interceptor trajectory is calculated from one set of initial conditions using orbital equations derived from the equations of motion. Inputs required are the target altitude and velocity; interceptor altitude, velocity, and flight path angle; and the initial difference in angular position of the two vehicles. The primary objective of the program is to furnish the following midcourse trajectory data as a function of time: (1) line-of-sight range between the two vehicles, (2) line-of-sight range rate, (3) line-of-sight elevation angle to the target (referenced to local horizontal), and (4) inertial line of sight angular rate. The program also computes the following information:

Interceptor - radius vector, velocity, flight path angle, position on trajectory.

Target - position on trajectory.

Equations and Method of Utilization

The detailed equations used in this program are listed in Table C-I. Conditions at the time the interceptor is injected into the intercept trajectory are used to calculate the parameters of the intercept ellipse and the position of the vehicle with respect to the pericynthion of its path. Time from pericynthion is used as the time reference. An investigation of the equations relating time and the true anomaly of an ellipse shows that the use of time as the independent variable is quite awkward,

$$t = (E - e \sin E) \times \text{constant}$$

$$\tan (E/2) = \text{constant} \times \tan (\phi/2)$$

Solving these equations for E and then ϕ would involve some trial and error or approximate method. By using the true anomaly as the independent variable, t can be readily calculated. For a given $\Delta\phi$, a corresponding Δt can be determined. New target and interceptor positions can be calculated.

$$\phi_{i2} = \phi_{i1} + \Delta\phi_i$$

$$\phi_{T2} = \phi_{T1} + (\text{average target angular velocity}) \times \Delta t$$

For each $\Delta\phi_i$, values of r, $\dot{r}$, α, $\dot{\theta}$, and the remaining trajectory data are calculated and printed. This process continues until the entire trajectory or any desired angular portion of the trajectory has been covered.

This program was written to calculate midcourse intercept trajectory data for a lunar orbital transfer. It is not restricted to lunar orbits and can easily be converted to give orbit data for any other body by changing the gravity constant.

TABLE C-I

MIDCOURSE INTERCEPT TRAJECTORY EQUATIONS

Characteristics of Elliptical Trajectory

Semimajor axis

$$a = \frac{\mu}{\frac{2\mu}{r_o} - v_o^2}$$

Semilatus rectum

$$p = \frac{(r_o v_o \cos g_o)^2}{\mu}$$

Eccentricity

$$e = \left(\frac{a - p}{a}\right)^{1/2}$$

Radius at pericynthion

$$r_p = a(1 - e)$$

Radius at apocynthion

$$r_a = a(1 + e)$$

Trajectory Parameters

Initial position with respect to pericynthion

$$\phi_o = \cos^{-1}\left(\frac{p - r_o}{r_o e}\right)$$

Eccentric anomaly

$$E = 2 \tan^{-1}\left[\left(\frac{1 - e}{1 + e}\right)^{1/2} \tan\left(\frac{\phi}{2}\right)\right]$$

TABLE C-I (Cont'd)

Time from pericynthion

$$t = \frac{(E - e \operatorname{Sin} E)}{\mu^{1/2}} \quad a^{3/2}$$

Radius vector of trajectory

$$r_i = \frac{p}{1 + e \operatorname{Cos} \phi_i}$$

Flight path angle

$$g_i = \left[\frac{ap}{r_i (2a - r_i)}\right]^{1/2}$$

Velocity

$$v_i = \frac{r_o V_o \operatorname{Cos} g_o}{r_i \operatorname{Cos} g_i}$$

Relative Position and Velocity Between Two Vehicles

(See Figure C.1 for sign conventions)

Line of sight range

$$r = (r_i^2 + r_t^2 - 2 r_i r_t \operatorname{Cos} \Delta\phi_o)^{1/2}$$

Elevation angle to command module relative to local horizontal

$$\alpha = \pm \frac{\pi}{2} \mp \operatorname{Sin}^{-1} \left(\frac{r_t \operatorname{Sin} \Delta\phi_o}{r}\right)$$

Line-of-sight range rate

$$\dot{r} = \pm \left[v_t \operatorname{Cos} (\alpha + \Delta\phi_o) - v_i \operatorname{Cos} (\alpha + g_i)\right]$$

Inertial angular rate of the line of sight

$$\dot{\theta} = \pm \left[\frac{v_t \operatorname{Sin} (\alpha + \Delta\phi_o) - v_i \operatorname{Sin} (\alpha + g_i)}{r}\right]$$

FIGURE C.1

SIGN CONVENTION

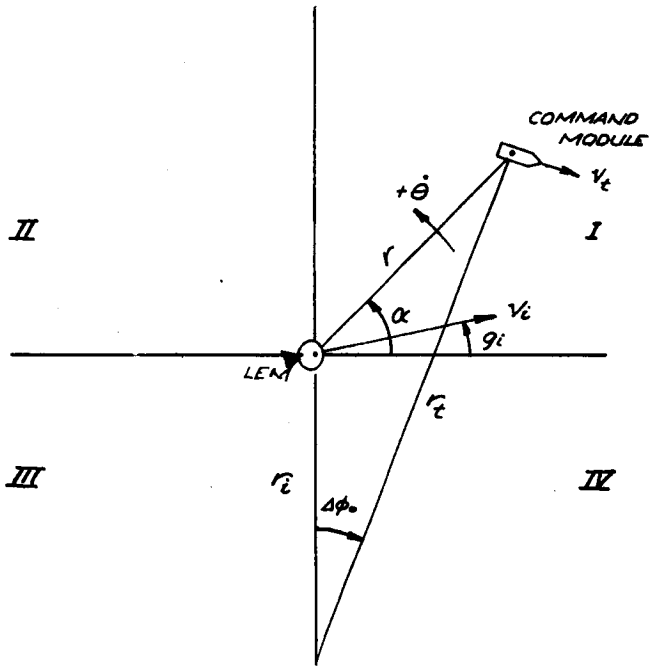

QUAD	α	$\Delta\phi_o$	$\dot{\theta}$	$\dot{r}$
I	+	+	+	*
II	+	-	+	*
III	-	-	+	*
IV	-	+	+	*

* $\dot{r}$ negative if vehicles closing, positive if vehicles moving apart.

APPENDIX D

DESCRIPTION OF THE SIMULATOR FACILITY

A detailed description is presented of all the major components included in the mechanization of the LEM Backup Guidance Simulation Program.

1. Moving Base Cockpit Simulator

Figure D-1 is a view of the simulator room showing the gondola mounted on the moving base inside the 20 foot diameter spherical projection screen. The safety console is also shown: its purpose is to monitor all moving base operations in order to protect personnel and apparatus. Figures D-2 and D-3 are side views of the gondola with the canopy open and closed. The interior lines are typical of a one-place, space glide type vehicle: the shell is a lightweight aluminum structure which is carried on a rigid, tubular steel, truss structure.

2. Master Control Station

The entire simulator operation is directed from a master control station (Figure D-4). Included in this station are a control console, plotters, intercom system controls, and generally all apparatus required to maintain complete control over the simulator operation. The control console contained several repeater instruments for the flight instruments in the cockpit.

3. Target and Starfield Projector

Figure D-5 is a photograph of the target projector; it is composed of two light beam projectors mounted on separate gimbals. The outer gimbal positions the target spot. The starfield effect is obtained with a perforated disk mounted on the second projector tube.

4. Lunar Scene Projector

The lunar scene projector (Figure D-6) is mounted on top of the gondola. It is suspended in a four gimbal arrangement, each axis of which is driven by a closed loop electromechanical servo with unlimited freedom.

5. Computer Facility

The portion of the LTV computer facility employed in the study is outlined in this section.

a. Digital and Conversion Equipment

Figure D-7 is a view of the ASI 210 digital computer. The digital-to-analog and analog-to-digital conversion equipment used was manufactured by Packard Bell.

The number of conversion channels employed is as follows:

A to D - 4

D to A -27 (4 time shared)

b. Analog Equipment

Approximately 100 analog operational amplifiers with the necessary accessories (pots, resolvers, limiters, etc.) were included in the simulation.

6. Instrument Panel Displays

The following displays were presented on the cockpit instrument panel. (See Figures D-8 and D-9.)

a. Three axis attitude ball

b. Present course indicator

c. Vertical velocity

d. Horizontal velocity

e. Altitude

f. %fuel remaining

g. Body axis rates

h. Abort light

j. Elapsed time register

k. Command module relative position and velocity (TV display)

(1) Range

(2) Range rate

(3) Bearing angle

(4) Bearing rate

(5) Elevation angle

(6) Elevation rate

The attitude ball was driven by ϕ, θ, and ψ. Maximum ranges on the vertical velocity instrument were 70, 700, and 7000 FPS. The voltmeter instrument for % fuel remaining was programmed to register descent fuel before staging and ascent fuel thereafter; 100% was indicated at the beginning of descent and again at staging. Range and range rate were displayed with numerical registers; whereas, elevation and bearing angles and rates were displayed with blips on the TV screen. A sketch of the TV display is shown in Figure D-10.

7. Cockpit Controls

The following manual controls were present in the cockpit.

a. Three axis side arm controller

b. Two axis docking throttle for $\pm$ X and $\pm$ Z thrusts

c. Descent engine on-off switch

d. Descent engine hi-low switch

e. Boost engine on-off switch

f. Pitch-Yaw hold switch

g. Starfield reset switch

h. Operate-reset switch

The side arm controller was used for vehicle orientation in the usual manner. The docking throttle had the capability of simultaneously thrusting in both the X and Z directions. Activation of the boost engine switch could be accomplished only with the descent engine switch off. Staging occurred the first time the boost engine switch was turned on. The single hold switch accomplished LEM orientation to force target elevation and bearing to zero.

8. Data Recording

Recording of necessary data was accomplished by means of rectangular plotters, strip chart recorders and digital readouts.

a. Plotters were used as follows:

(1) Polar plot of LEM altitude vs. down-range angle

(2) Orthogonal distances between vehicles referenced to LEM local coordinates (2 pens)

(3) Altitude vs. horizontal velocity

(4) Altitude vs. longitudinal range

The last two plots were terminated shortly after boost burnout.

b. Strip chart (time history) recorders were used for recording the following variables:

$\dot{h}$, h, V_H, $\textcircled{Y}_{RP}$, D_{X_O}, Fuel

c. Digital printouts were made at boost burnout and at the end of the run.

V_H	$\dot{Y}_O$	$\textcircled{Z}_{RD}$	$\dot{D}$
h	$\textcircled{Y}_{RP}$	m	t
$\dot{h}$		D	

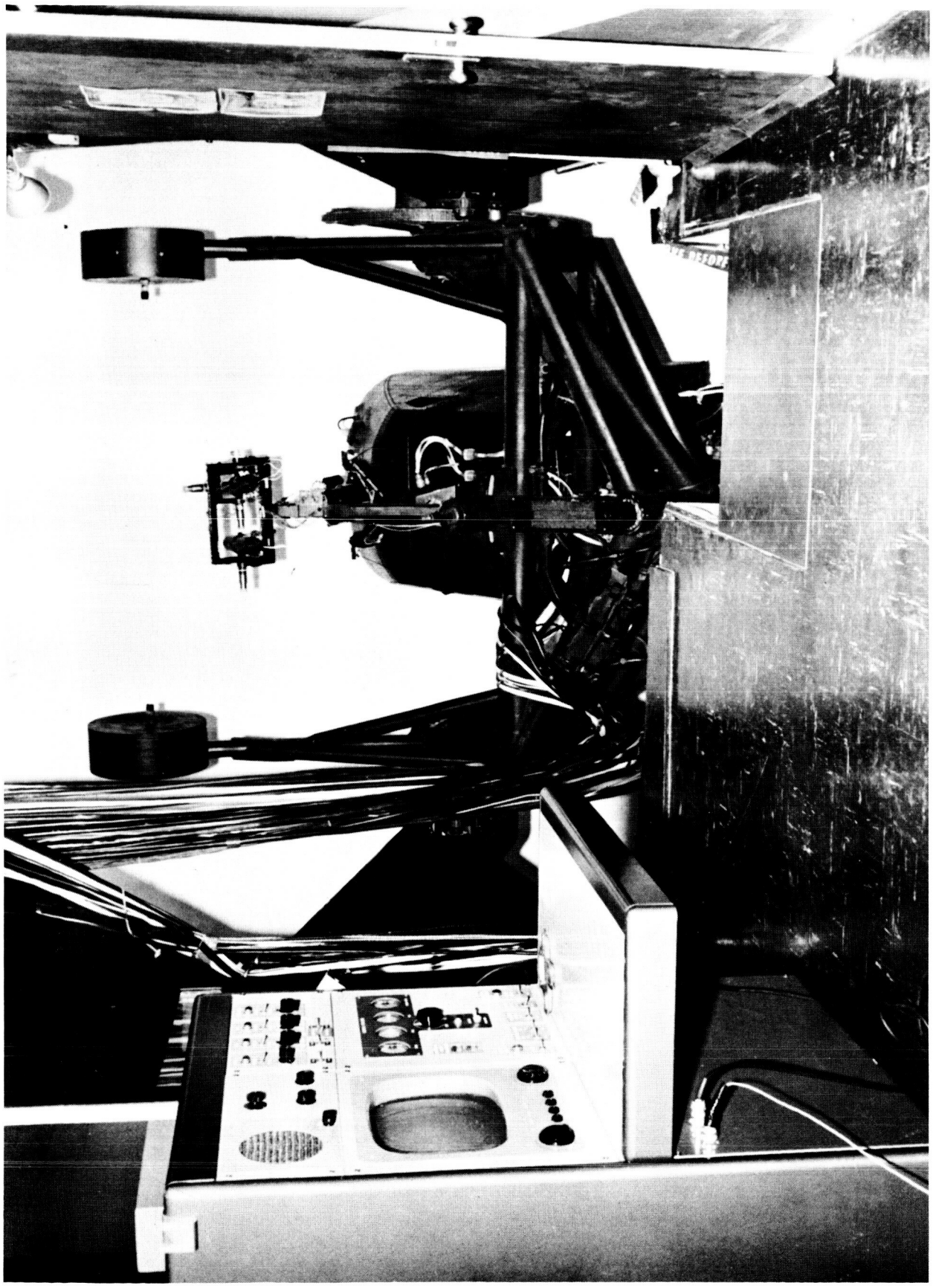

FIGURE D-1 MOVING BASE COCKPIT SIMULATOR WITH SPHERICAL PROJECTION SCREEN AND SAFETY CONSOLE

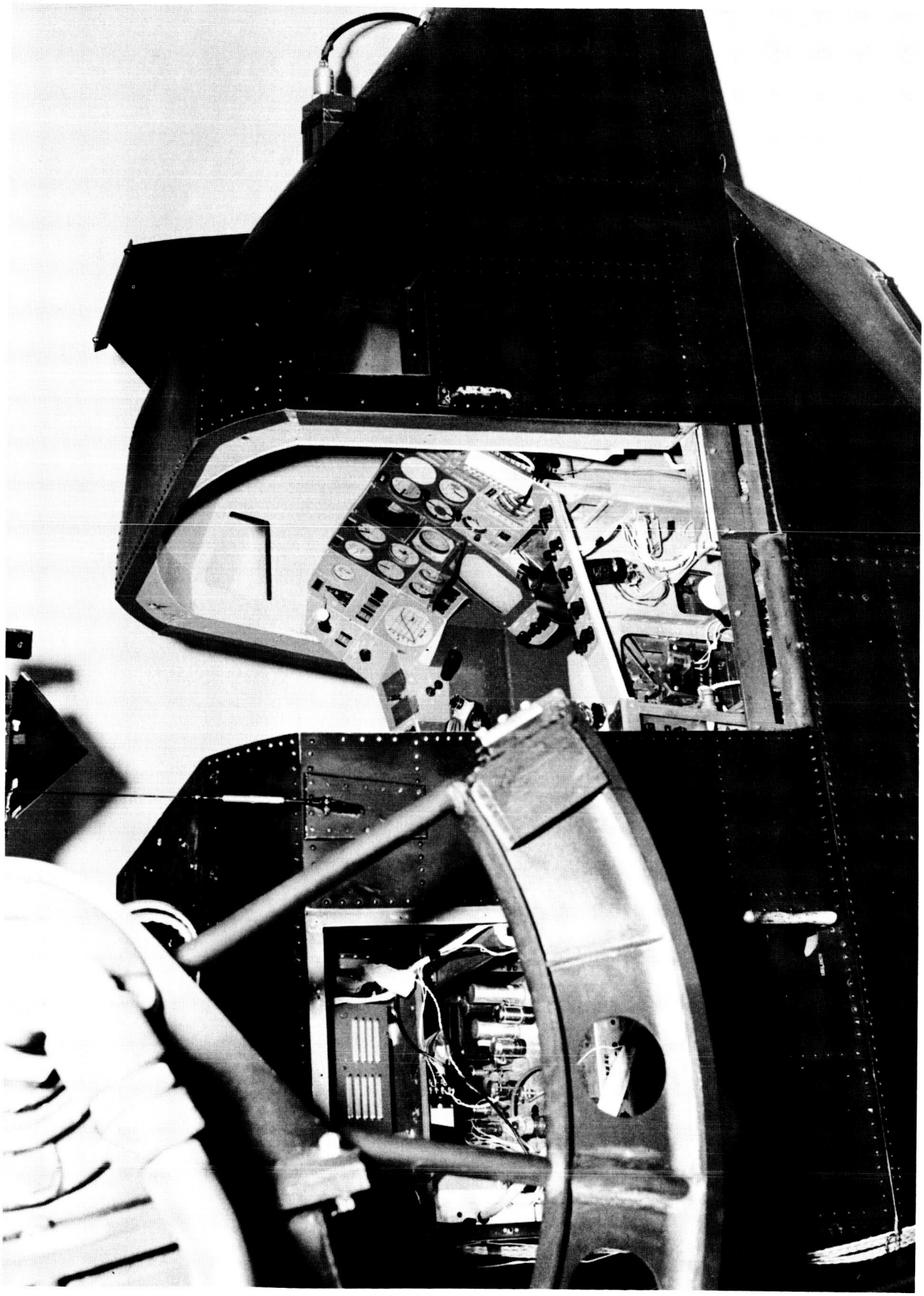

FIGURE D-2 MOVING BASE COCKPIT WITH CANOPY OPEN

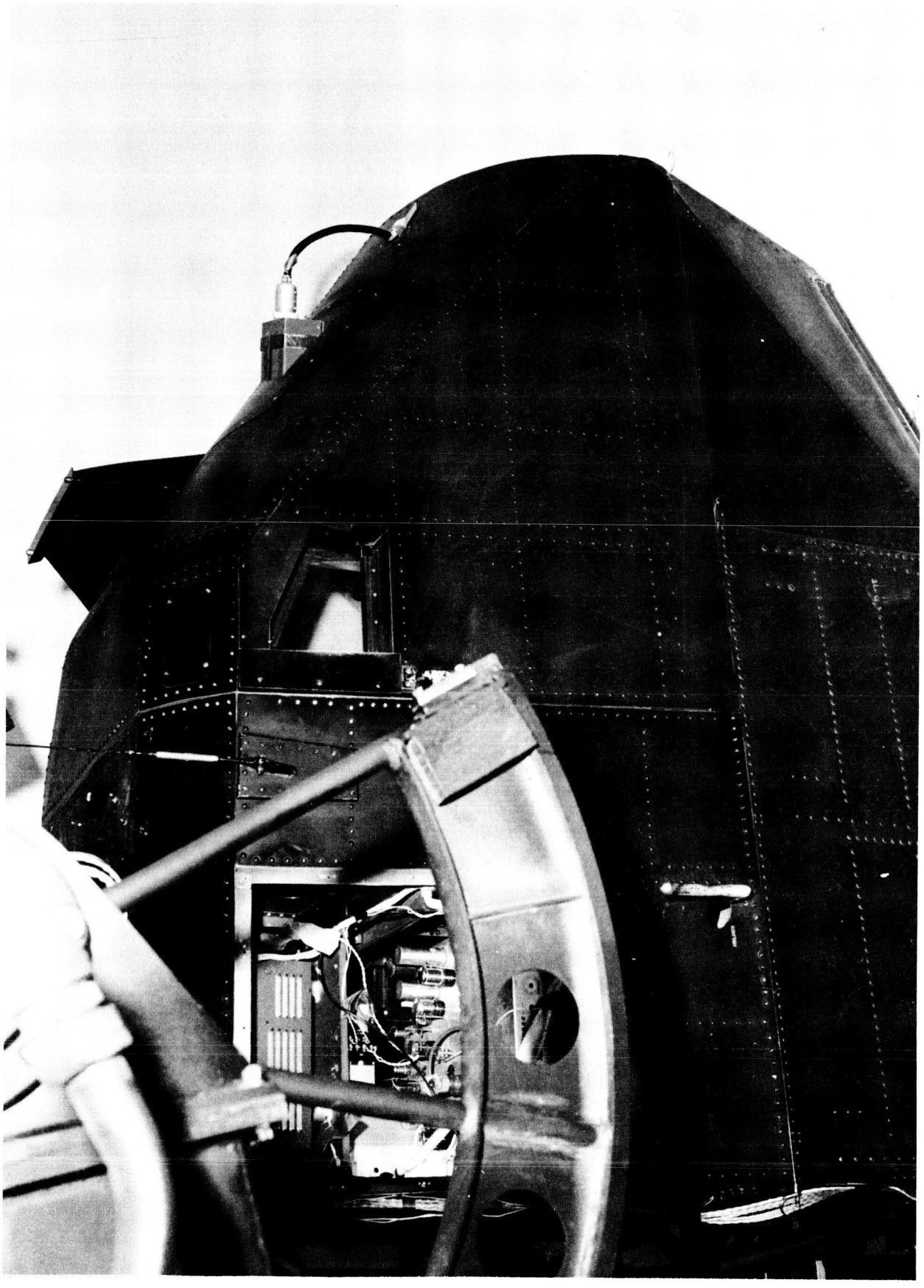

FIGURE D-3 MOVING BASE COCKPIT WITH CANOPY CLOSED

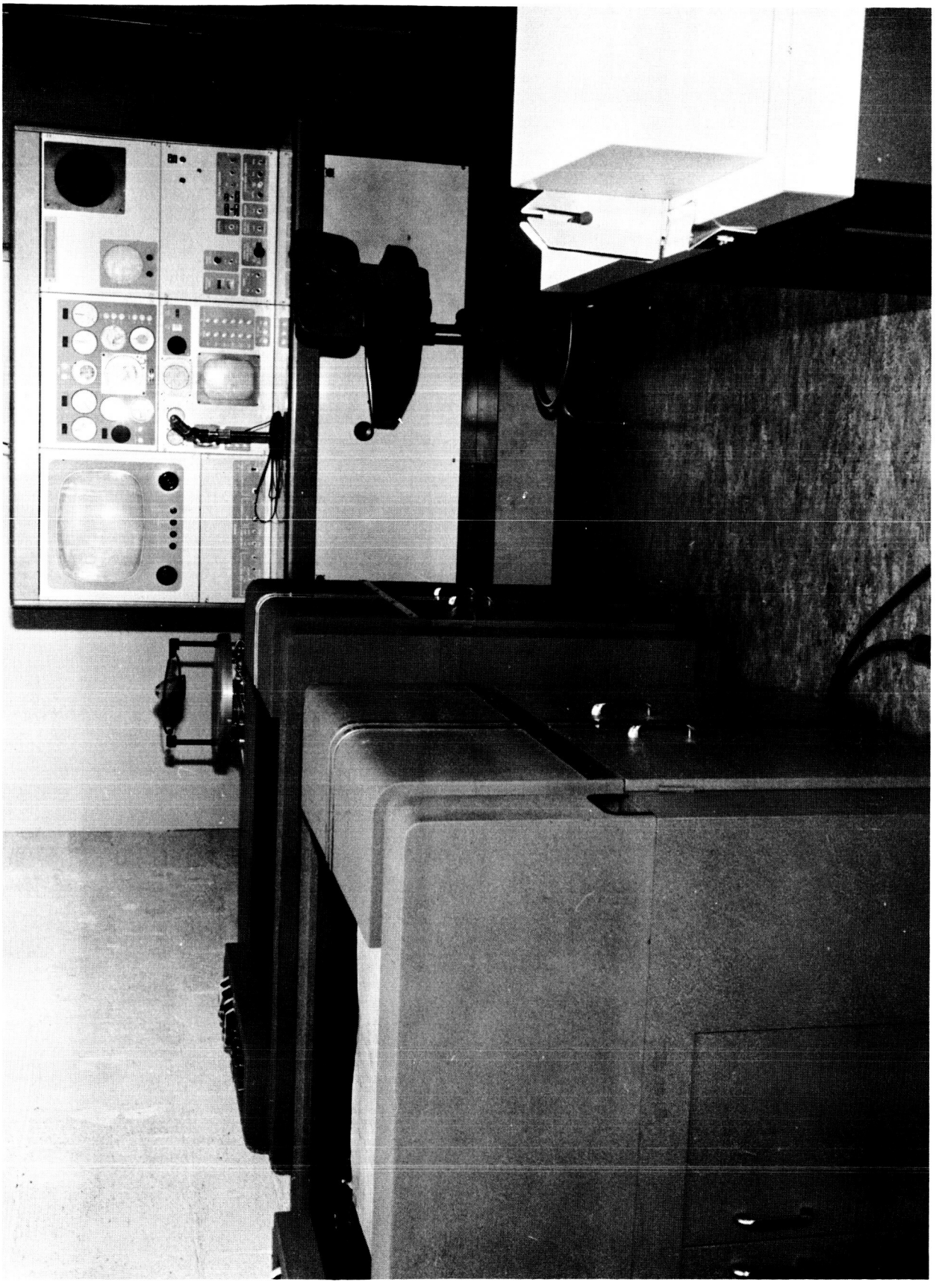

FIGURE D-4 MASTER CONTROL STATION AND PLOTTERS

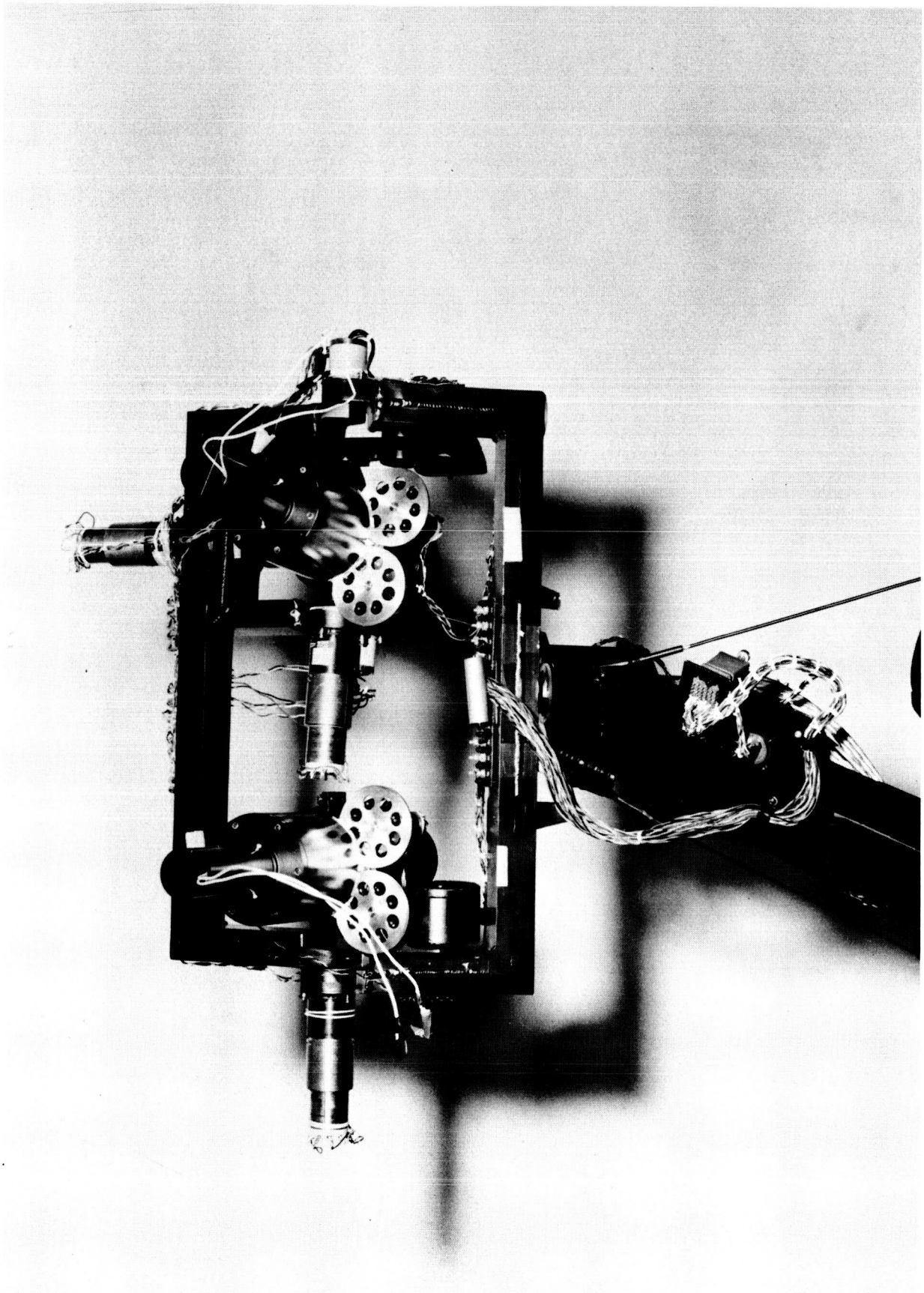

FIGURE D-5 TARGET PROJECTOR

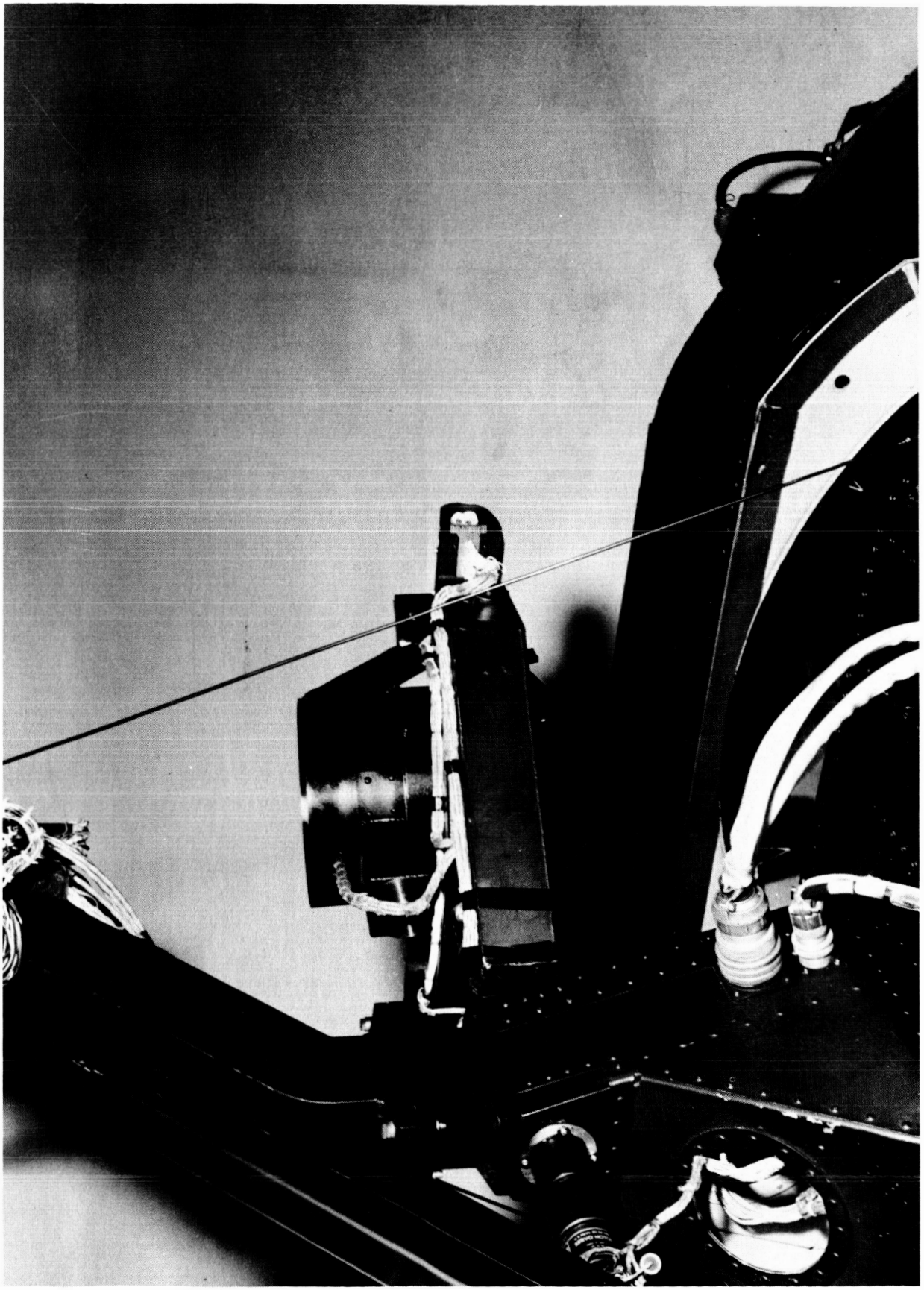

FIGURE D-6 LUNAR SCENE PROJECTOR

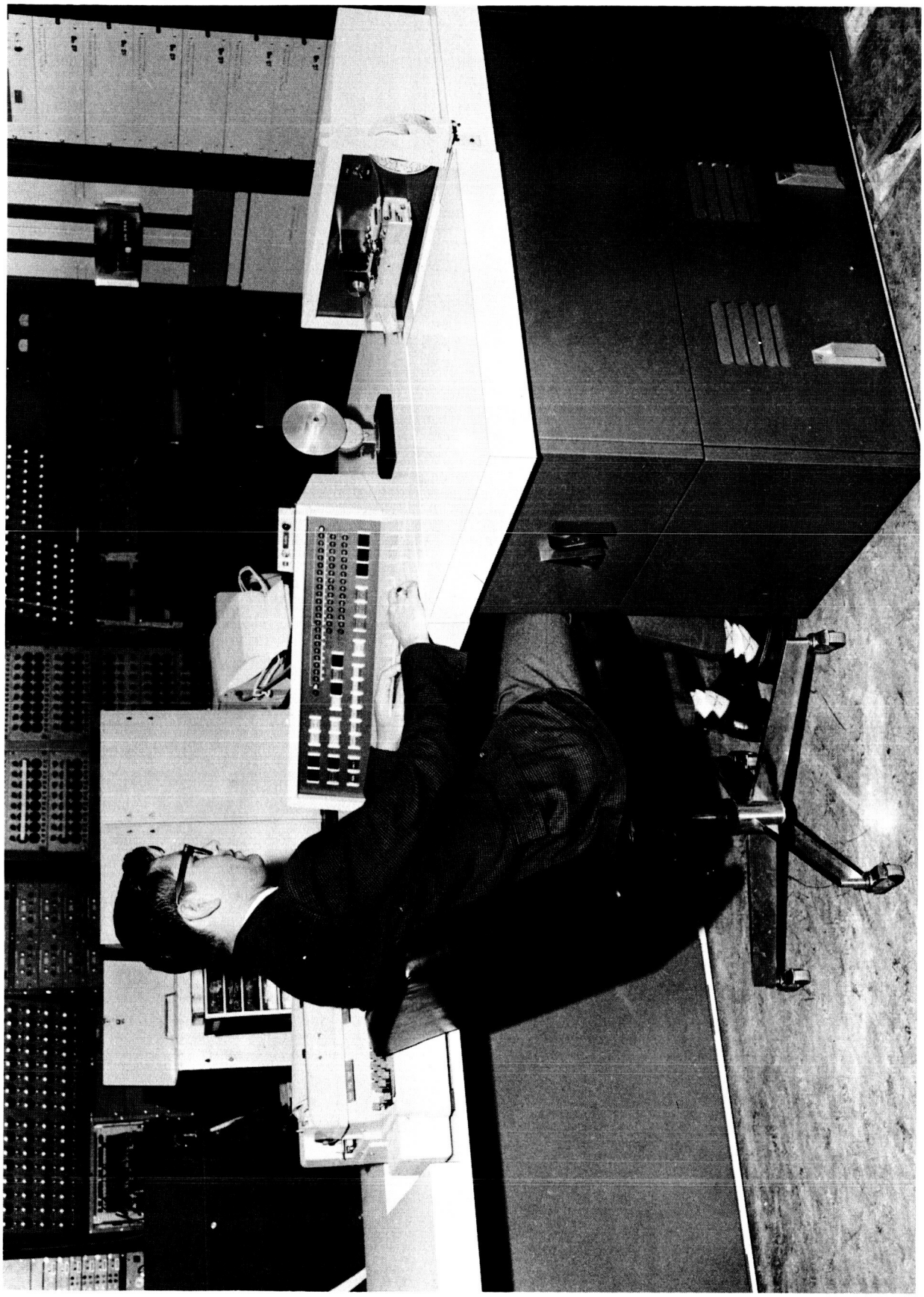

FIGURE D-7 ASI- 210 DIGITAL COMPUTER

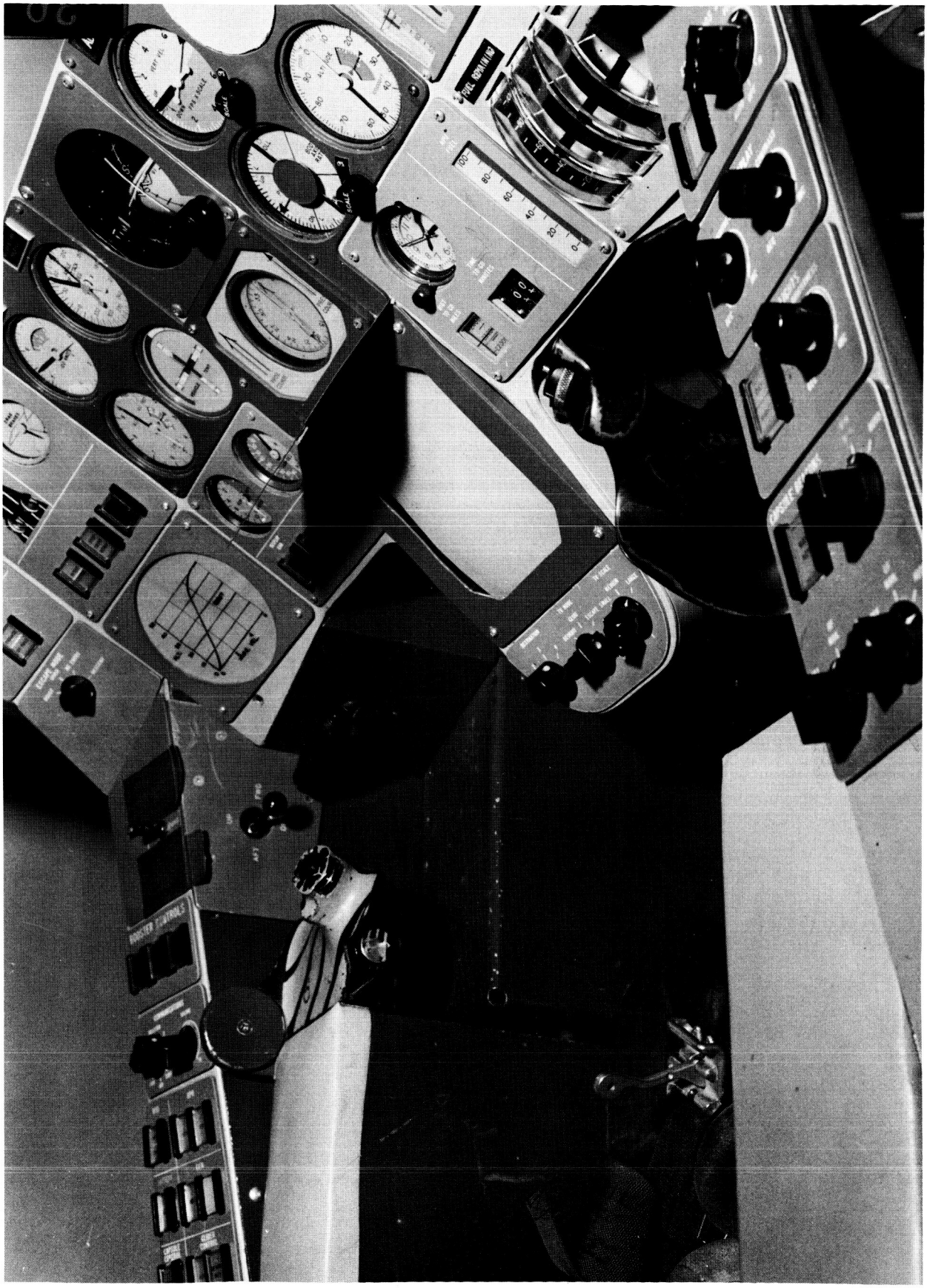

FIGURE D-8 INSTRUMENT PANEL - SIDE VIEW

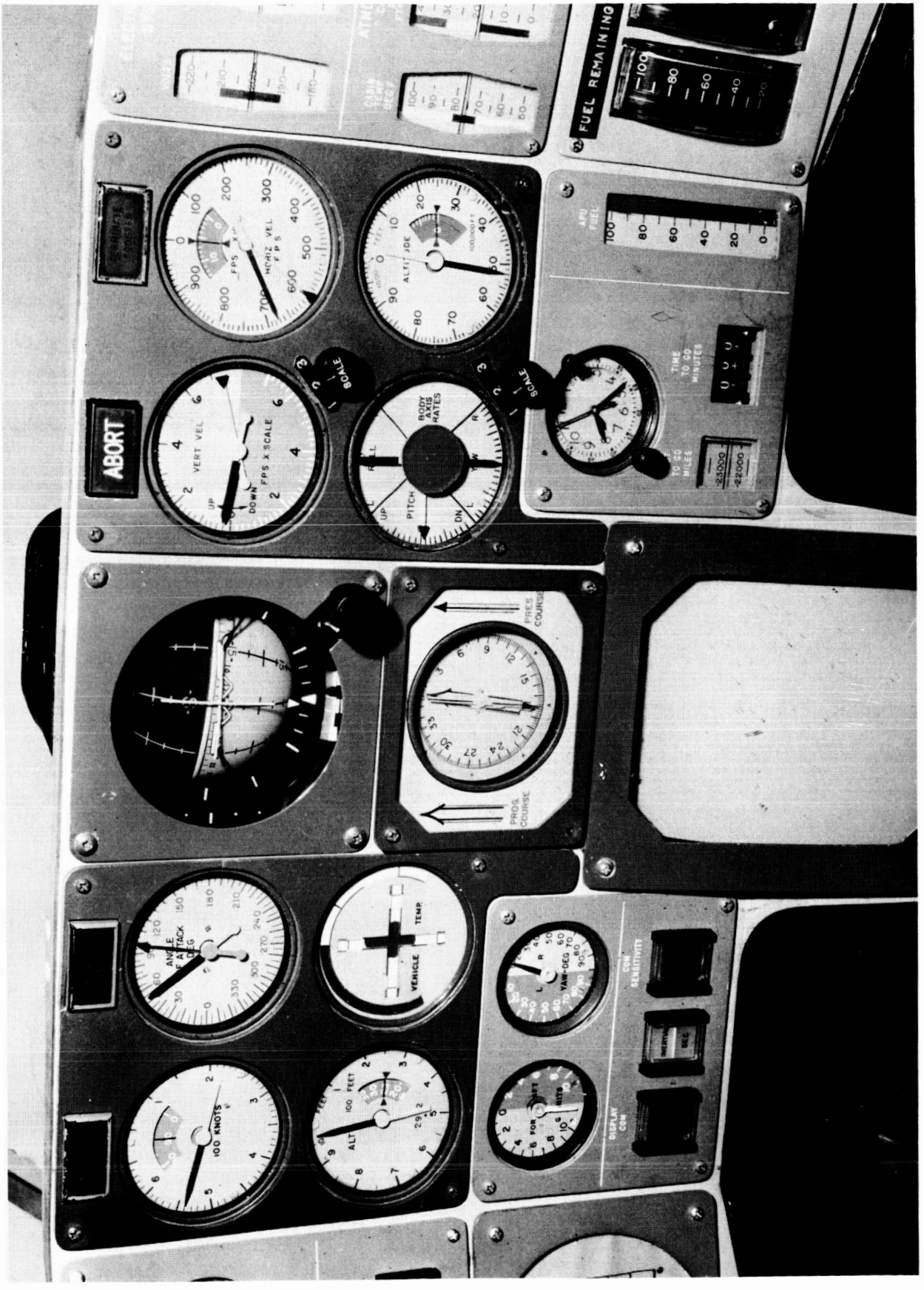

FIGURE D-9 INSTRUMENT PANEL - FRONT VIEW

FIGURE D-10

TV DISPLAY

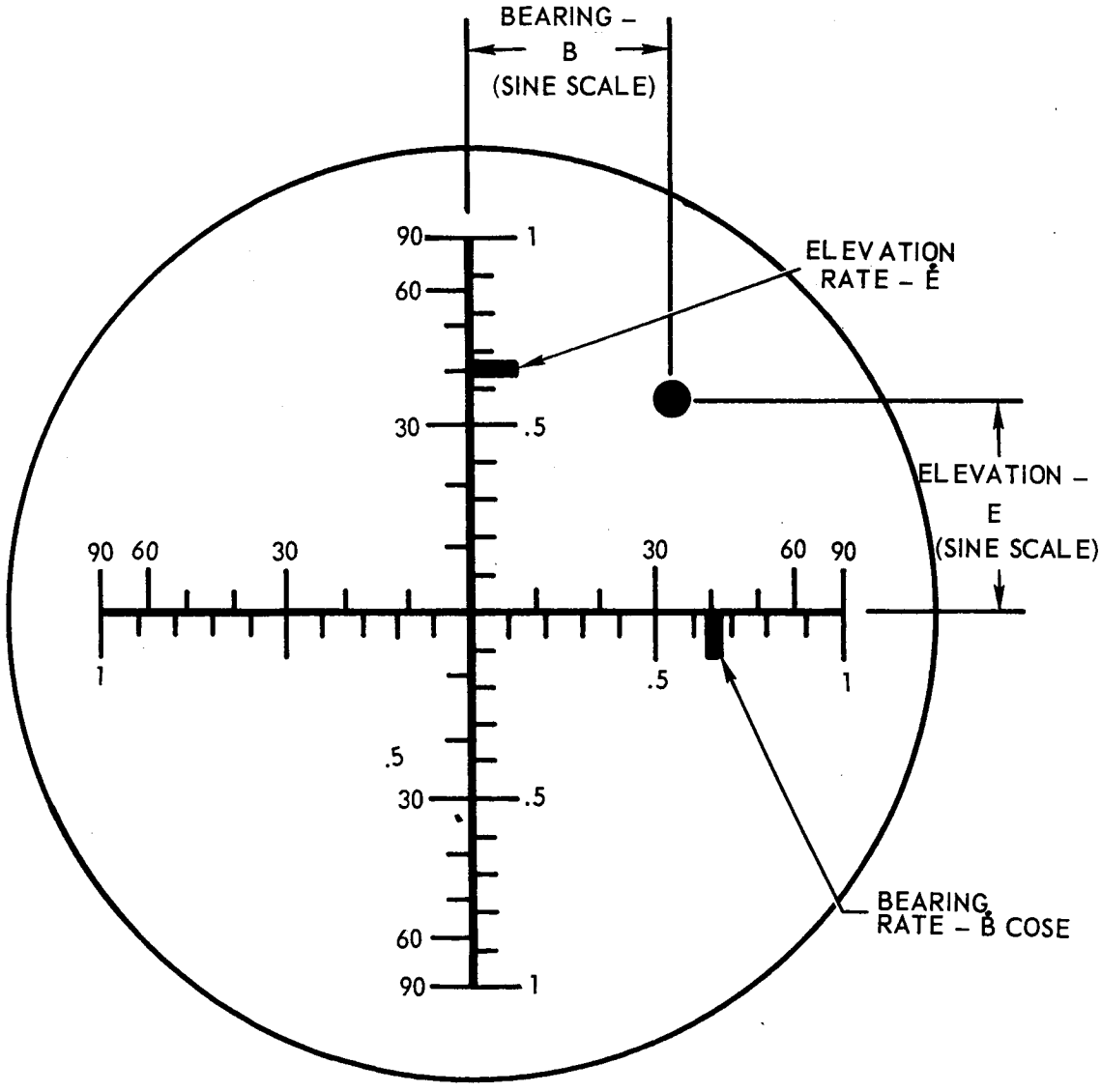

RANGE

1	1	2	3

RANGE RATE

+	2	6	3

SCALE	HIGH RANGE	MED. RANGE	LOW RANGE
B & E (DEG)	± 90	± 90	± 90
ḂcosE & Ė (RAD/SEC)	± 1 X 10^{-3}	± 1 X 10^{-3}	± 1 X 10^{-4}

APPENDIX E

SIMULATOR PROGRAMMING AND EQUATIONS

This section includes a brief description of the digital computer techniques employed for the LEM ballistic motion and Euler angle generation and provides the equations used for the LEM perturbations and control. Also listed are the drive equations for the lunar scene and target projectors and the moving base.

1. Digital Ballistic Routine

An inverse square law routine with a single attraction center was employed for the space mechanics calculations. The assumptions made were that the moon is a spherical, homogeneous, non-rotating body. The interation rate was 20 per sec and the worst condition of all combined errors averaged 0.0002 ft/sec^2. An execution time of 7.13 milliseconds was required for the program. The real-time precision was within $\pm$ 0.02%.

2. Euler Angle Generation

In order to drive the various displays, both three angle (ψ, Θ, ϕ) and four angle (ψ, ϕ_R, Θ, ϕ) Euler computations were accurately obtained in the digital computer. The basic attitude reference was a direction cosine set between the body axis system and the inertial axis system. The integration method was an incremental rotation about the instantaneous angular rate vector; it had a precision of $\pm$ 0.1%. The rate threshold was $\pm$ 0.01% of full scale. The Euler angles were derived from the direction cosines by algebraic relations and were between a local reference or any other reference base and body axis system. The Euler angle set was algebraically satisfied at each iteration point.

3. Equations - LEM Perturbations and Control

The six-degree-of-freedom body equations used for the manual portion of the runs were:

$$\dot{P} = -\delta_P \, P_{REF}$$

$$\dot{Q} = -\delta_Q \, Q_{REF}$$

$$\dot{R} = -\delta_R \, R_{REF}$$

$$M \quad \Delta \ddot{X}_B = T_{R_X}$$

$$M \quad \Delta \ddot{Y}_B = O$$

$$M \quad \Delta \ddot{Z}_B = -T_L - T_B + T_{R_Z}$$

$\dot{P}_{REF}$, $\dot{Q}_{REF}$, and $\dot{R}_{REF}$ are functions of mass and were used because suitable inertia data was not available. The reference functions provided the correct peak angular accelerations although coupling effects were not included.

The thrust levels were constant except for the descent engine which had a high and a low setting. The manual control equations are thus:

$$P_S = K_{S_P} \delta_{S_P} + K_{T_P} \delta_{T_P} \qquad -15^o \leq \delta_{S_P} \leq +15^o$$

$$Q_S = K_{S_Q} \delta_{S_Q} + K_{T_Q} \delta_{T_Q} \qquad -12^o \leq \delta_{S_Q} \leq +12^o$$

$$R_S = K_{S_R} \delta_{S_R} + K_{T_R} \delta_{T_R} \qquad -15^o \leq \delta_{S_R} \leq +15^o$$

$$P_E = P - P_S$$

$$Q_E = Q - Q_S$$

$$R_E = R - R_S$$

A $\pm$ 0.5^o/sec dead band was applied to the above error signals.

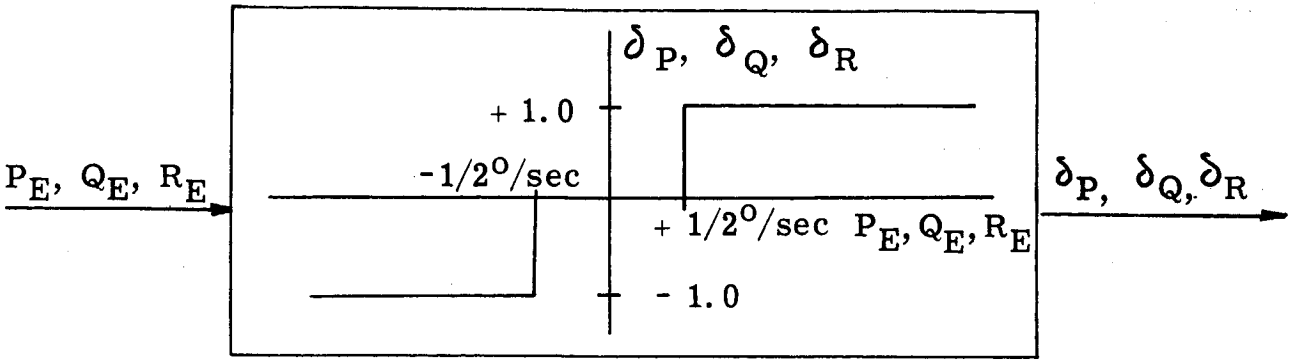

For the automatic descent to 6000 ft. altitude or to the abort, whichever occurred first, roll and heading were held at zero displacement and pitch was controlled with the following set of equations:

$$\dot{Q}_{auto} = - K_\Theta \Theta_E - K_Q Q_{auto}$$

$$\Theta_E = \Theta - \Theta_C$$

$$\Theta_C = K_I \int_o^t \left[(\Theta_{REF} - \Theta) - K_{\dot{h}} (\dot{h}_{REF} - \dot{h}) \right] dt$$

Θ_{REF} and $\dot{h}_{REF}$ were functions of altitude taken from the nominal descent data.

Automatic zero hold (manually engaged) of target line-of-sight elevation and bearing as seen from the LEM was accomplished by modifications of Q_E and R_E.

$$Q_E = Q - Q_S + K_1 \text{ Sin } E$$

$$R_E = R - R_S + K_2 \text{ Sin } B$$

Computations for fuel expended were accomplished as follows:

a. Descent Engine

$$M_{f_d} = \frac{1}{(32.2)(315)} \int_o^t T_L \, dt \quad \text{slugs}$$

b. Ascent Engine

$$M_{F_A} = \frac{1}{(32.2)(315)} \int_o^t T_B \, dt \quad \text{slugs}$$

c. RCS Translational (Docking) Engines

$$M_{F_R} = \frac{1}{(32.2)(315)} \int_0^t \left(|T_{R_X}| + |T_{R_Z}| \right) dt \text{ slugs}$$

Reaction jet fuel for attitude control was not included.

Drive equations for the moving base are written:

$$\text{Roll} = \left[0.3\, \dot{p} \left(\frac{1}{2S+1} \right) \right]_{LIM\ @\ \pm 20^\circ}$$

$$\text{Pitch} = \left\{ \left[1.61\, n_z \left(\frac{0.5S}{0.5S+1} \right) + 0.125\, (\Delta X_p \dot{Q} - \Delta Y_p \dot{P}) \right] \left(\frac{1}{2S+1} \right) \right\}_{LIM\ @\ \pm 10^\circ}$$

$$\text{Yaw} = \left\{ \left[1.61\, n_Y \left(\frac{0.5S}{0.5S+1} \right) + 0.05 (\Delta X_p \dot{R} - \Delta Z_p \dot{P}) \right] \left(\frac{1}{2S+1} \right) \right\}_{LIM\ @\ \pm 10^\circ}$$

$$\text{Gross Pitch} = \left\{ \begin{array}{l} \left[n_x \left(\frac{1}{2S+1} \right) \right]_{LIM\ @\ \pm 90^\circ} \\ + \left[9.55\, n_x \left(\frac{0.5S}{0.5S+1} \right) + 0.297 (\Delta Z_p \dot{Q} - \Delta Y_p \dot{R}) \right] \left(\frac{1}{2S+1} \right) \end{array} \right\}_{LIM\ @\ \pm 100^\circ}$$

The horizon-starfield projector was used to display a lunar scene and was driven by the necessary Euler displacements. The target projector displayed a target spot by means of the outer gimbal and a small starfield projected by the inner gimbal. Using E for elevation and B for bearing angle, the outer gimbal drive signals were obtained as follows:

$$E = SIN^{-1} \left[\frac{-D_{Z_B}}{D} \right]$$

$$B = SIN^{-1} \left[\frac{D_{Y_B}}{\sqrt{(D_{X_B})^2 + (D_{Y_B})^2}} \right]$$

The above equations represent input line of sight angles and were corrected for:

a. Position of projector beams relative to the pilot and sphere

b. The gimbaling system of the projector

The starfield center was positioned as an inertial line-of-sight expressed in the body axis system. Provision was made to center the starfield behind the target with a momentary contact panel switch. The position of the starfield on the spherical screen was corrected the same as the target beam.

4. Definition of Symbols Used

Symbol	Definition	Units
B	Bearing angle - LEM to target	rad.
D	Line-of-sight range between LEM and target	ft.
D_{X_B}, D_{Y_B}, D_{Z_B}	Orthogonal line-of-sight coordinates between LEM and target and referenced to the pilot	ft.
D_{X_O}, D_{Y_O}, D_{Z_O}	Orthogonal line-of-sight coordinates between LEM and target and referenced to the LEM local coordinates	ft.
E	Elevation angle - LEM to target	rad.
h	Distance above moon's surface	ft.
$\dot{h}_{REF}$	Nominal descent altitude rate	ft/sec
m	Mass	slugs
m_{f_A}	Mass of ascent fuel expended	slugs
m_{f_D}	Mass of descent fuel expended	slugs
m_{f_R}	Mass of docking fuel expended	slugs
n_X, n_Y, n_Z	Axial, lateral & normal accelerations	g units
P, Q, R	Body axis rates in roll, pitch & yaw	deg/sec
P_E, Q_E, R_E	Rate errors - roll, pitch & yaw	deg/sec
P_S, Q_S, R_S	Stick rate commands - roll, pitch & yaw	deg/sec
Q_{AUTO}	Body axis pitch rate - automatic descent	deg/sec

Definition of Symbols Used (Cont'd.)

Symbol	Definition	Units
$\dot{P}_{REF}, \dot{Q}_{REF}, \dot{R}_{REF}$	Body axis reference accelerations - roll, pitch & yaw	deg/sec
S	Laplace operator	---
T_B	Ascent thrust	lbs.
T_L	Descent thrust	lbs.
T_{R_X}, T_{R_Z}	Reaction control thrust - X & Z directions	lbs.
t	Time	sec.
V_H	Horizontal velocity	ft/sec
X_B, Y_B, Z_B	Body axes - Z_B is parallel to the pilot's spine, X_B parallel to the direction the pilot faces and Y_B is perpendicular to the $X_B Z_B$ plane.	ft.
ΔX_p, ΔY_p, ΔZ_P	Distances between the pilot C.G. and the vehicle C.G.	ft.
$\dot{Y}_o$	Lateral rate in LEM local horizontal plane	ft/sec
$\textcircled{Y}_{RP}$	Downrange angular displacement of LEM in target plane	deg.
$\textcircled{Z}_{RD}$	Angular displacement of LEM from target plane	deg.
δ_P, δ_Q, δ_R	Effective nozzle deflections - roll pitch & yaw	deg.
δ_{S_P}, δ_{S_Q}, δ_{S_R}	Stick displacements - roll, pitch & yaw	deg.
δ_{T_P}, δ_{T_Q}, δ_{T_R}	Trim displacements - roll, pitch & yaw	deg.
Θ	Euler displacement - pitch	deg.
Θ_c	Pitch command	deg.
Θ_E	Pitch error	deg.

Definition of Symbols Used (Cont'd.)

Symbol	Definition	Units
Θ_{REF}	Nominal pitch descent program	deg.
ϕ	Euler displacement - roll	deg.
ϕ_R	Euler displacement - redundant roll	deg.
ψ	Euler displacement - yaw	deg.

5. Control System Gain Settings

Gain	Setting
K_{SP}	1.33 sec^{-1}
K_{SQ}	1.67 sec^{-1}
K_{SR}	1.33 sec^{-1}
K_{TP}	0.05 sec^{-1}
K_{TQ}	0.05 sec^{-1}
K_{TR}	0.05 sec^{-1}
K_{Θ}	9.85 sec^{-2}
K_Q	3.14 sec^{-1}
K_I	1.0
$K_{\dot{h}}$	1.0^{o}/ft/sec
K_1	14.32^{o}/sec
K_2	14.32^{o}/sec